Dissolved Organic Matter in the Canadian Arctic & Sub-Arctic

Importance of DOM Quality & Quantity in a Warming Climate

by

Pieter Jan Karel Aukes

A thesis

presented to the University of Waterloo

in fulfillment of the

thesis requirement for the degree of

Doctor of Philosophy

in

Earth Sciences (Water)

Waterloo, Ontario, Canada, 2019

Examining Committee Membership

The following served on the Examining Committee for this thesis. The decision of the Examining Committee is by majority vote.

External Examiner	Dr. Susan Ziegler Professor
Supervisor(s)	Dr. Sherry Schiff Professor
Internal Member	Dr. Chris Parsons Research Assistant Professor
Internal-external Member	Dr. Roland Hall Professor
Other Member(s)	Dr. Igor Lehnherr Assistant Professor

AUTHOR'S DECLARATION

This thesis consists of material all of which I authored or co-authored: see Statement of Contributions included in the thesis. This is a true copy of the thesis, including any required final revisions, as accepted by my examiners.

I understand that my thesis may be made electronically available to the public.

STATEMENT OF CONTRIBUTIONS

Data chapters in this thesis have been written as publication units and were all conceived and developed by myself and Dr. Sherry Schiff. The thesis committee provided valuable input on all chapters through-out the duration of my thesis. Further, certain chapters in this thesis have benefited from the collaboration with the Government of the Northwest Territory:

Chapter 2 – Data was solely collected by the Water Resources Division, Environment & Natural Resources, Government of Northwest Territories and kindly provided by Robin Staples, GNWT. This data has been an ongoing collaboration with Mike Palmer (NWT Cumulative Impacts Monitoring Program) and Robin Staples.
Further, a version of this chapter will be submitted as a conference paper to the 22nd Northern Research Basins Symposia, Yellowknife, NT, August 2019.

Chapter 3 – Data collection from various sites involved numerous people, all of who can be found in the 'Acknowledgements'. All analyses, writing, and interpretation was done by myself with input from Dr. Schiff and the thesis committee.

Chapter 4 & 5 – Experimental design was developed by myself with input from Dr. Schiff and the thesis committee. All analyses, interpretation, and writing was done by myself with input from the committee.

Chapter 6 – A portion of the data was collected from public water quality records provided online by the Government of Northwest Territories Municipal and Community Affairs. All analyses, interpretation, and writing was done by myself with input from the committee.

Chapter 7 – The conceptual model was developed by myself with input from Dr. Schiff.

ABSTRACT

Dissolved organic matter (DOM) is a ubiquitous component of aquatic and terrestrial systems and an important constituent that can influence aquatic health and drinking water quality. For instance, DOM can act as an important nutrient for microbes or react with chlorine during treatment of drinking water supplies to form harmful disinfection by-products. As DOM is comprised of thousands of different organic molecules, the degree that DOM reacts with its surroundings depends not only on the amount of carbon, but also on its composition. A changing climate can influence DOM concentration and composition in a number of ways, such as by altering the residence time within the watershed or changing rates of DOM processing through warming temperatures. Recently, changes to DOM quality and quantity have been observed across surface waters in the northern hemisphere, which can complicate future drinking water treatment options. Organic-rich areas underlain with permafrost are found across the circumpolar north, leading to uncertainty over the effects of permafrost degradation on carbon release and fate, particularly upon downstream ecosystems and drinking water resources. Better prediction as to how DOM will respond under a warming climate requires an understanding of the variability in the amount and composition of DOM, as well as the drivers of DOM reactivity. However, the few arctic or sub-arctic locations with comprehensive DOM datasets can be difficult to compare due to the use of various DOM characterization techniques. Further, data are lacking, or entirely missing, in many areas of Canada's western sub-arctic. The overall goal of this thesis is to use field and laboratory measurements to quantify the heterogeneity encountered in DOM concentration and composition from a variety of hydrologic environments in three Canadian sub-arctic and arctic ecoregions, and to link this variability to DOM lability.

Statistical analyses of long-term monitoring of river hydrology and water quality provides a quantitative measure to the response of a watershed to a warming climate. Northern areas are quickly responding to a warming climate, yet few long-term monitoring records exist and most focus on large rivers draining directly into the Arctic Ocean. The Government of Northwest Territories have been collecting monthly river water quality parameters for the past 30+ years, providing a comprehensive dataset to quantify changes occurring to the Northwest Territories (NT) and define baseline conditions to help assess future change. Trend analysis was applied to mean annual and monthly air temperature, total precipitation, discharge, concentration, and load for

rivers draining the taiga shield (Yellowknife and Cameron Rivers) and taiga plains (Marian River) during the past 30 years. Mean annual air temperatures have significantly increased during the past 80 years (3.2×10^{-2} °C/yr), with significant increased winter monthly average temperatures (January to April). Large inter-annual variability was found in monthly average discharge for the Yellowknife and Cameron rivers, yet no significant change was found to the mean annual discharge during the past 80 years (the Marian River is ungauged). Winter flows have also increased over time within the Yellowknife River. Significant increases to mean monthly cation and anion concentrations occurred within the Yellowknife and Cameron rivers, but they did not result in significant changes to the annual loads. Baseline conditions can be easily determined for the Marian and Cameron rivers due the unchanging hydrologic and geochemical record. However, the Yellowknife River exhibits a uni-directional change in water quality, indicative of enhanced subsurface flow pathways even with no significant change to its discharge. These results indicate that annual variability in river discharge is important for determining differences in geochemical fluxes with a warming climate.

DOM composition can be quantified using a wide range of analytical techniques that vary in information obtained, cost, and analytical complexity. The overall objective was to use a readily available suite of DOM characterization techniques from surface and subsurface environments to determine which simple parameters explain the most variability within our DOM dataset, and use these parameters to create a simple, effective way to compare compositional differences in DOM. Samples were collected from surface and subsurface waters across northern freshwaters in Canada. DOM composition was quantified via absorbance, elemental ratios, and size-exclusion chromatography. Overall, DOM concentrations ranged from 0.5 mg C/L in surface water at high arctic sites to 273 mg C/L in NT subsurface environments. Composition measures that best explained DOM variability and were most unrelated in approach were specific absorbance at 255 nm (SUVA), ratio of dissolved organic carbon to dissolved organic nitrogen (DOC:DON), slope of absorbance between 275 to 295 nm ($S_{275\text{-}295}$), and humic substances fraction (HSF). Application of principal component analyses (PCA) quantified these independent measures of composition to explain up to 61% of the variability within the first three PCA axes. These four measures were used to create a 'Composition Wheel' to facilitate comparison of DOM across samples. A wide range in SUVA, $S_{275\text{-}295}$, DOC:DON, and HSF values were observed across DOM concentrations and spatial scales. Overall, subsurface DOM composition was similar across all locations, defined by high

amounts of humics, DOC:DON, and SUVA, and low $S_{275-295}$, while surface water DOM contained a variety of compositions across sites. Composition Wheels provide a simple way to visualize and compare DOM composition and quality, as well as efficiently communicate differences in DOM composition to a variety of scientific and interested audiences.

Microbial degradation is often the most important driver of DOM fate within aquatic systems. However, few measures of DOM microbial degradation rates are found among sub-arctic and arctic freshwater studies. The overall objective was to use a 30-day incubation experiment to determine how DOM composition influences microbial DOM degradation, and quantify microbial degradation rates for various surface and subsurface waters in the taiga shield (Yellowknife, NT), southern arctic (Daring Lake, NT), and northern arctic (Lake Hazen Watershed, NU). Proportion of DOM loss ranged from 1 to 27% across all samples with no clear association to initial DOM composition or hydrologic site. First-order degradation rates ranged from 0.4 to 11.2 $x10^{-3}$ d^{-1}, and were highest from DOM in the taiga shield subsurface and a southern arctic pond. Samples from the northern arctic contained the lowest rates and DOM loss, suggesting high arctic DOM may have undergone processing prior to the incubation experiment to more southern locations or no processing if the inoculum contained no viable microbes. Metrics of DOM composition responded differently to microbial degradation across all samples. Absorbance based measures ($S_{275-295}$, and SAC_{420}) have poor relationships to the proportion of DOM loss and 1st-order microbial degradation rates, whereas molecular size-based groupings were stronger predictors of degradation rate and proportion of DOM loss. Further, SUVA was a sensitive indicator of the microbial-induced change in DOM, and not a good predictor of biodegradability. DOM from all three northern ecoregions contained some degree of microbial-labile components that may not be well reflected using most measures of the initial DOM composition. Hence, the amount of DOM lost, degradation rate, and the uniqueness in the response of DOM at each location indicates a location-specific definition of DOM lability.

Photolysis is an important degradation pathway for DOM in northern systems due to the prolific number of shallow, exposed surface waters characteristic of many arctic landscapes. However, few DOM photodegradation rates have been published from Canadian arctic freshwaters. The objective of this data chapter was to determine how differences in DOM composition influence photo-lability and photodegradation rate from arctic and sub-arctic surface and subsurface waters in Canada. Degradation rates, calculated from the total DOM loss, were highest in subsurface samples (linear: 2 to 25 x 10^{-3} m^2/E; 1st-order: 4.1 to 17 $x10^{-4}$ m^2/E). Degradation rates were used to calculate total

DOM loss after 500 E/m^2 of photosynthetic active radiation (PAR) across all samples, equivalent to 18 and 13 days of sunlight in the high arctic and subarctic, respectively. Southern arctic subsurface and creek lost the highest amount of DOM (58 and 38%, respectively) while most other samples lost between 13 to 19%. The lowest proportion of DOM loss was observed from a taiga shield river (4%) likely due to pre-exposure among the landscape. No significant correlations were found between initial DOM composition and photolytic degradation rate. Alternatively, initial measures of SUVA and SAC_{420} predicted the proportion of photolytic DOM loss. Photolytic-induced changes to DOM were similar across all samples: decreased values of SUVA, DOC:DON, and SAC_{420}, and increased values of $S_{275\text{-}295}$. Hence, photolysis uniformly altered DOM regardless of initial composition or sample location. Specific measures of DOM composition, such as SUVA and SAC_{420}, provide sensitive indicators of photolytic processes and can be used to estimate the degradation rate and proportion of DOM loss.

Chlorine reacts with DOM to form harmful disinfection by products (DBP), yet the extent DOM forms DBP may depend upon the amount and composition of DOM. The objective of this data chapter was to determine how differences in DOM composition from sub-arctic freshwaters influences DBP formation. Samples were collected from Yellowknife, Wekweètì, and Daring Lake, NT, and a microbial and photolytic degradation experiment to understand how drivers of DOM fate influence DBP formation. Further, public water quality data records were used to determine the prevalence of DOM and DBP across NT water treatment records. DOM composition was characterized using overall concentration, SUVA, $S_{275\text{-}295}$, DOC:DON, and size-exclusion chromatography determined fractions of humic substances (HSF). Concentrations of trihalomethanes (THM) and haloacetic acids (HAA) were measured with equivalent chlorine residuals 24 hours after chlorine addition. Public water quality records indicate both DBP and DOM were ubiquitous in NT water sources and generally below health guidelines. DOM composition plays an important role for disinfection demand as no strong relationship was found between chlorine demand and DOM concentration. Simple measures of DOM composition, such as SUVA and $S_{275\text{-}295}$, resulted in stronger correlations with DBP concentration than overall DOM concentration. In particular, high molecular weight and aromatic humics, representative of terrestrial-like DOM sources, formed higher DBP concentrations. Microbial degradation led to higher DBP yields normalized to DOM mass while photolysis had little effect. We show various

compositions of DOM from across the NT lead to different but predictable differences in DBP concentration.

Data and interpretations from all chapters were brought together to form a conceptual diagram of DOM evolution in the NT. Different DOM compositions and changes related to microbial and photolytic degradation aided with categorization of different samples along a tri-axis plot of compositional end members: terrestrial, photolytic, and autochthonous. Not all DOM composition metrics respond the same way during degradation. Specific indicators of processes were identified from the degradation experiments: SUVA and SAC_{420} both responded oppositely to microbial and photolytic degradation, while $S_{275\text{-}295}$ only increased for photolysis. Although these processes appeared to align with the variation observed among high arctic DOM composition and sources, notable differences in high arctic DOM composition demonstrate the need for revision to incorporate other high arctic sites to the current DOM conceptual diagram. The conceptual diagram identified zones of 'labile' DOM composition, as well as zones of 'high-risk' DOM that have the potential to form high concentrations of DBP. The conceptual diagram provides a framework to focus and continue developing the impact of various drivers on DOM quantity and quality under different climate scenarios.

ACKNOWLEDGEMENTS

I'd like to thank Dr. Barry Warner, Dr. Igor Lehnherr, Dr. Michael English, and Dr. Sherry Schiff for being on my Thesis Committee and helping me create a solid work of science these past few years. I'd also like to thank Dr. Susan Ziegler, Dr. Chris Parsons, and Dr. Roland Hall for being on my examining committee and providing suggestions to make this thesis a better piece of science.

Research in the arctic is *incredibly* expensive. This thesis as benefited from the following funding organizations: Northwest Territories Cumulative Impact Monitoring Program (NWT CIMP), ArcticNet, Polar Continental Shelf Program (and for all the tremendous logistical work that goes into planning travel for a field season), Northern Scientific Training Program, NSERC, Government of Ontario (Ontario Graduate Scholarship), University of Waterloo, TD Friends of the Environment, Association of Canadian Universities for Northern Studies, and the Garfield Weston Foundation. Parks Canada helped with logistical support for work conducted at Lake Hazen, Quttinirpaaq National Park, Nunavut.

Many people have helped me during my time at the University of Waterloo. Sue Fisher, Lorraine Albrecht, and Chris Hanton-Fong have always been kind enough to help me wade through the logistics of Grad school. I'd like to thank Monica Tudorancea and Dr. Sigrid Peldszus for help with the LC-OCD, and Shoeleh Shams for her knowledge of DBP. I'd also like to thank Dr. Brewster Conant for all the organizational and teaching skills I learnt during my time as the field school TA.

There have been numerous people in the Environmental Geochemistry Laboratory who have helped by packing coolers, listening to my Hydromicros, prepping or running samples, bagging and labelling rubbermaids to send to Lake Hazen, etc.: Dr. Megan Larsen, Dr. Kateri Salk, Puru Shah, Jordyn Atkins, Mackenzie Shultz, Jeremy Leathers, Emily Barber, Rachel Henderson, Eric Mcquay, Bethany Gruber, Emma Jewett, Holden Little, Jenny Hickman, Erin MacDonald, Sarah Indris, and Amy Morrison. Thanks to Janessa Zheng for the tremendous help in the lab. A massive thanks to the mastermind behind all these people: Richard Elgood. I'm not sure if you know it but the support you give to us students is significantly greater than anything I could ever put in writing here (but maybe a fine scotch? Thanks Rich!). This thesis has also benefited from the countless discussions with Dr. Jason Venkiteswaran on all things science (and voetbal) and Dr. Maddy Rosamond for her insightful and always on-point science suggestions. Thank you to Paul Dainard for your help up at Hazen (So. Much. Filtering.) and for those interesting DOM discussions over the

years. I've been lucky to have Sarah Sine and Jenn Mead around for my whole thesis as they are both such wonderful, helping, and caring people who would drop anything to help. Sarah, thanks for all the positivity, Vin-Sam runs, support, and laughs over the years. Jenn, I've really enjoyed our DOM talks and witnessing your meticulous work ethic. You both have definitely made this much easier.

My trips to the Northwest Territories have always been greatly helped by a number of people. I'd like to thank the Community of Wekweètì and the Wek'èezhìi Land and Water Board for their support of this project. Thank you to Bruce Hanna, Ryan Fequet, and Dr. Sarah Elsasser for logistical help with the field work. Much of the work out on the land around Wekweètì would not have been possible without the help of Roy and Roberta Judas. This thesis has benefited from a number of interesting and fruitful discussions with Robin Staples, Mike Palmer, and Heather Scott. Field work around Yellowknife was also helped by Jordan Reid and Stefan Goodman.

High arctic field work can be exhausting but I've been lucky enough to have great collaborators to make it enjoyable. I'd like to thank the ever-patient Dr. Vince St. Louis (sorry for filtering so loud next to your tent) and Dr. Igor Lehnherr (no worries about the tritium and helium sampler) for teaching me how to plan and pack for the high arctic, and helping collect numerous samples both near and very far from camp. Thank you to Kyra St. Pierre for the laughs, jokes, and scientific discussions through-out our time at Hazen, as well as for experiencing that trip to Iqaluit where everything that could go wrong did go wrong. Thanks to Victoria Wisniewski, Maria Cavacao, Jessica Serbu, Steph Varty, Ashley Dubnick, and Brad Danielson who helped with field sampling, field laughter, and all sorts of helpful things with Lake Hazen.

Sometimes it's not the science that helps you through the thesis, but the little breaks in between. I'd like to thank the people who were very supportive and always up for a good laugh: Hilary White, Heather Shrimpton, Martin Pape, David Wilson, Katherine Hajdur, Colin McCarter, and the Courtney Family. Thank you to Allan, Erin, Steve, and Anita, for teaching me how to canoe and for the subsequent canoe trips we've been on (no more 4 km portages though). I'd like to thank Justin Harbin and Jess Leung not only for all the help in the isotope lab, but also for also being such caring, supporting, and positive people during my years at Waterloo. Thank you to my great friends Rowan Cockett and Kristyn Adams in Calgary for supporting this from afar. Thanks to Debbie, Richard, Ron, Barb, Chris and Steph for the support and attempts at understanding why your son/brother in law loves school so much. I can't wait to read this to you all!

I would really like to acknowledge the support and guidance from Sherry and Mike. It's one thing to supervise a student, but I really believe you have both been fantastic and inspiring mentors through-out my PhD. Mike, I've enjoyed working alongside you and learning about all the geologic and hydrologic aspects that make the arctic so confusing and interesting. Your sense of humour and curiosity for all things geochemistry have led to some great discussions and laughs! Sherry, I feel so lucky to have received that phone call way back when to start a MSc with you. I know I have learnt so many different things over the years that have made me a better scientist (especially the impromptu high arctic comprehensive exam on plumbing). You have definitely made this a wonderful experience and have really helped grow my excitement for science and research. Thank you so much for everything you have done these past few years.

I'd like to thank my sisters, Saskia and Fenna, for not only putting up with my pestering but also for being excited and interested in the work I was doing! Mom and Dad. Watching your kid stay in school for so long must have been somewhat worrying at times, but I want to thank you so much for supporting me through this. You were both always so interested, proud, and happy with even the smallest achievements that you made it easy for me to try for the impossible even if I failed. I know that I'll learn this from you two as I do the same for Finnley.

Amanda. You have always believed in what I could do and helped me through the times when it felt so very far away. You were always there and I feel incredibly lucky to have someone who just gets it, is so understanding, and is excited for where it will all take us. Throughout this PhD we've grown together, started a family, and had many great memories of our time here. I love you so much and know that wherever or whatever we do next won't matter as you and Finnley will be right there with me. (I know you wanted a poem here but I'm just terrible at that).

DEDICATION

This thesis is dedicated to my family (old & new).

Finnley,

You can't read this yet but I hope you find something you love to do each day as much as I found here.

TABLE OF CONTENTS

LIST OF FIGURES

LIST OF TABLES

LIST OF ABBREVIATIONS

BB	Building blocks
BDOM	Biodegradable DOM
BP	Biopolymers
CDOM	Chromophoric DOM
CW	Composition Wheel
DBP	Disinfection by products
DL	Daring Lake
DIC	Dissolved inorganic carbon
DOC	Dissolved organic carbon
DOC:DON	Molar ratio of dissolved organic carbon to dissolved organic nitrogen
DOM	Dissolved organic matter
DON	Dissolved organic nitrogen
GNWT	Government of Northwest Territories
HAA	Haloacetic acid (type of DBP)
HMW	High molecular weight
HSF	Humic substances like fraction
HZ	Lake Hazen Watershed
LC-OCD	Liquid chromatography – organic carbon detection
LMW	Low molecular weight
LMWN	Low molecular weight neutrals
MAC	Maximum acceptable concentration
NT	Northwest Territories
PAR	Photosynthetic active radiation (400 to 700nm)
PARAFAC	Parallel-factor analysis
PC1 and PC2	Principal component axis 1 or 2
PCA	Principal component analysis
POM	Particulate organic matter
RC	Reactivity-Continuum
$S_{275\text{-}295}$	Spectral slope between 275 and 295 nm
SAC_{420}	Specific absorbance coefficient at 420 nm
SCD	Specific chlorine demand (chlorine added per unit of DOM)
SOM	Soil organic matter
SUVA	Specific ultra-violet absorbance at 255 nm
TDS	Total dissolved solids
THM	Trihalomethane (type of DBP)
TP	Total phosphorus
UV	Ultraviolet
WK	Wekweètì
YK	Yellowknife

Chapter 1
Dissolved Organic Matter in Canada's North under a Changing Climate

1.1 Canada's Arctic Landscape

The arctic is an important part of Canadian identity with its three northern territories encompassing almost 40% of Canada's total land area. Defined as the area north of the Arctic Circle (66.5° N), the arctic is an environment of extremes and generally represented by long, cold winters and short, cool summers. Freeze-thaw cycles control many physical and geological processes, while moisture is generally stored during the winter as snow and released during the spring freshet[1]. These systems are uniquely defined by the abundance of small ponds and lakes due to the presence of permafrost[2–4]. Permafrost, defined as the subsurface where the mean annual temperature is below 0°C for two years, can range from discontinuous and sporadic in the south to continuous in the north[5]. The climate and physical features are unique and set these systems apart from anything else observed across the globe.

The Quaternary (~2.6 mya) period represents a time of planetary cooling with alternating glacial and interglacial periods. The northern Canadian physical landscape seen today is a result from processes during the deglaciation of ice sheets and glaciers that covered Canada approximately 13,000 to 6,000 years before present[1]. Retreating glaciers scoured and exposed Precambrian bedrock across much of the Northwest Territories, leaving behind rolling topography and post-glacial deposits[6], while sedimentary bedrock was exposed in the high arctic[7,8]. Areas in the high arctic are defined as a polar desert due to the lack of moisture. Here, vegetation is sparse and growth is limited as plant life adapts to low-nutrient and low solar radiation conditions with a tolerance towards desiccation, snow, and frost[1]. In contrast, lower arctic areas can contain trees and shrub vegetation, especially in areas where the southern-most limits encounter the boreal ecotone[9]. These unique features of the arctic govern much of the distribution and functioning of surface water systems found today.

Climate change occurs globally yet northern systems are the most sensitive to a warming north, exhibiting clear and rapid changes due to anthropogenic influences[10,11]. Specifically, certain areas are undergoing permafrost degradation, shifts in vegetation, increased mean annual air and

subsurface temperatures, changes to lake ice thickness and duration, and changes to the timing and form of precipitation, all of which can alter hydrologic flow pathways, aquatic health, and elemental cycling[12–21]. Further, the everyday lives of northern community members are directly affected, whether it be changes to safe passageway to hunting areas, continual road maintenance from permafrost degradation, increased occurrence and severity of fires, or changes to drinking water quality[22]. Ultimately, the uncertainty towards the future environmental responses to a warming climate greatly influences environmental, social, and economic sectors in the North.

1.2 Carbon in a Warming North

The release of carbon currently frozen and 'immobilized' within the subsurface due to permafrost degradation will significantly alter the global carbon cycle[23]. Permafrost areas are predicted to become a net carbon source to the atmosphere by 2100[24] with current estimates of 1700 Pg of carbon currently stored within permafrost across the circumpolar north[25,26]. Carbon can be released in particulate form, dissolved phase, or as a greenhouse gas (namely carbon dioxide or methane from surface waters and vegetation)[15,18,27–35]. Attempts have been made to predict the vulnerability of stored carbon, such as through use of C:N[36]. Shallow ponds and lakes across the arctic landscape are know to be biogeochemical hotspots[3,37–39] and can determine whether carbon is released to the atmosphere or sequestered into the sediments. Changes to the carbon cycle have been quantified through the release of greenhouse gases from either permafrost thaw[23,37,40–43] or increased terrestrial and aquatic productivity[44–46]. Recent work encompassed the lateral transfer of carbon across terrestrial-aquatic linkages[18,47]. Further, the use of stable and radioactive isotopes have been incorporated to better understand the portioning of old, permafrost derived carbon versus recent carbon[48]. Hence, rapid changes to climate have the potential to greatly influence the global carbon cycle by altering the amount, form, and rate of carbon transferred between northern terrestrial and aquatic ecosystems.

1.3 Importance of Dissolved Organic Matter

1.3.1 Role of DOM in the Natural Environment

Dissolved organic matter (DOM) is a ubiquitous component found among terrestrial and aquatic environments. Although DOM is comprised of thousands of different molecules with varying structural and chemical properties, the overall amount can be quantified by the concentration of

dissolved organic carbon that passes through an operational filter size (commonly ranges between 0.2 to 0.7 μm). Sources of DOM within a system are categorized as being formed *in situ* (termed autochthonous) or transported into the system from the surrounding environment (termed allochthonous; Figure 1.1). Differences in DOM source and processing, whether it be physical, chemical, or biological, within the watershed dictates the amount and form of DOM available for further reactions[49–51].

Dissolved organic matter plays a number of important roles within the environment. Within aquatic systems, DOM transports carbon between aquatic and terrestrial systems[18], regulates pH[52], absorbs solar radiation[53,54], impacts visibility and thermal regimes within surface waters[55,56], acts as an important energy source for microbes[57], and influences redox conditions and biogeochemical reactions[58]. Drinking water quality is affected by the amount and form of DOM. There are no Federal Canadian water quality guidelines for a maximum acceptable concentration for DOM, but provincial governments have set an aesthetic objective value, between 2 to 5 mg C/L, to reduce colour, odour, taste, and microbial regrowth within water distribution infrastructure[59]. Metals can complex with and be transported by DOM[60–62] while differences in DOM concentration and composition influences mercury bioaccumulation in invertebrates and fish[63]. The single-largest determinant of water treatment cost is the removal of organics as filtration, coagulation, flocculation, or ultra-violet light are required to lower the amount of organic matter within water supplies[64–66]. Further, during the disinfectant stage of water treatment, DOM can react with chlorine to produce various carcinogenic disinfection by-products (DBP; Krasner et al. 2006). However, the amount of DBP formed, and its toxicity, depend upon the concentration and composition of DOM[68]. Hence, both the amount and composition of DOM are important parameters that dictate aquatic ecosystem health and drinking water quality.

1.3.2 DOM Quantity versus Quality

The reactivity of DOM to the surrounding environment depends upon the amount and specific mixture of organic molecules present. The term 'DOM quality' is often used to describe different mixtures of DOM, but the term is ambiguous as it can refer to a number of different characteristics depending upon the parameter and role under question. For instance, DOM quality as defined by its ability to absorb ultraviolet and visible light could be completely different from DOM quality as defined by its ability to complex and mobilize trace metals. Hence, different roles of DOM within

the environment result in different qualities of DOM. This confusion can be simplified by referring to variations in DOM composition, rather than quality, which will be used for this thesis.

Differences in DOM composition are commonly characterized by the light-absorbing components (chromophoric DOM), specifically by quantifying ultraviolet and visible light absorption or fluorescence-emission excitation[69–73]. However, these techniques only provide information on the chromophoric components, and could also include interference from the matrix solution (such as iron; Poulin et al. 2014). Regardless, absorbance and fluorescence metrics provide an economic and relatively simple method to characterize DOM. Other methods include the use of molecular groupings[75,76], elemental ratios[77,78], or specific molecular structures via mass spectrometry[79,80]. These techniques can be used to quantify differences in DOM composition, each with their own advantages and disadvantages. However, differences in absorbance wavelengths or methodology used across published studies make it difficult to holistically compare DOM across studies.

Degradation of DOM is dependent upon its concentration and composition. Ultimately, the persistence of DOM within the environment is controlled by DOM intrinsic properties, such as specific molecular groups or characteristics[81]. Changes to DOM as a result of processing can be quantified using laboratory experiments that determine the amount of DOM loss over time using biotic[82–85] and abiotic processes (in particular solar radiation[86,87]). However, differences in experiment duration, filter sizes, or addition of nutrients make it difficult to compare the percentage of microbial or photolytic labile DOM across sites. Regardless, these examinations quantify the rate of DOM change, indicate how DOM composition is affected, and provide tools to predict the responses of DOM under different climate change scenarios.

1.4 The Role of DOM in a Changing North

The responses of DOM to a warming climate have global implications for water quality, carbon cycling, and climate feedback systems. For instance, warmer temperatures could increase the export of DOM among major northern river systems draining into the Arctic Ocean[88], enhancing the transfer of carbon from freshwater terrestrial systems into the marine environment. Increased amounts of DOM, particularly terrestrial-derived DOM, have been observed across the northern hemisphere[55,89] and resulted in changes to water transparency. Further, differences in aquatic-terrestrial linkages could increase the variability in DOM composition found in surface waters as

observed across Finnish thaw ponds[90]. The darkening of surface water colour in the northern hemisphere, a phenomena termed 'brownification', results from changes in DOM and iron export from the surrounding catchment and can influence thermal regimes, water clarity, and drinking water treatment options[34,55,91,92]. Hence, the connection between a changing terrestrial environment upon surrounding aquatic systems in terms of subsurface processing and hydrologic flow paths has important consequences upon water quality.

Degrading permafrost among organic-rich substrates can contribute very old, low molecular weight, low aromatic, and microbially-labile DOM to nearby surface waters[32,93–98]. Although photolysis accounts for 70 to 95% of DOM processed in shallow Alaskan surface waters[99], permafrost-derived DOM seems to be unaffected by photolysis[100]. Further, DOM change via photo-oxidation and photochemical transformation is found to be more common than complete mineralization of DOM into carbon dioxide[99,101]. Differences in the processing and transport of DOM can alter subarctic pond bacterial communities [90], influence future drinking water treatability[66,102], and promote acidification of the East Arctic Shelf[103]. The response of the carbon cycle to a changing climate will directly influence DOM in northern waters, thus understanding the role DOM composition plays in dictating its fate will aid in predicting how DOM affects various aquatic ecosystem functions and drinking water quality.

1.5 Thesis Rationale and Objectives

Studies on climate change in the Arctic come from a select few sites that have been extensively studied[104], likely due to the high costs of arctic field work[105]. Many northern-based DOM studies are found in Siberia[15,28,29,32,46,96,106–108], Alaska[82,99,109–116], and Nordic countries[90,98,117–120]. In Canada, the main sites include the Yukon River Basin[30,121–126], Mackenzie Delta[127–132], and select high arctic sites (Bylot Island[101,133] and Cape Bounty[134–138], Nunavut). However, few data are found from large areas of Canada's arctic and sub-arctic that describe ice-poor, subarctic shield sites[139,140], let alone published rates of DOM degradation via biotic or photolytic pathways. There is a need in the scientific community to pursue how process-based knowledge of the landscape can be used to understand controls of DOM fate that help to link climate-driven changes with the impact on DOM composition[141]. Although much information can be found over freshwater northern carbon cycling under a changing climate, there are still large geographic areas of Canada lacking important information.

The overall goal of this Ph.D thesis is to determine how DOM amount and composition differs between different arctic and sub-arctic environments, and understand how these differences in DOM composition affect aquatic ecosystem health, drinking water quality, and the ultimate environmental fate of DOM. This goal will be accomplished by combining field data with laboratory experiments to answer three specific objectives: 1) how does DOM composition vary? 2) how does DOM composition influence microbial and photolytic degradation rates? and 3) how does DOM composition relate to drinking water quality and aquatic ecosystem health (Figure 1.2).

This thesis is organized into five data chapters, followed by one chapter that synthesizes the results into a conceptual model of DOM composition in the environment and tests that model on DOM from the high arctic, and a final chapter that summarizes the key original findings in this thesis. In the first data chapter, long-term river water quality data records will be used to determine how rivers near Yellowknife, Northwest Territories (NT), have changed during the past 30 years, and whether baseline conditions can be defined (Chapter 2). A suite of simple DOM characterization methods from samples spanning a large range of Canadian ecoregions (from Southern Ontario to the NT) will be used to determine which measures of DOM composition best represent differences in DOM (Chapter 3). These select compositional measures will be used to determine how DOM composition influences microbial (Chapter 4) and photolytic (Chapter 5) degradation. The influence of DOM composition on drinking water quality will be assessed by comparing differences in DOM with the formation of disinfection by-products (Chapter 6). Finally, results from the previous chapters will be combined to form a conceptual diagram of DOM evolution in the NT (Chapter 7), which will be used to compare with changes to DOM along well-defined high arctic flow path to assess whether similar processes and drivers dictate DOM fate.

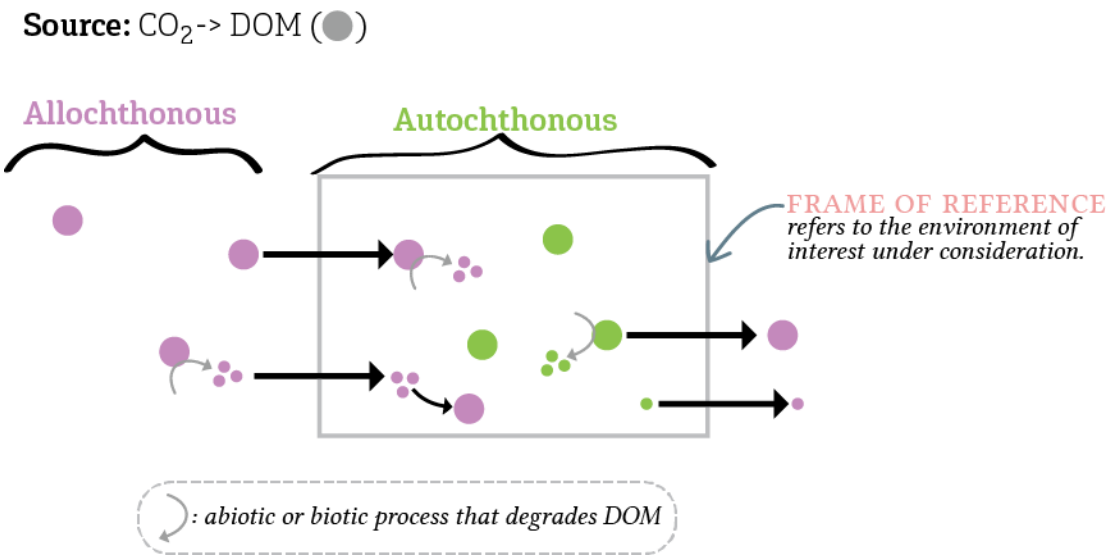

FIGURE 1.1: A general schematic to illustrate the definitions for dissolved organic matter (DOM) source as it is converted between inorganic carbon dioxide (CO_2) to DOM and transferred across systems.

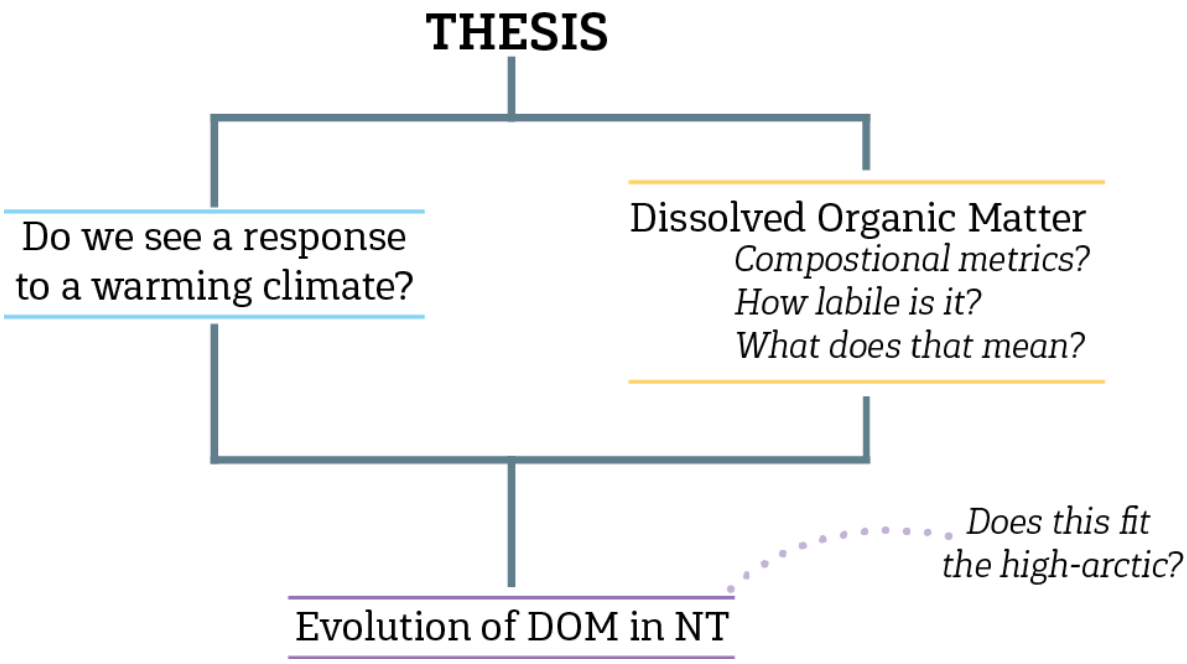

FIGURE 1.2: Simplified outline of this thesis, combining long-term environmental records in the Northwest Territories (NT; left side) with field and laboratory analyses of dissolved organic matter (DOM; right side). These two aspects are combined to create a synthesis of DOM evolution, which will also be compared to DOM collected from a high arctic location.

Chapter 2
Trends in Water Quality from Three Rivers near Yellowknife, Northwest Territories

2.1 Introduction

Long-term monitoring of river water quality provides hydrologic and geochemical insight of the surrounding watershed. Statistical analyses of discharge and chemical fluxes can identify environmental responses to climate or anthropogenic drivers[142,143]. Significant changes in nutrient exports have been linked to combinations of anthropogenic and climate influences[144,145]. For instance, increased summer temperatures and changes to land management in the United Kingdom led to the enhanced release of dissolved organic carbon (DOC) from upland peat catchments[146]. Determining drivers of change within watersheds, and how different watersheds respond to such changes, can be addressed by the analysis of long-term monitoring records of water quantity and quality.

The Northwest Territories (NT) is an area of Canada that is most sensitive to a warming climate. Air temperatures in the arctic have increased in recent decades, concurrent with decreases to annual snow depth[13,147]. A shift in precipitation from snow to rain has been observed in the sub-arctic and is expected to continue with a changing climate[17,148], ultimately affecting the seasonal hydrological balance of many northern systems. Understanding how arctic and sub-arctic ecosystems respond to a warming climate on a watershed scale is difficult due to high costs associated with routine field work and a lack of technical infrastructure. In terms of natural resource extraction in the NT, degrading permafrost allows for new subsurface connections to nearby surface waters that can complicate industrial waste disposal[107]. Drinking water sustainability can also be altered as many NT communities solely rely on rivers as sources of drinking water, which are already affected by high turbidity, colour, and particulate trace metals[149]. Understanding how arctic rivers respond to a warming climate is important for predicting effects on future aquatic and community health.

Northern systems are already responding to a changing climate. Discharge in Eurasian rivers has significantly increased and contributed the highest combined average discharge of all circumpolar

rivers to the Arctic Ocean between 1964 to 2000[150]. Annual discharge from 42 northern Canadian rivers has increased by 18% between 1989 and 2013 and at a rate greater than that of northern Eurasian rivers[151]. Increasing temperatures and changes to precipitation are the main drivers of change to river discharge[151]. Further, increased flows within the Mackenzie River Basin have been correlated with long-term atmospheric processes, such as the Pacific Decadal Oscillation[152], signifying a response of these watersheds to climatic drivers at longer time scales.

Permafrost thaw can influence watershed processes and nutrient export. Permafrost degradation is linked with increased winter base flow due to enhanced subsurface water capacity[14]. However, recent studies find enhanced late fall storage, rather than increased groundwater contribution, may be responsible for increased winter base flow within sub-arctic creeks[153]. Increasing active-layer thicknesses, thermokarst processes, and degrading permafrost can enhance weathering and mobilization of previously-frozen solutes and nutrients within permafrost, including carbon, inorganic nitrogen, and phosphorus[116,122,132,154,155]. Further, mineralization incubation experiments on thawing Swedish peatlands found significant releases of nitrogen with warming temperatures[156]. Such changes have the potential to alter in-river and downstream productivity of many arctic systems[157]. Concentrations of major ions are predicted to increase with permafrost degradation as flow paths become less confined to upper, organic rich layers and move into deeper, mineral-rich subsurface material[158–160]. The Arctic may change from a surface to subsurface dominated system[161], affecting geochemistry of waters that eventually discharge to surface water systems.

Of further concern are the large stores of carbon found within permafrost[162]. However, there is uncertainty in how degrading permafrost influences DOC concentrations in arctic rivers. Some studies expect DOC to decrease with permafrost degradation due the exposure of mineral soils and increased adsorption[158,160] or from increased subsurface transit times and microbial mineralization[163]. Further, increased subsurface contributions resulting from permafrost thaw in the Yukon and Alaska decreased DOC export, as well as altered DOC quality[121,123]. Alternatively, DOC loading has increased with time in circumpolar rivers draining into the Arctic Ocean due to climate change[164]. Large amounts of carbon within permafrost may be released with permafrost thaw, as observed in Siberia[15,28,29]. Within the Mackenzie watershed, NT, thawing permafrost has led to increased DOC export over time[132], while monthly summer DOC fluxes have increased in the Yukon River Basin[122]. There is much uncertainty over the response of permafrost to a warming climate and the role that DOC plays.

Many studies have focused on the export of nutrients from large rivers into the Arctic Ocean, generally in areas draining an ice-rich subsurface where slumping and thermokarst processes may be responsible for increased nutrients within rivers. The overall objective of this study is to provide a better understanding of how three rivers near Yellowknife, NT, are responding geochemically and hydrologically to a changing climate, as well as determine local baseline conditions and natural variability. This will be accomplished with two specific objectives: 1) determine if there are significant changes to hydrologic discharge, solute concentrations, and geochemical fluxes over time in three rivers near Yellowknife, NT, and 2) quantify changes to local climate and whether these changes are reflected in the geochemical record in these rivers.

2.2 Site Descriptions

The Yellowknife, Cameron, and Marian Rivers all drain into the northern end of Great Slave Lake, NT (Figure 2.1). These rivers were chosen for this study as they have long-term records of water quality and discharge that represent two prominent ecozones in the NT. In addition, the Yellowknife and Cameron rivers drain a similar ecozone but differ in watershed area, providing a scale-component to this study. The Yellowknife and Cameron rivers drain the Taiga Shield ecozone (basin area: 19,353 km^2 and 3,630 km^2, respectively), while the Marian River flows between the Taiga Shield and Taiga Plains ecozones (basin area: 23,608 km^2). The Taiga Shield is underlain with Precambrian bedrock, till deposits, eskers, and peat plateaux[165] while the Taiga Plains is comprised of extensive peatlands and till plains[166]. Both are below the treeline. In the NT, permafrost extent ranges from sporadic and discontinuous in the south, to continuous in the north[5,167]. Extensive discontinuous permafrost is found around Yellowknife in areas with forested systems, whereas increased bedrock exposure results in sporadic discontinuous areas[168]. Hydrologic flow in the Taiga Shield follows a subarctic nival flow regime, characterized by highest flows during spring due to snowmelt, followed by a gradual decline to baseflow during the winter[169]. The area around Yellowknife is hydrologically characterized by a series of lakes connected by wetlands and streams, where flow through the system can be defined as a 'fill-and-spill' system[170].

2.3 Methods

2.3.1 Data Collection

Historical daily climate data were retrieved online from Environment Canada (http://www.climate.weather.gc.ca). Mean daily temperature (°C) and total daily precipitation (mm) were taken from the Yellowknife Airport Station #1706 (from 1942 to 2013) and Station #51058 (from 2013 to 2016). Daily data were aggregated into monthly and yearly averages. Hydrological data were taken from the WaterOffice Government of Canada (http://wateroffice.ec.gc.ca), for the Yellowknife and Cameron rivers. Currently, there is no gauging of the Marian River.

Water samples were collected once a month between 1985 and 2013 by the Northwest Territories Water Resources Division, Environment Natural Resources, Government of Northwest Territories. Depending on season, water was collected from shore in open water, or from an auger hole in the middle of the river during winter. Collection from the Marian River began in September 1997. In-field parameters include pH and specific conductivity. The sample was kept in a cooler until same-day filtering was completed at the Taiga Environmental Laboratory, Yellowknife, NT. Field and travel blanks were included.

All samples were run by the Taiga Environmental Laboratory where data were quality-checked as received. Samples were run for cations (potassium, K^+; sodium, Na^+; calcium, Ca^{2+}; magnesium, Mg^{2+}), anions (chloride, Cl^-; sulphate, SO_4^{2-}; alkalinity), nutrients (ammonia, NH_3; nitrate plus nitrite, $NO_3^-+NO_2^-$; total phosphorus, TP; DOC), and other parameters (total dissolved solids, TDS). It is estimated that quality assurance/quality control samples accounted for ~20% of all samples submitted (Robin Staples, GNWT; *pers. comm.*). Any field or travel blank parameter that measured above detection limits were flagged, reviewed, and re-analyzed with samples from the same batch. Values under analytical detection limits were kept in the dataset at the concentration of the detection limit (Appendix A). Any parameters that measured replicates greater than 15% of each other were flagged and reviewed. Re-run values replaced original values. Finally, outliers were flagged if any of the above occurred, or if the value was outside of 1.5x the interquartile ranges. Professional judgement was used to remove outliers if numerous validation tests had failed, or significant field sampling events occurred (i.e: no gloves, high wind).

2.3.2 Statistical Analyses

2.3.2.1 Calculation of Fluxes

Mean annual fluxes for cations, anions, nutrients, and TDS were calculated for the Yellowknife and Cameron Rivers by combining geochemical and hydrological datasets. Fluxes could not be calculated for the Marian River as hydrological data for this river does not exist. All monthly and annual fluxes were calculated using LOADEST [171] via LoadRunner[172]. Briefly, LOADEST runs a number of predefined models to find the best fit for flow and concentration data, then uses that model to calculate the load[171]. To minimize the influence of the linear time functions within LOADEST, monthly concentration data and monthly-averaged discharge data were run using a series of 5-year increments as done by other time-trend analysis of northern rivers[122,132].

2.3.2.2 Significant Trends

Significance of annual and seasonal trends were calculated using the non-parametric Mann-Kendall test for temperature and precipitation averages, seasonal averages in concentration, annual geochemical flux, and hydrologic discharge. Annual concentration data were averaged by season and compared over time. Data were first 'pre-whitened' to remove autocorrelation based on the serial correlation within a time series using the R package 'zyp', then statistically analyzed for significance[173]. Monthly and annual z-scores were also calculated for temperature and precipitation data (Appendix A).

2.4 Results

2.4.1 Climate Data

Mean annual air temperatures near Yellowknife significantly increased during the past 80 years (Sen's slope: 3.2×10^{-2} °C/yr, $p<0.05$; Figure 2.2a), while total annual precipitation increased but not significantly (Figure 2.2b). Monthly average temperatures significantly warmed over the years in the months of January to April, June, and July (Figure 2.3a). Most significant increases were found during winter months (December to April; Sen's slope: 5.0×10^{-2} °C/yr, $p<0.05$), June (3.5×10^{-2} °C/yr, $p<0.05$), and July (2.6×10^{-2} °C/yr, $p<0.05$). The largest range in average monthly temperatures per month were found during winter (November to May), while summers (June to October) exhibited a narrow range in temperatures across years. Total monthly precipitation was

consistent across most months, except for increased values in January (Figure 2.3b). Most precipitation fell from July to September, with lower values from October to June.

2.4.2 Hydrological Data

The Cameron River has a lower discharge than the Yellowknife River (Figure 2.4) but contains similar yields when normalized for watershed area (Appendix A). Large variability in the average monthly discharge between May and August is observed over the three decades, with a greater variability (up to ~5x) in the Cameron River than the Yellowknife River. Average monthly discharge for the Cameron River did not significantly change over the three decades other than a decrease in August (Figure 2.4a). The Yellowknife River increased in average monthly discharge over time for the months of January to May (Figure 2.4b). No significant change to mean annual discharge was found for either the Yellowknife or Cameron River (Figure 2.5). Distinct seasonal patterns were identified in daily discharge data, illustrated by the timing of peak and low flow periods. Lowest flows from the Yellowknife and Cameron Rivers occurred during winter months (December to April), followed by a rise in the annual hydrograph during spring melt (termed 'freshet'; May to June), peak flow during the summer (July to August), and a gradual decline in discharge during the fall (September to November; Figure 2.6).

2.4.3 Geochemical Concentrations and Loads

2.4.3.1 Cation Concentrations

The Cameron, Yellowknife, and Marian rivers contained similar concentrations of K^+ and Na^+ Figure 2.7a). The Marian River had higher concentrations of Ca^{2+} and Mg^{2+} than either the Cameron or Yellowknife rivers. Lowest concentrations of K^+ and Na^+ in the Yellowknife and Cameron rivers occurred around 1995, followed by an increasing trend annually across all seasons. In the Yellowknife River, significant increases in Ca^{2+} and Mg^{2+} concentrations occurred across all seasons, but only in spring for K^+ and both spring and summer for Na^+ (Table 2.1; Figure 2.7a). All cation concentrations significantly increased across all seasons within the Cameron River. A significant decrease in K^+ occurred in the Marian River during spring.

2.4.3.2 Anion Concentrations

On average, Cameron River Cl^- concentrations were higher than either the Yellowknife or Marian rivers. The Cameron and Yellowknife rivers contained similar SO_4^{2-} concentrations, while

alkalinity was higher in the Cameron than the Yellowknife River. The Marian River had higher concentrations of both SO_4^{2-} and alkalinity compared to all other rivers in the study (Figure 2.7b).

Anion concentrations in the Yellowknife River increased significantly during the spring and summer. Alkalinity increased significantly across years in all seasons in both the Yellowknife and Cameron rivers (Figure 2.7b). Chloride concentrations in the Cameron River increased significantly across years for each season, while SO_4^{2-} increased significantly during the fall and winter. Spring Cl^- concentrations in the Marian River decreased significantly in spring, while SO_4^{2-} significantly decreased in fall. Alkalinity increased significantly during summer.

2.4.3.3 Nutrient Concentrations

All three rivers had similar nutrient concentrations (Figure 2.7c). Overall, average inorganic nitrogen species were slightly higher in the Marian River than either the Cameron or Yellowknife rivers. Lowest DOC concentrations were found in the Yellowknife River compared to either the Cameron or Marian river. Concentrations of TP in the Yellowknife and Cameron rivers were lower than in the Marian River.

All rivers exhibited seasonality in NO_3^-+NO_2^- and TP concentrations, with high concentrations in the fall and winter, and lower concentrations during the spring and summer. Concentrations of NH_3 decreased across all rivers and seasons with time. However, summer NH_3 concentrations in the Marian River increased between 2005 and 2010 (Figure 2.7c). Concentrations of NO_3^-+NO_2^- increased across all seasons in the last ten years among all three rivers. Concentrations of NO_3^- +NO_2^- significantly increased during the fall within the Cameron River, and significantly increased during winter and fall in the Marian River. DOC concentration increased across all seasons within the Yellowknife and Marian rivers, while the Cameron River exhibited no change in concentration with time. Total phosphorus concentrations within the Yellowknife River significantly increased in spring, while winter TP concentrations significantly declined in the Marian River.

2.4.3.4 Other Parameters

Concentrations of TDS were highest in the Marian River, followed by the Cameron River and Yellowknife River (Figure 2.7d). Specific conductivity was highest in the Marian River, followed by the Cameron and Yellowknife river.

Concentrations of TDS significantly increased during the spring in the Yellowknife River and during the fall in the Cameron River (Figure 2.7d). Measurements of specific conductivity significantly increased across all seasons for both the Yellowknife and Cameron rivers. All rivers were neutral to slightly basic. Significant increases to pH were only observed during summer in the Marian River, and in all seasons but winter in the Cameron River.

2.4.3.5 Annual Cation & Anion Loads

The Yellowknife River had higher cation and anion loads than the Cameron River (Table 2.2). Both rivers exported higher loads of Ca^{2+} than the other cations. Although cation loads in the Yellowknife River increased between 1985 and 2013, annual cation and anion loads from the Cameron and Yellowknife rivers did not significantly change over the time period (Figure 2.8a).

2.4.3.6 Annual Nutrient & TDS Loads

Inorganic nitrogen loads were an order of magnitude higher in the Yellowknife River than the Cameron River (Table 2.2; Figure 2.8c). The Yellowknife River exported higher DOC and TP loads than the Cameron River. NH_3 loads did not change over time in the Cameron River, but significantly decreased in the Yellowknife River (Figure 2.8c). NO_3^-+NO_2^- loads in both rivers show no change over time. DOC loads increased over time in the Yellowknife River, but significantly decreased in the Cameron River. TP load in the Yellowknife River have increased with time, but exhibited a decreasing trend since 2005. TP load within the Cameron River gradually decreased over time.

Higher TDS loads are found in the Yellowknife River than the Cameron River (Table 2.2; Figure 2.8d). Annual loads of TDS within the Yellowknife and Cameron rivers increased over time (Figure 2.8d). However, from 2000 onward, annual loads of TDS decreased in the Cameron River.

2.5 Discussion

2.5.1 Changes to Climate & River Flow in the Northwest Territories

Climate can be an important driver of change to arctic rivers, influencing watershed processes and flow pathways[151,152,174]. For instance, warming air temperatures in Sweden led to increased active-layer thicknesses and permafrost degradation[175,176]. Warming temperatures in Yellowknife could influence subsurface contribution to surface water quantity and quality, especially in areas where

discontinuous permafrost continues to degrade. Permafrost degradation has already been found to occur in the area[168], potentially influencing flow pathways; however, insulating peat layers, commonly found around Yellowknife, can limit effects of increased air temperatures upon subsurface processes[168,177]. Annual discharge has not changed in the Yellowknife or Cameron rivers (Figure 2.5), suggesting no clear response between permafrost degradation and discharge in these systems. This may be in part due to the lack of significant increase to total precipitation in the area (Figure 2.3b), potentially coupled with estimated increased evapotranspiration rates across the circumpolar north[164,178]. Rivers in this study drain smaller watersheds and may not be as responsive to a warming climate compared to the previously-studied, larger systems[132,150,151]. Further, the presence of large lakes can attenuate streamflow to reflect a prolacustrine regime[148], which could minimize or dampen the effects of hydrologic changes associated with permafrost degradation. Although temperatures are warming in the area, there appears to be no significant change to the amount of water draining these systems over the time record.

Changes to temperature and precipitation around Yellowknife during the past seven decades did not occur uniformly over the yearly cycle (Figure 2.2). Increased winter temperatures and increased precipitation around the late summer and fall are similar to studies predicting a seasonal regime shift in the area[148,153]. This shift can enhance winter streamflow by increasing late-season hydrologic storage by soils and lakes, and is observed in the significant increase in average monthly winter discharge within the Yellowknife River (Figure 2.4b). Annual discharge of the Cameron River showed no significant change during the past seven decades and contradicts previous findings of significant increases to both winter base flow and mean annual flow[14]. These increases were linked to enhanced permafrost degradation in the watershed that resulted in increased subsurface capacity during winter. The discrepancy between trends in this study and the work of St. Jacques and Sauchyn[14] lies in the time periods being considered, as the previous dataset ended in 2007 during an upward trend in discharge. More recent measurements of discharge (2008 to 2014) show an annual decline. Results from this study provide evidence of enhanced base flow during winter months within the Yellowknife River, but also highlight the importance of long-term monitoring to acknowledge influences of cyclic processes on flow in northern watersheds.

2.5.2 Geochemical Response in the Yellowknife, Cameron, and Marian rivers

Geochemical differences between rivers can be attributed to underlying geology and watershed characteristics. The Yellowknife and Cameron rivers drain the Taiga Shield, which consist of shallow glacial tills and Precambrian bedrock [165,179], while the Marian River flows between the Taiga Shield and Taiga Plains. The Taiga Plains are comprised of deeper glacial tills and calcareous soils[166] and are relatively easier to erode than the Precambrian igneous bedrock, resulting in higher concentrations of dissolved Ca^{2+}, Mg^{2+}, SO_4^{2-}, alkalinity, and TDS in the Marian River. Similarity among trends in cation and anion concentrations between the Yellowknife and Cameron rivers, compared to the Marian River, reflect the role watershed characteristics have upon water quality.

With no change to annual discharge in the Yellowknife River, positive Sen-Thiel slopes in loads, although not statistically significant, for most constituents indicate increased export of solutes from the watershed. Increases to solute fluxes were observed in the Yukon River Basin and Mackenzie River and linked with increased active-layer thicknesses and enhanced weathering[122,132]. Similar patterns are seen in the Yellowknife River; however, not at the significance found in these larger systems. Watersheds underlain with ice-rich permafrost are susceptible to thermokarst processes that can release large amounts of particulate and dissolved materials to surface waters[154,180,181], which may result in a more pronounced response than in rivers draining ice-poor areas. Regardless, results of increased solute fluxes are similar to other studies that have identified the influence of permafrost degradation on river geochemistry[161,182].

Increased active-layer thicknesses and permafrost degradation can result in two water quality scenarios: 1) flow pathways deepen into mineral layers and enhance the export of inorganic solutes while decreasing DOC concentrations[183], or 2) organic-rich layers become unfrozen and increase the release of organic carbon and nutrients[184]. Although data in this study cannot identify a singular factor like permafrost degradation, increasing trends in solute concentrations and increasing NO_3^-+NO_2^- loads are evidence of changing water quality. The lack of change in DOC concentration concurrent with increases to inorganic solutes corroborates the idea that flow pathways are deepening into mineral-rich layers. Further, as there are no significant increases to total precipitation, changes in concentrations and fluxes would be more representative of subsurface flow pathways responding to warming air temperatures on the Taiga Shield.

Changing flow pathways in the sub-arctic can alter seasonal water chemistry. Increased winter baseflow and solute concentration within the Yellowknife River could result from enhanced soil and lake storage before freeze-up. This has been found to be responsible for fueling increased winter streamflow and solute, nutrient, and DOC export in the area[140,153]. Buildup of inorganic nitrogen during the winter within subarctic lakes may provide a source for increased annual nitrate and nitrite fluxes while annual discharge remains static. Further, recent (>2010) increases to NO_2^-+NO_3^- concentrations during the fall and winter, concurrent with stable TP concentrations and decreased TP loads (Figure 2.7c, Figure 2.8c) suggest there is no increase in river productivity to take up extra nitrogen. The fall and winter represent seasons of decreased productivity due to colder temperatures and less light, thus enhanced contributions of inorganic nitrogen may accumulate. Nutrient limitation and changes to food webs can result from permafrost-thaw induced changes to nutrients and DOC within Alaskan thaw lakes[182]. These rivers exhibit similar changes and indicate that they may not be able to compensate for higher nutrients, especially as TP loads, an important nutrient that can limit microbial activity, have decreased since 2005 (Figure 2.8c). Hence, productivity within these rivers may not be able to reduce future increases to inorganic-nitrogen.

Sporadic and sudden environmental events can impact water quality. Wildfires occurring in the boreal forest, especially the NT, have increased in severity and occurrence[185,186]. Wildfires result in increased exports of nutrients and major ions from a boreal and mixed-conifer watershed[187,188] and can decrease DOC loading among arctic rivers[164]. Large fires have occurred in the Yellowknife and Cameron watersheds in 1998 and 2014, while the Marian River watershed experienced fires in 2008 and 2014[189]. Although the scope of this paper was not to identify wildfire effects upon water quality, long-term datasets may reflect these effects via higher summer concentrations of inorganic nitrogen and DOC after wildfires (Figure 2.7).

2.5.3 DOC in the Northwest Territories

In terms of the global carbon cycle, much uncertainty surrounds the response of carbon stocks as northern watersheds begin to warm and expose previously-frozen carbon within permafrost. In watersheds underlain by carbon-rich permafrost, DOC export during spring contained higher contributions of recently-fixed carbon, whereas late summer to winter flows contained a greater amount of old carbon derived from a deepened active-layer and permafrost degradation[30,96,125,190]. DOC concentrations found in this study are comparable to DOC concentrations in other

permafrost-affected streams[191] but no significant change in concentration is found in any river over time (Figure 2.7c). Increased concentrations and fluxes of major cations and anions suggest that if permafrost degradation in the area is leading to enhanced subsurface flow, these flow pathways may be travelling through inorganic, till layers, rather than mobilizing permafrost-derived DOC.

High DOC concentrations in streams and rivers have been correlated to a higher percentage of wetlands or peatlands in a watershed[192,193]. However, the presence of permafrost in the northern half of West Siberia reduced the export of high DOC concentrations from high-organic environments[28]. Further, it was determined that a mean annual air temperature above -2°C represents a threshold where higher DOC concentrations are exported from peat-derived watersheds. Within the NT, mean air temperatures exceeded this threshold in 1998, and have been close-to or surpassed this limit during the past decade (Figure 2.2a). A large area of the NT contains organic-rich permafrost[194] that may export higher DOC loads as temperatures continue to meet or exceed this threshold. Further, climate driven changes to hydrologic flow pathways have the potential to connect previously-isolated bogs[174], further enhancing the susceptibility of high-organic areas around Yellowknife to increase DOC export. Hence, the increasing trend in mean annual air temperatures around Yellowknife signifies the potential for increasing DOC loads from these areas.

2.5.4 Baseline Conditions

Long-term records of water quality and discharge can be used to define 'baseline' conditions for the area. Baseline conditions of river concentrations and export for the whole NT cannot be completely defined using only three rivers presented here; however, relative changes in water quality over time provide an opportunity to assess how local and similar sub-arctic rivers may respond. Although not significant, the steady increase to the load of major cations, anions, and all nutrients (except NH_3) within the Yellowknife River suggests that annual baseline conditions may be beginning to change. Importantly, increasing winter temperatures and increasing average winter discharge result in a dynamic baseline for the Yellowknife River. Based on concentration data for the Marian River, increases to alkalinity, and more recently nutrients, suggest enhanced weathering in the watershed, similar to other Mackenzie Basin systems[132,195]. The baseline for the Cameron River is more easily defined due to relatively unchanging annual discharge and solute fluxes. Analyses of these three

rivers shows the importance of year-long monitoring to compare how different rivers in ice-poor systems respond to a warming climate.

2.6 Conclusions & Future Trends

Long-term meteorological and water quality records of three rivers around Yellowknife indicate a geochemical response to a warming climate. Temperatures have significantly increased during the past 80 years, while average annual discharge for the Yellowknife and Cameron rivers show no significant change. Instead, the magnitude of solute and nutrient export into Great Slave Lake are determined by variations in the monthly average discharge, more-so than the uni-directional change over time. Hence, changes to discharge will dictate the load of dissolved constituents into Great Slave Lake rather than slight changes to concentration. Combined results of increasing solute concentrations, increasing cation fluxes, and stable DOC concentrations suggest an increasing contribution from mineral-rich subsurface flow pathways, altering water quality over time. Results show how increased inorganic nitrogen export during the winter, previously observed within smaller catchments[153], can be observed in larger systems. However, the lack of increasing river productivity may result in the continual increase in nutrients. Geochemical and hydrological analyses of the Yellowknife, Cameron, and Marian rivers find the importance of annual variability and enhanced subsurface flow pathways play an important part dictating water quality in the NT.

Defining baseline conditions in these rivers allows for a determination of impacts upon water quality and quantity resulting from future resource development or a warming climate. Static baseline conditions are difficult to define in the Yellowknife River due to increasing cation concentrations and increasing winter discharge. Cameron and Marian River geochemical and hydrological baselines were more simple to define due to the relatively unchanging annual discharge and geochemical flux within the Cameron River, and lack of geochemical trends in the Marian River.

Northern rivers will continue to change given future climate scenarios of increased temperatures and changes to precipitation regimes[196,197]. Future work could focus on specific years that reflect future conditions (i.e. dry summers or wet falls) to understand the geochemical response within these three rivers. Further, discharge-solute relationships (Appendix A) could be further explored to create discharge-solute relationships to predict exports of certain constituents into Great Slave Lake. In terms of environmental consequences to a changing climate, subsurface warming could

result in increased risk of contaminating freshwater sources from anthropogenic activities as municipal and industrial waste can be mobilized into sources via permafrost degradation[107,198]. Enhanced export of nutrients due to permafrost thaw could have similar results to thaw-induced slumping in small lakes, such as increasing biological productivity[127]. Increased temperatures may also enhance peatland carbon decomposition, enhancing the export of DOC and nutrients into Great Slave Lake. The rate and magnitude of these processes are still uncertain; however, changes to water quality observed in these three rivers over the past three decades suggest a variable but uni-directional geochemical response to a warming climate.

TABLE 2.1: Summary of the Mann-Kendall statistical analyses on concentrations of various water quality parameters over time for different seasons in the Yellowknife (YK), Cameron (CAM), and Marian (MAR) rivers. Shapes represent the river, size of symbol represents the significance, and colour represents the direction of the trend.

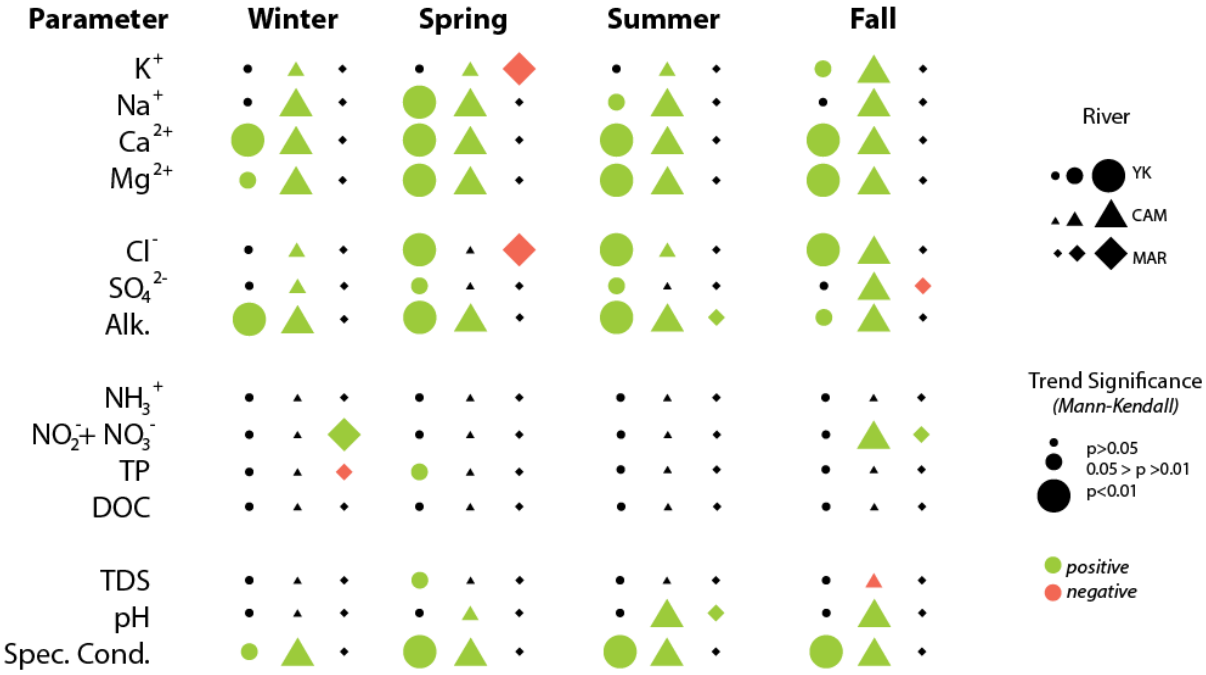

TABLE 2.2: Average annual loads for various chemical parameters for the Yellowknife and Cameron rivers, Northwest Territories, Canada. Included are 1-standard deviation (σ) and total number of values (*n*). Alkalinity is measured as total concentration as $CaCO_3$.

	Yellowknife			Cameron		
Parameter	*Avg (Gg/yr)*	*σ (Gg/yr)*	*n*	*Avg (Gg/yr)*	*σ (Gg/yr)*	*n*
K^+	1.2	0.5	27	0.2	0.1	29
Na^+	2.2	1.1	27	0.5	0.2	29
Ca^{2+}	6.6	3.0	27	1.8	0.9	29
Mg^{2+}	2.4	1.1	27	0.5	0.3	29
Cl^-	2.2	0.9	27	0.5	0.3	29
SO_4^{2-}	4.2	1.7	27	0.9	0.5	29
Alkalinity	23	10	26	5.7	2.8	29
N-NH3	1.6E-02	1.1E-02	24	2.0E-03	9.2E-04	22
$N\text{-}NO_3^-+NO_2^-$	4.5E-02	1.9E-02	24	5.2E-03	3.2E-03	19
TP	1.5E-02	9.1E-03	24	2.7E-03	2.3E-03	19
DOC	6.5	2.8	27	1.6	0.7	19
TDS	40	17	27	9.9	5.4	22

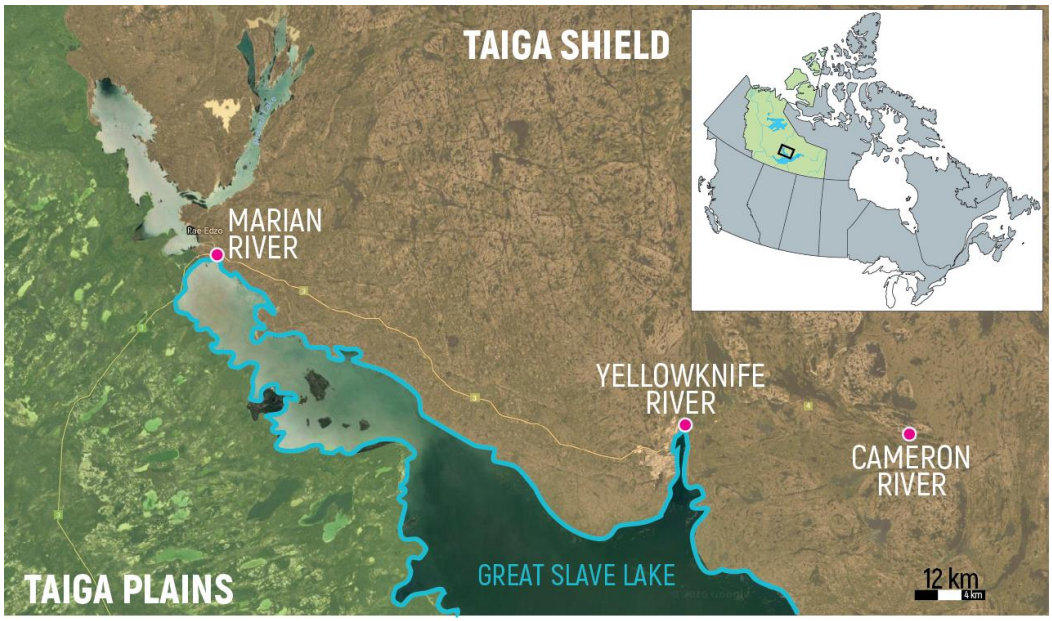

FIGURE 2.1: Sampling locations for the three rivers and their geographical location. Different ecozones are shaded (green: Taiga Plains; orange: Taiga Shield).

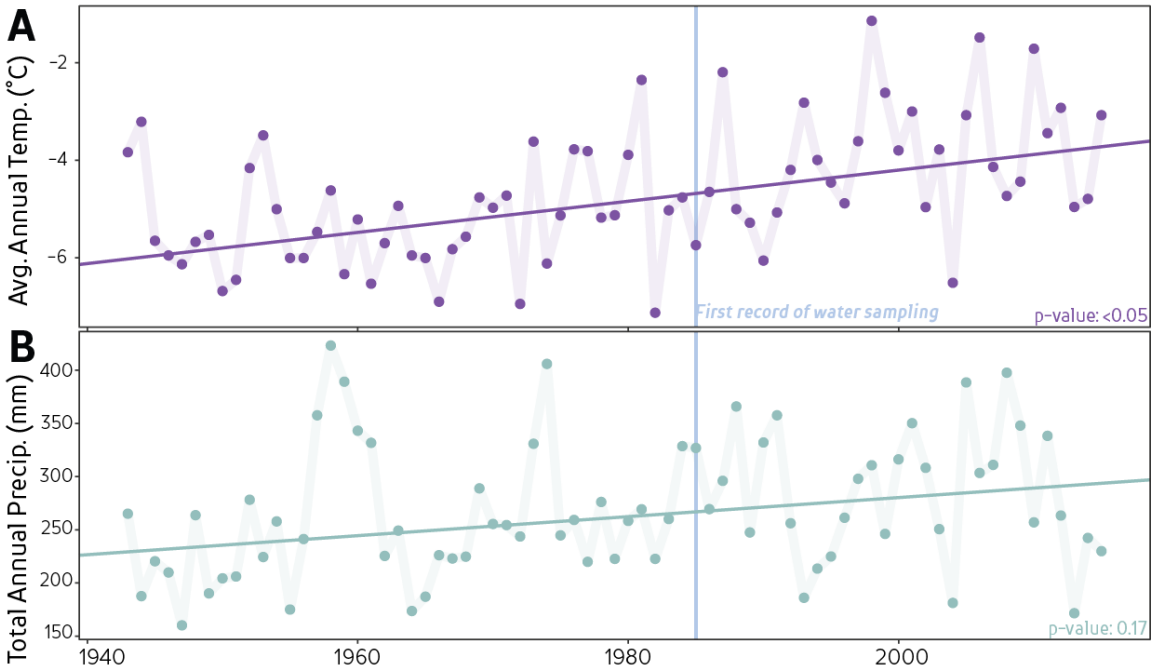

FIGURE 2.2: Average annual air temperature (A) and total annual precipitation (B) for the city of Yellowknife, NT. Included are linear regressions through the entire time period, as well as the beginning of water sampling (blue vertical line). Significance in the trend is determined using a Mann-Kendall test.

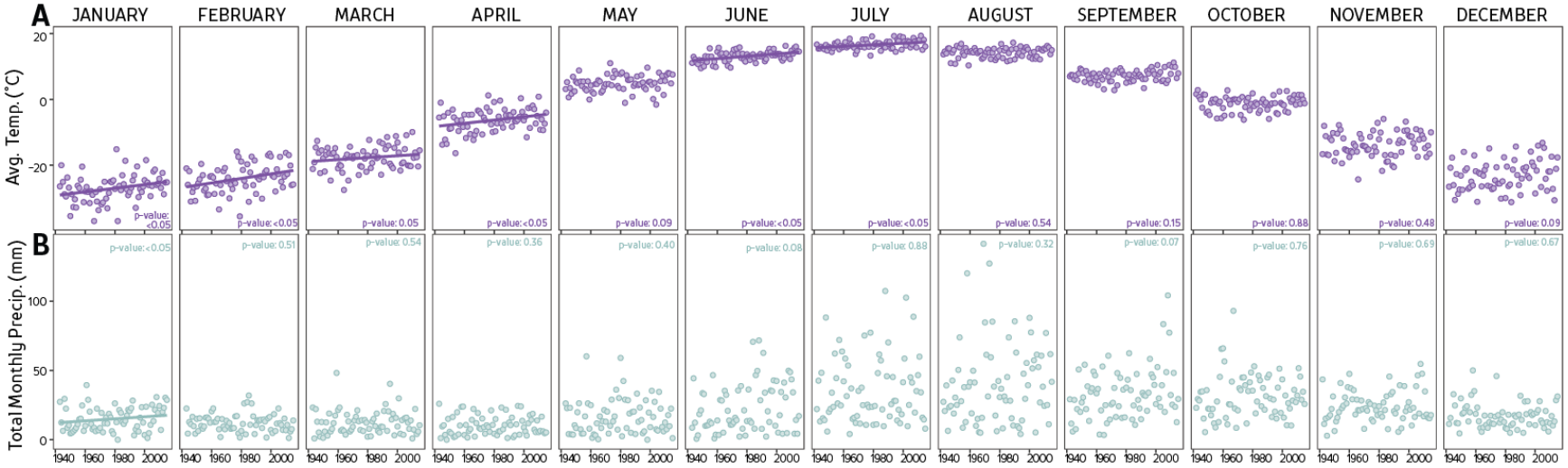

FIGURE 2.3: Average monthly temperature (A) and total monthly precipitation (B) per year for the city of Yellowknife, NT. Lines represent significant monotonic changes (Mann-Kendall) over the time period.

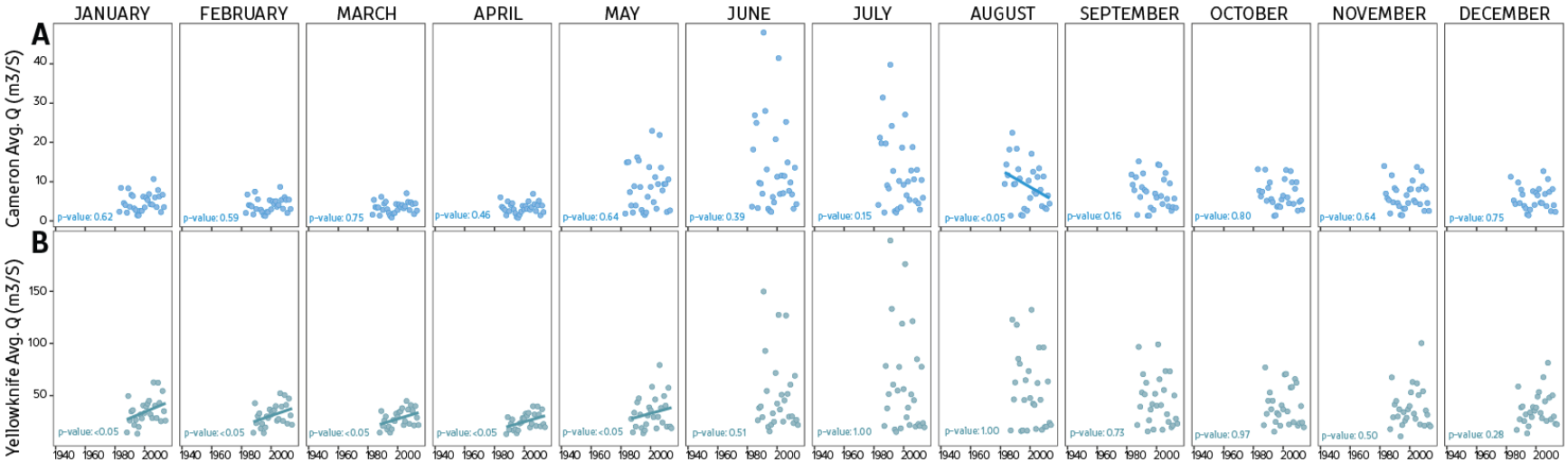

FIGURE 2.4: Average monthly discharge for the Cameron (A) and Yellowknife (B) rivers over time. Lines represent significant monotonic changes (Mann-Kendall) over the time period.

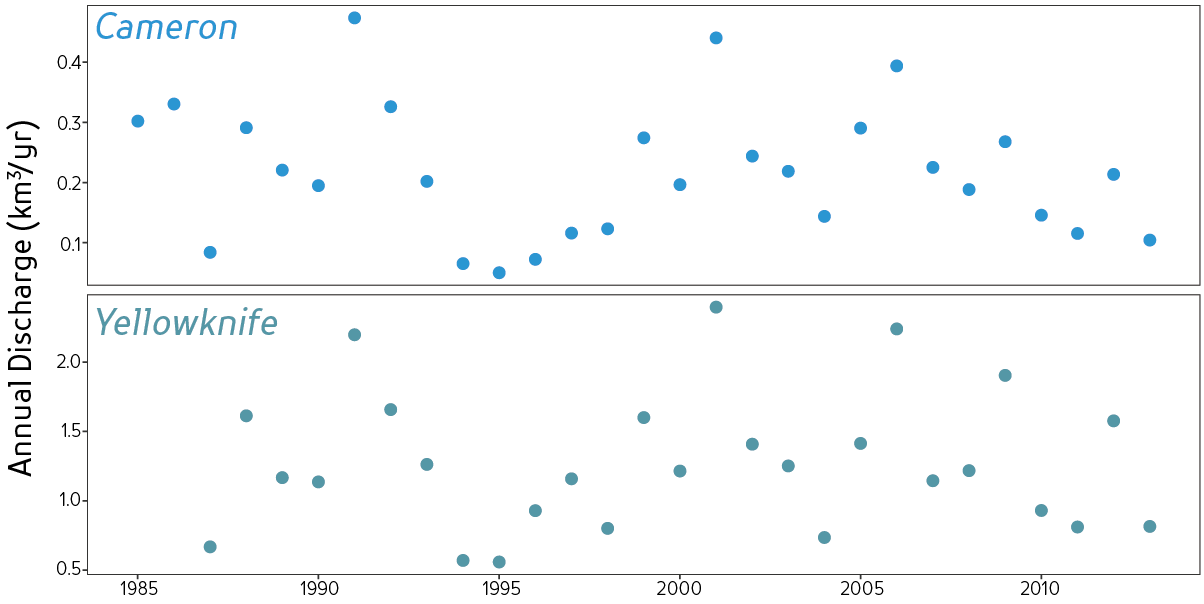

FIGURE 2.5: Average annual discharge for the Cameron (top panel) and Yellowknife (bottom panel) rivers.

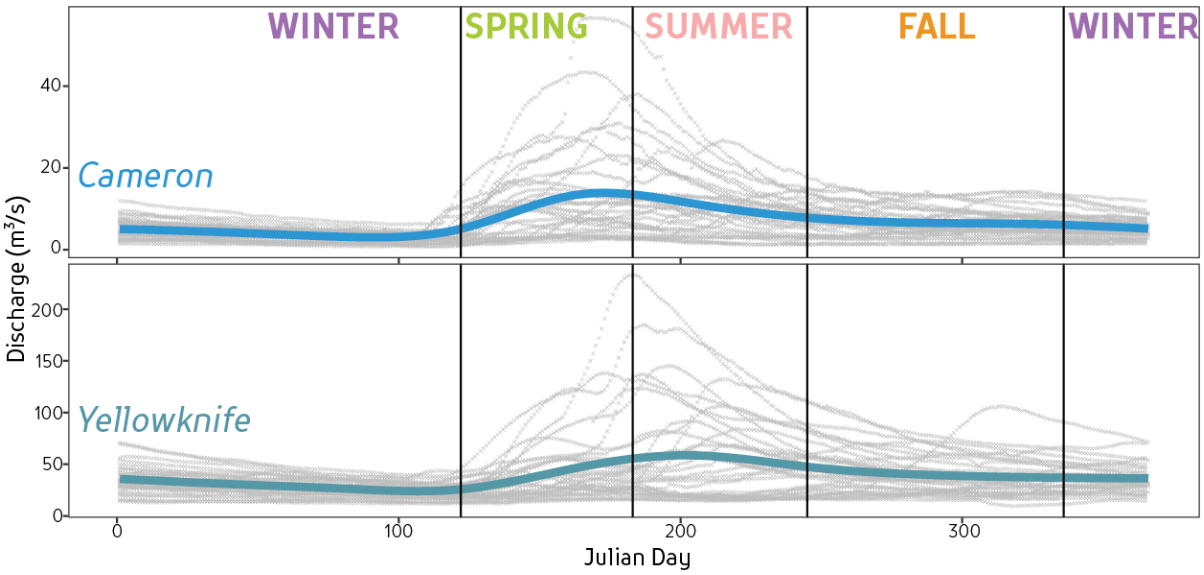

FIGURE 2.6: Daily average discharge for the Cameron (A) and Yellowknife (B) rivers. Light grey points indicate individual data points for different years, while solid coloured lines represent averages on each day. Included are divisions for each season based on the hydrograph.

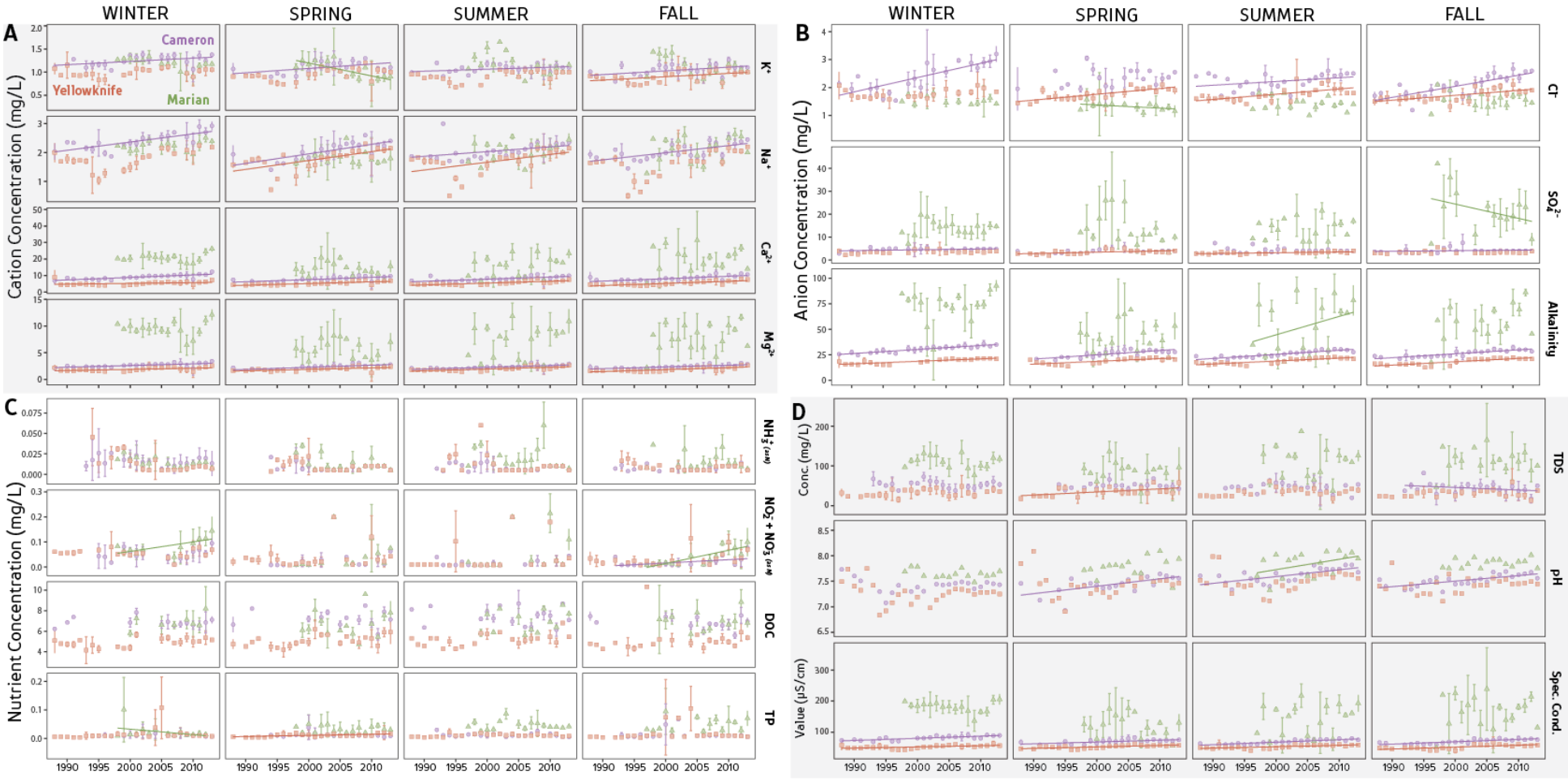

FIGURE 2.7: Season-averaged concentration for cations (A), anions (B), nutrients (C), and other parameters (D) for the Yellowknife (red square), Cameron (purple circle), and Marian (green triangle) rivers over time. Each data point is an average for the months included in that season for that year. Lines represent significant trends over the time period (Mann Kendall).

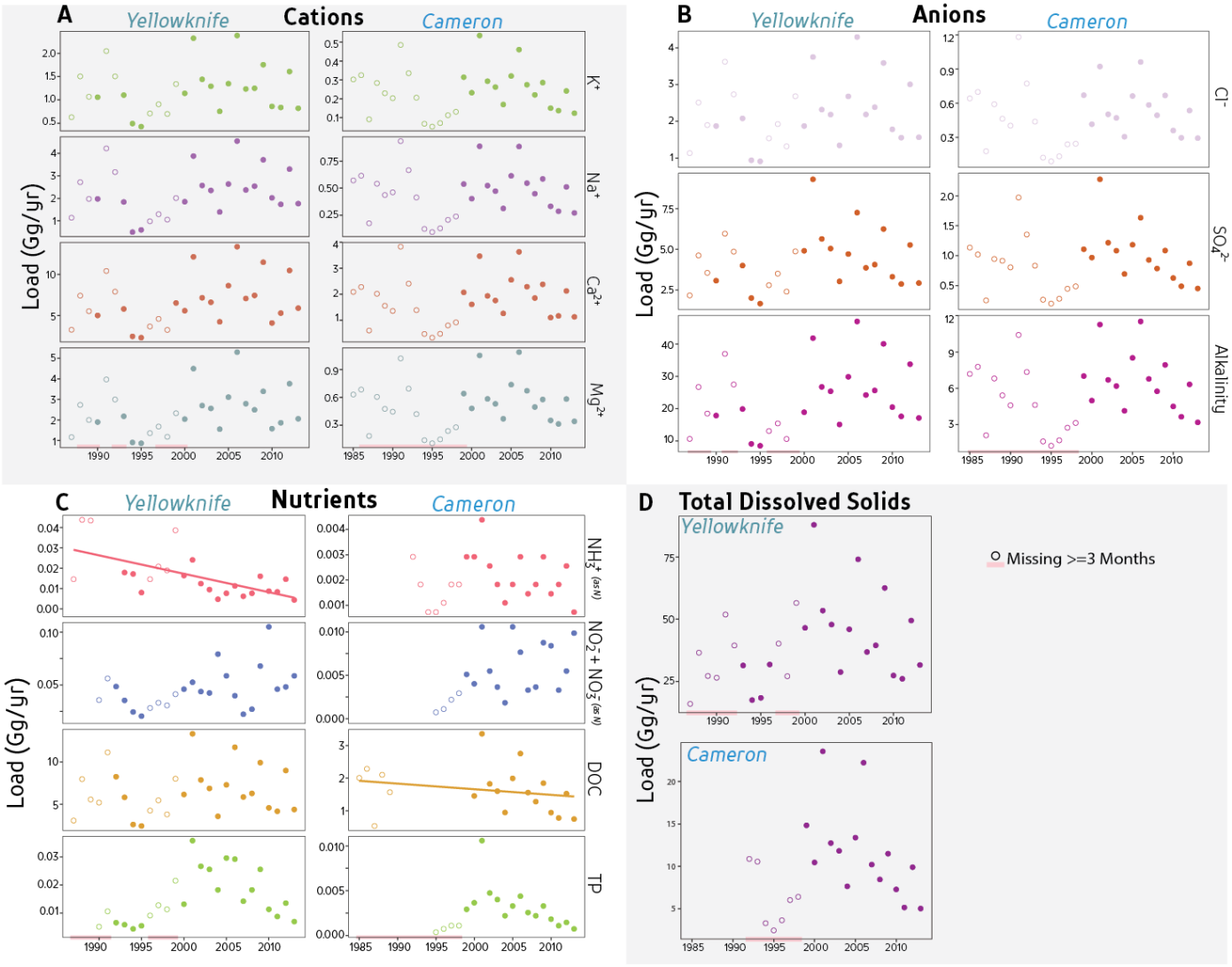

FIGURE 2.8: Calculated annual loads for cations (A), anions (B), nutrients (C), and total dissolved solids (D) in the Yellowknife and Cameron rivers. Hollow symbols represent years that were missing three or more months of data. Lines represent significant trends over the time period (Mann Kendall).

Chapter 3
Visualizing Dissolved Organic Matter Using Common Composition Metrics across a Variety of Canadian Ecoregions

3.1 Introduction

Dissolved organic matter (DOM) is a ubiquitous component of terrestrial and aquatic environments and an important determinant of overall water quality. For example, DOM dictates thermal and pH regimes within lakes[55], complexes with and mobilizes metals[61], and acts as an important redox constituent for biogeochemical reactions[58]. Further, DOM affects drinking water quality through taste, odour, and colour[65], and reacts with chlorine during drinking water treatment processes to form carcinogenic disinfection by-products[67]. The overall reactivity of DOM is determined by its mixture of thousands of organic molecules with differing structural and chemical characteristics. Increased DOM concentrations in surface waters have been observed across the United Kingdom, Europe, and North America[55,89] and have been linked with declines to water transparency[55,92]. These changes can have significant effects upon future drinking water treatment options[66,102], yet little information is found on how DOM composition changes[141]. Hence, quantifying changes to the amount and composition of DOM across temporal and spatial scales allows for a better understanding of future changes to DOM and its influence upon water quality.

Measures of DOM concentration and composition are used to identify source, quality, and fate of DOM within the environment. The overall DOM concentration is operationally defined as the concentration of carbon molecules passing through variable filter sizes (generally between 0.2 and 0.7 μm). Compositional measures commonly used include ultraviolet or visible light absorbance[71,73,199], fluorescence[70,72], elemental ratios[77], molecular weight and size[75], and mass spectrometry[79,80]. Differences in DOM composition have been used to quantify hydrologic mixing and changes to redox potential[200]. Differences in DOM absorbance parameters have been useful for tracking changes to DOM composition within riverine systems[73] and coastal wetlands[200], but can be susceptible to interference from other molecules within the sample, such as nitrate or iron[71,74]. Corrections for such interference are dependent upon DOM quality, so there is circularity if corrected and subsequently used to infer quality[201]. Thus, use of various characterization techniques can provide an holistic representation of the components that comprise DOM.

Dissolved organic matter is the net representation of varying sources and degrees of processing at that point within the watershed. Climate, hydrology, land cover, and nutrients have all been found to influence lake DOM composition[49–51,202]. Quantifying changes to DOM composition along a hydrologic continuum can provide information on dominant sources or processes that influence DOM evolution[203]. Laboratory experiments have been used to isolate specific DOM compositional changes resulting from either microbial or photolytic degradation[83,204]. Catchment-scale observations of DOM composition have identified a gradient along the aquatic continuum where soil-derived aliphatic components of DOM are preferentially lost as water moves from subsurface to surface waters. Here, aromatic, high-nominal oxidation state DOM becomes further degraded along the fluvial network to more aliphatic, low nominal oxidation state DOM[79,81]. Increased degradation and processing of DOM along a system reduces its chemodiversity, with persistence of specific components linked to the original DOM composition[50,81,205]. Hence, compositional measures provide quantitative information along the aquatic continuum that could be used to trace the evolution or reactivity of DOM.

Recent progress in the understanding of DOM and carbon cycling has led to a change in the importance of characterizing DOM composition. Specifically, the conceptualization of the genesis of soil organic matter (SOM) is undergoing a paradigm shift. Previously, it was thought that SOM within subsurface environments would continually evolve towards recalcitrant forms that were resistant to further degradation. Recent findings view organic matter as a continuum of decomposed and re-generated components that can be protected from further alteration by the surrounding soil and mineral matrix[206–208]. Further processing enhances the solubility of SOM, transporting large volumes of labile, microbial-derived carbon into aquatic systems. Once in the aquatic system, differences in DOM properties and composition, or intrinsic controls, are thought to dictate DOM fate more-so than extrinsic controls such as temperature, nutrients, sunlight exposure[81]. Modelling of the rates at which microbes process DOM in surface waters have included approaches that treat DOM as a heterogeneous mixture of compounds with varying decay rates, rather than a 0- or 1-order rate[209–211], allowing for specific DOM components to dictate overall degradation kinetics. Hence, understanding kinetics and fate of DOM is closely linked to quantifying and comparing compositional changes over spatial and temporal scales.

Comparison of different DOM measures have generally focussed on single hydrological environments (i.e. solely lakes) or one or two measures across spatial scales and varying

environments. More recent studies have looked to pair optical properties with advanced compositional methods[79,80]. The use of various and complimentary measures of DOM composition can provide a better characterization of DOM among samples. There are various options to characterize DOM within the environment, but many are expensive, require complicated analysis, or are not accessible. For instance, Fourier-transform infrared spectroscopy (FTIR) analyses provides insightful and novel information on DOM composition[79,80] but is not readily available. Although fluorescence and subsequent parallel factor analyses (PARAFAC) are commonly used to characterize DOM, we chose to focus on a variety of available UV-visible light absorbance parameters. The objective of this study is to use a relatively simple suite of DOM characterization techniques from surface and subsurface environments to determine which parameters explain the most variability within a DOM dataset from various ecoregions across Canada, and use these parameters to create a simple, effective tool to compare compositional differences in DOM. This will be accomplished in three parts: 1) determine which measures of DOM composition explain the most variability, 2) identify how these measures relate to DOM quantity and site, and 3) create a new visualization tool to easily compare different DOM samples based upon these composition measures.

3.2 Methods

3.2.1 Sites & Sampling

Locations were selected where DOM was expected to differ due to differences in surrounding watershed characteristics (e.g. land use, climate, and vegetation). Surface and subsurface samples were collected from the Northwest Territories (Yellowknife, Wekweètì, Daring Lake), Nunavut (Lake Hazen Watershed), and Ontario (IISD-Experimental Lakes Area) (Figure 3.1; Appendix B). Surface water samples included lakes, rivers, creeks, and ponds, and were collected 0.25 m below the surface. Subsurface samples from northern locations (Yellowknife, Wekweètì, Daring Lake, Lake Hazen) were collected from the deepest extent of the active-layer, just above the permafrost boundary (0.1 to 0.5 m below surface). Additional samples were collected at Turkey Lakes Watershed (ON), Nottawasaga Valley (ON), Grand River (ON), Mackenzie River (NT), and Black Brook Watershed (NB), but were only measured for overall DOM concentration and select composition measures.

Surface water samples were collected using a 60 mL syringe and filtered using 0.45 µm syringe-tip filter (Whatman GD/X 45mm) into 40 mL pre-washed glass vials. Subsurface samples were collected using a peristaltic pump with an attached 0.45 µm syringe-tip filter. Vials and filters were pre-rinsed with filtered sample water before collection. Samples were kept cool (<4°C) and in the dark until analysis within three weeks of collection.

3.2.2 DOM Quantity & Composition Analyses

Dissolved organic carbon and total nitrogen concentrations were measured using the Shimadzu Total Organic Carbon (TOC-L) Combustion Analyzer with TNM-1 module. Dissolved organic nitrogen (DON) was calculated as the difference between total dissolved nitrogen concentration and sum of the inorganic nitrogen species (nitrate, nitrite, and ammonium). Inorganic nitrogen species were measured using SmartChem 200 Automated Chemistry Analyzer (Unity Scientific, MA United States).

Absorbance was measured using a Cary 100 UV-VIS Spectrophotometer (Agilent, CA United States) at 5 nm increments from 200 to 800 nm. Deionized water was used to zero the machine, and was run intermittently during analyses to correct for baseline drift. The Naperian absorption coefficient (a; m^{-1}) was calculated using:

$$a_\lambda = \frac{ln(10) \times A_\lambda}{L}$$

where A is the baseline-corrected absorbance at wavelength λ and L is the cell length (m). A suite of absorbance characteristics were then calculated (Table 3.1).

DOM composition was determined using a size exclusion chromatography technique (Liquid Chromatography – Organic Carbon Detection, LC-OCD[75]), at the University of Waterloo. Briefly, the sample was diluted to within 1 – 5 mg C/L and injected through a size-exclusion column (SEC; Toyopearl HW-50S, Tosoh Bioscience) that separated DOM based on hydrodynamic radii into five hydrophilic fractions (from largest to smallest): biopolymers (BP; polysaccharides or proteins), humic substances fraction (HSF; humic and fulvic acids), building blocks (BB; lower weight humic substances), low molecular weight neutrals (LMWN; aldehydes, small organic materials), and LMW-acids (LMWA; saturated mono-protic acids). Based on elution time, a number average molecular weight was derived only for the HSF. Duplicates run at six concentrations yield a precision for the LC-OCD of less than ±0.09 mg C/L for all fractions. Concentrations of each fraction were calculated

using specialized software (ChromCALC, DOC-Labor, Germany) that integrated chromatograms from the LC-OCD.

3.2.3 Statistical Analyses & Composition Wheel Design

Data were analysed using unconstrained ordination analysis via principal components analysis (PCA) on a subset of samples that contained all composition measures (n=130). Data were scaled before PCA, and analysed using R Statistical Software[212].

A Composition Wheel (CW) is a representation of various composition measures using a polygon. Differences in shape can be easily used to compare different DOM compositions. Composition Wheel parameters were chosen based on the highest contribution of variables explaining the first two principal component axes (Appendix B). Further, independent measures of DOM composition were chosen to minimize overlap in information between similar techniques. Each Composition Wheel axis corresponds to a specific parameter. For each axis, the individual value for each sample is normalized as a value between the maximum and minimum encountered for that parameter in the dataset.

3.3 Results

3.3.1 DOM Concentration & Composition

DOM concentrations ranged from 0.1 to 273 mg C/L, with highest mean values in subsurface, pond, and creek samples (Appendix B). Highest DOM concentrations were found from subsurface environments in Yellowknife, while the lowest concentrations were found in high arctic environments (Figure 3.2). High arctic seeps, rivers, and lakes contained the lowest average DOC:DON values, but higher average specific ultra-violet absorbance at 255 nm (SUVA) and HSF values than other locations. SUVA values ranged from 1.1 to 21 L/(mg·m) and were similar between ponds, lakes, and rivers. Highest SUVA values were found from the bottom of a boreal lake and high arctic subsurface. Spectral slope values ranged from 0.005 to 0.032 nm^{-1}, and were highest in high arctic surface waters. Values of DOC:DON ranged between 9 to 124, and were lowest in rivers and samples from high arctic sites. Proportion of humics (HSF) ranged from 14% to 85%, and on average were lowest in lakes. Overall, subsurface samples contained the highest SUVA and DOC:DON values, and lowest $S_{275\text{-}295}$ and HSF values. Hence, DOM concentration and composition vary across geographic scales and hydrological environments.

3.3.2 PCA on DOM Composition

The first three principal component axes explained 61% of the variance in the dataset, with PC1 and PC2 accounting for 51% of the variability. Comparison of the first two principal components yield four distinct groupings of strongly-contributing measures: I) SUVA, SAC_{420}, SAC_{350}; II) HSF, HS MW; III) $S_{275-295}$, E_2:E_3, and S_R; and IV) BB, LMWN, and BP. Groups I and II were negatively associated to groups III and IV. Highest contributions to PC1 and PC2 axes were HSF, SAC_{350}, $S_{275-295}$, and SUVA. Variables with contribution to PC1 and PC2 lower than 2% were E_4:E_6, DOC:DON, $S_{350-400}$, and LMWA (Appendix B). Absorbance parameters normalized to DOM concentrations (SAC_{350}, SAC_{420}, and SUVA) all plotted closely to each other and trended positively with measures of HSF, HSF molecular weight, and DOC:DON. Absorbance techniques plotted perpendicular to LC-OCD measures (Figure 3.3). Thus, based on contribution and characterization technique, this study focussed on four independent measures to define DOM composition that include three high-contributing variables to PC1 and PC2 axes (SUVA, $S_{275-295}$, and proportion of HSF) and DOC:DON.

3.3.3 Composition Wheel Axes

Four DOM composition measures that explained the most variability within the dataset were used to compare DOM across a larger dataset. Composition Wheel axes were defined using absorbance measures (SUVA, $S_{275-295}$), HSF, and DOC:DON. Although two absorbance measures are used, they represent independent measures of DOM composition as one characterizes the amount of UV-absorbing components normalized to DOM concentration (SUVA) and the other is correlated with DOM molecular weight ($S_{275-295}$). Shapes varied across hydrologic and geographic settings, with larger shapes corresponding to samples with higher values of compositional measures. Ponds and lakes tended to have lower values of SUVA and DOC:DON while subsurface DOM contained higher HSF and SUVA values (Figure 3.4:). Representation of different measures using these four axes allows for a facile comparison of DOM composition among samples.

3.4 Discussion

3.4.1 Comparison of DOM Composition Measures

Collection of samples from various locations and hydrological environments resulted in a wide range in values for each composition metric within the dataset. Four distinct PCA clusters contained characterization methods that responded to different components of DOM (i.e:

independent measure of either size-based grouping, absorbance, or elemental ratio). Further, chromophoric (CDOM) and non-chromophoric components of DOM were well represented within the dataset as absorbance measures plotted perpendicular to elemental and size-based fractionation methods (Figure 3.3). Similar studies using PCA to assess relationships across various DOM characterization techniques have found higher explained variability in the first two principal component axes than this study[83,213]. However, those studies used only absorbance parameters to describe DOM composition from leachates and surface waters in a subtropical coastal wetland. Representing a single location or source likely results in a higher explained variance than studies using a suite of DOM characterization techniques[202] due to the simplification of quantitative DOM information[214]. Further, data from this study represent various sites along the aquatic continuum. Although the dataset contains a wide range of values in all characterization methods, statistical analyses indicates that DOM composition could be easily represented by certain measures across spatial scales.

Of all compositional measures used in this study, simple absorbance parameters that are normalized to the concentration of DOM explained the highest variability within the dataset. This suggests there are a wide range to the CDOM components encountered across various environments. Although various wavelengths could be selected, an excellent correlation was found when predicting the absorbance of a sample at a specific wavelength using different wavelengths across the absorbance spectra[203]. Absorbance at different wavelengths within a sample are closely related and should provide similar interpretations of DOM composition, and is further supported by the grouping of specific absorption coefficients within the PCA (Figure 3.3). Although absorbance parameters are easily measured and helpful in comparing different DOM compositions, they do not accurately reflect non-CDOM components that could be important for overall DOM composition. The difficulty with characterizing DOM composition is that there are a number of parameters that could be used to represent specific components of a whole. These results illustrate how relatively simple measures of absorbance provide a limited, but quantifiable, component that represents DOM.

Intrinsic DOM properties can be assessed through positive associations between different measures, allowing for a detailed interpretation of the overall DOM composition. For instance, the similar direction of both HSF and DOC:DON PCA vectors indicate that humic-like molecules within DOM likely contain the minority of nitrogen moieties. A similar interpretation of DOM was observed in Swedish lakes[202] and northern German streams[215]. Further, positive associations

between concentration-normalized absorbance parameters to other forms of characterization (such as size-based groupings or DOC:DON) indicate that CDOM may be primarily associated with high molecular weight, low-N containing humic-like components. Slope ratio (S_R) is inversely-related to overall molecular weight[199], further supporting these findings by plotting oppositely of HSF but similarly to degraded components of HSF (such as BB[216]). Similar associations between DOM characterization techniques are found in other studies using different DOM sources[217]. Comparison with highly detailed characterization of DOM using FTIR shows agreement with certain LC-OCD fractions and fluorescence components[79]. Associations between different characterization techniques not only help determine measures most useful to describe DOM composition, but also avoid overlap of information.

In contradiction, we find both high-molecular weight (BP) and low-molecular weight (LMWN) variables plotting closely on the PCA (Figure 3.3). LC-OCD quantifies different size-based DOM groupings as a proportion, removing the influence of overall concentration when comparing LC-OCD groupings across samples. However, the HSF generally comprises the dominant fraction of DOM[75] and could lead to a negative correlation to other components (i.e: higher HSF inherently leads to lower proportions of BP and LMWN). Hence, when humics do not comprise the majority of DOM, the dominant molecular-size fraction shifts to either larger (BP) or smaller (LMWN) components for either surface or ground waters, respectively (Appendix B). Differences in the proportions of either high or low molecular weight components do not influence most absorbance-based parameters as they plot perpendicular to the LC-OCD vectors, further supporting the concept that these independent measures of composition can be used together to gain a better understanding of absorbing and non-absorbing components of DOM.

3.4.2 How Compositional Measures Relate to DOM Concentration or Site

This large dataset incorporating both DOM quantity and composition provides an opportunity to compare the two. While some studies find correlations between the amount of DOM and its quality across continental USA (lakes, streams, and estuaries[218]) others do not (boreal streams[79] and north temperate lakes in Wisconsin[219]). In this study, DOM concentrations from high arctic creeks were orders of magnitude different than subsurface DOM at Yellowknife, yet contained similar SUVA values (Figure 3.2a). Although DOM concentration is not adequate to determine its composition,

concentrations of DOM are necessary for calculating mass balances, fluxes, biogeochemical rates, or observing net effects of mixing and should be measured concomitantly with compositional metrics.

The general perception is that watershed vegetation governs the type of DOM. However, CWs suggest this is not the case. Similar DOM compositions are observed regardless of the range of vegetation types and sites that span areas of peat palsas (taiga shield), boreal shield watersheds, tundra heath ecosystems (Southern Arctic), and the high xeric arctic with relatively productive wetlands (Figure 3.4). Instead, differences in DOM composition are more apparent between subsurface and surface water DOM than between sites; all subsurface DOM samples exhibit a high proportion of large, humic, UV-absorbing components. The various sampling locations are very different in terms of vegetation and hence terrestrial sources of DOM, yet CWs indicate similarities across different ecoregions.

The range in values found across the four compositional measures also compared well with DOM from other studies, indicating that DOM composition may not be unique to its locale. Concentrations of DOM and SUVA values from rivers in this study compared well to the comprehensive study of United States rivers[73] and Canadian boreal lakes[49]. Across lakes, streams, and estuaries in the United States, similar ranges in DOM concentration, SUVA, and DOC:DON were found[218]. However, much higher SUVA values were found in non-riverine environments, particularly in subsurface samples from organic-rich wetlands. Hence, DOM from northern regions contain similar compositions as DOM from areas with different climate and vegetation characteristics.

Commonalities in DOM composition across concentrations and spatial gradients could identify similarities in DOM sources or processing, or reflect the presence of common molecular moieties that persist within the environment. In a 120-lake survey of boreal lakes in Sweden, 95% of all unique molecular DOM compounds within the dataset were identified after only 45 lakes[50], indicating a commonality in DOM composition transcending spatial scales and environmental gradients. The similarity in varying compositional measures across different studies indicates DOM composition is not vastly different across environmental or latitudinal gradients, and differences in certain measures could be easily used to observe the evolution of DOM composition across the aquatic continuum.

3.4.3 Visualizing Differences in DOM Composition

Expressing DOM composition with only four concentration-independent parameters excludes advantages of other techniques not used in this study. However, there is agreement between multiple parameters that allow for the use of surrogates in the CW. LC-OCD is not widely available but many studies have traditionally used resins[73,220,221] or other size-exclusion columns[214,222] to characterize DOM. Further, LC-OCD fractions of humics have been well correlated to measures of ^{13}C-NMR and more accessible fluorescence measures such as HIX[79,215,223]. Although fluorescence was not used in this study, strong associations between certain fluorescence parameters and absorbance or molecular-weight groupings could be used to replace LC-OCD defined fractions, such as using PARAFAC modelling to discern components most similar to HSF[79,215] (Appendix B). These fluorescence parameters are also independent measures of DOM composition and could be readily substituted into the CW. Elemental ratios of DOC:DON were positively correlated with humic-like fluorescence and negatively correlated to protein-like components[202]. Slope ratio and E_2:E_3 (see Table 3.1 for description) are potential surrogates for $S_{275\text{-}295}$ (Figure 3.2). Measurements of SUVA could be substituted with SAC_{420}, SAC_{350}, or E_4:E_6, as well as HIX if not used for HSF[81,202]. Although SUVA has been correlated to fluorescence component C3 [81,202], the opposite has also been found[215]. Associations between different characterization techniques allow for mixing and comparison of different variables, indicating a wide-range of applicability of CW for use within environmental sciences.

Clear communication of science and its relevance to society is becoming increasingly important for informing public and supporting evidence-based policy decisions. This visualization method provides an efficient communication tool not only among scientists, but also between scientists and other parties concerned with water quality, ranging from stakeholders to community members. It is clear how DOM composition differs due to the variations in shape, whereas changes in the numerical value of metrics are better understood by those with adequate background who are familiar with the methods. Further, changes to composition resulting from DOM degradation could be used to trace DOM evolution, while different shapes of DOM could be associated with certain parameters of interest (i.e. disinfection demand, metal mobility). By reducing the complexity of independent DOM measures and creating an easily comparable shape, differences in DOM composition can be easily compared and communicated to larger audiences.

TABLE 3.1: Dissolved organic matter composition as described by chemical, absorbance, and molecular-size based measures.

Parameter	Equation	Unit	Characteristic	Reference
Chemical				
DOC:DON	$M_C \div M_N$	-		77
Absorbance				
E_2:E_3	$A_{255} \div A_{365}$	-	Inversely related to molecular size	69
E_4:E_6	$A_{465} \div A_{665}$	-	Humic molecular weight and size	224
SAC_{350}	$\frac{ln(10) \times A_{420}/L}{[DOC]}$	$\frac{cm^2}{mg\text{-}C} \div 1000$	Specific colour	225
SAC_{420}	$\frac{ln(10) \times A_{420}/L}{[DOC]}$	$\frac{L}{mg \times m}$		
SUVA	$\frac{ln(10) \times A_{255}/L}{[DOC]}$	$\frac{L}{mg \times m}$	Correlated to degree of aromaticity	71
$S_{275\text{-}295}$	$a_\lambda = a_{\lambda_{275}} e^{-S(\lambda-275)}$	nm^{-1}	Inversely related to MW	199
$S_{350\text{-}400}$	$a_\lambda = a_{\lambda_{350}} e^{-S(\lambda-350)}$	nm^{-1}		199
S_R	$\frac{S_{275-295}}{S_{350-400}}$	-	Inversely related to overall molecular weight; integrative indicator of CDOM history	199
Size Exclusion Chromatography				
Biopolymers (BP)	-	% of DOM	Polysaccharides, proteins	75
Humic substances (HSF)	-	% of DOM	Humic or fulvic-like components	75
Building Blocks (BB)	-	% of DOM	Degraded HS	75
Low-molecular weight neutrals (LMWN)	-	% of DOM	Aldehydes, small organic materials	75
Low-molecular weight acids (LMWA)	-	% of DOM	Saturated mono-protic acids	75
HS molecular weight (HS MW)	-	g / mol	Nominal average molecular weight of HS	75

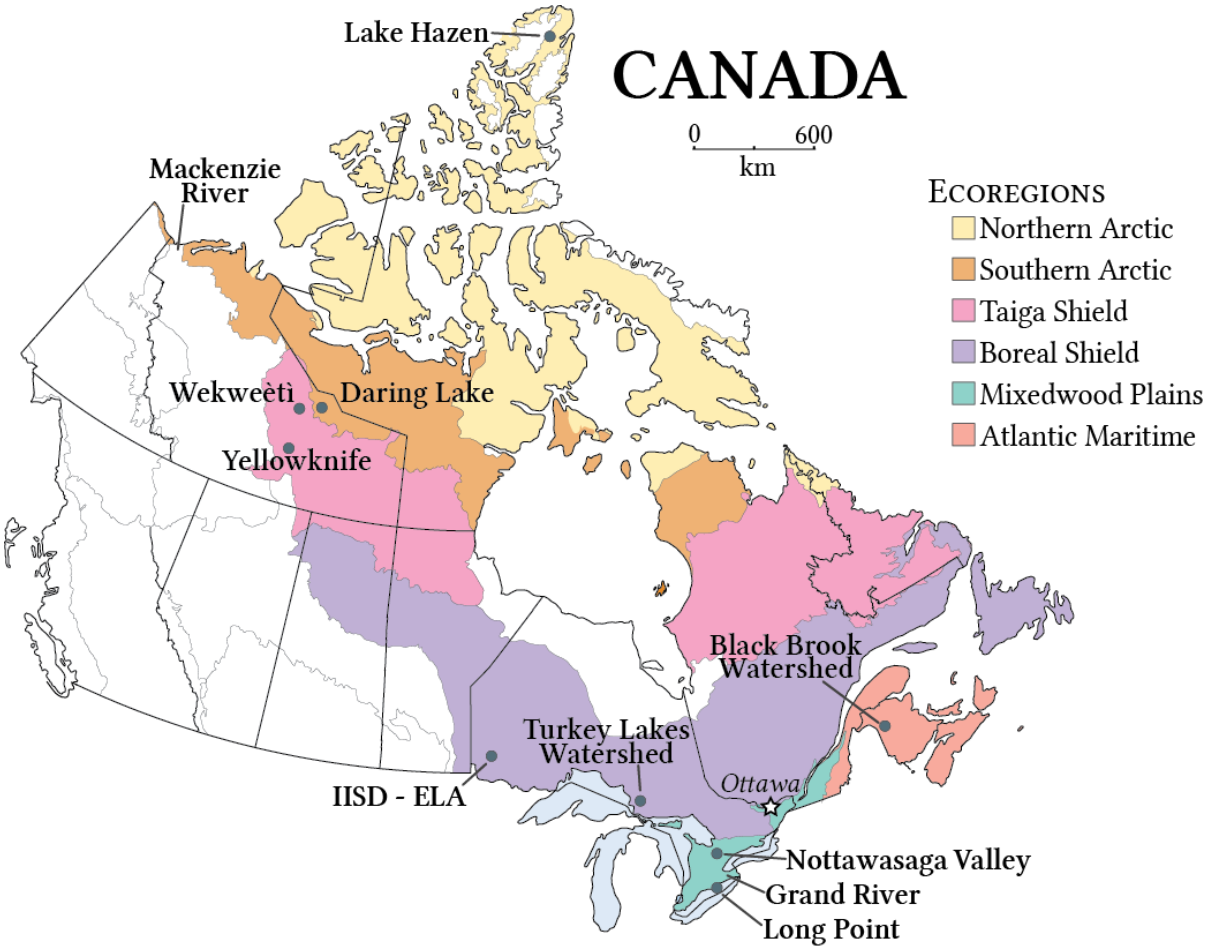

FIGURE 3.1: Locations of sampling sites and ecoregion. River locations (Grand River, ON; Mackenzie River, NT) labelled at the mouth of the river.

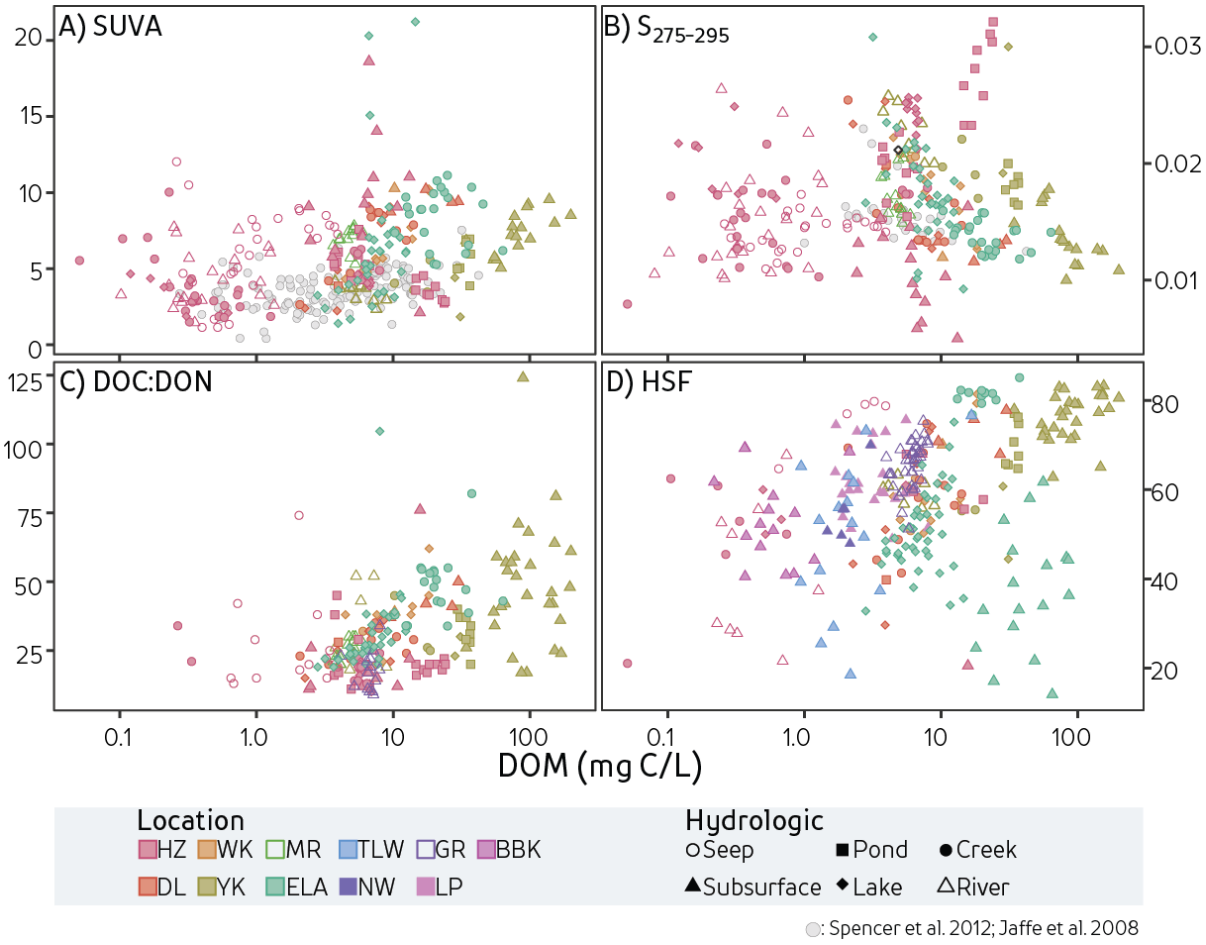

FIGURE 3.2: Compositional measures versus overall DOM concentration (mg C/L). Measures include A) specific ultraviolet absorbance at 255 nm, B) slope between 275 to 295nm, C) DOC:DON, and D) proportion of humic substances. Colours represent geographical sampling locations (HZ: Lake Hazen Watershed, NU; DL: Daring Lake, NT; WK: Wekweètì, NT; YK: Yellowknife, NT; MR: Mackenzie River, NT; ELA: IISD-Experimental Lakes Area, ON; TLW: Turkey Lakes Watershed, ON; NW: Nottawasaga Valley, ON; GR: Grand River, ON; LP: Long Point, ON; BBK: Black Brook Watershed, ON) while shapes represent hydrologic environments. Light grey circles represent two other DOM characterization studies conducted at similar scales.

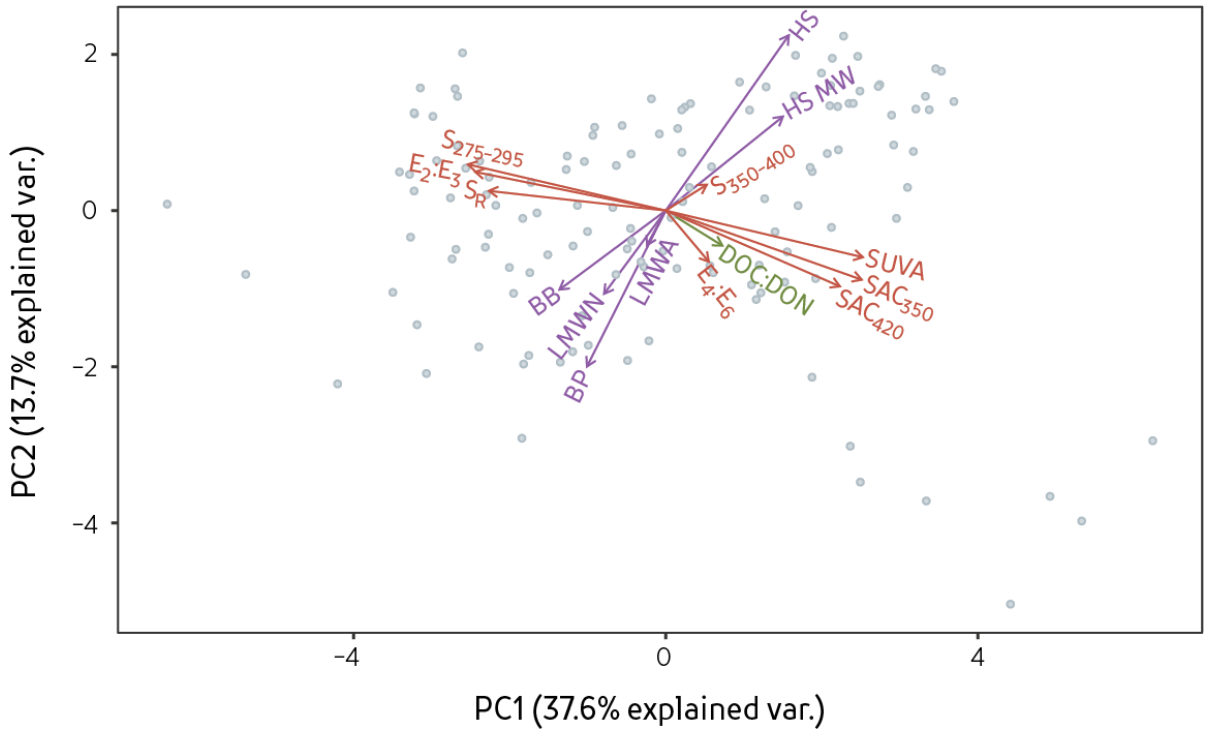

FIGURE 3.3: Principal component analysis for samples that contained measures of absorbance (red), elemental ratios (green), and LC-OCD (purple) (n=143). Grey dots represent individual samples.

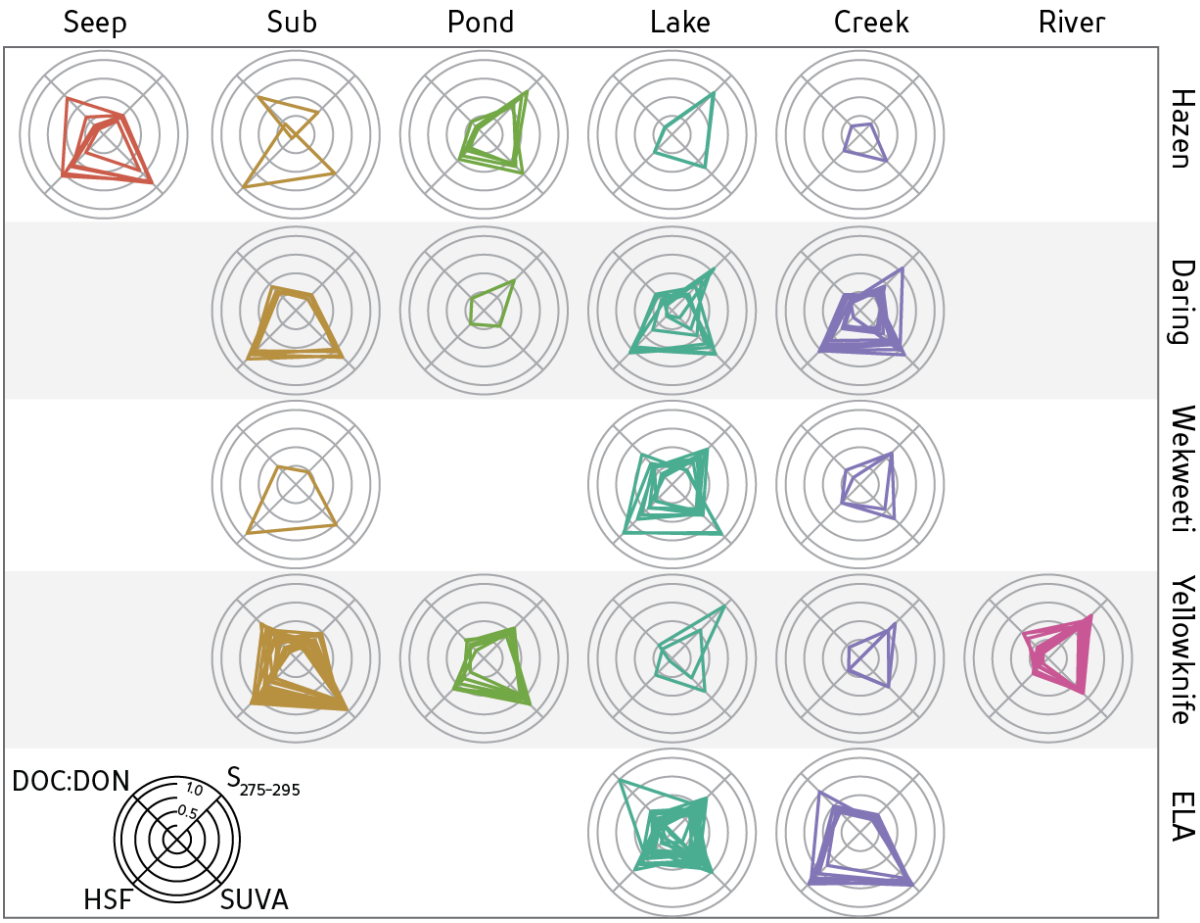

FIGURE 3.4: Composition Wheels for different hydrological environments at different locations. Axes represent the normalized value for each parameter (parameter axis in bottom left). Different samples from the same hydrological and geographic setting are plotted within the same wheel.

Chapter 4
How Dissolved Organic Matter Composition from Freshwaters in the Western Canadian Sub-Arctic to High Arctic Influences Loss and Degradation Rate during a Microbial Degradation Experiment

4.1 Introduction

Northern environments are some of the most sensitive to a warming climate and are experiencing rapid changes that affect carbon cycling, aquatic ecosystem health, and drinking water quality. Across the circumpolar north, large reserves of carbon are frozen within organic-rich permafrost[162,194] but changes to temperature and hydrology have led to the mobilization of this carbon[15,18,30,33]. In particular, release of carbon as dissolved organic matter (DOM) can transfer carbon between aquatic and terrestrial systems. The overall amount of DOM in a sample is quantified by the concentration of dissolved organic carbon that passes through variable filter sizes. However, DOM is comprised of thousands of organic molecules with varying structural and chemical properties that can influence the reactivity of DOM with its surroundings. For instance, depending upon its composition, DOM can influence water transparency and thermal regimes within lakes[55], provide an important energy source for aquatic food webs[3], influence subarctic lakes and pond bacterial community composition and diversity[90], or act as an important biogeochemical constituent in redox reactions[58]. In terms of drinking water resources, DOM affects water colour, taste, and odour, and reacts to form carcinogenic disinfection by-products during water treatment[65–67]. Increases to surface water DOM concentrations have been observed, most notably among northern environments, and can complicate future drinking water treatment options[89,92,102]. Determining what drives differences in DOM concentration and composition in northern environments would better allow for predictions to the impact of changing DOM upon aquatic health and drinking water resources.

Recent studies have focussed on the effects of permafrost degradation and subsequent carbon release on the overall carbon cycle and aquatic ecosystem. Carbon from thawing permafrost is old and can be easily utilized by microbes[96,134,226] in comparison to active-layer DOM which has been

subjected to substantial degradation before reaching surface waters[98]. In northern environments, subsurface DOM characteristics are becoming increasingly dominant within surface water DOM[34] and could lead to enhanced bacterial production within peatland lakes[227]. Further, thaw ponds with high DOM and nutrients in the eastern Canadian Arctic have higher microbial activity and higher water methylmercury concentrations[228]. In ice-rich areas, warming of the subsurface results in active-layer detachments and thermokarst that leads to sudden influxes of permafrost carbon and nutrients into surface waters[128,136,229]. Hence, the responses of northern areas to a warming climate have direct implications on the carbon cycle and aquatic ecosystem health as there is the potential for large amounts of previously immobilized carbon to enter aquatic systems.

Biodegradation is an important driver of DOM concentration and composition in the environment. The intrinsic (compositional) properties of organic matter can dictate how easily DOM can persist or degrade, termed lability, within the environment[81,230,231]. Optical properties of DOM, such as fluorescence and ultraviolet (UV)-visible absorbance, have been used as qualitative indicators of biodegradation[82,83]. Generally, DOM transported into surface waters from terrestrial environments (allochthonous DOM) is typically considered more difficult to biodegrade, or recalcitrant, compared to DOM produced *in situ* (autochthonous DOM). However, recent studies have found otherwise[209,232,233]. Similarly, the traditional approach to the labile-recalcitrant categorization was based on a size-reactivity continuum, where high molecular weight DOM was more labile than low molecular weight components[234]. Recent findings suggest that bioavailable DOM components are influenced by the diversity of the DOM mixture in the system[84,85], thus it is possible for labile components to be molecules of either low molecular weight (LMW)[211] or high molecular weight (HMW)[108]. Characterizing DOM composition provides a way to quantify how biological processing alters DOM concentration and composition.

Northern surface waters act as biogeochemical hotspots for carbon and nutrient cycling[3,37], thus better predictions of carbon cycling and carbon fate in northern systems can be achieved by quantifying the rates and processes that dictate DOM evolution. Most biodegradation studies have been conducted in Siberia, Alaska, and Sweden, while Canadian experiments have focused on northern Quebec[235,236] or the Mackenzie Delta[129,229]. There is a wide range in the fraction of DOM that is biodegradable (BDOM) among these systems. For instance, within thaw slump only incubations, BDOM ranged from >40% in Siberia[32,96] to between 1 and 12% in the NT[129]. Large differences in the proportion of BDOM are found, yet few estimates of BDOM exist, let alone

microbial degradation rates with paired measures of DOM composition for wide areas of northern Canada. Degradation rates provides a quantifiable value to predict and model the response in DOM concentration to a changing climate based on known parameters, such as changes to nutrient levels, water residence times, or temperatures.

The overall objective of this study is to quantify the range of BDOM and microbial degradation rates of DOM across various hydrologic sites from the western sub-arctic and high arctic in Canada. This will be accomplished using three specific objectives: 1) quantify the concentration of BDOM and microbial degradation rate for each site, 2) determine how microbial degradation changes measures of DOM composition from different northern sites, and 3) determine whether initial DOM composition can be used to predict microbial degradation rate. Various hydrologic sampling sites along a latitudinal gradient will be used to provide a range in DOM compositions that span differences in watershed characteristics, sources, and processes.

4.2 Methods

4.2.1 Sample Collection

Bulk water was collected from creeks, lakes, ponds, and subsurface sites across the Northwest Territories (late July; Yellowknife (YK), Daring Lake(DL)) and the Lake Hazen Watershed, NU (HZ; early July; Figure 4.1). Subsurface water was collected from the deepest extent of the active-layer. An aliquot of each sample was taken as the 'inoculum' and filtered only to 1.2 μm to remove large particulates and allow for the ambient microbial consortium to pass through. The remaining water was filtered in the field to 0.45 μm. It should be noted that filtering to 0.45 μm does not eliminate all microbes and render the solution sterile, but was chosen to be consistent with previous characterization of DOM samples (i.e. Chapter 3). Both filtered water and inoculum were kept cool (<4°C) and in the dark until experiments were conducted (within 2 weeks) at the University of Waterloo. For logistical reasons, Lake Hazen experiments were conducted on site.

4.2.2 Microbial Degradation Experiment Setup

Similar to the majority of reported microbial incubation studies, the concentration of BDOM was defined as the loss in DOM concentration during the duration of the experiment (Table 4.1) and calculated as:

$$BDOM = DOC_0 - DOC_{30}$$

where DOC_0 represents the initial concentration of dissolved organic carbon and DOC_{30} represents the final concentration. Percentage of BDOM was calculated by dividing the BDOM concentration by DOC_0. Use of this common methodology to calculate BDOM allowed for the comparison of results from this study to other reported values across the circumpolar north. It should be noted that this definition of BDOM assumes DOM loss results only from mineralization into CO_2 or incorporation into biomass. Very few studies include 'control' treatments to assess changes in DOM without inoculum (Table 4.1). Over time, DOM can be lost to flocculation processes or adhere to container walls during storage in the absence of microbial activity. Thus, reported estimates of BDOM include these dark abiotic losses. Controls were included in this experiment in order to calculate the minimum proportion of DOM loss due to microbial degradation. Total DOM loss, which may include abiotic losses, was used to calculate degradation rates and compare proportions of BDOM using consistent BDOM definitions encountered in the published literature.

Microbial degradation experiments were conducted using duplicate sacrificial bottles at the following time points: 0, 4, 7, 14, and 30 days. These sampling times capture the majority of DOM change and provide high-resolution sampling during initial rapid degradation. Half of the filtered water was mixed with inoculum (10% by volume), well stirred, and poured into a series of either 250 mL acid-rinsed glass bottles (YK and DL) or 5 L Tedlar bags (HZ). The remaining sample was used as a Control treatment to compare loss of DOM without inoculum. Control treatments were not prepared for Lake Hazen. Containers had sufficient air in the headspace to avoid oxygen limitation during DOM decomposition. Bottles and Tedlar bags were gently agitated daily to ensure the water did not become anoxic. Experiments were conducted in the dark and at room temperature.

4.2.3 Laboratory Analyses

Samples were re-filtered to 0.45 µm at each sacrificial time point and run for subsequent geochemical analyses. Samples were quantified for concentrations of dissolved organic carbon (DOC; mg C/L) and total nitrogen (TDN; mg N/L) using a Shimadzu Total Organic Carbon (TOC-L) Combustion Analyzer with TNM-1 module (precision of ±0.3 mg C/L; ±0.3 mg N/L). Inorganic nitrogen species (NO_2^-, NO_3^-, NH_4^+) were analysed using SmartChem 200 Automated Chemistry Analyzer (NO_2^- and NH_4^+ precision of ±0.1 mg N/L, precision NO_3^- of ±0.15 mg N/L; Unity Scientific, MA United States).

DOM was characterized primarily using UV and visible absorbance and DOC:DON ratios. Absorbance was measured using a Cary 100 UV-VIS Spectrophotometer (Agilent, CA United States) at 5 nm increments from 200 to 800 nm. Deionized water was used to zero the machine, and run intermittently during analyses to correct for baseline drift. The Naperian absorption coefficient (a; m^{-1}) was calculated using:

$$a_\lambda = \frac{ln(10) \times A_\lambda}{L}$$

where A is the baseline-corrected absorbance at wavelength λ and L is the cell length (m). The specific UV-absorbance at 255 nm (SUVA) and visible absorbance at 420 nm (SAC_{420}) were calculated by dividing the Naperian absorption coefficient by the overall DOM concentration. The spectral slope between 275 and 295 nm was also calculated[199].

Initial DOM composition was further characterized using molecular size-based groupings determined by liquid-chromatography organic carbon detection (LC-OCD). Detailed methodology can be found elsewhere[75]. Briefly, the sample passed through a size-exclusion column (SEC; Toyopearl HW-50S, Tosoh Bioscience) that separated DOM based on hydrodynamic radii into five hydrophilic fractions (from largest to smallest): biopolymers (BP; polysaccharides or proteins), humic substances fraction (HSF; humic and fulvic acids), building blocks (BB; lower weight humic substances), low molecular weight neutrals (LMWN; aldehydes, small organic materials), and LMW-acids (LMWA; saturated mono-protic acids). Duplicates run at six concentrations yield a precision for the LC-OCD of less than ±0.09 mg C/L for all fractions. For this study we focussed on BP, HSF, and LMWN as they provide information on three different size-groupings and have been determined to be most useful to differentiating different DOM compositions (Chapter 3).

Composition wheels (CW) were used to visually compare differences in DOM composition between initial and final samples (Chapter 3). Composition Wheels use a polygon to represent different metrics of DOM composition that best explain the variability in DOM encountered across a variety of environments. Independent measures were chosen to provide an encompassing representation of various DOM characteristics and include: SUVA (measure of UV-absorbing capability), spectral slope ($S_{275\text{-}295}$; inversely related to overall molecular weight of UV-absorbing components), DOC:DON (indication of source and nitrogen content), and SAC_{420} (measure of water colour and humic material). Values were normalized as a proportion of the maximum and minimum value encountered from a larger dataset of various ecoregions across Canada.

4.2.4 Statistical Analyses

The correlation between DOM composition and BDOM measurements were calculated using the non-parametric Pearson coefficient correlation. Linear and 1st-order degradation rates were calculated in R[212]. The Reactivity-Continuum (RC) Model, derived from marine environments, has been applied to model the rate of degradation of DOM in freshwater systems[209,211,236]. This approach treats DOM as a distribution of labile and recalcitrant components that change over time, based on changing 1st-order degradation rates[237]. The change in DOM over time was calculated as:

$$\frac{DOC_t}{DOC_0} = \left(\frac{\alpha}{\alpha + t}\right)^{\nu}$$

where α is the average life-time of more reactive components, ν relates to the quantity of recalcitrant components, and t is age (days)[209]. The initial 1st-order decay rate constant (k) can be calculated as ν/α (d^{-1}) and represents the expected value from the initial gamma distribution of reactive and recalcitrant DOM components[210]. These measures not only provide degradation rates, but also provide information on differences in DOM lability.

4.3 Results

4.3.1 DOM Concentration and Composition

A range in DOM concentration and composition were measured across various hydrologic environments in different ecoregions. Samples from YK contained the highest DOM concentrations (16 to 84 mg C/L) while HZ samples contained the lowest (2.5 to 6.2 mg C/L; Table 4.2). Subsurface sites contained higher DOM concentrations than surface waters for all locations but HZ (Figure 4.2). Differences between surface and subsurface water DOM composition were more apparent than differences in composition across a latitudinal gradient. Initial measures of SUVA ranged from 4.0 to 9.1 L/(mg·m) with lowest SUVA values from YK and DL creeks and highest values from YK and DL subsurface DOM (Table 4.3). Similar spectral slope values were found for most samples across sites, ranging between $1.3x10^{-2}$ to $1.7x10^{-2}$ nm^{-1}. Across all sites, surface waters contained higher spectral slope values than subsurface DOM with the highest slopes found from DOM in a YK creek and HZ lake (Table 4.3). DOC:DON of initial samples were highest at YK (31 to 56) compared to either DL (21 to 42) or HZ (13 to 28). Subsurface DOM contained the highest DOC:DON from YK and DL samples (56 and 42, respectively). Measures of SAC_{420} ranged from 0.19 to 0.75 L/mg·m, with lowest values from surface water DOM (HZ lake, DL creek, and YK creek). Similar DOM CW

were found in YK and DL subsurface, YK pond, and DL creek (DAR 8; Figure 4.3). Use of a suite of compositional metrics indicated that subsurface DOM is compositionally different than surface water DOM due to differences in UV-absorbing capabilities and DOC:DON.

4.3.2 BDOM and Degradation Rates

The proportion of BDOM after 30 days varied across all sites. Degradation experiments quantified a total loss in DOM that ranged from 1 to 27% of the initial concentration, with an average loss of 11% (n=9) over 30 days (Table 4.2). The majority of DOM loss occurred within 14 days (Figure 4.2). The total loss of DOM was higher in samples with high initial DOM concentrations. In particular, YK samples had higher initial DOM concentrations and a greater DOM loss over 30 days than either DL or HZ samples. DOM loss in Control treatments ranged from 4 to 14% and resulted in minimum microbial loss proportions from 1 to 13% (Table 4.2). The average difference in proportion of BDOM and minimum microbial loss was 8%. Thus, DOM at all these sites is biolabile. Although the total DOM loss was greater in samples with added inoculum, the addition of Control treatments provide an estimate to the minimum microbial contribution.

A range of microbial degradation rates were quantified from different initial DOM compositions. Different models were used to account for limited data availability (linear model), comparison to traditional methods (first-order), and use of newer approaches (RC Model). Similar patterns in the relative magnitude of linear and 1st-order derived degradation rates were observed among different samples; however, unlike other models the RC model predicted a higher initial degradation rate from YK pond than YK subsurface (Table 4.4). The highest linear and 1st-order degradation rate was found from a DL creek (DAR10) and YK subsurface, while the lowest rate was from HZ subsurface (Table 4.4). Degradation rates in all surface waters were comparable. Predicted initial RC Model degradation rates were highest from DL creek, YK subsurface, and YK pond, and much lower for the remaining samples (Table 4.4). Hence, 1st-order and linear rates were similar in relative magnitude across different locations and identify DOM samples that are more easily degraded than others.

RC modelling rates were calculated for all but three samples (where the model was unable to converge). The highest initial rates were determined for YK samples (9 to 34 x10^{-3} d^{-1}) and a DL creek (99 x10^{-3} d^{-1}) and lowest from LH (1 to 3 x10^{-3} d^{-1}). Similar α values from YK subsurface, YK creek, and DL subsurface samples indicate higher average lifetimes of the more reactive components (11, 14, 9 d, respectively) compared to other samples. Use of the RC Model resulted in

similar trends in the relative magnitude of degradation rates compared to the other two models, and provided a method to quantify the relative abundance of labile and recalcitrant DOM components.

4.3.3 Microbial Degradation and the Influence of DOM Composition

The DOM composition of most samples changed in response to the loss in DOM concentration (Figure 4.3). Only DL subsurface and DL creek had little compositional change, even after a 5 and 11% total loss in DOM concentration (Table 4.2). SUVA values increased after 30 days of microbial degradation for all sites except DL subsurface and LH subsurface, with the largest increases found in YK subsurface, DL creek, and HZ seep. Measures of SAC_{420} increased for most samples except in DOM from DL subsurface, DL creek, and HZ subsurface. Overall, various metrics of DOM composition did not respond uniformly when compared across different samples with changes being unique to each sample.

Absorbance-based measures of initial DOM composition were not good *a priori* predictors for 1st-order degradation rates, 30-day concentration of BDOM, or proportion of BDOM (Figure 4.4). Conversely, initial proportions of different molecular-based size DOM groupings were significantly correlated to the proportion of BDOM and 1st-order degradation rate (Table 4.5). The majority of DOM was comprised of high molecular weight components (total of BP and HS proportions: 73 to 80%) and a smaller contribution of LMWN (3 to 12%; Figure 4.5). Subsurface samples contained the highest proportions of HS (71 to 78%), while creeks contained the highest amount of BP and LMWN. Hence, characterization of DOM based on size-based groupings may provide better predictive capability to the susceptibility of DOM to microbial degradation than absorbance based measures.

The magnitude of change in some parameters can be used as a surrogate for predicting the proportion of BDOM. Little change was observed in $S_{275\text{-}295}$ (between -3 to 5% after 30 days) while large changes were observed in SUVA, DOC:DON, and SAC_{420} (Table 4.2**;** Figure 4.6). The change in SUVA was significantly correlated to the proportion of BDOM over the 30-day microbial experiment (r: 0.92, $p<0.05$; Figure 4.6).

4.4 Discussion

4.4.1 Experimental Influences on BDOM Determination

Comparison of laboratory biodegradation results can be difficult because measured BDOM values are influenced by differences in temperatures, inoculum filter sizes, incubation durations, and nutrient additions[238]. However, use of different methodology during soil DOM biodegradation experiments resulted in comparable final BDOM values, supporting comparison across different studies regardless of experimental design[239]. Our laboratory experiments were set up to quantify BDOM amount and degradation rate based on previous BDOM definitions using the host microbial consortia and ambient nutrient levels at each site. Although this limits our ability to compare rates with other studies using different filter sizes or nutrient additions, it quantifies a representative proportion of BDOM for each of our studied systems.

Even within a site a whole range of factors including nutrient availability, *in situ* temperature, and microbial community, to name a few, can result in different rates of degradation. Transport and mixing along hydrologic flow paths can change the conditions and thereby increase or decrease degradation rates. Similarly, hydrologic residence time can affect the actual amount of degradation at each site as longer residence times allow for more processing within the environment. Another important consideration is the time it takes for microbial populations to establish within the containers. All efforts were made to minimize the effect of transit time (kept cold and quick setup of the incubations) but this may have affected the microbial consortium added to the samples. Thus, both environmental and experimental design features are important to understand when comparing differences in BDOM and degradation rates.

Quantifying the explicit contribution between biotic and abiotic DOM loss during incubation experiments is difficult. During the incubation, DOM loss can result from microbial mineralization into carbon dioxide, formation of biomass, or from altered DOM solubility, sorption to biomass, and flocculation as particulate organic matter. The inclusion of Controls shows that DOM loss occurs even without inoculum addition (Table 4.2). Approximately 95% of bacteria can still pass through a 0.3 μm filter size[240] likely contributing to DOM degradation within Control samples. Further, one study was able to culture bacterial communities that passed through 0.1, 0.45, and 0.7 μm filter pore sizes[241], signifying that Control samples still include some of the native microbial consortia. Alternatively, abiotic microparticle formation occurs within filtered samples[242]. Re-filtration of

samples before analyses would encompass DOM loss from both biomass growth and abiotic flocculation, as well as microbial respiration. Few studies report changes to dissolved inorganic carbon (DIC) when assessing microbial degradation of DOM, but those that have observe increased DIC concentrations over the duration of the experiment[93,94,243]. Select YK samples analyzed for DIC indicated little change to DIC concentration over the incubation (Appendix C) suggesting some DOM loss may be attributed to biomass growth or flocculation rather than mineralization into inorganic carbon. Samples with high proportions of minimum microbial contributions showed large changes to DOM composition (Figure 4.3; Table 4.2). The lack of including and reporting Control results (Table 4.1) indicates that caution should be taken when referring to DOM loss as BDOM as filtration to 0.45 μm may allow a sufficient population of microbes through that continues DOM degradation at slower rates. Hence, the loss of DOM within this study is due to both biotic and abiotic processes over the 30 day incubation.

4.4.2 Comparison of DOM Composition and BDOM Proportion with Other Circumpolar Studies

As discussed in Chapter 3, differences in DOM composition were more apparent between subsurface and surface water samples than samples across a latitudinal gradient. There is similarity in the composition of subsurface DOM in this study to terrestrial-like DOM observed across other northern systems[34,244,245]. Further, characteristics of surface water DOM, such as higher BP and $S_{275-295}$, reflect either photodegradation or biotic *in situ* DOM contributions[90,130,199]. Hence, differences in DOM composition likely span a gradient of sources and amounts of previous processing. This provided a comprehensive dataset to relate differences in DOM composition to microbial degradation rates and BDOM amounts.

The proportion of DOM lost from samples in this dataset are well within the range of BDOM reported across the circumpolar North for similar incubation lengths. DOM from the sub-arctic contains greater BDOM proportions and degradation rates compared to high arctic DOM (Table 4.2). Further, samples in this study had the highest DOM loss reported in the NT when compared to one other similar experimental setup (Table 4.1). However, BDOM proportion in this study was lower when compared to studies conducted in Siberia and Alaska (>40% [96,108] ; Table 4.1). Linear degradation rates are similar to values found from freshwaters in Russia and Alaska, and initial 1st-order decay rates determined from the RC Model were higher in this study than reported from either Swedish lakes or Canadian boreal streams[209,236]. Thus, northern ecoregions sampled in this

study all contained DOM with some degree of microbial-labile components with comparable degradation rates to areas with different climate and vegetation; however, the sites in this study contained a lower proportion of BDOM compared to other circumpolar areas.

4.4.3 Different DOM Samples Respond Uniquely to Microbial Degradation

Previous studies of surface water DOM in northern regions found biolabile DOM to consist of LMW and low-aromaticity components[96,108,129]. With this definition, both YK creek and HZ lake DOM have high proportions of biolabile components but neither had the highest degradation rates (Figure 4.4). Strong correlations between the proportion of BDOM to both large and LMW groupings suggest biolability may not be simply defined by different molecular-sizes of DOM as suggested by others[234]. Rather, the definition of biolabile DOM components may differ across various systems depending upon the preferences of the ambient microbial community[84,85]. Essentially, the DOM components that are microbially labile may differ across sites.

Certain measures of DOM composition are not good *a priori* predictors of microbial DOM quality. For instance, unlike in this study, measures of initial spectral slope and elemental ratio have been shown to correlate to microbial DOM quality in soil, lakes, and rivers[108,209,239,243]. In general, high SUVA has been associated with lower BDOM proportions[32,111,115,129] (Figure 4.7), attributed to the preferential microbial degradation of non-UV or visible light absorbing LMW DOM[93]. However, some studies find no relation between BDOM and initial SUVA[246,247], as was the case with this dataset.

Measures of DOM composition do not always respond to microbial degradation, as seen from DL subsurface and creek DOM. Similar results were observed during a 3.5 year dark incubation as fluorescence indices did not change even though DOM decreased by 40% [247]. Further, measures of SUVA and fluorescence did not change during a boreal lake water DOM incubation[246]. Hence, use of absorbance-based measures of initial DOM composition are not always effective to predict microbial DOM lability.

The magnitude of change in SUVA is a better indicator to the proportion of BDOM than the initial SUVA value as an *a priori* indicator. Changes to DOM composition are unique for different samples and few composition measures were able to predict the microbial lability of DOM. Thus, measures of SUVA may be better suited to determine changes to DOM during microbial degradation rather than predict its initial microbial quality.

The unique response of each sample to microbial degradation and range in DOM degradation rates encountered suggest that sample location is more important for microbial degradation than initial DOM composition. Differences in climate, microbial consortia, and nutrients may control degradation rates. Regardless, certain measures of DOM composition provide an excellent indicator to the influence of microbial degradation upon DOM composition, with some measures that are more sensitive to microbial degradation than others. In particular, the preferential loss of non-UV and visible light absorbing components are easily captured with increased SUVA and SAC_{420} values. This is further supported by the significant positive relation between BDOM and the non-UV absorbing BP fraction[75] (Figure 4.6) suggesting that changes to SUVA and SAC_{420} act as indicators of microbial processing. Hence, measures of DOM composition are useful to track changes to DOM but the overall proportion of DOM loss and rate of microbial degradation are location dependent.

4.4.4 Microbial Degradation and DOM Fate in a Changing Climate

The distribution of sites across a latitudinal gradient provides a simplistic comparison of different physical controls on DOM composition and lability. From south to north, the landscape generally becomes colder, drier, and soils contain lower soil organic content, all of which are important factors that regulate biodegradation rates[82]. Low microbial degradation rates in high arctic sites (Table 4.4) indicate that DOM has either been heavily processed in the terrestrial environment, or the microbial community does not process the DOM as extensively as other sites. Conversely, sub-arctic sites contain DOM that is readily lost over 30 days, indicating that microbial DOM quality differs widely across the latitudinal gradient. Degradation constants need to be quantified for specific locations as 1st-order degradation rate constants could differ by up to 10x across all samples. Doing so will help constrain the rate at which carbon may be cycled through the system due to microbial degradation. Although the proportion of BDOM and degradation rate constants all differ, every location contained some component of BDOM that could act as an energy source for downstream biogeochemical reactions.

Subsurface processing can alter the form and amount of DOM exported to surrounding surface waters. Changing hydrologic flow pathways due to deepening active-layer thicknesses, increasing subsurface temperatures, and changes to the timing and amount of precipitation[17,132,148] could all affect subsurface residence times and carbon processing. However, permafrost and active-layer leachates in Finland were found to be of low quality as only 3% was mineralized after a week[98].

Scaling of laboratory to field studies is difficult to extrapolate as thawed cores or leachates represent the immediate lability of leached DOM and not necessarily what will be transported into surface water systems. Further, the variability in subsurface DOM degradation rate constants among different ecoregions (up to 7x difference) indicates that changes to the subsurface residence time and thawing of permafrost could alter the amount of DOM processed within the terrestrial landscape.

Nutrient deficiency within oligotrophic systems can hinder DOM degradation. The release of dissolved inorganic and organic nitrogen resulting from permafrost thaw could accelerate microbial processing of subsurface DOM[82,116,156]. Both inorganic and organic forms of nitrogen can be utilized by bacteria for cell growth depending on the availability of other nutrients, such as phosphorus. DOM can act as an important source of nitrogen as bacteria can grow more efficiently on DOM with low DOC:DON[78,230,248,249]. In Greenland arctic lakes, DOM was a readily-available source of N for microbial nutrient demands[250]. Inorganic nitrogen, phosphorus, and DON did not hinder DOM processing among thermokarst slumps and water tracks in Alaska[111] while a meta-analysis of northern DOM incubation studies found inorganic nutrient addition to have little influence on BDOM[238]. DOC:DON decreased in most samples during the experiment suggesting the loss of N-poor components or the production of N-rich dissolved organic products (Figure 4.3). We did not find any correlation between initial DOC:DON and either degradation rate or proportion of BDOM (Table 4.5) indicating the microbial community are not utilizing DOM as a source of nitrogen. Although DOM may supply a source of nitrogen to these systems, the lack of correlation between initial DOC:DON and proportion of BDOM indicates differences in DOC:DON is not a sensitive indicator of DOM lability at any of our sites.

4.5 Conclusion

A series of incubation experiments were conducted to quantify the importance of initial DOM composition in terms DOM loss and degradation rate. Differences in the amount and composition of DOM across hydrologic and geographic sites that included rivers, creeks, pond, and subsurface waters were greatest between subsurface and surface waters, rather than across locations. Although we report the highest BDOM proportions in the NT, overall BDOM proportion was generally lower than incubations conducted at other circumpolar areas. However, 1st-order and RC Model microbial degradation rates were relatively similar to other studies. Differences in microbial

DOM qualities across three Canadian arctic ecoregions are evident and result in a range of 1st-order degradation rate constants (up to 10x among all samples). The highest BDOM proportions, or most labile DOM, was found in low arctic subsurface waters and creeks. Not all metrics respond the same to microbial degradation. Changes to DOM composition were not uniform across sites and resulted in a unique final composition for each sample. Size-based groupings of DOM and the increases to SUVA and SAC_{420} were found to be strong predictors of BDOM proportion. Hence, the unique response of each sample, the wide variation in degradation rate constants, and the lack of relationship between initial DOM composition and BDOM proportion, all indicate that location may be more important for determining DOM lability than initial DOM characteristics. This outlines the importance of conducting microbial incubation experiments to obtain relevant and applicable BDOM amounts and degradation rates for specific environments.

TABLE 4.1: Summary of microbial degradation experiments for arctic and sub-arctic environments. Included are site characteristics (area and sample), definition of biodegradable dissolved organic matter (BDOM), duration of experiment, whether nutrients were added (Nutri.), incubation temperature (Temp.), inclusion of a control or Control, and the microbial degradation model used to calculate rates. A linear degradation rate was calculated from studies that did not include rates in the dataset (termed 'calc. here').

SITE		MICROBIAL INCUBATION SETUP						BDOM RESULTS				
Area	**Sample**	**BDOM Definition**	**Duration (d)**	**Nutri.**	**Temp. (°C)**	**Inoculum**	**Control?**	**Initial DOM (mg C/L)**	**BDOM (%)**	**Degrad. Model Used**	**Degrad. Rate (d-1)**	**Reference**
Russia	Yedoma thaw	Difference in DOC before and after 28d	28	No	20	Filtered to 0.7um	None	131	47.2	Linear (calc. here)	0.017	32
Russia	Erosion streams							30	17.5		0.006	
Russia	Streams							20	13.3		0.005	
Russia	Minor tribs							9.2	21		0.008	
Russia	Major tribs							6.1	12.2		0.004	
Russia	Kolyma River							5.1	14.6		0.005	
Russia	Kolyma River - Average							9.6	8.8		0.003	
Russia	*Kolyma River - Minimum BDOC*	Difference in DOC before and after 28 days	28	No	20	Filtered to 0.7um	None	*2.7*	*0.1*	Linear (calc. here)	*0.000*	108
Russia	*Kolyma River - Maximum BDOC*							*13.2*	*20.4*		*0.007*	
Russia	Yedoma thaw streams	DOC loss after 28 days	28	No	20	Filtered to 0.7um	Unfiltered river water	155	41	Linear (calc. here)	0.015	96
Russia	Soil pore waters	5-day biological oxygen demand difference	5	No	15	Filtered to 0.7um	None	43	3.9	Linear (calc. here)	0.008	251
Russia	Streams							12	3.2		0.006	
Russia	Rivers							4.9	6.2		0.012	
Russia	Kolyma mainstem							3.6	4.5		0.009	
Russia	Kolyma River main stem	Percent loss over incubation time	28	No	20	Filtered to 0.7um	None	5.5	6.6	Exp. Decay (3 parameter)	0.09	226
Russia	Permafrost thaw stream A							152.4	52.2		0.12	
Russia	Permafrost thaw stream B							165.8	61.9		0.19	
AK, USA	Soil leachate (Nonacidic tundra)	Difference in DOC over incubation	14	No	4	Inoculum prepared from unfiltered leachate	Blank of inoculum added to deionized water	117	46	Linear (calc. here)	0.033	252
AK, USA	Soil leachate (Acidic-1)							113	34		0.024	
AK, USA	Soil leachate (Acidic-2)							117	36		0.026	
AK, USA	Permafrost soil leachate	DOC loss entirely due to microbial uptake	8.3	Yes	20	1.6um inoc added	None	18	53.5	Linear (calc. here)	0.064	93
AK, USA	Kuparuk River (May to July average)	Difference in DOC over incubation	30	No	20	Filtered to GF/F (0.7um)	None	10	11.3	Linear (calc. here)	0.004	114
AK, USA	Upper Kuparuk River (May to July average)							5.6	8.3		0.003	

AK, USA	Colville River (May to July average)	Difference in DOC before and after 30d	30	No	25	Common inoculum added	None	6.5	13.5	Linear (calc. here)	0.004	78
AK, USA	Sagavanirktok River (May to July average)							4.0	6.9		0.002	
AK, USA	Bog leachate							27.1	27		0.009	
AK, USA	Forested Wetland leachate							32.1	23		0.008	
AK, USA	Fen leachate							14.6	42		0.014	
AK, USA	Upland Forest leachate							9.2	29		0.010	
AK, USA	Bog stream	Difference in DOC before and after 30d	30	No	25	Common inoculum added	None	17.5	17.5	Linear (calc. here)	0.006	253
AK, USA	Forested wetland stream							18.7	12.6		0.004	
AK, USA	Upland forest stream							5.5	22.9		0.008	
AK, USA	Main-stem stream (Peterson Creek)							8.4	16.1		0.005	
AK, USA	Main-stem stream (McGinnis Creek)							1.4	30.1		0.010	
AK, USA	Main-stem stream (Fish Creek)							5.0	19.8		0.007	
AK, USA	Feniak streams	Percent DOC loss over time	40	Yes	20	Inoculated	None	3.7	38.1	Linear (calc. here)	0.010	115
AK, USA	Toolik streams							3.1	18.5		0.005	
AK, USA	Anaktuvuk streams							13	9.6		0.002	
AK, USA	Outflow - No thermo-degradation	DOC drawdown after 10 and 40 days	40	Yes	20	Common inoculum added	None	8.7	12.8	Linear (calc. here)	0.003	111
AK, USA	Outflow - Active thermo-degradation							27	40.9		0.010	
AK, USA	Outflow - Moderate thermo-degradation							34	31.8		0.008	
AK, USA	Outflow - Stabilized/limited thermo-degradation							13	20.6		0.005	
AK, USA	C2 Stream	Loss of DOC after incubation time	40	No	25	Glass fibre filter added to promote natural assemblage of microbes	None	3	15.3	Linear (calc. here)	0.004	112
AK, USA	C4 Stream							2.9	35.6		0.009	
AK, USA	C3 Stream							6.2	4.4		0.001	
AK, USA	S-C3a Spring							15	15		0.004	
AK, USA	S-C3b Spring							1	46.9		0.012	
AK, USA	S-C4a Spring							1.7	35.2		0.009	
AK, USA	K1 Thermokarst							37	8.9		0.002	
AK, USA	K2 Thermokarst							31	6.8			
NT, Canada	Upstream Thaw Slump	Percent loss over incubation time	28	No	20	Filt. To 0.7um with 1.2um inoc (Upstream)	None	11	1.6	Linear (calc. here)	0.001	129
NT, Canada	Within Thaw Slump							9.0	11.8		0.004	
NT, Canada	Downstream Thaw Slump							12	8.3		0.003	

Sweden	Lake	Cumulative DOC loss per unit time step	12	No	3.5	Lake Filtered to 0.7um	None	5.82	16.3	Linear	0.015	[118]
Sweden	Fen leachate							8.91	56		0.055	
Sweden	Active Layer leachate							11.29	32.5		0.034	
Sweden	Permafrost leachate							19.78	21.7		0.023	

TABLE 4.2: Initial and final dissolved organic matter (DOM) concentrations for all samples in a 30-day microbial incubation experiment. The biodegradable DOM (BDOM) is calculated as the amount of DOM lost during the experiment. Included are the final concentrations of 'Control' samples (non-inoculated water) and calculation of the minimum microbial contribution to the BDOM value (calculated as the percentage control loss subtracted from the percentage total loss). No control samples were done at Lake Hazen.

		Initial DOM	Final DOM	Total Loss (BDOM)		Final - Control	Control Loss	Min. Microbial
	Hydro. Env.	(mg C/L)	(mg C/L)	(mg C/L)	(%)	(mg C/L)	(%)	(%)
Yellowknife	Subsurface	84.2	69.7	14.4	17.1	78.2	7.1	10.0
	Pond	36.0	32.7	3.3	9.2	33.9	5.9	3.3
	Creek	15.9	13.9	2.0	12.7	14.7	8.0	4.7
Daring Lake	Subsurface	29.9	28.5	1.5	4.9	28.9	3.7	1.3
	Creek (DAR 10)	5.1	3.8	1.4	26.5	4.4	13.9	12.7
	Creek (DAR 8)	7.7	6.8	0.8	11.0	6.9	10.3	0.7
Lake Hazen	Subsurface	5.2	5.2	0.0	0.6	-	-	-
	Lake	6.2	5.9	0.3	4.7	-	-	-
	Seep	2.5	2.2	0.3	10.8	-	-	-

TABLE 4.3: The proportion of total dissolved organic matter (DOM) loss and corresponding initial and percent change in DOM composition over the 30-day microbial incubation experiment. DOM composition measures include specific UV-absorbance at 255 nm (SUVA), spectral slope between 275 and 295nm ($S_{275-295}$), dissolved organic carbon to dissolved organic nitrogen molar ratio (DOC:DON), and specific absorption coefficient at 420 nm (SAC_{420}).

		DOM Loss	SUVA		$S_{275-295}$		DOC:DON		SAC_{420}	
	Hydro. Env.	%	Initial	Change (%)	Initial	Change (%)	Initial	Change (%)	Initial	Change (%)
Yellowknife	Subsurface	17	7.7	13	1.3E-02	-1.6	56	-57	0.46	78
	Pond	9.2	7.7	4.5	1.6E-02	1.0	44	-26	0.57	3.9
	Creek	13	3.9	1.4	2.1E-02	4.2	31	-30	0.24	-9.9
Daring Lake	Subsurface	4.9	9.4	-3.1	1.3E-02	0.7	42	12	0.75	-5.0
	Creek (DAR 10)	27	4.3	20	1.7E-02	-1.7	21	-21	0.31	34
	Creek (DAR 8)	11	8.0	2.8	1.4E-02	1.1	29	-5.4	0.67	-3.6
Lake Hazen	Subsurface	0.6	6.7	-5.4	1.5E-02	4.6	28	-31	0.59	-23
	Lake	4.7	4.3	1.4	2.5E-02	-2.2	28	-20	0.19	46
	Seep	11	7.2	-1.2	1.6E-02	-3.0	13	0.2	0.58	13

TABLE 4.4: Calculated linear, 1st-order, and Reactivity-Continuum (RC) model rates (k) with standard error (SE). Linear regression and Spearman rank correlations were used to determine the goodness of fit between the data and degradation models. RC Model parameters could not be computed for DAR8, Lake Hazen lake, and Lake Hazen seep.

		Linear k			1st-order k			Reactivity Continuum Model					
	Hydro. Env.	10^{-3} (d^{-1})	SE (±)	R^2	10^{-3} (d^{-1})	SE (±)	R^2	α (d)	SE (±)	v	SE (±)	Fit	Initial k 10^{-3} (d^{-1})
Yellowknife	Subsurface	6.7	1.3	0.76	7.3	1.4	0.87	11.1	27.0	0.157	0.237	0.92	14.1
	Pond	3.7	0.8	0.58	3.9	0.8	0.87	0.8	0.2	0.026	0.002	1.00	33.9
	Creek	5.0	1.2	0.67	2.5	0.5	0.86	14.0	50.5	0.133	0.313	0.86	9.4
Daring Lake	Subsurface	1.8	0.3	0.74	1.9	0.3	0.87	9.3	17.1	0.035	0.039	0.91	3.8
	Creek (DAR 10)	9.9	2.3	0.34	11.2	2.5	0.80	0.7	1.4	0.072	0.045	0.93	99.0
	Creek (DAR 8)	3.4	1.1	0.44	3.6	1.2	0.68	-		-		-	-
Lake Hazen	Subsurface	0.3	0.2	0.07	0.3	0.2	0.39	1.5	9.4	0.003	0.007	0.55	2.0
	Lake	1.3	0.3	0.72	1.3	0.4	0.91	-		-		-	-
	Seep	3.4	0.8	0.57	3.6	0.8	0.79	-		-		-	-

TABLE 4.5: Matrix of Pearson moment correlation coefficients for dissolved organic matter (DOM), molar dissolved organic carbon to dissolved organic nitrogen ratio (DOC:DON), specific ultraviolet absorbance at 255 nm (SUVA), spectral slope between 275 and 295nm (S275-295), proportion of biopolymers (BP), proportion of humic substances (HS), proportion of low-molecular weight neutrals (LMWN), biodegradable dissolved organic matter (BDOM), Reactivity-continuum model degradation rate (k – RC), linear degradation rate (k – linear), and 1st-order degradation rate (k – first order). Highlighted cells represent significant correlations ($p<0.05$).

	DOM (mg C/L)	DOC:DON	SUVA	S275.295	SAC420	BP (%)	HS (%)	LMWN (%)	BDOM (%)	BDOM (mg C/L)	k - RC	k - linear	k - first order
DOM (mg C/L)	1												
DOC:DON	0.91	1											
SUVA	0.40	0.43	1										
S275.295	-0.42	-0.35	-0.82	1									
SAC420	0.11	0.18	0.94	-0.83	1								
BP (%)	-0.09	-0.16	-0.77	0.41	-0.76	1							
HS (%)	0.22	0.25	0.81	-0.48	0.77	-0.98	1						
LMWN (%)	-0.11	-0.21	-0.67	0.31	-0.64	0.74	-0.77	1					
BDOM (%)	0.22	-0.02	-0.31	-0.12	-0.36	0.77	-0.70	0.69	1				
BDOM (mg C/L)	0.96	0.78	0.23	-0.37	-0.04	0.06	0.06	0.11	0.38	1			
k - RC	-0.06	-0.14	-0.37	-0.01	-0.31	0.72	-0.65	0.61	0.78	0.02	1		
k - linear	0.27	0.05	-0.32	-0.13	-0.37	0.78	-0.70	0.67	0.99	0.41	0.81	1	
k - first order	0.27	0.05	-0.19	-0.23	-0.24	0.67	-0.57	0.63	0.95	0.41	0.85	0.96	1

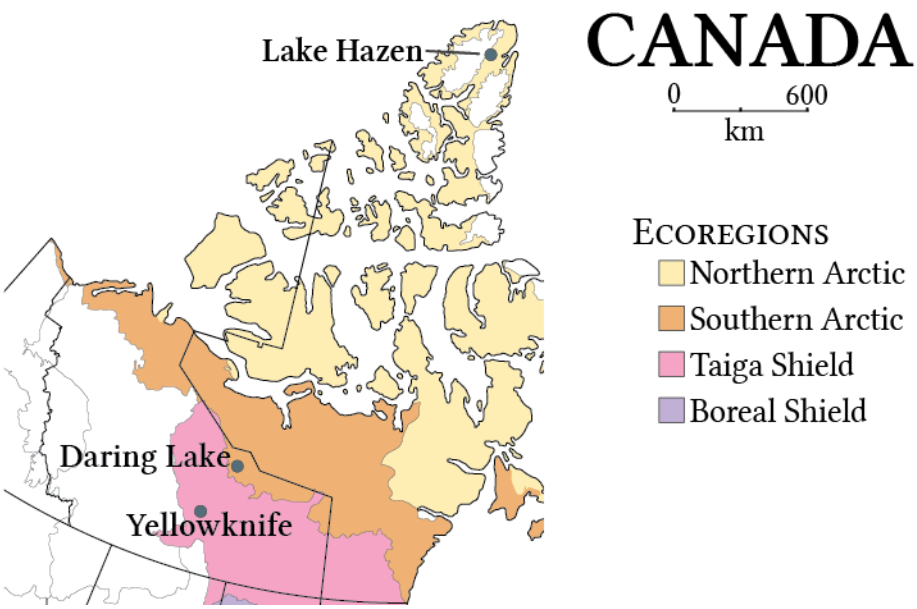

FIGURE 4.1: Locations of sampling sites and corresponding ecoregions in the Northwest Territories, Canada.

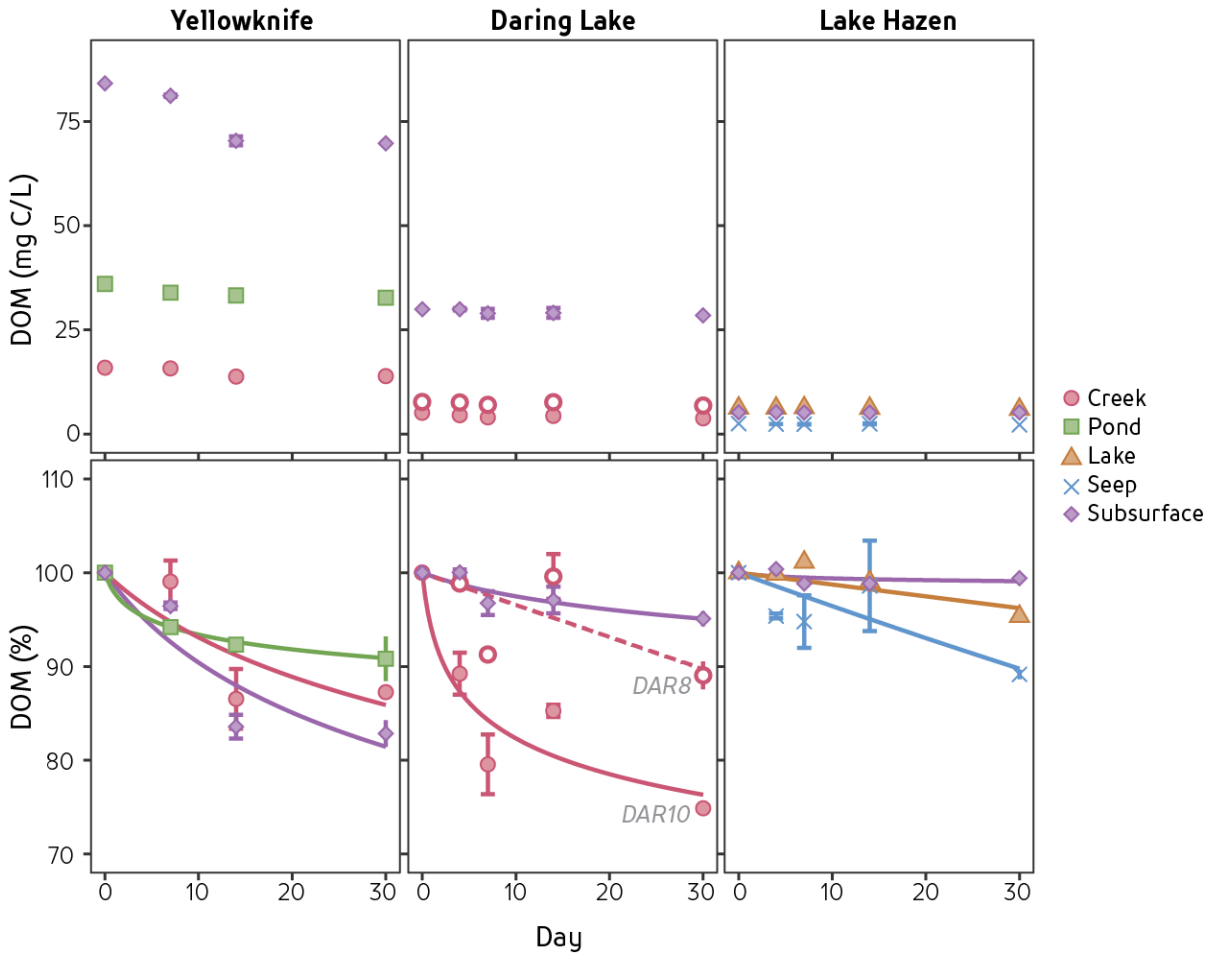

FIGURE 4.2: Changes to the overall concentration of dissolved organic matter (DOM; top panel) and proportion (bottom panel) over time for different sites.

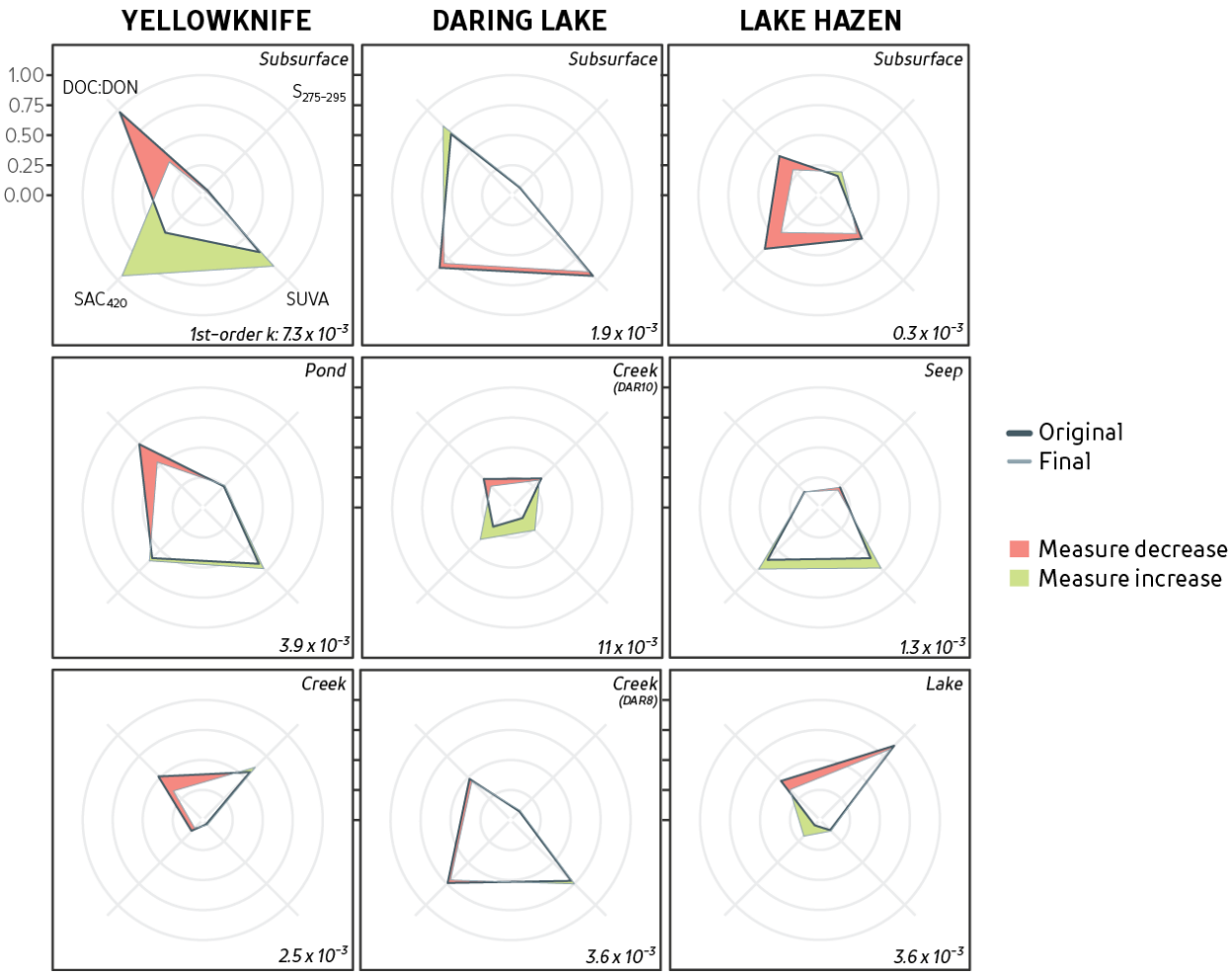

FIGURE 4.3: Composition wheels for initial (thick line) and final (thin line) dissolved organic matter for different samples. Shaded red area means a loss in parameter over the experiment, whereas green represents an increase in parameter. Value in the bottom right represents the 1st-order degradation rate constant.

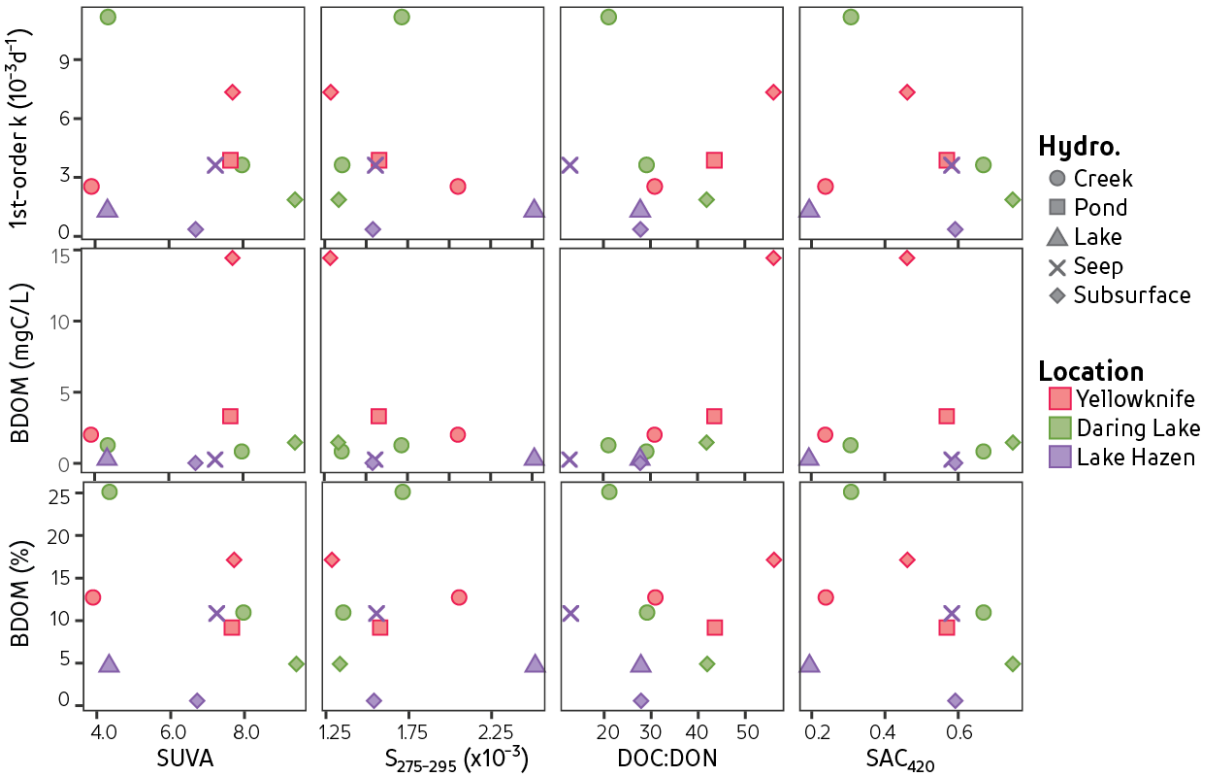

FIGURE 4.4: Degradation rate (top row), biodegradable dissolved organic carbon (BDOC; middle row), and proportion of BDOC (bottom row) for different DOM compositional measures: specific UV-absorbance at 255 nm (SUVA), spectral slope ratio between 275 and 295 nm (S275-295), molar ratio of dissolved organic carbon to dissolved organic nitrogen (DOC:DON), and specific absorption coefficient at 420nm (SAC_{420}). Symbols represent different hydrological environments while colour represent geographic location.

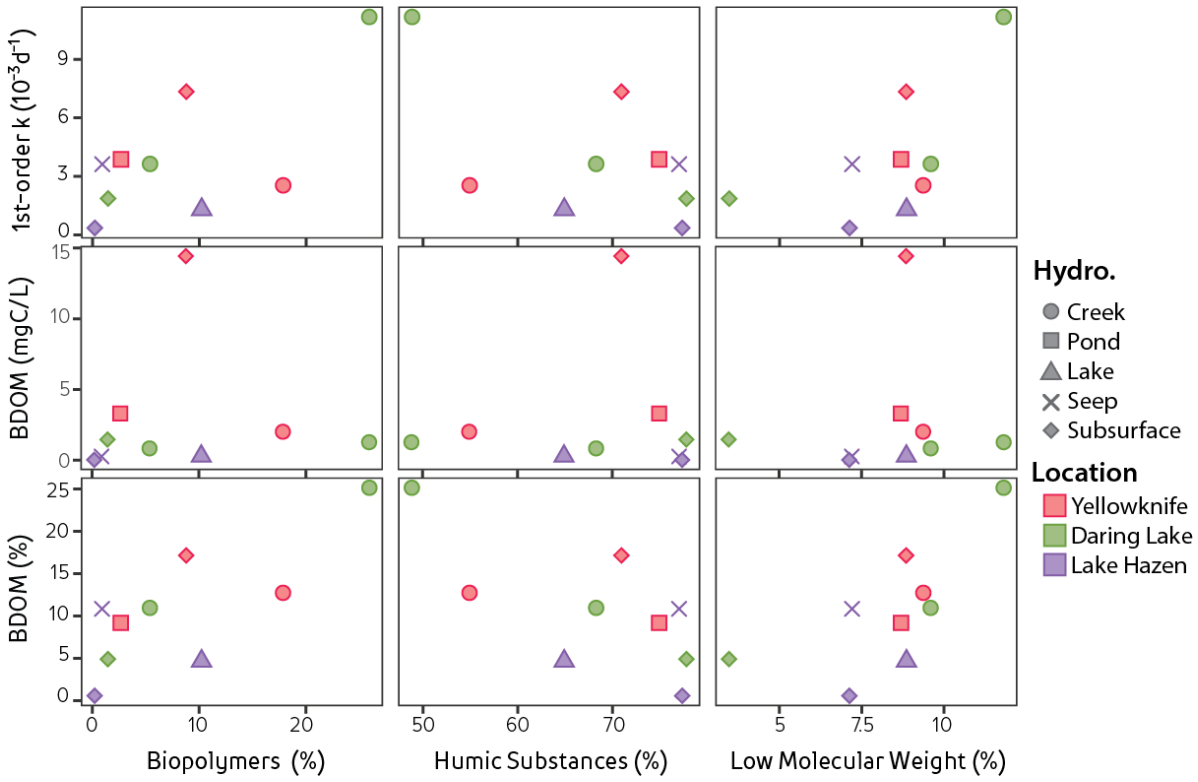

FIGURE 4.5: Degradation rate (top row), biodegradable dissolved organic carbon (BDOC; middle row), and proportion of BDOC (bottom row) for different LC-OCD groups: biopolymers (BP), humic substances (HS), and low molecular weight neutrals (LMWN). Symbols represent different hydrological environments while colour represent geographic location.

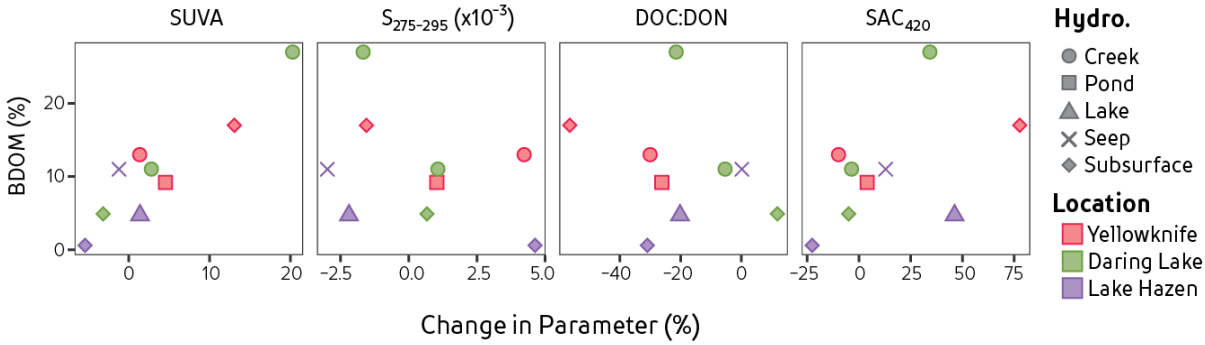

FIGURE 4.6: Percentage of biodegradable dissolved organic matter (BDOM) versus change in different compositional parameters after 30-day incubation: specific UV-absorbance at 255 nm (SUVA), spectral slope ratio between 275 and 295 nm (S275-295), molar ratio of dissolved organic carbon to dissolved organic nitrogen (DOC:DON), and specific absorption coefficient at 420nm (SAC_{420}).

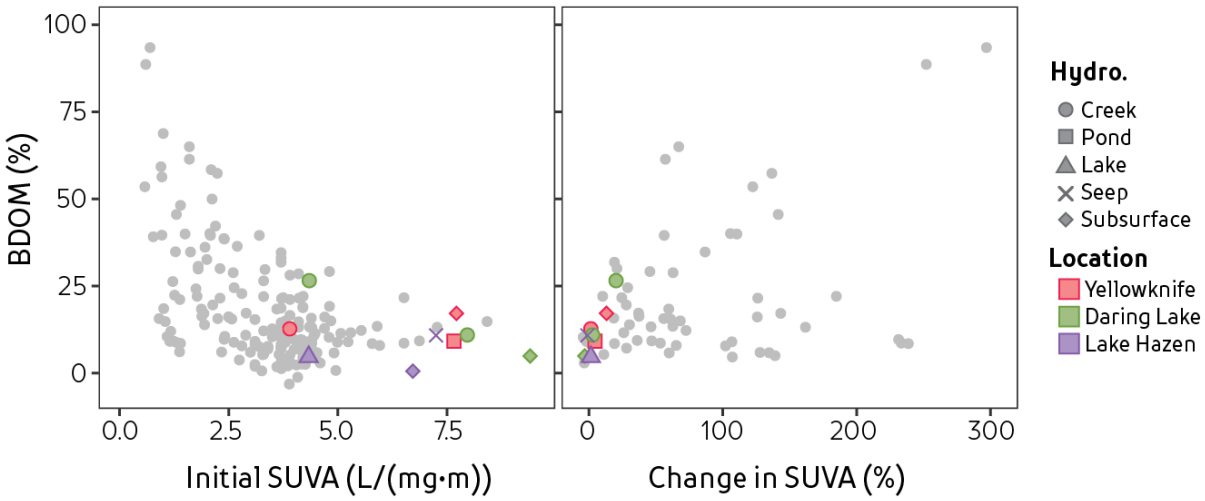

FIGURE 4.7: Percentage of biodegradable dissolved organic matter (BDOM) versus the initial specific ultraviolet absorbance at 255 nm (SUVA; left) and the overall change in SUVA during an incubation experiment (right) for data in this study (coloured) and across literature (grey dots). The literature data does not include specific hydrologic categorization (i.e. dot does not represent a creek).

Chapter 5
Dissolved Organic Matter Composition is Important for Photolysis among Surface and Subsurface Freshwaters in the Canadian Sub-Arctic and Arctic

5.1 Introduction

Dissolved organic matter (DOM) is an important constituent regulating aquatic health and quality of drinking water resources. For instance, DOM is known to absorb sunlight and regulate thermal regimes in surface waters, as well as act as an important microbial nutrient source[55,57]. In terms of carbon cycling, DOM is an important intermediary in the transfer of terrestrial carbon to the atmosphere as a greenhouse gas. The extent DOM reacts with its surroundings depends upon its concentration and composition. Various organic carbon sources and processes encountered within a watershed can influence the mixture of organic molecules that comprise DOM[49–51]. Increasing surface water DOM concentrations have been observed across the northern hemisphere [89,92] and are a concern for treatment of future water supplies[102]. However, there is much less information on how DOM composition is changing under a warming climate[141]. Hence, DOM concentration and composition are both important aspects of DOM that influence water quality.

Northern environments are undergoing vast changes in response to a warming climate that directly influences ecosystem function and carbon cycling. Permafrost degradation, increased mean annual air and subsurface temperatures, changes to lake ice, and changes to the timing and form of precipitation can alter carbon sources, rates of cycling, residences times, and flow pathways[13,15,17–19]. In particular, large reserves of carbon are currently immobilized within permafrost[162,194], yet a warming climate, and the resulting environmental consequences, have the potential to release this carbon into surrounding surface water systems[18,28,29,32]. This is of particular concern for many northern communities that rely on surface waters for fish and drinking water supplies as changes to the amount and form of DOM impacts ecosystem health and drinking water quality. Quantifying the effects and rates of DOM degradation allow for a better estimation on how quickly these changes affect DOM reactivity.

Exposure to sunlight drives changes to DOM concentration and composition. Photo-oxidation of DOM results in the production of different, lower molecular weight components or carbon dioxide (CO_2)[87,192,254]. Like any light-absorbing component, DOM absorbs among three spectral bands: ultraviolet (UV)-A (315-400 nm), UV-B (280-315 nm) and photosynthetic active radiation (PAR; 400-700 nm). Rapid attenuation of UV-radiation within the water column is due to both UV and PAR absorbing components[255]. Differences in DOM composition result in different amounts of UV attenuation within surface waters[131] and seasonal changes to DOM composition result in changes to DOM photoreactivity[256]. For instance, DOM formed from *in situ* processes (autochthonous) are less susceptible to photolysis than terrestrial-derived DOM (allochthonous)[84,254]. Aromatic components within DOM are the primary absorber of light in surface waters and have traditionally been thought to control the susceptibility of DOM to photolytic degradation[100,257]. However, recent studies have determined that aromatic components control the rate of light absorption rather than predict the degree DOM will photo-oxidize when exposed to solar irradiation[87,258]. Rates of DOM photodegradation are calculated using either 1st-order decay rates[236,259] or apparent quantum yields that focus on the photoreactions and products formed per absorbed photon[87,260]. Further, photolytic degradation rates are dependent upon the total amount of irradiation energy received rather than the instantaneous intensity [259]. Hence, monitoring DOM composition is important when quantifying the susceptibility of DOM to photo-degradation.

The degradation of DOM by sunlight is an important driver of DOM fate in northern surface waters. Arctic environments are characterized by large numbers of shallow ponds and lakes that act as biogeochemical hotspots[3,37,38] and provide ideal settings for photolytic DOM transformation. Chromophoric DOM (CDOM), defined as the part of DOM responsible for absorbing UV and PAR wavelengths, is more susceptible to photolytic degradation within northern freshwaters due to low bacterial respiration rates and the presence of shallow and unshaded surface waters[99,113]. For instance, photochemical oxidation of DOM accounted for 70 to 95% of DOM processing within arctic freshwaters and was much higher than bacterial respiration[99]. Although important for northern waters, photolysis is less important than microbial degradation on a global scale as a driver of CO_2 emissions from lakes[261]. Photolytic experiments have generally focussed on the mineralization of DOM into CO_2; however, intermediate, photochemical-transformed products are also important as they may act, depending on the microbial community, as labile substrates for

microbial mineralization[85,99,101]. Hence, surface waters in northern systems are important regulators of carbon cycling and drivers of DOM reactivity among these systems.

A number of studies have quantified the importance of photolysis as a driver of DOM quality and fate within changing arctic systems. Active-layer detachments into surface waters on Melville Island, Canada, resulted in DOM with enhanced biological and photolytic lability[136]. Further, permafrost-leached DOM from Alaska was found to be more susceptible to photo-oxidation than DOM leached from the active-layer[87]. Conversely, ancient permafrost-derived DOM in Siberian streams was not photolabile[100]. Photolytic changes to DOM can also influence aquatic health. Enhanced photoproduction within high-DOM thaw ponds on Bylot Island, Canada, increased the ponds susceptibility to methylmercury photodemethylation[262]. Most northern photolytic studies have focussed on Siberia[100,108], Alaska[85,87,99], Sweden[261,263,264], and Quebec[235,236], with few studies focussed on Canada's vast arctic[101,136]. Further, there is a need for temporal studies on DOM transformation to better understand the relative importance of different drivers of DOM fate[264].

The importance of photolysis in regulating the fate of northern DOM relies on differences in DOM composition. Northern environments have the added complexity of a rapidly warming environment and an abundance of shallow surface waters. Understanding the rate of photodegradation would help quantify how quickly DOM changes with photolysis; however, few rates have been published especially for much of Canada's sub-arctic and arctic. The objective of this paper was to quantify the rate and change in DOM due to photolysis across different hydrologic sites and ecoregions in Canada's North. This was accomplished through three parts: 1) quantify photolytic degradation rates from different sites, 2) determine how photolytic degradation influences DOM concentration and composition, and 3) determine whether DOM composition influences overall DOM degradation rate.

5.2 Methods

5.2.1 Experimental Setup

Samples were collected between June and July across three different arctic ecoregions: taiga shield (Yellowknife, NT), southern arctic (Daring Lake, NT), and northern high arctic (Lake Hazen Watershed, NU; Figure 5.1; Table 5.1). From each location, bulk surface water was collected from the surface (<0.25 m) of creeks, lakes, and ponds, while subsurface water was collected from

previously installed PVC piezometers (Yellowknife, YK) or drive-point piezometers (Daring Lake, DL, and Lake Hazen, HZ) at the deepest extent of the active-layer (~0.5 m below surface). Samples were filtered in-field to 0.45µm (Whatman GD/X 45mm), kept cool (<4°C) and dark until the experiment could be conducted at the University of Waterloo. For logistical reasons, Lake Hazen experiments were conducted at the field camp.

Filtered water was placed inside of 3 or 5 L Tedlar bags (SKC Inc., USA) using a 1:1 ratio of water to air to ensure enough oxygen was available for DOM oxidation by photolysis. All bags were placed in low-lipped white containers in full sunlight and surrounded, but not submerged, by water to minimize temperature fluctuations during the experiment. 'Light' treatments were exposed to full sunlight while 'Dark' treatments were covered with aluminum foil to observe the final loss of DOM over the course of the experiment without sunlight exposure. Bags were gently agitated each day to avoid anoxia and maintain a mixed sample. Samples were either taken before and after the experiment (YK) or every few days (DL and HZ), at which point the known volume of removed water was replaced with an equal volume of ambient air as to not create any pressure differences between air and water. The amount of visible light over the duration of the experiment was quantified using a PAR sensor (HOBO, Hoskin Scientific) logging PAR measurements every 1-5 minutes. Cumulative PAR was calculated by averaging the PAR measurements over the logging interval, multiplying it by the time step, and adding it to the previous cumulative PAR value. Although PAR measurements were taken outside the bag, attenuation of UV-A and PAR by Tedlar bags has been shown to be minimal[265].

5.2.2 Laboratory Analyses

All samples were run for concentrations of dissolved organic carbon (DOC) and total dissolved nitrogen (TN) using a Shimadzu Total Organic Carbon (TOC-L) Combustion Analyzer with TNM-1 module (precision of ±0.3 mg C/L; ±0.3 mg N/L). Dissolved organic nitrogen (DON) was calculated as the difference between TN concentration and sum of the inorganic-nitrogen species (nitrate, nitrite, and ammonium). Inorganic nitrogen species were measured using a SmartChem 200 Automated Chemistry Analyzer (NO_2^- and NH_4^+ precision of ±0.1 mg N/L; NO_3^- precision of ±0.15 mg N/L; Unity Scientific, MA United States).

Absorbance of DOM was measured using a Cary 100 UV-VIS Spectrophotometer (Agilent, CA United States) at 5 nm increments from 200 to 800 nm. Deionized water was used to zero the

machine, and run intermittently during analyses to correct for baseline drift. The Naperian absorption coefficient (a; m^{-1}) was calculated using:

$$a_\lambda = \frac{ln(10) \times A_\lambda}{L}$$

where A is the baseline-corrected absorbance at wavelength λ and L is the cell length (m). Specific absorption coefficients at 255 nm (SUVA), 350 nm (SAC_{350}) and 420 nm (SAC_{420}) were calculated by dividing a_λ by the overall DOM concentration.

Initial DOM composition was further characterized using liquid chromatography organic carbon detection (LC-OCD)[75]. Briefly, the sample passed through a size-exclusion column (SEC; Toyopearl HW-50S, Tosoh Bioscience) and was separated based on hydrodynamic radii into five hydrophilic fractions defined by Huber et al. (2011)[75]. Here we compare the proportions high molecular weight components (HMW; the humic substances fraction and 'Building Blocks') and low-molecular weight neutrals (LMWN). The precision for the LC-OCD is less than ±0.09 mg C/L for all fractions.

Composition Wheels (CW) were used to compare differences in DOM composition over the course of the experiment (Chapter 3). This method creates a polygon from four measures that relate to different DOM characteristics. Values for each parameter were normalized to the maximum and minimum values encountered from a larger DOM dataset that encompassed various ecoregions across Canada. The selected measures were DOC:DON (measure of DOM source and lability[78]), $S_{275\text{-}295}$ (molecular size[199]), SUVA (UV-absorbing components[71]), and SAC_{420} (visible absorbing components and humics[92]). These specific measures provide information on different aspects of DOM composition, are easily measured, and are commonly used in other studies.

5.2.3 Calculation of Photolabile DOM & Photolytic Rates

Among northern-based photolytic experiments, the total loss in DOM concentration with cumulative irradiation has been used to represent the proportion of photolabile DOM and determine photodegradation rates[100,101,236]. One study defined photolabile DOM to be the difference between light and dark treatments, but did not calculate rates[108]. Here the proportion of photolabile DOM is calculated as the amount of DOM lost within the Light treatment subtracted from DOM lost within the Dark treatment. However, for comparative reasons, rate calculations are determined from total DOM loss in Light treatments only. First-order degradation rates are quantified using DOM concentrations from the Light treatments with more than two time points using:

$$\frac{DOM}{DOM_0} = e^{-k \cdot PAR}$$

where DOM represents the concentration of DOM of a sample (mg C/L), DOM_0 is the initial DOM concentration, k is the first-order degradation rate constant (m^2/E), and PAR is the cumulative PAR at that time (E/m^2). A 0-order equation was used for samples with only two time points (initial and final):

$$DOM = -k \cdot PAR + DOM_0$$

The concentration of DOM lost after 500 E/m^2 was calculated using the previously calculated linear or 1st-order degradation rate constants. This PAR value represented an average amount of solar radiation that all samples were exposed and allowed for the comparison of DOM lost to different locations with different cumulative PAR exposures.

Statistical correlations between degradation rates and DOM composition measures were calculated using a Spearman rank correlation to better account for outliers and non-linear relationships. All analyses were conducted in R[212].

5.3 Results

5.3.1 Initial DOM Characteristics

Initial DOM concentrations were highest from subsurface sites at YK and DL and lowest from YK and DL creeks and a HZ seep (Table 5.2). Overall, YK contained higher DOM concentrations than either DL or HZ. The range in DOM concentrations encountered were low at HZ (from 2.3 to 6.1 mg C/L) compared to either DL or YK. DOM concentrations at DL and YK were notably higher among subsurface sites than any of the surface water sites (Table 5.2). Differences in DOM concentration reflect both a latitudinal gradient, with lower concentrations observed at northern sites, and between subsurface and surface water DOM.

DOM composition varied among and across all three sampling locations (Figure 5.2). YK subsurface and pond samples were characterized by high DOC:DON, SUVA, and SAC_{420}, and low $S_{275\text{-}295}$. Creek and river DOM at YK differed from subsurface DOM by having lower SUVA and SAC_{420} and higher $S_{275\text{-}295}$. Similar compositions between the DL subsurface and creek (DAR8) samples were identified by high SUVA and SAC_{420} compared to the other creek sample (DAR10).

DL samples contained lower DOC:DON than YK. Similar to YK and DL subsurface samples, HZ subsurface contained higher SAC_{420} and SUVA than HZ lake. HZ lake contained higher $S_{275-295}$ than other HZ DOM, while DOC:DON values were similar across HZ samples. Seep DOM from HZ closely resembled HZ subsurface except for the higher SUVA in seep DOM. Surface water DOM composition varied across all three locations, yet subsurface DOM composition was similar across the three locations.

5.3.2 Photolytic Degradation – DOM Concentration & Composition

Exposure to sunlight resulted in decreases to DOM concentration across most sites (Figure 5.3). Different total cumulative PAR amounts ranged between 290 to 1030 E/m^2 as a result of conducting experiments in the natural environment rather than a solar simulator. The highest proportion of total DOM loss across all sites was observed in subsurface samples (Figure 5.4). The proportion of total photo-labile DOM ranged from 20-35% in subsurface samples to negligible loss in surface waters (Table 5.2). Little difference in concentration between Light and Dark treatments were observed for YK river and all HZ samples, while DL creek (DAR10) concentration did not change. Although DOM decreased in the Dark treatments, for most sites photolysis in Light treatments generally lead to a greater loss of DOM. Further, a subset of samples analysed for dissolved inorganic carbon (DIC) concentrations indicated higher DIC in the photolysed sample than either the original or dark (Appendix C). Hence, changes to DOM concentration and composition are related to the influence of photolysis.

Across all sites, subsurface samples contained higher 1^{st}-order photolytic degradation rates than surface waters. Although all samples could be compared using linear degradation rates, with highest rates found from subsurface DOM (Table 5.3), photolysis is best represented using a 1^{st}-order rate equation. Linear rates would over-calculate DOM loss at higher cumulative PAR values. Highest 1^{st}-order DOM degradation rate constants were observed from DL subsurface (1.7×10^{-3} m^2/E) and creek (9.6×10^{-4} m^2/E) and lowest from HZ surface waters (Table 5.3; Figure 5.4). Similar photolytic degradation rates were found between YK and HZ subsurface samples. Comparing 1^{st}-order degradation to initial DOM composition identified strong relationships but no statistical significance with any compositional metric (Figure 5.5). High 1^{st}-order rates were observed from DOM with high values of SUVA and SAC_{420} or low $S_{275-295}$. Across all sites, subsurface DOM characteristics resulted in higher 1^{st}-order photolytic degradation rates.

The amount of cumulative irradiation was normalized to compare the amount of DOM lost during photodegradation across sites. The proportion of DOM lost after 500 E/m^2 ranged between 3.7 to 19% for most samples, except for DL samples that contained the highest proportions (subsurface: 58%; DAR8: 38%). Higher DOM amounts were lost from sub-arctic subsurface DOM after 500 E/m^2 (between 11.5 and 17.7 mg C/L; Table 5.3) while lower concentrations were lost from a YK river (0.2 mg C/L) and both HZ surface waters (lake: 0.5 mg C/L ; seep: 0.3 mg C/L). Comparison of initial DOM composition with proportion of DOM loss found strong, statistically significant correlations with $S_{275\text{-}295}$ (ρ: -0.618, $p=0.05$), SUVA (ρ: 0.664, $p<0.05$) and SAC_{420} (ρ: 0.645, $p<0.05$), but no correlation with DOC:DON (Figure 5.6). Size-based chromatography did not result in significant relationships between proportion loss and either HMW or LMW components, but a greater proportion loss was found from samples with high HMW DOM (Figure 5.7). A similar result was observed between 1st-order rates and HMW and LMWN proportions, with higher rates associated to DOM with higher HMW proportions. Thus, initial DOM composition can be used to predict the proportion and rate of DOM lost to photolysis.

Photolysis resulted in similar changes to the overall composition of DOM across all sites. Dark treatment samples contained compositions more similar to the original composition than the Light treatment, indicating changes to DOM due to photolytic degradation. Final compositions had lower DOC:DON, SUVA, and SAC_{420}, and higher $S_{275\text{-}295}$ than initial compositions (Figure 5.8). Similarities in the final DOM composition were observed among HZ samples, DL creek (DAR10), YK creek, and YK river. These samples had high $S_{275\text{-}295}$ and low SUVA and SAC_{420}. The effect of photolysis was similar across a variety of DOM compositions from different sites. In some cases, photodegradation resulted in similar final DOM compositions regardless of initial DOM amount or composition.

5.4 Discussion

5.4.1 Similarity in the Response of DOM to Photolytic Degradation

A number of samples with different DOM compositions all responded similarly to photolysis. For instance, a suite of complementary measures simultaneously shifted towards a unique composition: increased spectral slope indicating loss of large, UV-absorbing components with a decrease to DOC:DON ratios (Figure 5.8). Similarly, photolytic incubations of DOM from Southern Ontario surface waters[266], boreal forest[267], tundra thaw ponds[101], and a Siberian river underlain by

continuous permafrost[108] resulted in a decrease to terrestrial-derived humics, aromatics, and CDOM components, and an increase in protein-like fluorescence and LMW components. Data from this study illustrates how photolysis results in predictable changes to DOM composition, regardless of initial composition, that results in a reduction to both the amount and heterogeneity of DOM within the environment.

Sampling along a latitudinal gradient encompassed sites that were quite different in terms of vegetation and terrestrial sources of DOM. However, as discussed earlier in Chapter 3, DOM composition is not that different across locations (i.e. subsurface looks like subsurface; Figure 5.2). In particular, subsurface sites contained a unique compositional signature across all locations, identified by higher compositional metrics than surrounding surface water DOM, and contained the most photo-labile components. These environments form humic and aromatic terrestrial components that are light-sensitive[84,136,254] contributing to higher concentrations of photo-labile DOM when exposed to light. Although the high photolability of subsurface or terrestrial DOM has been observed in other northern systems[136,209,263], we further show how surface water DOM with terrestrial-like signatures result in higher rates and proportions than other surface waters. For instance, YK pond, DL creek (DAR8), and HZ seep are similar to their respective subsurface DOM and were more photolytically labile than nearby surface water DOM (Figure 5.8). Thus, we are able to characterize specific compositional metrics that relate to the degree of DOM photo-lability observed among different environments.

5.4.2 Quality over Quantity: DOM Composition Influences Photolytic Degradation

A number of cumulative factors affect the overall rate of photolytic degradation within surface water systems. Hydrology (such as mixing, surface water depth, and residence time), irradiation intensity (clouds and latitude), other suspended or dissolved constituents influencing attenuation coefficients (such as particulate matter or iron), and the amount and form of CDOM can all affect DOM photodegradation[84,113]. Hence, experimentally derived rates of DOM decomposition may differ than what is actually found within the environment. Although these factors were not in the scope of this study, our objective was to quantify the rate and interaction between photolysis and DOM composition, assessing how intrinsic properties regulate or alter photolability across northern sites.

Quantifying degradation rate and proportion of photo-labile DOM in this study provided data for an area of the circumpolar north underrepresented in the literature. Photolytic degradation rates are important to determine as they can be used to better predict the response of DOM and refine carbon flux estimates under various future climate scenarios. The variability among subsurface and surface water 1st-order degradation rate constants (4x and 6x, respectively) provide a possible range of values to be used to model photolytic degradation in these systems. Comparison of our results with reported values elsewhere are difficult due to differences in experimental design, such as use of natural sunlight versus solar simulators, or the amount of total irradiation. Calculation of a photo-labile yield (the concentration of photo-labile DOM divided by the cumulative irradiation) across studies indicate lower yields from samples in this study compared to others (Table 5.4). Thus, DOM from these sites contain lower proportions of photo-labile components compared to other northern sites, but still exhibit some degree of photolability with degradation constants within a relatively constrained range.

Photolysis can alter the composition of DOM with little influence on the overall DOM concentration, as was observed in DOM from HZ and a DL creek (Table 5.2; Figure 5.3). For instance, DAR10 had little decrease in DOM concentration but its final composition reflected photo-processing through increased spectral slope and decreased DOC:DON and SUVA values (Figure 5.8). Similarly, significant losses to UV-absorbing components with no change in fulvic and humic concentrations were observed during photolytic degradation of Alaskan stream and lake DOM[268], while changes to CDOM were greater than changes in overall DOM concentration within Canadian thaw ponds[101]. Further, photochemical processes were unimportant in terms of DOM cycling within an estuary along the Texas coast due to the lack of absorbing components and greater importance of biological processes within the system[269]. Such changes are thought to result from photolytic changes to larger molecules without fully mineralizing these products into CO_2[209]. Stubbins et al.[100] found photo-modification of permafrost DOM to occur with little loss to DOM concentration, suggesting photo-induced cleaving of aromatics into non-coloured, non-aromatic DOM. Changes to DOM composition that occur independently of its overall concentration highlight the importance of monitoring DOM characteristics that directly influence DOM quality and reactivity across the aquatic continuum.

5.4.3 Importance of Photolysis in Relation to Ecosystem Processes

Rates of photolytic degradation can be compared to microbial rates from Chapter 4 to elucidate the relative importance of these two drivers of DOM fate. Although the rate constants contain different units, the proportion of DOM remaining after photolytic or microbial degradation can be compared after 30 days (Table 5.5). Average daily PAR values for YK and DL were assumed to be 39.5 E/(m^2·d) (eight year average from May to August at Daring Lake[270]) and 28 E/(m^2·d) for HZ (ocean near south-eastern Ellesmere Island[271]). Over the month, photolysis plays a greater role degrading and altering DOM composition. However, attenuation of UV and PAR within the water column could alter the amount of processing within coloured or deep surface waters, altering the amount of DOM available for photolysis. These experiments provide a way to quantify the impact of each degradation pathway separately, but in reality there is likely interplay between the two. For instance, photolysis produces more labile components that would enhance microbial degradation[85,101]. Regardless, these rates allow for the comparison of different drivers of DOM fate across a variety of DOM compositions.

Although location was more important for microbial degradation than initial DOM composition (Chapter 4), we find DOM composition to be important for photolytic lability. Similar changes in DOM composition were observed across locations and the proportion of DOM loss was predicted by initial SUVA or SAC_{420} values (Figure 5.6). Further, not all metrics respond the same way and specific indicators of processing can be identified based on differences to the change in DOM composition. Decreases to SUVA and SAC_{420} during photolysis are opposite to microbial-induced changes to DOM composition. Further, $S_{275\text{-}295}$ only responded to photolytic degradation, indicating that these measures are useful indicators of processes. These results highlight the use of certain DOM composition metrics to discern processing history.

DOM concentrations represent the largest difference among sites and can be important when considering carbon export. The circumpolar north contributes large amounts of organic carbon to the Arctic Ocean relative to all other basins[272]. Hence, the degree of processing among the terrestrial landscape will dictate organic carbon fate and reactivity in the ocean. Our results found similar losses in the amount of DOM (after 500 E/m^2) between hydrologic sites across geographic locations (Table 5.3); however, this loss comprised much more of a significant proportion of DL subsurface DOM than at YK. The high arctic subsurface had comparable 1st-order degradation rates as YK subsurface DOM, yet the low overall loss in DOM concentration (between 0.4 and 1.1 mg C/L)

may make it a minor influence for downstream systems. In terms of carbon export and cycling, subarctic and low arctic sites contain higher proportions of photo-labile carbon than the high arctic.

The impact of changing DOM sources or solar UV radiation upon the environment are complex and can have significant and uncertain effects upon the fate of DOM in northern systems[33,273]. Coloured DOM has been observed to preferentially degrade in sunlight[225,274]; however, this is not always the case and may depend upon whether the system is dominated by 'brown water' or 'clear water' regimes[264]. Dark water colour among certain Swedish lakes were found to be consistent across a seven-year record as CDOM-removing processes were too slow to result in measurable declines in water colour, suggesting some regimes may remain 'brown'. Alternatively, clear-water regimes were found in lakes where photochemical processing led to significant decreases in DOM and CDOM[264]. The ability to predict how drivers of degradation alter DOM composition becomes increasingly important to quantify as the subsequent impact upon water transparency negatively affects fish, thermal regimes, and other important ecosystem processes that impact aquatic health[55,56,275].

A similar hypothesis proposed by Cory et al.[113] focussed on 'process' rather than 'regime', finding photolytic loss of DOM to reflect either light-limited systems (high CDOM concentrations or low light exposure) or substrate-limited systems (high photolability or low CDOM concentrations). Our results support this hypothesis as high concentrations and little change to the overall molecular weight of UV-absorbing constituents, as defined by $S_{275\text{-}295}$, suggested YK and DL subsurface DOM may represent light-limited systems with high CDOM concentrations (Figure 5.8). Conversely, YK creek, river and all HZ samples support substrate-limited systems due to large changes to DOM composition and low initial water colour. Linking DOM composition with ecosystem functioning provides information on how these systems will respond to changing landscape drivers[141]. Hence, characterizing DOM composition can help predict the susceptibility of a watershed to a changing climate in terms of DOM evolution and water clarity.

5.5 Conclusion

A uniform response in DOM composition to photolysis was observed across all sites and was comparable to photolytic-induced changes to DOM reported in literature elsewhere. In general, reductions in DOM concentration due to photolysis resulted in decreases to the molecular weight of UV-absorbing components, regardless of differences in initial DOM composition and concentration.

First-order photolytic degradation rates ranged from $1.6x10^{-4}$ m^2/E in DOM from a high arctic lake to $1.7x10^{-3}$ m^2/E in DOM from the tundra subsurface. Initial DOM composition is an important determinant for the proportion of DOM loss due to photolysis. Not all metrics respond the same way, with decreases to SUVA and SAC_{420} representing sensitive indicators of photolysis. However, compositional measures could not provide statistically-significant relationships to 1^{st}-order degradation rate constants. These results highlight how DOM with different compositions respond to photolytic degradation across a variety of ecoregions. Differences in the magnitude of change among samples support the occurrence of light or substrate based systems that identify the dominant drivers of DOM fate within northern surface waters. Quantifying the range in photodegradation rates with a suite of DOM characterization methods evidences the similarity in DOM response to photolytic degradation across different ecoregions in Canada's arctic and the use of specific measures, such as SUVA, $S_{275-295}$, and SAC_{420}, to discern between different degradation processes.

Table 5.1: Site descriptions for each sample used in the photolytic experiment.

Location	Site Characteristics	Sample	Info
Yellowknife	62° 27' 14"N, 114° 22' 18"W; Taiga Shield High Boreal, landscape characterized by Precambrain bedrock outcrops, glaciolacustrine sediments, and peat plateaux; mean annual precipitation between 280-360 mm; mean annual temperature between -3 to -6C; trees consist of jack pine and aspen; underlain by sporadic discontinuous permafrost	Subsurface 1 (P2)	~0.89 m.b.g.s; located ~40m away from Pond
		Subsurface 2 (P5)	~0.27 m.b.g.s; located ~40m away from Pond
		Pond	10300m2; surrounded by peat plateaux
		Creek	Baker Creek, drains series of lakes on Taiga Shield
		River	Yellowknife River, drains chain of lakes on Taiga Shield
Daring Lake	64° 31' 29"N, 111° 40' 24"W; Tundra Shield Low Arctic; mean annual precipitation 201-300mm; mean annual temperature -9 to -12C; fractured Precambrian granite and sedimentary bedrock with small eskers and erratics; above treeline, mesic heath upland to moist shrub lowland, underlain by continuous permafrost	Subsurface	Esker Lakes Basin
		Creek 1 (DAR8)	Peregrine Basin inflow to Daring Lake, longer lower section of lateral flow through shrub/meadow adjacent areas
		Creek 2 (DAR10)	Raven Basin inflow to Daring Lake, upland and topography, less organic plateaus and more exposure/retention in lakes
Lake Hazen	81° 49' 30"N, 71° 19' 26"W; Polar desert; bedrock consists of calcareous and dolomitic sandstone with igneous intrusions within the Grant Land Mountains; mean annual precipitation of <150mm; mean annual temperature -20°C; heavily glaciated dominated landscape that also contains small, productive subcatchments in a thermal oasis; continuous permafrost	Subsurface	~0.25 m.b.g.s; productive meadow, underlain by mineral-rich sediment, next to 'Lake'
		Lake	14,400 m^2 and 4.5m maximum depth; samples taken near shore
		Seep	Seasonal spring at relatively high elevation; flows out from rock talus slope

TABLE 5.2: Changes in dissolved organic matter (DOM) concentration for the samples exposed to light ('Final-Photo') and those that were not ('Final-Dark'). Calculation of photolabile DOM included the difference between light and dark treatments. Included are the amount of cumulative photosynthetic active radiation (PAR) for each sample.

			DOM		**Total Loss**	**Photolabile**	**Cumulative PAR**
Location	**Sample**	Initial	Final - Photo	Final - Dark	Prop. of DOM	Prop. of DOM	E/m^2
Yellowknife	Subsurface 1 (P2)	83.6	58.3	75.2	30%	20%	1030
	Subsurface 2 (P5)	72.6	59.6	74.9	18%	21%	1030
	Pond	36.8	31.2	-	15%	-	514
	Creek	15.6	12.8	-	18%	-	514
	River	5.03	4.65	4.81	8%	3%	1030
Daring Lake	Subsurface	30.4	18.5	29.1	39%	35%	290
	Creek 1 (DAR8)	7.61	5.76	7.82	24%	27%	290
	Creek 2 (DAR10)	4.80	4.98	5.02	-4%	1%	290
Lake Hazen	Subsurface	5.28	4.17	4.39	21%	4%	619
	Lake	6.05	5.44	5.41	10%	-1%	619
	Seep	2.29	1.93	2.06	16%	6%	619

TABLE 5.3: Calculated linear and 1st-order degradation rates with standard error (SE) and model fit results. The loss in dissolved organic matter (DOM) after 500 E/m^2 of irradiation is based on previously calculated degradation rates. Linear rates are used to calculate the loss after 500 E/m^2 for those samples without 1st-order rates.

		Linear *k*			**1st-order *k***			**Loss after 500 E/m^2**	
Location	**Sample**	m^2/E	SE (±)	R^2	m^2/E	SE (±)	Fit	mg C/L	Prop. of DOM
Yellowknife	Subsurface 1 (P2)	3.0E-02	3.0E-03	0.95	4.2E-04	3.3E-05	0.97	15.8	19%
	Subsurface 2 (P5)	1.3E-02	-	-	-	-	-	6.31	8.7%
	Pond	1.1E-02	-	-	-	-	-	5.45	15%
	Creek	5.5E-03	-	-	-	-	-	2.73	17%
	River	3.7E-04	-	-	-	-	-	0.18	3.7%
Daring Lake	Subsurface	4.3E-02	2.9E-03	0.98	1.7E-03	5.6E-05	0.99	17.7	58%
	Creek 1 (DAR8)	6.4E-03	1.0E-04	0.99	9.6E-04	6.4E-06	0.99	2.89	38%
	Creek 2 (DAR10)	-4.3E-04	4.2E-04	0.53	-	-	-	-0.21	-4.4%
Lake Hazen	Subsurface	2.0E-03	1.5E-04	0.94	4.2E-04	3.4E-05	0.97	1.00	19%
	Lake	9.4E-04	3.2E-05	0.99	1.6E-04	6.1E-06	0.99	0.47	7.8%
	Seep	6.1E-04	3.8E-05	0.97	2.9E-04	1.9E-05	0.98	0.31	13%

TABLE 5.4: Percentages of total dissolved organic matter (DOM) from this study (Yellowknife (YK), Daring Lake (DL), Lake Hazen (HZ)) compared to published values in other northern environments. Photolabile concentrations were included in brackets (calculated as loss of DOM in dark subtracted from the light treatment and divided by the initial DOM concentration). Only Mann et al. (2012) calculated photolabile DOM in a similar manner. Included are the methods of photolytic degradation, total amount of irradiation the sample received, and photolabile yield (the concentration of DOM lost divided by the total amount of irradiation). Yields were not calculated for Mann et al. (2012) and Vachon et al. (2017) due to insufficient information.

Location	Hydro	Initial DOM (mg C/L)	DOM Loss (%)	Photolysis Method	Amount of Irradiation	Units	Photolabile Yield	Reference
YK	Subsurface 1 (P2)	83.6	30 (20)	Natural sunlight	1030	E/m^2	1.6E-02	This Study
	Subsurface 2 (P5)	72.6	18 (21)	Natural sunlight	1030	E/m^2	1.5E-02	
	Pond	36.8	15	Natural sunlight	514	E/m^2	-	
	Creek	15.6	18	Natural sunlight	514	E/m^2	-	
	River	5.0	8 (3)	Natural sunlight	1030	E/m^2	1.5E-04	
DL	Subsurface	30.4	39 (35)	Natural sunlight	290	E/m^2	3.7E-02	
	Creek 1 (DAR8)	7.6	24 (27)	Natural sunlight	290	E/m^2	7.1E-03	
	Creek 2 (DAR10)	4.8	-4 (1)	Natural sunlight	290	E/m^2	1.4E-04	
HZ	Subsurface	5.3	21 (4)	Natural sunlight	619	E/m^2	3.5E-04	
	Lake	6.1	10 (-1)	Natural sunlight	619	E/m^2	-5.7E-05	
	Seep	2.3	16 (6)	Natural sunlight	619	E/m^2	2.1E-04	
Siberia	Permafrost Thaw Stream	3	-3	Solar Simulator	6	E/m^2	-1.6E-02	[100]
	Stream (Y3)	24.4	40	Solar Simulator	6	E/m^2	1.7E+00	
	Stream (Y4)	21.4	28	Solar Simulator	6	E/m^2	1.0E+00	
	Pantileikha River	12.1	31	Solar Simulator	6	E/m^2	6.6E-01	
	Kolyma River Mainstem	4.8	26	Solar Simulator	6	E/m^2	2.2E-01	
	Kolyma River Main	8.6 to 13.9	12.2 to 29.9*	Natural sunlight	14	days	-	[108]
Quebec	Lac Simoncouche	6.3	12	Solar Simulator	1000	KJ/m^2	-	[236]
	Chicoutimi	8.2	30	Solar Simulator	1500	KJ/m^2	-	
	Abitibi	11.1	21	Solar Simulator	2550	KJ/m^2	-	
Bylot Island	BYL1	8.5	3	Natural sunlight	0.119	E/m^2	2.1E+00	[101]
	BYL38	13.1	-4	Natural sunlight	0.119	E/m^2	-4.4E+00	

TABLE 5.5: Comparison of photolytic degradation rates with microbial degradation rates calculated in Chapter 4 and the proportion of DOM remaining after 30 days of photolytic or microbial degradation. Average daily photosynthetic active radiation (PAR) values for Yellowknife and Daring Lake were assumed to be 39.5 E/(m^2 d) (eight year average from May to August at Daring Lake[270]) and 28 E/(m^2 d) for HZ (ocean on south-eastern Ellesmere Island[271]).

		Photolysis		**Microbial**		**PHOTOLYSIS**	**MICROBIAL**
Location	**Sample**	Linear (m^2/E)	1st Order (m^2/E)	Linear (d^{-1})	1st Order (d^{-1})	*Prop. After 30d*	*Prop after 30d*
Yellowknife	Subsurface 1 (P2)	3.0E-02	4.2E-04	6.7E-03	7.3E-03	0.61	0.80
	Subsurface 2 (P5)	1.3E-02	-	-	-	0.79*	-
	Pond	1.1E-02	-	3.7E-03	3.9E-03	0.65*	0.89
	Creek	5.5E-03	-	5.0E-03	2.5E-03	0.59*	0.93
	River	3.7E-04	-	-	-	0.91*	-
Daring Lake	Subsurface	4.3E-02	1.7E-03	1.8E-03	1.9E-03	0.13	0.95
	Creek 1 (DAR8)	6.4E-03	9.6E-04	3.4E-03	3.6E-03	0.32	0.90
	Creek 2 (DAR10)	-4.3E-04	-	9.9E-03	1.1E-02	1.11*	0.72
Lake Hazen	Subsurface	2.0E-03	4.2E-04	3.4E-04	3.5E-04	0.70	0.99
	Lake	9.4E-04	1.6E-04	1.3E-03	1.3E-03	0.87	0.96
	Seep	6.1E-04	2.9E-04	3.4E-03	3.6E-03	0.79	0.90

*Linear photolytic degradation rate used

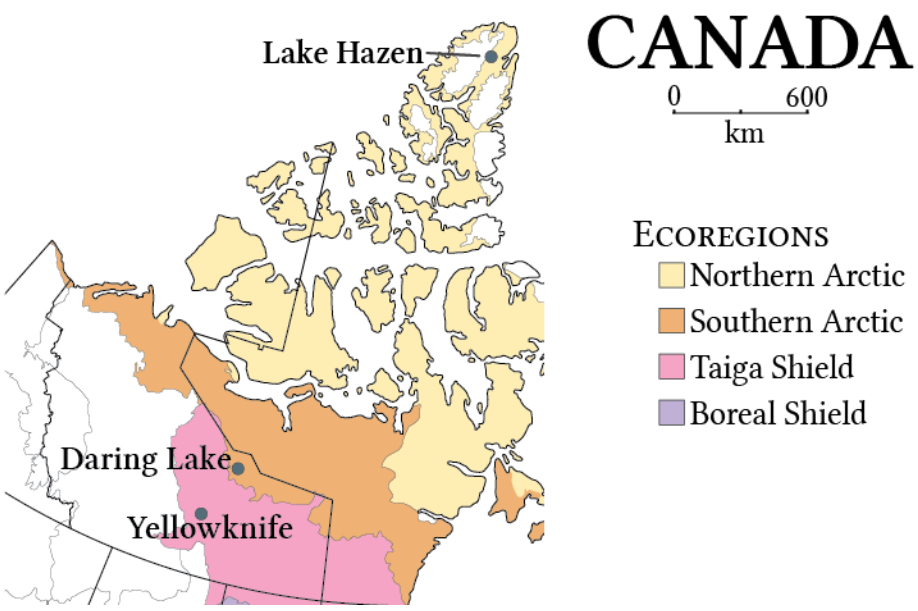

FIGURE 5.1: Locations of sampling sites and respective ecoregion [276]

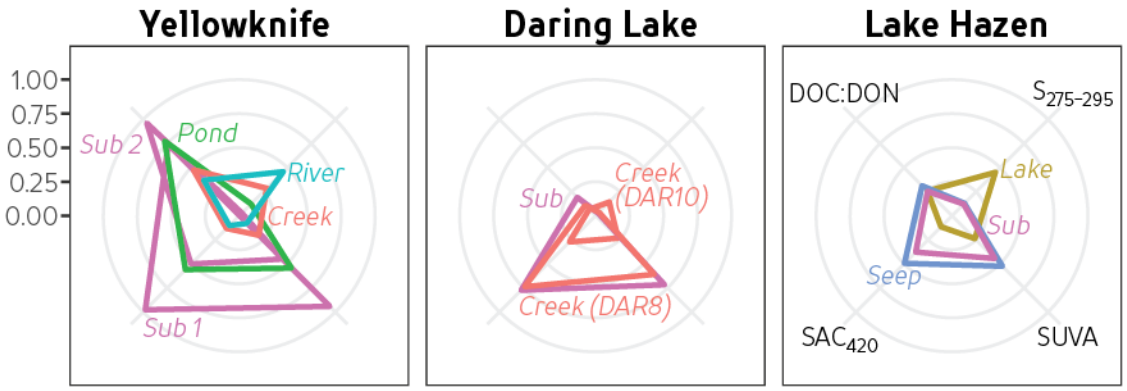

FIGURE 5.2: Initial dissolved organic matter (DOM) Composition Wheel for all samples. Each axis is normalized for the maximum and minimum value for each parameter: molar DOC:DON, slope from 275 to 295nm (S275), specific UV-absorbance at 255nm (SUVA), and specific absorption coefficient at 420nm (SAC420). Colours represent different hydrological environments.

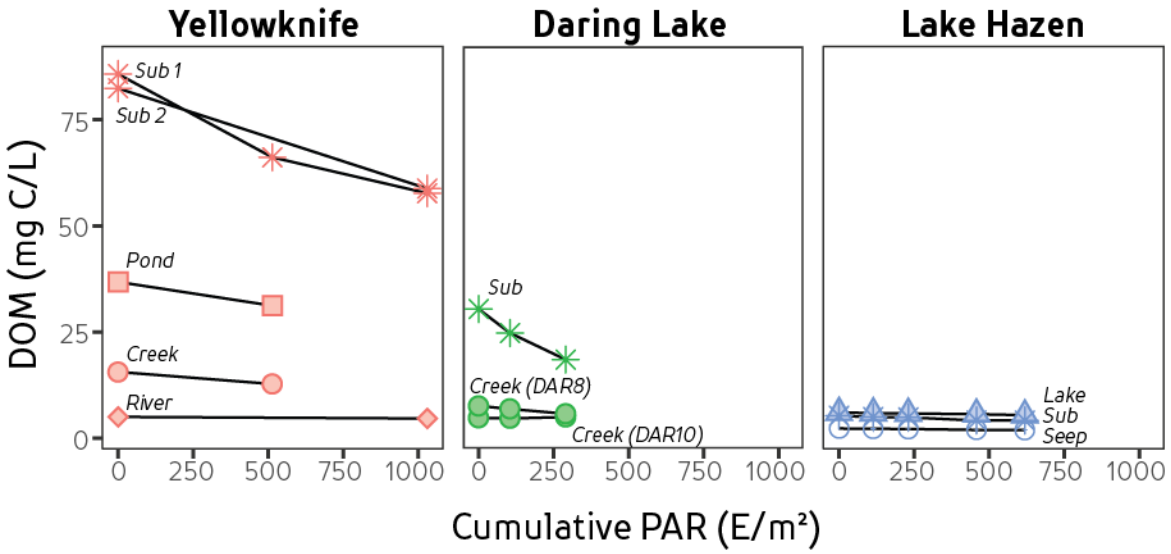

FIGURE 5.3: The change in dissolved organic matter concentration (mg C/L) over cumulative photosynthetic active radiation (PAR; E/m2) for each site.

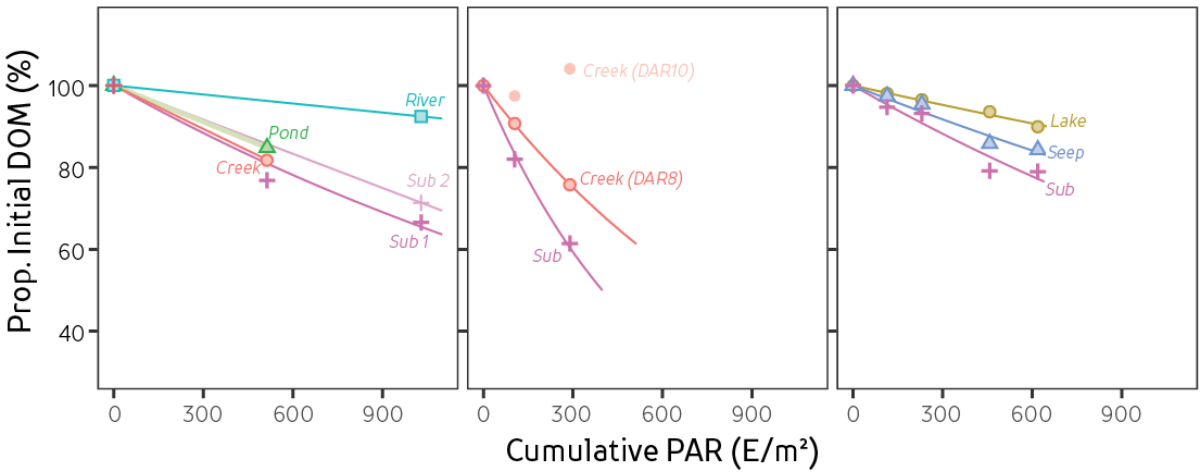

FIGURE 5.4: The proportion of dissolved organic matter remaining with increasing cumulative photosynthetic active radiation (PAR) for each site.

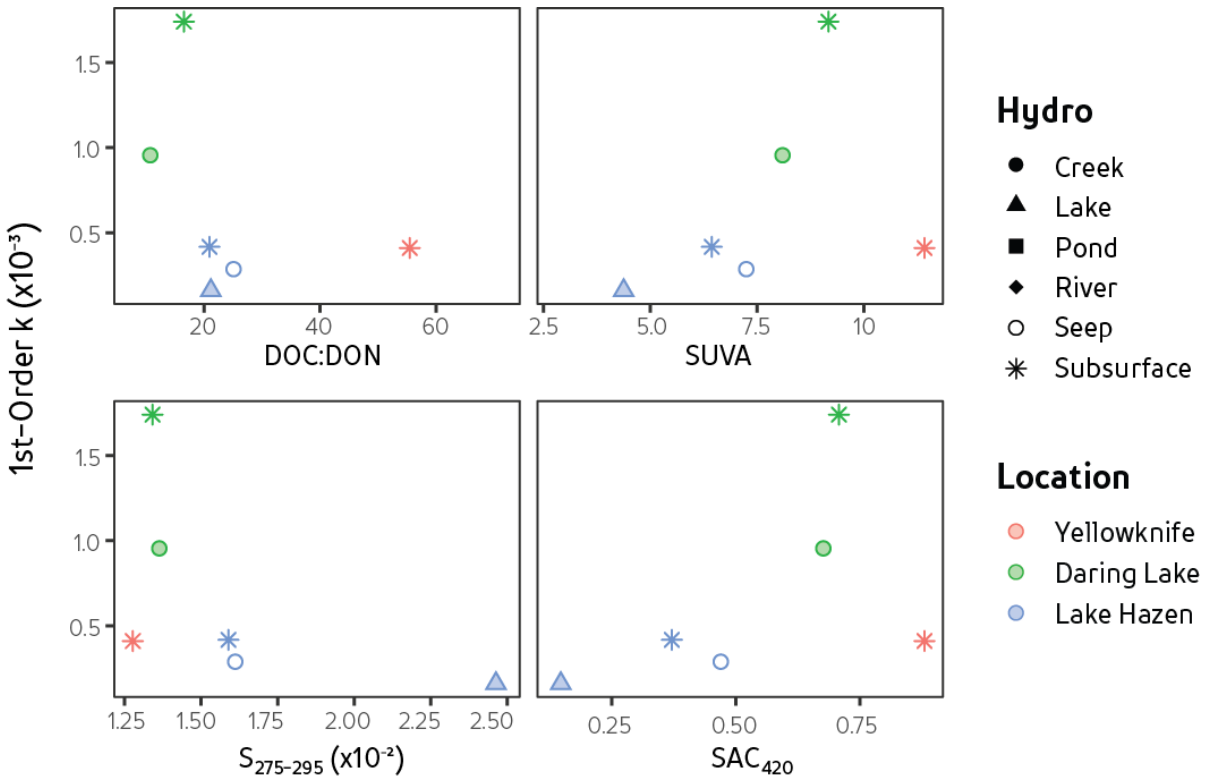

FIGURE 5.5: Comparison of samples with 1st-order degradation rates to different measures of dissolved organic matter composition: a) molar DOC:DON, b) specific UV-absorbance at 255nm (SUVA), c) spectral slope between 275 and 295nm (S275), and d) specific absorption coefficient at 420nm (SAC420). Different shapes correspond to different hydrological environments, while different colours refer to geographic location.

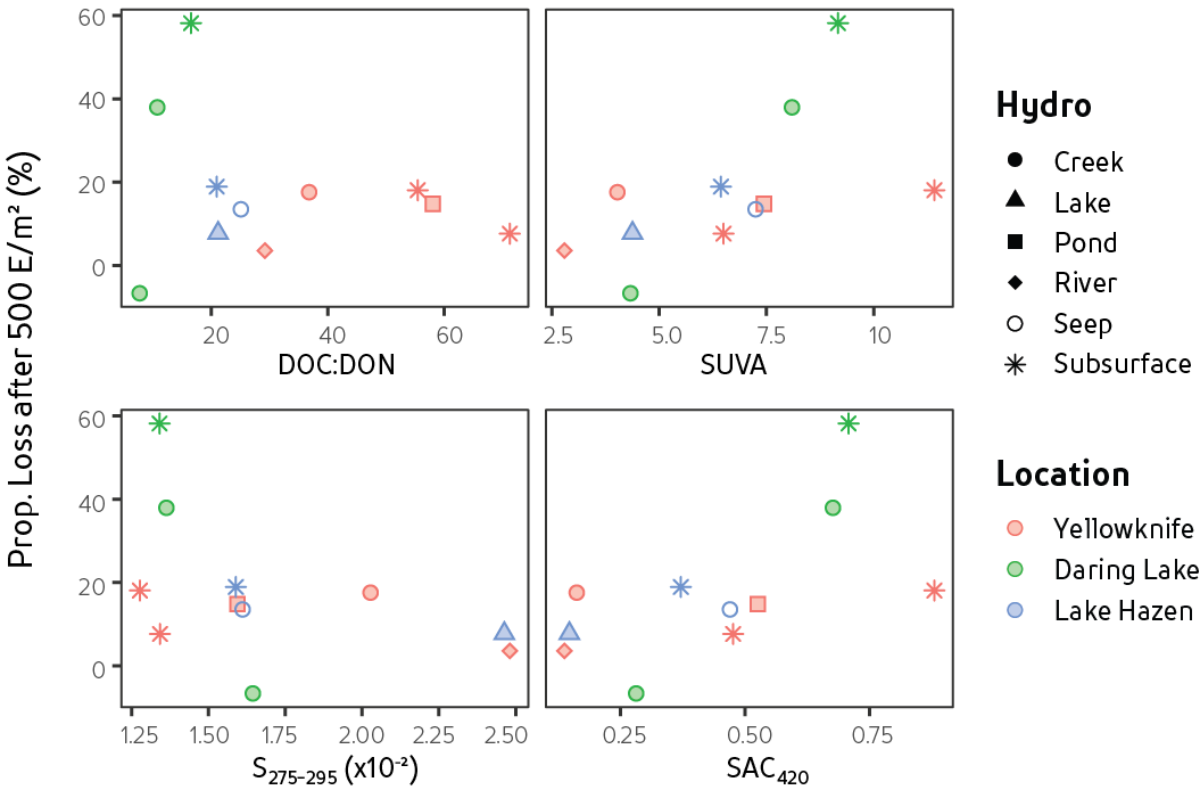

FIGURE 5.6: Comparison of the proportion of dissolved organic matter (DOM) loss after a set irradiation amount (500 E/m2) with initial DOM composition: a) molar DOC:DON, b) specific UV-absorbance at 255nm (SUVA), c) spectral slope between 275 and 295nm (S275), and d) specific absorption coefficient at 420nm (SAC420). Different shapes correspond to different hydrological environments, while different colours refer to geographic location.

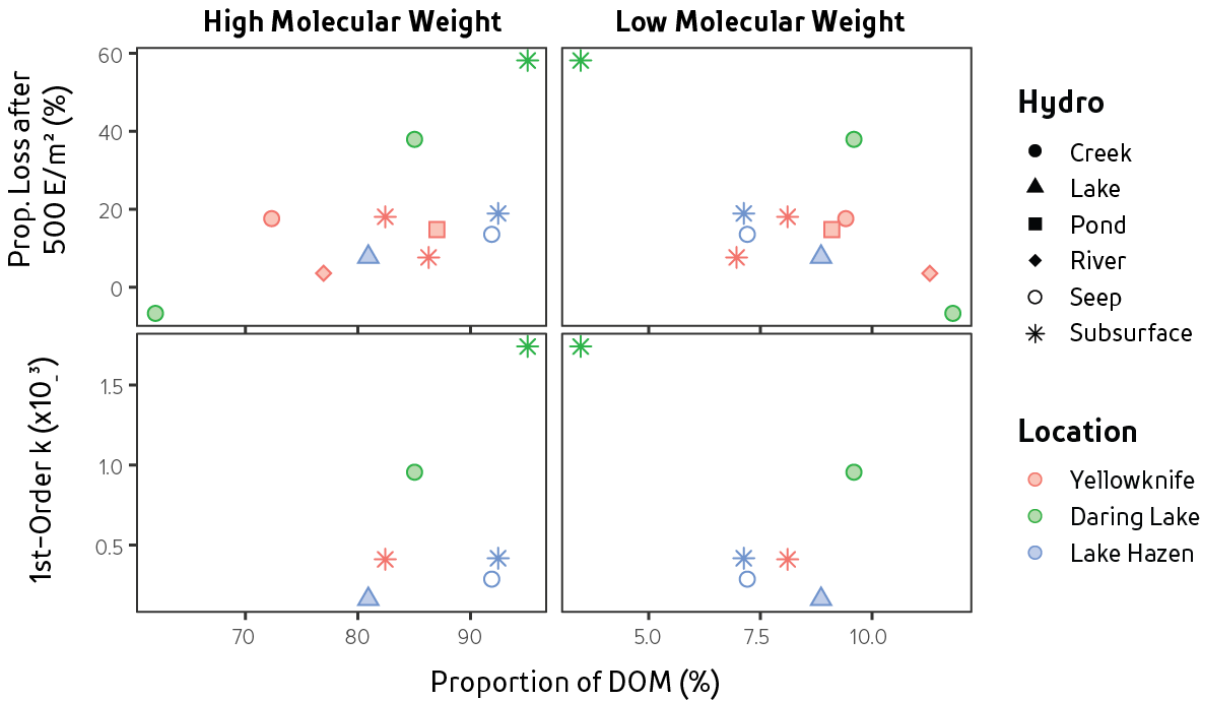

FIGURE 5.7: Comparison of the proportion of DOM loss after 500 E/m^2 (top graph) and 1st-order degradation rate (lower graph) for size-exclusion chromatography determined proportion of high molecular weight (HMW) and low-molecular weight (LMWN) components of dissolved organic matter. Different shapes correspond to different hydrological environments, while different colours refer to geographic location.

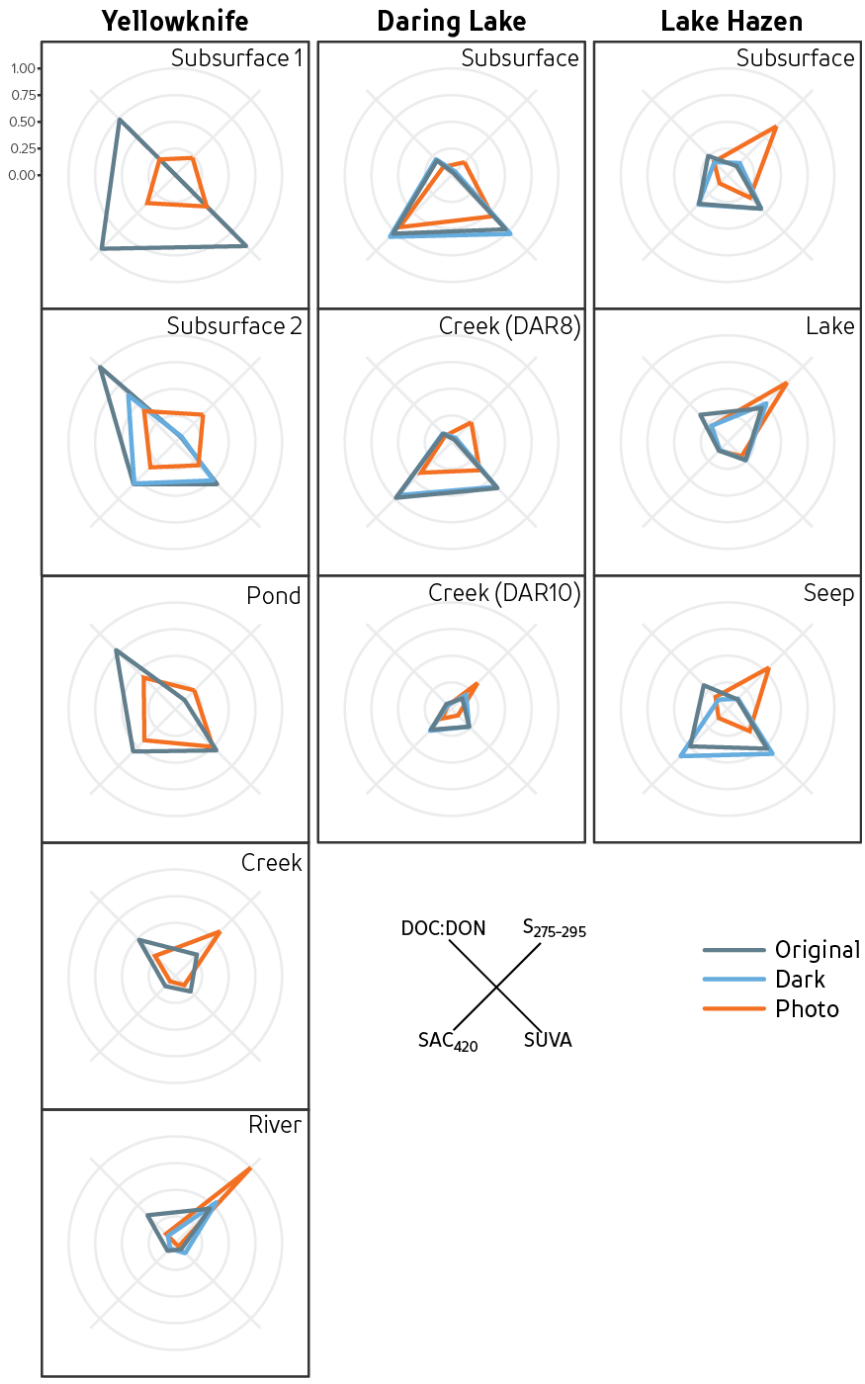

FIGURE 5.8: Composition Wheels for each sample representing the initial composition (black), light treatment (orange) and dark treatment (blue). Dissolved organic matter composition is represented by molar DOC:DON, slope from 275 to 295nm (S275), specific UV-absorbance at 255nm (SUVA), and specific absorption coefficient at 420nm (SAC420). Each axis is normalized for the maximum and minimum value for each parameter. Yellowknife subsurface 1, pond, and creek did not contain 'Dark' treatments.

Chapter 6

Quality over Quantity: Characterizing Dissolved Organic Matter and Formation of Disinfection By-Products at Three Locations in the Northwest Territories, Canada

6.1 Introduction

Dissolved organic matter (DOM) is a ubiquitous component across aquatic systems and an important factor influencing drinking water treatment and quality. For instance, DOM influences drinking water taste, colour, and odour, and can stimulate microbial growth within water infrastructure[65]. DOM is comprised of thousands of different organic molecules with differing structural and chemical characteristics that determine its overall reactivity. Differences in organic source, residence time, and environmental processing can alter DOM reactivity along the aquatic continuum[38,80,202], which can have an effect on drinking water treatment options, cost, and overall water quality. Although Canadian guidelines do not state a maximum acceptable concentration for DOM, provincial governments have set specific concentrations for aesthetic values (between 2 to 5 mg C/L) to maintain water colour, taste, and odour[59,277]. However, DOM can react with other substances to form more toxic and problematic compounds.

Organic matter can react with chlorine, a common disinfectant used in water treatment, to form various carcinogenic disinfection by-products (DBP)[278,279]. DBP are commonly found within water treatment plants, with new and more toxic DBP being discovered as technology advances and detection limits improve[280–284]. Disinfection by-products encompass thousands of different compounds, some more carcinogenic than others, making it difficult to measure and regulate every known compound. Thus, DBP are generally quantified and regulated using concentrations of the two most common groups: trihalomethanes (THM) and haloacetic acids (HAA).

In terms of water treatment, DOM concentration has previously been used to predict DBP formation and chlorine addition[285]. However, the reactivity between DOM and chlorine depends upon both the concentration and composition of DOM. Seasonal changes to DOM composition result in varying THM concentrations[286], while differences in DOM composition influence DBP formation rates[287,288]. Quantifying variations in DOM composition found within the environment

could help identify waters susceptible to forming higher DBP concentrations. Complex models have incorporated various components of DOM (UV-absorbance, fluorescence, and apparent molecular weight) to identify DOM precursors of THM formation[68]. Low molecular weight (LMW) and UV-absorbing components of DOM can both be important for DBP formation[287,289–292]. Although UV-absorbing methods are popular, they do not account for DBP precursors with low-UV absorbing properties that can also be important predictors of DBP formation[71,293]. Hence, DOM composition and the processes that alter DOM play an important role regulating DBP formation within water supplies.

Shallow surface waters are a characteristic feature of arctic environments and act as important drinking water resources for many northern communities. In particular, communities across the Northwest Territories (NT), Canada, rely primarily upon surface waters for drinking water sources. Three of thirty water treatment plants use only chlorination as their primary treatment option, while the majority of water treatment systems are Class I and II, and seven communities relying on Small Systems[294]. Some communities rely on the use of water trucks to transport chlorinated water into large storage tanks within personal residences. Although residual chlorine within treated water is required to ensure safe drinking water standards, there is a preference for non-chlorinated water in many northern communities, which in itself carries a risk of gastrointestinal illness[295,296]. Water treatment and storage within the NT involves various environmental, economical, and societal influences that may be exacerbated by a changing climate.

Changes to hydrological processes and carbon cycling can alter DOM concentration and composition among northern surface waters. Within the NT there is the potential for increasing active-layer thickness and permafrost thaw to mobilize large stores of previously-frozen carbon, solutes, and nutrients into surrounding surface waters[132]. Increased surface water DOM concentrations have been observed across the northern hemisphere and are linked with increased terrestrial contributions[34,297,298]. There is concern regarding changes to the amount and form of DOM within drinking water sources and its impact upon future water treatability[102,298], especially in northern communities[299–301]. Enhanced terrestrial DOM in surface waters could alter the amount of humics or UV-absorbing components, both thought to result in higher DBP formation. As various drivers of DOM fate can have different influences on DBP formation[302], it is important to better understand the relationship between DOM and DBP formation, providing better predictive abilities for northern water security.

The relationships between DOM composition, disinfection demand, and DBP formation are important when considering drinking water treatment options. As a warming arctic may rapidly alter DOM sources and fate, simple characterization techniques that are able to predict DOM-DBP reactivity becomes increasingly important for monitoring changes to DOM within remote communities. The overall objective of this study was to quantify how DOM composition relates to DBP formation across various hydrological sites in the NT. This was accomplished with two specific objectives: 1) use NT water treatment plant records to assess the prevalence and range of DOM and DBP across NT communities, and 2) determine how differences in DOM compositional measures relate to concentrations of DBP (both THM and HAA). Further, the impact of DOM fate and DBP formation was assessed using 30-day microbial and 12-day photolytic degradation experiments.

6.2 Methods

6.2.1 Public Water Quality Records

Public water quality records for NT water treatment plants were obtained from online records found from the Government of Northwest Territories Water Quality Database (www.nwtdrinkingwater.ca/operations/water/water_raw.asp). Samples were collected from various locations, including water treatment plants, water trucks, and local water taps (i.e., schools, hamlet offices, hotels; Appendix D). Measures compiled were True Colour, DOM concentration, and THM concentration. As no consistent data were available for the individual THM species concentration to convert to mg-C/L, the summation of THM species are in µg/L. Data were sporadic but spanned from 1994 to 2015 for 31 water treatment systems. Values outside of 1.5x the interquartile range for THM and DOM data were removed from the original dataset as major outliers were observed when compiling the data (i.e., THM of 60 mg/L).

6.2.2 Field Collection

Samples were collected between July and October 2013 to 2016 from surface and subsurface waters across three locations in the NT: Yellowknife (YK), Wekweètì (WK), and Daring Lake (DL) (Figure 6.1; Appendix D). Yellowknife and Wekweètì are situated on taiga shield and are found in discontinuous and sporadic continuous permafrost zones, respectively. Daring Lake is situated above the treeline in the southern arctic ecoregion, underlain by continuous permafrost. Surface

water samples were collected ~0.25 m from the surface and filtered in the field. All subsurface samples were collected from the deepest extent of the active layer above the permafrost boundary using either pre-installed PVC piezometers 0.50 m below surface (YK) or drive-point piezometers installed 0.25 to 0.50 m below surface (WK and DL). Piezometers were purged by three pore volumes prior to sampling and water collected using a peristaltic pump. All samples were filtered to 0.45 µm into pre-rinsed, acid-washed glass vials and kept cool (<4°C) and dark until further analyses.

6.2.3 Laboratory Analyses

6.2.3.1 Geochemistry & DOM Characterization

Concentrations of DOM (as dissolved organic carbon) and total nitrogen (TN) were measured using a Shimadzu Total Organic Carbon (TOC-L) Combustion Analyzer with TNM-1 module (precision of ±0.3 mg C/L; ±0.3 mg N/L). Inorganic nitrogen species (nitrite, nitrate, and ammonium) were analyzed using a SmartChem 200 Automated Chemistry Analyzer (NO_2^- and NH_4^+ precision of ±0.1 mg N/L, precision NO_3^- of ±0.15 mg N/L; Unity Scientific, MA United States). Dissolved organic nitrogen was calculated as the difference between TN and the sum of inorganic nitrogen species and used to calculate molar DOC:DON. DOM absorbance was measured using a Cary 100 UV-VIS Spectrophotometer (Agilent, CA, United States) at 5 nm increments between 200 to 800 nm. Deionized water was used to zero the machine, and run intermittently during analyses to correct for baseline drift. The Naperian absorption coefficient (a; m^{-1}) was calculated using:

$$a_\lambda = \frac{ln(10) \times A_\lambda}{L}$$

where A is the baseline-corrected absorbance at wavelength λ and L is the cell length (m). Specific absorbance at 255 nm (SUVA) was calculated by dividing the absorption coefficient at 255 nm by the overall DOM concentration. The slope ($S_{275\text{-}295}$) of the log-transformed absorption coefficients was measured between 275 and 295 nm and is inversely related to molecular weight[199]. DOM composition was also characterized using size exclusion chromatography (Liquid Chromatography – Organic Carbon Detection, LC-OCD[75]) run in the Department of Civil and Environmental Engineering, University of Waterloo. Briefly, the sample was diluted to within 1 to 5 mg C/L and injected through a size-exclusion column (SEC; Toyopearl HW-50S, Tosoh Bioscience) that separated DOM based on hydrodynamic radii into five hydrophilic fractions (from largest to

smallest): biopolymers (BP; polysaccharides or proteins), humic-substances like fraction (HSF; humic and fulvic acids), building blocks (BB; lower weight humic substances), low molecular weight neutrals (LMWN; aldehydes, small organic materials), and LMW-acids (LMWA; saturated mono-protic acids). Composition Wheels (CW) were used to compare differences in DOM composition, which uses four independent measures of composition (Chapter 3). Each scale represented a measure of composition and normalized based on the maximum and minimum values encountered from a larger dataset encompassing various ecoregions across Canada.

6.2.3.2 Disinfection By-Product Determination

All disinfection by-product analyses were conducted at the Clean Water Laboratory, Civil and Resource Engineering, at Dalhousie University using Standard Methods for the Examination of Wastewater Method 5710 and HACH Method 8021. Samples were first diluted to a range between 1 to 10 mg C/L to obtain acceptable levels of chlorine addition and DBP formation. Briefly, sodium hypochlorite was added to the samples until a chlorine residual of 1 ±0.4 mg/L at pH 8 remained after 24 h at 20°C. At this point, the maximum amount of DBP have been formed. Concentrations of THM and HAA were analysed using a Varian CP-3800 Gas Chromatograph equipped with a CP-8400 Autosampler. Total THM concentration (mg C/L) were calculated as the sum of bromodichloromethane, bromoform, chloroform, and dibromochloromethane concentrations in mg C/L. Total HAA concentration (HAA; mg C/L) were calculated as the sum of chloroacetic acid, bromoacetic acid, dichloroacetic acid, trichloroacetic acid, bromochloracetic acid, dibromoacetic acid, bromodichloroacetic acid, chlorodibromoacetic acid, and tribromoacetic acid concentrations in mg C/L.

6.2.3.3 Microbial & Photolytic Treatments

Select samples were subjected to microbial (5 samples) and photolytic (3 samples) treatments. Microbial treatments were conducted by adding 120 mL of 0.45 µm-filtered sample to a series of acid-rinsed 220 mL glass bottles. An inoculant (same sample but filtered to 1.7µm) was added (10% by volume) and bottles were gently mixed and left lightly capped to allow for oxygen exchange. Photolytic treatments were setup by filtering 2.5 L of sample to 0.45 µm, transferred into 5 L Tedlar bags (SKC Inc., USA), injected with 2.5 L of air, and exposed to 12 days of sunlight on the roof at the University of Waterloo. Samples were then re-filtered to 0.45 µm and analysed for DOM characteristics and DBP concentrations at the beginning and end of both treatments.

6.2.3.4 Statistical Calculations

Significance of correlation between variables was calculated using Spearman's rank correlation using non-linear least squares ('nls' package) in R[212]. Reported are both the correlation (ρ) and the p-value between the data and the non-linear least squares model.

6.3 Results

6.3.1 Government of Northwest Territories Water Quality Records

The presence of DBP and DOM were ubiquitous within NT water treatment systems regardless of water source or type of water treatment (Figure 6.2). Measures of True Colour were, on average, similar across water sources and communities, while raw samples contained the highest values of True Colour (Figure 6.2a; Table 6.1). DOM concentration among natural and treated waters ranged from 0.01 to 22 mg C /L with highest DOM concentrations found from lake sources (7.2 ±5.4 mg C/L; Figure 6.2b). Lower DOM concentrations were found from communities using either rivers (4.3 ±2.6 mg C/L) or groundwater (5.7 ±3.3 mg C/L) as a water source. The majority of water sources remained below the Canadian federal maximum acceptable concentration (MAC) for THM (0.1 mg/L; Figure 6.2c) and only 56 of 520 records exceeded this limit. Large ranges between maximum and minimum THM concentrations were observed across all sites, with a range of up to 0.15 mg/L at some communities. No relationship between DBP and True Colour was observed (Appendix D); however, higher DOM concentrations generally had higher True Colour values (Appendix D). Ratios of THM:DOM varied across communities with no apparent trend with water source or type of water treatment (Figure 6.2d). Hence, treated water within the NT communities contained low but measurable concentrations of DBP and DOM at the sampling location, which varies from taps to plants at different communities.

6.3.2 DOM Concentration, Composition, and DBP

Samples from a variety of hydrological environments had a large range in both DOM (2.3 to 87 mg C/L) and DBP concentrations (5 to 317 µg C/L). The amount of chlorine added to maintain a residual after 24 h varied with DOM concentration (Figure 6.3). The lack of linear relationship between these variables indicates the specific chlorine demand (SCD; chlorine demand per unit of DOM) varied across samples. DBP yields, the amount of DBP formed normalized to DOM concentration on a weight carbon basis (mg C-DBP : mg C-DOM), varied across various hydrologic

and geographic sites (Figure 6.4). The largest range in THM yield was found from subsurface DOM (2 to 106 $x10^{-4}$) while surface water DOM ranged between 5 to 77 $x10^{-4}$. Similar trends were found in HAA yields as subsurface DOM had the largest range (3 to 104 $x10^{-4}$) while surface waters had yields between 11 to 91 $x10^{-4}$ (Figure 6.4b). Similar yields between THM and HAA were found for most samples except for higher HAA yields found from creeks, and lakes from DL and WK. Differences in DBP:DOM indicate that not all DOM produces the same amount of DBP. Further, a significant relationship was observed between DOM concentration and C-THM (ρ=0.57, $p<0.05$) but not for C-HAA (ρ=0.46, $p>0.05$) concentrations (Appendix D). The amount of chlorine added did not result in the same amount of DBP formed as DBP:Chlorine values varied across hydrologic sites (Figure 6.4c,d). Although THM and HAA produce similar yields, a large range of values were observed across hydrological sites. Subsurface and lake DOM contained the largest range in THM:Chlorine (Figure 6.4c). Differences in DBP:Chlorine values indicate the amount of chlorine added is not a good predictor of overall DBP concentration.

Measures of DOM composition were significantly correlated to the concentration of DBP formed. SUVA values covered a wide range from 2.4 to 10.3 L/(mg·m) with high-SUVA samples forming high DBP concentrations (Figure 6.5a). Spectral slopes ranged from $1.20x10^{-3}$ to $2.48x10^{-3}$ nm^{-1} and were highest in a YK river and lakes from WK and DL (Figure 6.5b). The HSF comprised the majority of DOM for most samples with highest proportion found from YK and WK samples (Figure 6.5c). Across all sites, subsurface DOM contained the highest HSF proportion. Measures of DOC:DON ranged from 23 to 62 and were not correlated with DBP concentration (Figure 6.5d). A significant positive correlation was found between DBP concentrations and SUVA, while a significant negative correlation was found for $S_{275\text{-}295}$. Both THM and HAA had similar trends across most measures of DOM composition. Concentrations of HAA were more strongly correlated with measures of SUVA and $S_{275\text{-}295}$ than THM. Although some measures were auto-correlated (namely $S_{275\text{-}295}$ and SUVA; Appendix D), DOM compositional measures provided better predictive capabilities of DBP formation than DOM concentration.

Composition Wheels provide an efficient tool to integrate various measures and visualize differences in DOM composition (Figure 6.6). Highest DOM and DBP concentrations were observed from WK subsurface and YK pond DOM, characterized by high SUVA and HSF. Alternatively, Composition Wheels with low SUVA, HSF, and high $S_{275\text{-}295}$ resulted in the lowest DBP concentrations, as seen by YK River, DL creek (DAR11), and WK lake (WK6). Comparison of

various DOM samples by similar hydrological environment found similarities in subsurface DOM composition across locations. Lake DOM composition differed between WK and DL as WK lakes plotted more closely with subsurface samples. WK and DL lakes with similar Composition Wheels to subsurface samples also contained higher DBP concentrations. Assessing DOM composition using a suite of quasi-independent types of measures identified DOM composition that had a higher propensity to form higher DBP concentrations.

6.3.3 Effects of Microbial & Photolytic Degradation on DBP

Degradation experiments were used to quantify how DBP formation was influenced by changes to DOM concentration and composition. DOM loss in a 30-day incubation experiment resulted in a 5 to 22% decrease in DOM concentration while photolysis resulted in a 8 to 30% decrease (Table 6.2). All five microbial treatments increased THM:DOM ratios after 30 days. Conversely, THM:DOM ratios had either no change or a slightly decreased during photolysis (Figure 6.7). Microbial degradation decreased the amount of chlorine needed per molecule DOM for all samples except the two subsurface sites. Photolysis decreased the amount of chlorine needed per molecule DOM for the single river sample but increased the ratio for both subsurface samples (Table 6.2). DOM loss in both experiments was accompanied by a compositional change of DOM. Microbial degradation resulted in increasing SUVA values and altered DOC:DON, but had little change to other DOM compositional measures (Figure 6.8). LC-OCD analyses were not completed on two samples and thus HSF data were not included. Photolysis greatly altered subsurface composition, as seen by decreased SUVA, proportion of HSF, and DOC:DON, and increased $S_{275\text{-}295}$. However, little compositional change was observed from photolysis of YK River DOM. Subsurface DOM composition wheels subjected to photolysis appeared similar to the Composition Wheel of YK River. Microbial and photolysis degradation had different effects upon DOM composition and DBP:DOM yields.

6.4 Discussion

6.4.1 DBP in the Northwest Territories as Observed from Community Water Records

Low concentrations of DBP in treated water indicate that although these constituents are present in most systems they pose little concern for human consumption at point of testing. Differences in handling and methodology, such as storage times, point of sampling, different analytical

laboratories, and time left to react, can all influence the amount of DBP formed making comparisons among sites difficult. For instance, DOM and DBP can differ within a community depending upon where the sample was taken (Appendix D). Comparison with other reported values provide an indication of how concentrations of DBP and DOM within NT water systems relate to other water treatment systems. Alaskan water treatment plants had similar DOM concentrations but higher True Colour and DBP concentrations compared to NT systems[282]. Water treatment systems in the NT contained the lowest DBP yields across various published laboratory values and water treatment plants in Scotland and Alaska[282,290] but were relatively similar to treatment plants in North Carolina[280]. The variability and low DBP concentration among NT data could result from post-treatment handling, making it difficult to directly compare results to other studies. Regardless, municipal water quality data indicates DBP and DOM to be variable but ubiquitous across the NT.

The discrepancy in DBP concentrations between field data and the NT water quality database likely reflects the analysis of post-treated samples among the NT water quality database. Although field samples contained DBP concentrations significantly above the MAC, they represent untreated samples directly from the environment and not drinking water from the tap. Pre-treatment of drinking water, such as by ozone or chlorine dioxide, is known to lower both DOM and THM concentrations[287]. NT communities rely on filtration or conventional (coagulation, flocculation, sedimentation, and filtration) steps to treat water[294]. Although concentrations are different, relationships found between DOM and DBP based on field samples provide field-based relationships to identify DOM susceptible to higher DBP formation in similar waters. Further, field samples are needed to supplement the NT water quality database by providing true chlorine consumption and DBP formation as there are no data on the amount of chlorine needed to form the residual.

Chlorine consumption results from both organic and, to a lesser extent, inorganic constituents such as ammonia, halides, iron, manganese, and sulphur[303] but DBP production can only result from the interaction with organic matter. For northern communities, chlorine consumption directly affects cost due to the amount of chlorine required to produce safe drinking water. The range encountered in SCD and DBP:Chlorine across sites indicate there are factors that control chlorine consumption but do not produce DBP (Figure 6.3, Figure 6.4). The range in DBP:DOM (Figure 6.4a,b) illustrate that different mixtures of DOM influence the formation of DBP, as well as the consumption of chlorine. No relationship was observed between DBP production and DOM

concentration within Alaskan treatment plants[282], yet our results did find a correlation with DBP concentration on a per-carbon basis, rather than by summation of individual weights of THM species (Appendix D). Long-term records of NT water sources illustrate the presence of DBP and DOM within treated northern water supplies, but these measures may not be effective to properly predict or monitor changes to chlorine consumption and DBP formation in the north. Thus, measures of DOM composition, which are not reflected by the overall DOM concentration, are required to accurately forecast changes to future water treatability.

Differences in concentrations of DOM, DBP, and True Colour across NT water treatment plants suggest not all DOM is the same among water sources. DOM can be a major contributor to overall water colour as True Colour of lake water has been found to be a good predictor of long-term DOM concentration among boreal lakes[304]. This attribute reflects differences in the type, or composition, of DOM. The lack of relationship within the water quality records between DOM concentration and DBP (Appendix D), as well as the lack of linear relationship between DOM and chlorine (Figure 6.3), reflect the importance of quantifying differences in both the amount and composition of DOM. Both field and community water quality data show a good relationship between DOM and colour (Appendix D), indicating the importance of DOM composition. Hence, DOM composition must also be important for chlorine consumption and DBP formation when considering a variety of water sources with different amounts and forms of DOM.

6.4.2 DBP and DOM Concentration & Composition

Watershed characteristics can dictate the composition of DOM due to various DOM sources and processing mechanisms[72,236,305]. Unique DOM compositions or 'signatures' can be used to predict the susceptibility of drinking water to DBP formation by identifying components susceptible to DBP formation[288]. Further, understanding how composition changes temporally or spatially would allow for a better prediction to future DBP formation. Certain Composition Wheels of samples were representative of a terrestrial-like DOM signature observed across arctic systems: higher humic and SUVA values and lower $S_{275\text{-}295}$ [34,80,81,244,245] (Figure 6.6) These samples also contained high concentrations of DBP. Conversely, lakes with aquatic or photobleached signatures (lower DOC:DON, high $S_{275\text{-}295}$, low SUVA) contained the lowest DBP concentrations. Humics have been associated with high DBP formation[68,278], yet all DOM contains some proportion of humic substances (Figure 6.6) thus a single measure is not sufficient to predict DBP formation. Our results

indicate that surface or subsurface DOM defined by low $S_{275-295}$, high HSF, and high SUVA, characteristic of terrestrial-like DOM, are susceptible to forming high DBP concentrations.

Differences in DBP concentrations are influenced by variations in both UV and non-UV absorbing components of DOM. Strong correlations previously observed between DBP concentration and UV-absorbance components[282,289] were also observed here (Figure 6.5). Similarly, the proportion of HSF were positively correlated to THM concentrations (ρ=0.47, p=0.07) indicating HSF or UV-absorbing measures would provide similar estimates of DBP concentration. Positive and similar correlation coefficients between DBP concentration and either simple or complex DOM characterization techniques were observed in DOM among Scottish water treatment plants[290]. This is also found in this study as more complex methods, such as LC-OCD (Figure 6.5), also provide similar information to more simple UV-absorbing techniques. Further, UV-absorbing techniques may better predict HAA than THM formation (Figure 6.5). Thus, the use of relatively simple DOM composition measures are better to use as a simple tool to monitor changes in DOM composition, ultimately providing an indication of the effect upon DBP formation within NT water sources.

Processing of DOM within the landscape will influence the ability of DOM to consume chlorine and produce DBP. Microbial and photolytic degradation experiments provided DOM degradation compositions representative of enhanced processing and its ability to further form DBP. Photolytic formation of LMW compounds have been reported to increase chlorine demand and DBP formation on a weight basis of DOM[287,292]. However, in our experiments, although there was a shift towards LMW UV-absorbing components as seen by the increase in $S_{275-295}$, the DBP:DOM remained relatively constant (Table 6.2; Figure 6.7). Further, photolytic degradation had different effects on DBP based on the original DOM composition (Table 6.2). Although a loss in overall DOM concentration was observed, changes to DOM composition resulted in differences in DBP:DOM, implying photolytic degradation does not necessarily relate to decreased DBP formation. Conversely, microbial degradation resulted in higher THM:DOM values. This is similar to a study into the biodegradation of plant leachates that resulted in higher DBP-forming components remaining in recalcitrant DOM components[306,307]. Hence, the continual evolution of DOM that result in changes to DBP:DOM along the aquatic continuum has important implications for drinking water treatability across northern systems.

6.4.3 Implications for Northern Drinking Water Quality

In terms of treatment options, our results indicate higher DBP concentrations were formed from HMW and aromatic DOM, which are characteristics of DOM that is easily removed via coagulation and flocculation[64]. Water treatment plants in the NT are being upgraded to avoid chlorine-only systems, introducing more filtration and coagulation[294]. However, increases to both DOM and coagulant would generate more waste that would need to properly disposed of[65]. Although changes to DOM concentration and composition can complicate its removal, these results suggest that surface water sources from similar environments in the NT may be easily treated by conventional methods, helping to reduce DBP formation within drinking water sources.

Our results indicate that biodegradation can result in higher DBP formed per carbon molecule in DOM, which can influence water quality within both drinking water sources and infrastructure. Laboratory studies have identified organic matter produced from algal exudates to produce significant levels of DBP[308]. Expected increases to mean annual air and subsurface temperatures, enhanced mobilization of solutes and nutrients from degrading permafrost, and longer ice-off periods, could promote the eutrophication of shallow ponds and lakes[34,116,132,155,309,310] and lead to increased autochthonous DOM production. Both photolysis and microbial degradation are the main drivers of DOM fate, with photolysis being important for shallow lakes[99]. The importance of the balance between these two drivers can have significant effects upon DBP formed from the resulting DOM, as photolysis resulted in lower production of THM per amount of DOM than microbial degradation (Table 6.2). Quantifying the role and relative importance of biodegradation on DOM in northern surface waters will be an important component of northern water security in terms of DOM and DBP formation.

Storage and transportation of treated water in northern communities can have implications for DBP within drinking water sources. Long storage times and trucking of chlorinated water may lead to the degassing of THM[311,312]. The more carcinogenic HAA may have the potential to remain in solution due to its high polarity and low volatility. Further, storage of drinking water in large containers within houses and lack of routine cleaning can lead to the growth of biofilms and other contaminants[301,313]. The growth of biofilm within water infrastructure can lead to both the consumption of DOM and production of microbially-derived DOM, which can contribute to chlorine consumption and DBP formation outside of the water treatment plant[314]. The communities of Rigolet and Nain in Nunatsiavut, Labrador, Canada, consistently found low levels of free-chlorine

within drinking water sources[300], hence there is the potential for DOM produced from biofilm to react with the residual chlorine within water supplies and form additional DBP.

Different climate scenarios projected for a warming Arctic can lead to various responses in terms of DOM fate and export. In particular, DOM concentration and composition would be influenced by changes to hydrologic pathways and residence times within the watershed[15,18,28,29,80] ultimately affecting the propensity of DOM to form DBP. For instance, higher concentrations of terrestrial-derived DOM from permafrost thaw into surface waters[34] would result in the need for higher chlorine additions and higher DBP concentrations in systems with minimal pre-treatment. Longer transit times in organic-rich subsurface environments could enhance microbial degradation of organic matter and result in DOM with higher DBP yields. Alternatively, longer ice-off periods in shallow northern ponds and lakes could enhance photolytic degradation of DOM as sunlight in shallow northern water systems can process the majority of DOM[99]. Photolysis may provide 'natural remediation' in terms of DBP formation as irradiation would lower DOM concentrations and break down terrestrial components into lower molecular weight molecules or CO_2 [87,101,199]. These results highlight the importance of the relationship between DOM and both chlorine consumption and production of DBP when considering projections of future drinking water supplies and treatment options in the NT.

6.5 Conclusion

Low concentrations of DBP are ubiquitous across various water treatment plants in the NT. DOM composition from three different locations in the NT indicate not all DOM is the same and certain measures of composition reflect DBP formation better than overall DOM concentration. DBP concentration was not easily predicted by either the amount of DOM or amount of chlorine added. We find high molecular weight, aromatic, humic-like DOM to produce higher DBP concentrations. Use of Composition Wheels with DBP formation provided a tool to identify aquatic environments susceptible to forming higher DBP concentrations. Hence, DOM from subsurface environments, or terrestrial-like DOM in surface waters, are at a higher risk to form high DBP concentrations within chlorinated water sources without any pre-treatment. Although impossible to predict the response of northern systems to a warming climate, our results highlight the importance of DOM composition and use of simple UV-absorbing parameters to monitor relevant changes to DOM composition. Changes to DOM composition due to biodegradation are of great concern as higher

DOM:DBP yields were found, while photolytic degradation of DOM could help reduce the amount of chlorine needed to treat water sources. Impacts of DBP, DOM, and future water treatment are not only approached with technical or engineered solutions, but are also greatly influenced by cultural and socio-economic factors of northern communities. The evolution of DOM composition through out the aquatic continuum presents itself as a dynamic determinant of drinking water quality in northern systems.

Table 6.1: Summary of True Colour, concentration of dissolved organic matter (DOM), and total trihalomethane (THM) concentration compiled from public drinking water quality records for communities of the Northwest Territories for both treated and raw waters separated by source water. Parameters include number of samples (n), maximum, minimum, average, and standard deviation for each parameter per hydrological environment.

	True Colour (TCU)					DOM (mg C/L)					Total THM (mg/L)				
TREATED	*n*	*Max*	*Min*	*Avg*	*SD*	*n*	*Max*	*Min*	*Avg*	*SD*	*n*	*Max*	*Min*	*Avg*	*SD*
Groundwater	57	20	2	7	4	22	14.0	0.5	5.7	3.3	44	0.150	0.002	0.030	0.036
Lake	169	457	0	13	38	101	22.0	0.2	7.2	5.4	273	0.159	0.000	0.051	0.042
Reservoir											1	0.040	0.040	0.040	NA
River	74	70	2	16	15	67	11.2	0.0	4.3	2.6	142	0.140	0.001	0.039	0.029
RAW															
Groundwater	29	35	2	16	10	4	8.6	5.0	7.4	1.6	8	0.110	0.001	0.020	0.038
Lake	111	111	1	19	23	76	22.0	1.6	10.2	5.3	28	0.085	0.000	0.032	0.024
Reservoir	5	12	3	7	4	5	7.6	5.0	6.5	1.0	1	0.005	0.005	0.005	NA
River	123	864	2	14	78	34	18.9	0.6	5.4	4.3	24	0.075	0.001	0.010	0.020

Table 6.2: Changes to dissolved organic matter (DOM) concentration, trihalomethane (THM) yield (THM/DOM), THM concentration, and ratio of chlorine demand to DOM from microbial and photolytic degradation experiments.

	DOM (mg C/L)			THM/DOM		THM (mg C/L)			Chlorine / DOM	
Sample	*Initial*	*Final*	*% Change*	*Initial*	*Final*	*Initial*	*Final*	*% Change*	*Initial*	*Final*
MICROBIAL										
YK Subsurface	86.7	69.7	-20%	0.00612	0.00739	0.53	0.51	-3%	1.04	0.80
YK Pond	36.8	32.7	-11%	0.00662	0.00886	0.24	0.29	19%	0.48	0.58
YK Creek	17.8	13.8	-22%	0.00079	0.00447	0.01	0.06	339%	0.41	0.38
DL Subsurface	29.9	28.5	-5%	0.01059	0.01087	0.32	0.31	-2%	0.64	0.26
DL Creek	7.7	6.8	-11%	0.00306	0.01078	0.02	0.07	213%	0.34	0.50
PHOTOLYSIS										
YK Subsurface	8.4	5.8	-30%	0.00369	0.00372	0.031	0.022	-30%	2.17	3.50
YK Subsurface 2	7.0	6.0	-15%	0.00723	0.00596	0.051	0.036	-30%	2.07	2.18
YK River	5.0	4.7	-8%	0.00305	0.00273	0.015	0.013	-17%	2.14	1.37

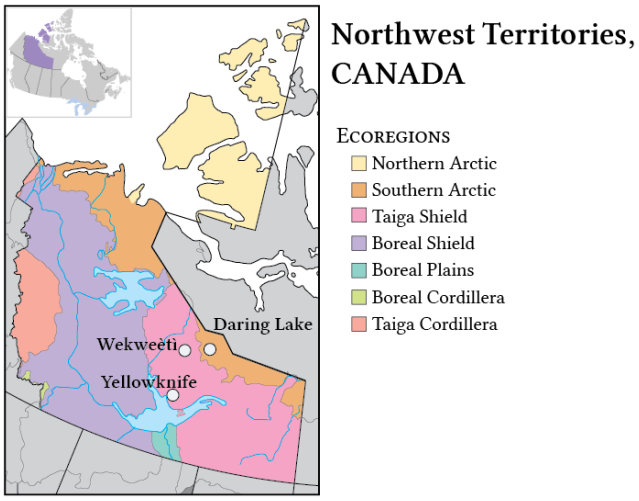

Figure 6.1: Field sampling locations for Yellowknife, Wekweètì, and Daring Lake in the Northwest Territories, Canada. Highlighted areas represent the various ecoregions.

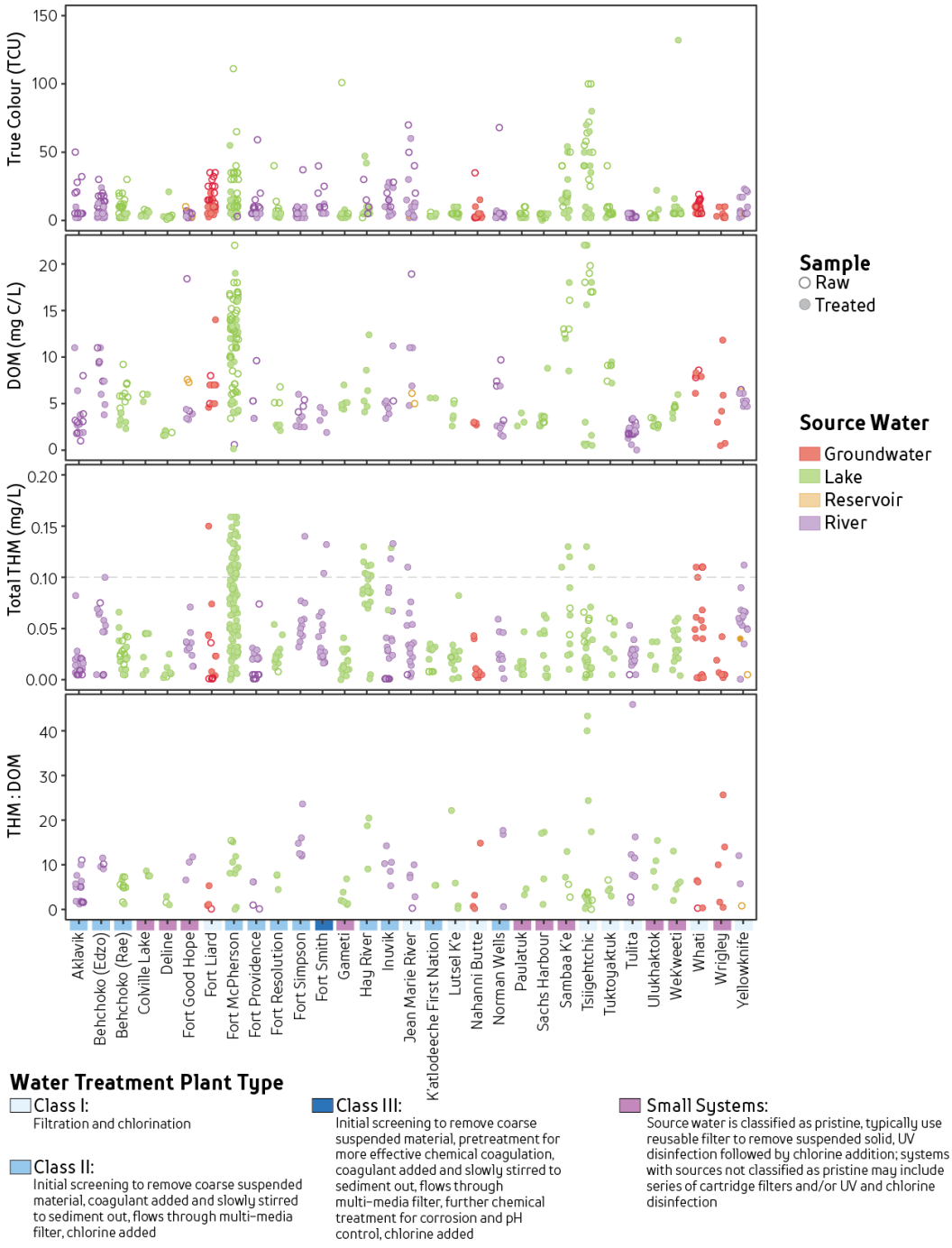

FIGURE 6.2: Public water quality records for various communities across the Northwest Territories for treated (solid circles) and raw (open circles) for different water sources (lakes, streams, groundwater, reservoir) represented by different colours. Sampled parameters include: True Colour (True Colour Units), dissolved organic matter (DOM; mg C/L) concentration, total trihalomethane concentration (THM), and THM yield. Description of water treatment plants are included and represented by a colour bar on the x-axis. The line on the plot of THM is the Maximum Acceptable Concentration for Canadian drinking waters.

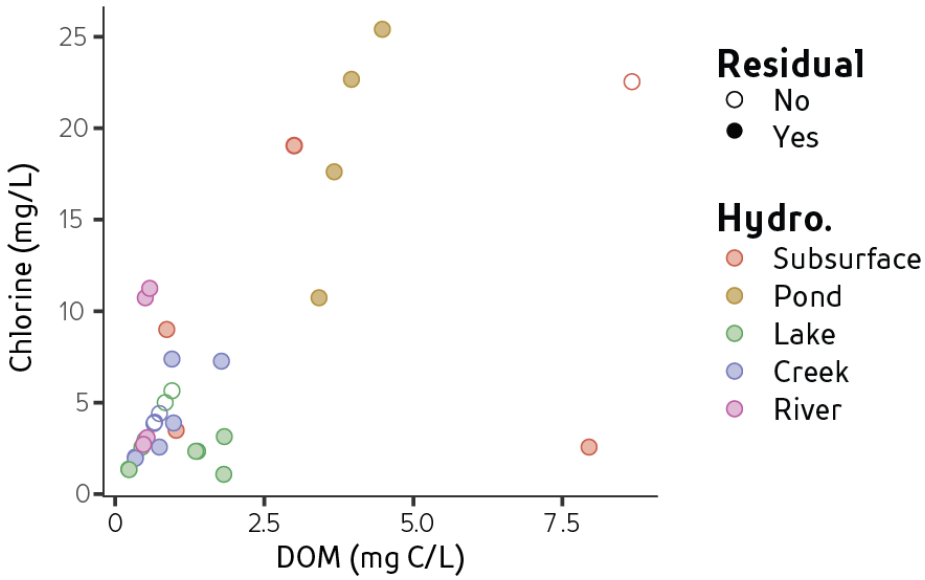

FIGURE 6.3: Concentration of chlorine added to create a potential residual concentration after 24h versus dissolved organic matter concentration (DOM). Solid dots represent samples that achieved the residual whereas hollow dots did not. Different colours represent hydrological environments sampled.

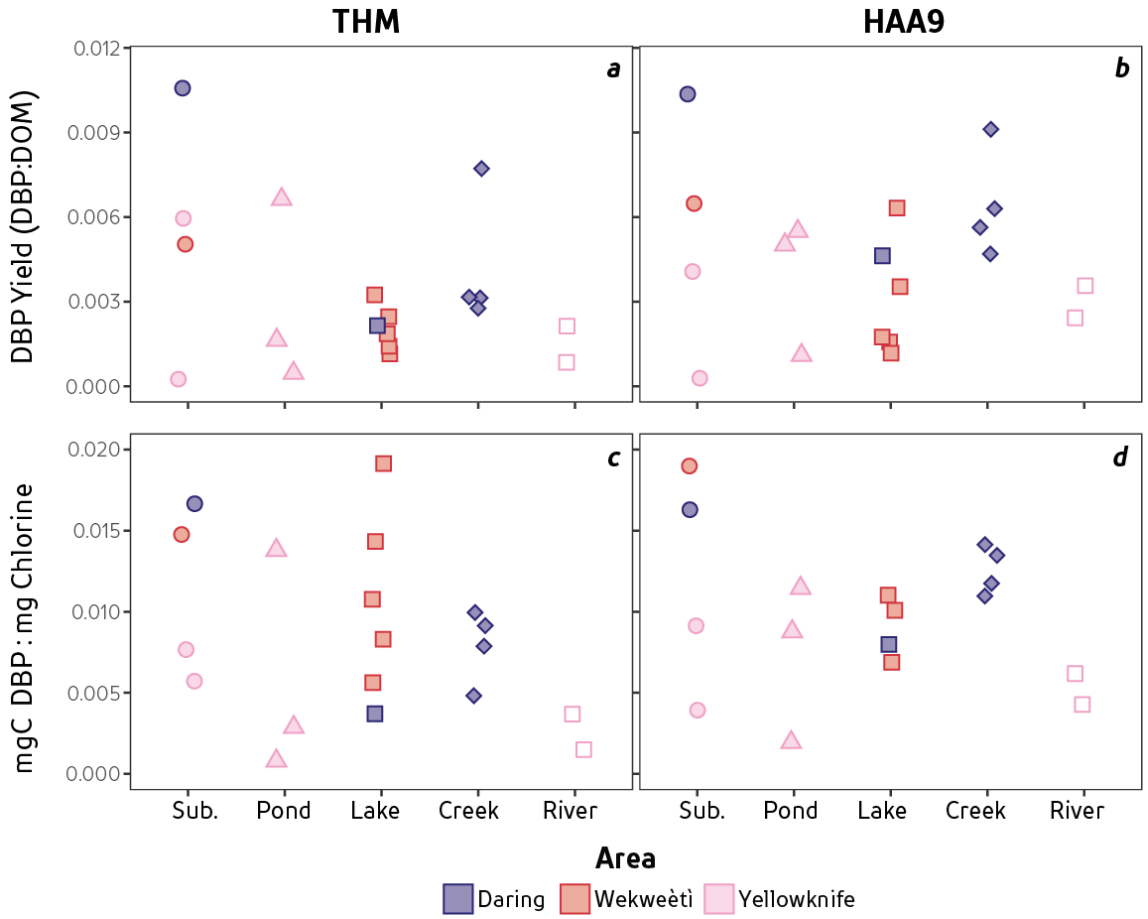

FIGURE 6.4: Ratio of formed trihalomethane (a) and haloacetic acid (b) concentration per dissolved organic matter (DOM) concentration, and ratio of trihalomethane (c) and haloacetic acid (d) to added chlorine for different hydrologic environments. Colours represent the different sites (Yellowknife (YK), Wekweètì (WK), and Daring Lake (DL)) and may include similar locations sampled at different times.

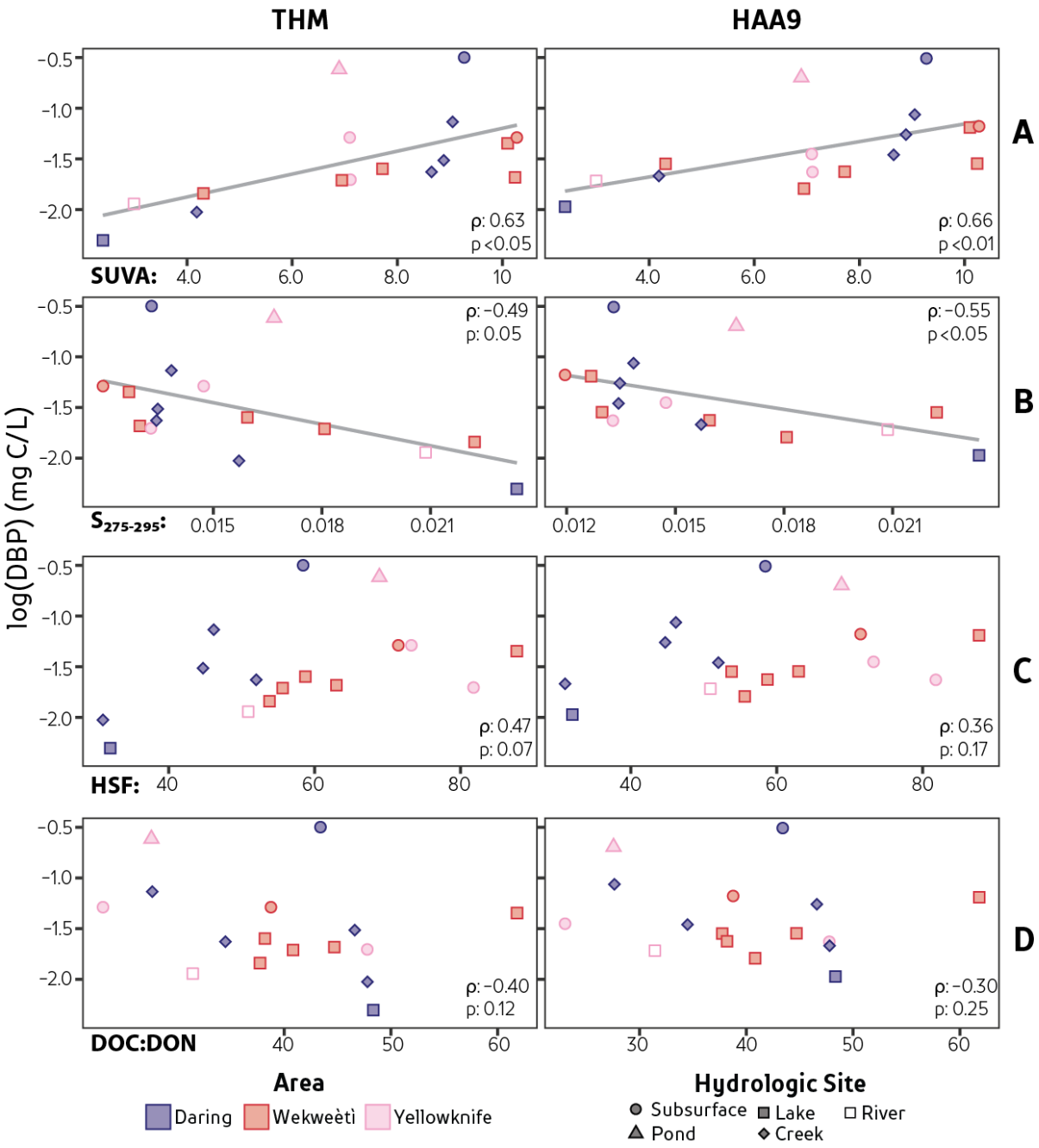

FIGURE 6.5: Disinfection by-product (DBP) concentration versus various measures of dissolved organic matter (DOM) composition that include specific UV-absorbance at 255nm (SUVA; a), slope between 275 and 295nm ($S_{275-295}$; b), proportion of humic substances fraction (HSF; c), and ratio of dissolved organic carbon to dissolved organic nitrogen (DOC:DON; d). Shapes represent various hydrologic environments while colours represent different geographic locations. Grey lines illustrate the line of best fit with the degree of correlation using Spearman Rank correlation (ρ) and associated p-value between the model and actual data.

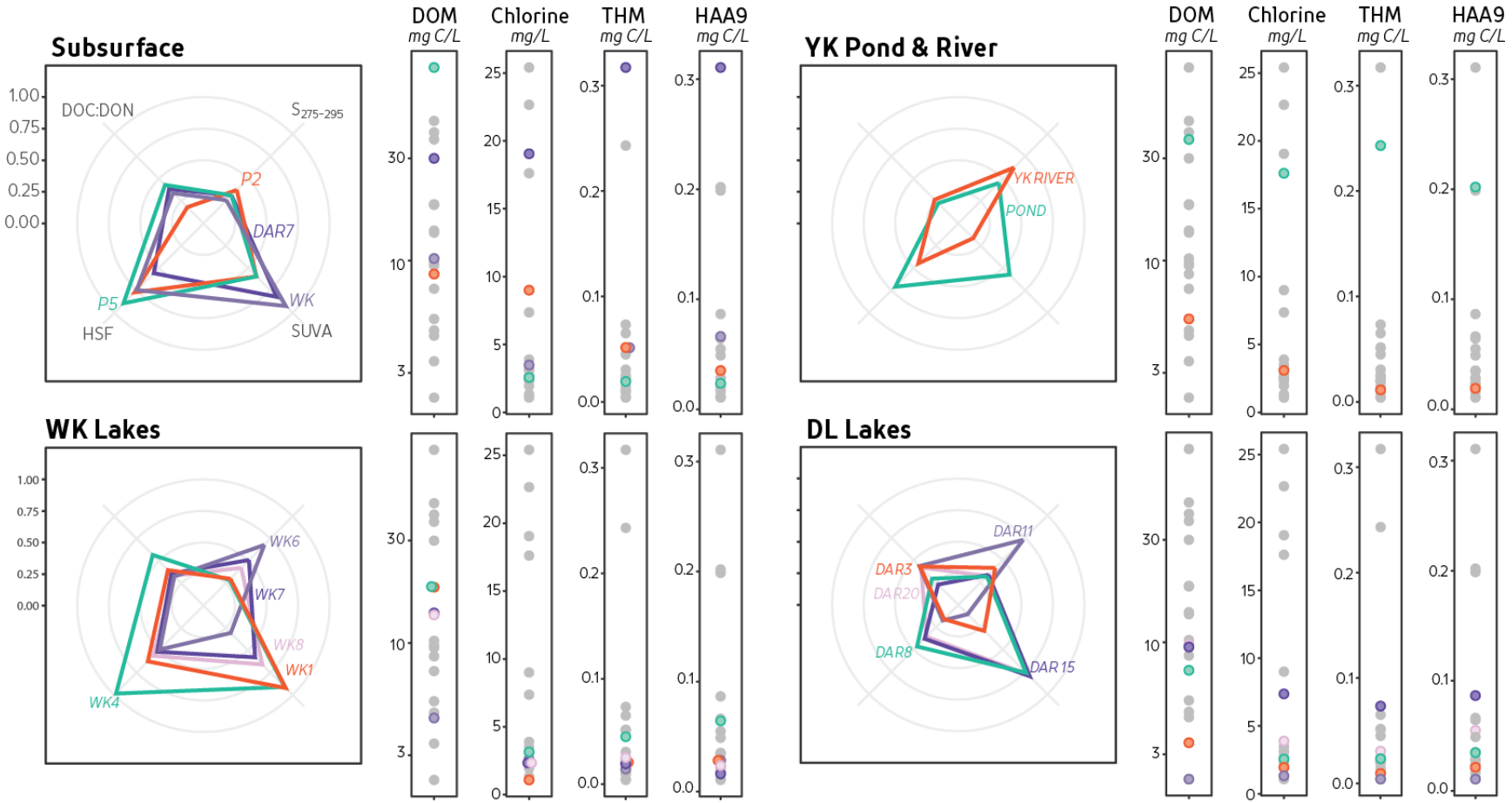

FIGURE 6.6: Various Composition Wheels with associated overall dissolved organic matter concentration (DOM; mg C/L), amount of chlorine added (mg/L), concentration of trihalomethanes (THM; mg C/L) and concentration of haloacetic acids (HAA9; mg C/L). Different axes represent normalized values for DOC:DON (top left), $S_{275\text{-}295}$ (top right), SUVA (bottom right), and proportion HSF (bottom left). Groupings are based on hydrological environment and location: subsurface samples (a), YK surface waters (b), WK surface waters (c), and DL surface waters (d).

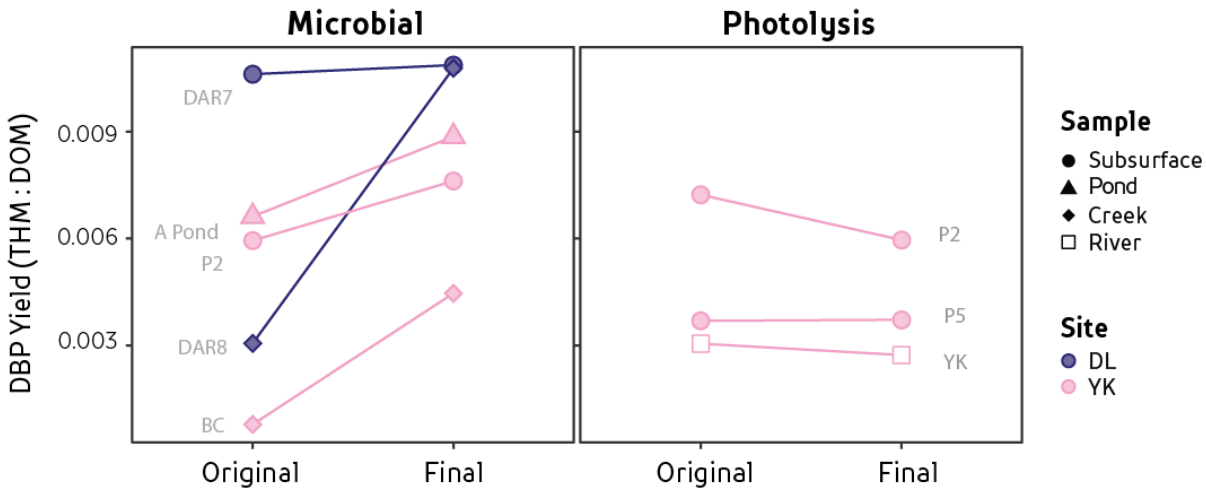

FIGURE 6.7: Ratio of trihalomethane (THM) to dissolved organic matter (DOM) concentration for microbial (left panel) and photolytic (right panel) degradation.

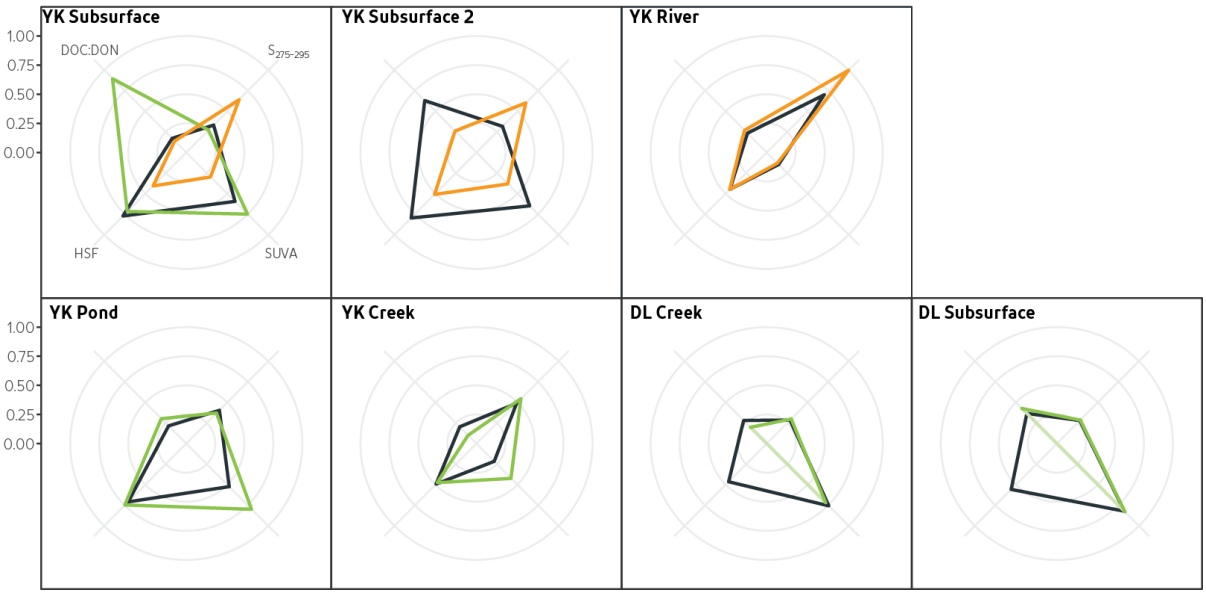

FIGURE 6.8: Composition Wheels illustrating the difference between original (dark line) and final samples for microbial (green) and photolytic (orange) degradation experiments. Different axes represent normalized values for DOC:DON (top left), $S_{275\text{-}295}$ (top right), SUVA (bottom right), and proportion HSF (bottom left).

Chapter 7
Synthesis of Thesis: Conceptual Diagram of Dissolved Organic Matter Evolution in the Northwest Territories

7.1 Creating a Conceptual Diagram

This thesis illustrates how dissolved organic matter (DOM) from the taiga shield to northern arctic differs across surface and subsurface systems in terms of DOM composition and response to microbial and photolytic processing. Integrating the results from Chapters 3, 4, and 5 provides a basis to categorize similarities in DOM composition, using Composition Wheels (CW), based on location and processing characteristics. The objective of this brief synthesis is to combine information generated across the previous chapters to form a conceptual diagram depicting the evolution of DOM composition along a flow path in the Northwest Territories (NT). The formation of this simplistic conceptual diagram of DOM evolution in the NT uses the idea that DOM composition reflects dominant source and processing characteristics, similarly to studies that have found DOM intrinsic properties to dictate DOM persistence in the environment[81]. In addition, process-based changes to DOM composition (Chapters 4 and 5) can be used to predict the evolution of DOM concentration and composition among different hydrological sites.

In this synthesis, the overall amounts of DOM are compared across the aquatic continuum to understand how DOM quantity evolves across the landscape. Then, DOM composition and lability, based on laboratory experiments, are compared to discern similarities and differences across different DOM samples. Differences in DOM concentration and composition will be used to form a conceptual diagram and compared to a well-defined flow path in the northern arctic to test the applicability of the framework to a system with greatly different climate and vegetation.

7.2 Setting the Conceptual Framework – DOM Source & Processing

Flow along the aquatic continuum originates from the subsurface and flows out of the watershed via creek or river. Differences in the overall amount of DOM are found along this flow path. High-organic peat plateaux samples in Yellowknife (YK) had the highest DOM concentrations (up to 273 mg C/L) while Daring Lake (DL) lakes (6.1±2.8 mg C/L, n=7) have the lowest average concentration

(Figure 7.1). DOM concentrations are highest from subsurface sites across all ecoregions, and decline along the aquatic continuum (Figure 7.1). Subsurface DOM concentrations from continuous permafrost (Wekweètì (WK) and DL) have lower concentrations than YK, but are higher than surrounding surface waters at each location. The highest surface water DOM concentrations are observed in YK ponds (34.0±2.4 mg C/L, n=2), while the lowest is from a DL creek (2.1 mg C/L). YK has higher surface water DOM concentrations than either WK and DL. Hence, a wide range of DOM concentrations are encountered not only across a latitudinal gradient in the NT, but also across a relatively small spatial scale within each ecoregion.

Photolytic and microbial degradation experiments were used to quantify the magnitude of change across different measures of composition (Chapters 4 and 5). Although initial DOM composition are not strong predictors of microbial degradation rate, changes to composition can be used to quantify the effect of both microbial and photolytic degradation. The amount of DOM lost and changes to composition resulting from photolysis are consistent across different sites with different DOM; however, microbial degradation is more dependent upon location characteristics and may differ depending upon host microbial consortia or availability of nutrients. For this reason, the average percent change between the final and initial SUVA, $S_{275\text{-}295}$, SAC_{420}, and DOC:DON across all samples are plotted, along with the largest percent increase and decrease observed (Figure 7.2), providing a range of DOM change that is expected for DOM in similar environments. In particular, degradation Composition Wheels show that the loss of non UV-visible absorbing components and decrease to DOC:DON would be the most notable changes resulting from microbial degradation. Conversely, photolysis results in a notable increase to $S_{275\text{-}295}$ and a net decrease in all other composition measures. Changes to DOM composition differ between photolytic and microbial degradation in ways that allow for the identification of DOM that has been previously altered due to photolysis.

7.2.1 End-members of the DOM Conceptual Diagram

Three distinct end-member groups can be defined based on similarities in DOM compositional metrics to literature, hydrologic sources, and degradation experiments. First, DOM compositions were grouped into three sections based on how similar each CW was and whether they contained characteristics similar to the final degradation DOM CW. This divided the composition into terrestrial, intermediate, or photolytic groups (Figure 7.3). The mixture of molecules that comprise

DOM at the point of sampling is dependent upon its source, degree of processing, and hydrologic mixing. For this reason, a plot that allows various combinations of sources and characteristics is used to portray variations in DOM composition. This approach is not able to determine the exact source or amount of processing required to produce each individual DOM sample; rather, this dataset provides the first step to understand whether DOM differs across landscapes and whether these differences can be used to understand DOM evolution along the aquatic continuum. Categorization of CW into these three groups was used to help constrain the end-members found on the DOM conceptual diagram.

7.2.1.1 Terrestrial End Member

Subsurface sites are important sources of organic matter within the NT as they contain much higher DOM concentrations than downstream surface water systems. Further, the unique signature of subsurface CWs are easily identified by the presence of large, humic, aromatic components. These characteristics have been used to define terrestrial DOM in other environments[34,80,81,244,245]. This signature is not only unique to the subsurface. Surface water DOM can be highly influenced by surrounding soil properties[4] resulting in identical subsurface and surface water CWs in areas with strong terrestrial-aquatic linkages. As subsurface sites generally contain higher DOM concentrations than surface waters (Figure 7.1), only a small contribution of subsurface DOM would be required to imprint a terrestrial signature within surface waters. Hence, subsurface environments are included as an end-member within the conceptual diagram and represent an important component dictating DOM composition in the NT.

7.2.1.2 Photolysis End Member

Photolytic degradation of DOM imprints a clear signature on various DOM compositions. Changes to DOM composition during photolysis (Figure 7.2) are consistent with other studies[199]. Samples with a unique photolytic signature are identified by an abundance of low molecular weight components (high $S_{275\text{-}295}$), and a low proportion of both aromatic (low SUVA) and humic components (either as HSF, or SAC_{420} as a proxy; Figure 7.3). The prominent effect of photolysis upon DOM composition results in unique and consistent changes to DOM composition regardless of source.

7.2.1.3 Autochthonous End Member and Other Samples

Autochthonous DOM is another important source of DOM within the aquatic environment. Shallow, hydrologically isolated ponds in the subarctic contain an important input of autochthonous DOM from macrophytes and benthic production that can be internally recycled on long timescales[4,90,130,315,316]. Autochthonous DOM is characterized by a low amount of UV-visible absorbing components, high protein and nitrogen content, and overall low molecular weight[34,244,317]. However, such characteristics of DOM are also representative of photolytically-degraded DOM. The importance of the autochthonous contribution to northern DOM is addressed in the conceptual diagram by defining this as an end-member that describes DOM with low DOC:DON and high $S_{275-295}$.

Variations in DOM sources, hydrologic mixing, or DOM degradation processes not accounted for in this thesis can result in CWs that are difficult to categorize. In particular, river DOM samples identified by high humic and low-molecular weight UV-components (high $S_{275-295}$) were found at both Yellowknife and Daring Lake; however, high $S_{275-295}$ that is indicative of extensive photolysis should also result in a low proportion of humics (Figure 7.3). These river samples may represent a mixture of DOM photolysed in upstream lakes, in-river production or mineralization of DOM, or a contribution of downstream terrestrial sources that may not have been fully processed. The conceptual diagram proposed here is not all encompassing, but does provide a basis to simplify, characterize, and eventually predict DOM evolution across hydrologic systems in the NT.

7.2.2 The DOM Conceptual Diagram

The three end-members represent a framework from which to compare differences in DOM composition (Figure 7.4). For instance, photolytic degradation acts universally across all sample types and will generally conform DOM to be more similar to the 'Photolysis' end member. Mixing of different DOM sources can also alter DOM composition, but the extent of change would depend upon a number of factors, such as the relative amount of mixing or the compositions being mixed. DOM composition can dictate different microbial or photolytic regimes within headwaters[264] or determine whether the system may be light (lacking solar energy to conform DOM) or substrate (lacking UV-absorbing components) limited in terms of photolytic degradation[113]. The conceptual diagram can be used to trace changes to DOM composition in response to a changing climate.

The conceptual diagram presented here, and data found in this thesis, support several conceptual hypotheses recently outlined by Creed et al.[141] that focusses on the response of northern DOM composition to global change. For instance, it was hypothesized that global change will introduce higher contributions of allochthonous DOM into lakes, altering water processes and influencing internal food webs. The focus on a shift towards greater allochthonous contributions among northern surface waters suggests the 'Autochthonous' end member in this model may be under-represented with a warming climate. However, our model supports this hypothesis as we find certain surface water DOM to have similar DOM compositions as the surrounding subsurface, suggesting DOM composition can be used to identify areas susceptible to enhanced allochthonous supply. Further, certain metrics of DOM composition differ in their response to different drivers of DOM fate. Overall, the conceptual model presented here aligns closely with previous hypotheses outlined by Creed et al.[141] that quantify the effects of certain landscape controls (photolysis and microbial degradation) on DOM composition and fate.

7.3 DOM Conceptual Diagram as a Predictive Tool

The DOM conceptual diagram provides a framework to track changes to DOM in response to a changing climate. The NT is projected to become warmer and drier[318], which can lead to increased water residence times in surface and subsurface systems and a lack of terrestrial-surface water connections[319]. In turn, mobilization of terrestrial DOM sources into surface waters may rely on infrequent rainfall events. Identifying how DOM composition influences drinking water treatability and how a warming climate may alter surface water characteristics via changes to transport pathways may be helpful for water managers. Results from this thesis found that microbial degradation of DOM, as well as high subsurface DOM concentrations, result in increased DBP formation on a carbon basis, while the opposite was observed from photolytic degradation. Mapping 'high-risk' DOM compositions on the conceptual diagram is possible by incorporating known relationships between DOM composition and certain water quality parameters, such as DBP (Figure 7.5). Further, incorporation with DOM loss rates will allow for a determination to the net effect of changing DOM composition on drinking water (i.e. DOM may become more terrestrial but enhanced retention time in reservoirs may reduce the amount and form of DOM entering the water treatment facility). This creates a tool that can be used to track the potential impact of DOM evolution in both concentration and composition under different climate scenarios.

7.4 Comparison to the High Arctic

The DOM conceptual diagram is based on samples from the NT. Northern arctic samples from the high arctic (Lake Hazen Watershed, NU) have DOM from very different sources, surrounding vegetation, and climate. In comparison to the NT, the Lake Hazen Watershed is colder, remains frozen for longer periods of time, receives much less precipitation, and generally contains sparse vegetation except for a few productive meadows[45]. The DOM conceptual diagram is used to trace DOM along a flow path through a representative sub-catchment near Lake Hazen. Flow begins from a talus seep, into a wetland, through a series of lakes and ponds, and eventually discharges via a creek into the larger Lake Hazen[320]. This flow-path provides a simple and constrained continuum to evaluate whether the DOM conceptual diagram can be easily adapted to represent different high arctic systems.

DOM concentrations increase along the continuum, beginning around 1.0 to 3.3 mg C/L at the seep, and increasing to 8.3 mg C/L in the subsurface and 6.3 mg C/L within a small lake. Glacial creeks contain the lowest concentrations (0.3 to 0.7 mg C/L; Figure 7.6). DOM compositions differ at each hydrologic site. Seep DOM is characterized by high HSF, moderate SUVA, and low DOC:DON and $S_{275\text{-}295}$, while subsurface DOM is characterized by high SUVA and low values for all other parameters (Figure 7.6). Pond and lake DOM contain high $S_{275\text{-}295}$, moderate HSF, and low DOC:DON and SUVA values. Glacial creeks have a variety of DOM compositions but generally contain lower measured values for all metrics compared to other sites. First-order microbial and photolytic degradation rates are much lower compared to NT, with photolysis resulting in higher DOM loss than microbial degradation (Chapter 4; Chapter 5). Microbial rates varied by 10x and was highest from seep DOM, while photolytic rates ranged by 1.5x and highest from subsurface DOM.

The lack of specific UV and visible absorbing components in northern arctic surface and subsurface DOM resulted in a position near the ‘substrate limited’ and ‘clear water’ regimes on the conceptual diagram. Further, all DOM samples from the Lake Hazen Watershed responded similarly in terms of DOM metrics to photolysis (Chapter 5), characteristic of other clear-water regime systems. These samples also plot closely to NT DOM with strong photolytic characteristics (Figure 7.7). Grouping of DOM compositions in the NT DOM conceptual diagram may also be applicable to other locations. These groupings provide information on processes that drive DOM composition across these systems.

The NT DOM conceptual diagram may not accurately incorporate the diversity of high arctic DOM composition. Creek DOM did not contain comparable compositions to any of the end members (Figure 7.7). Further, lower proportions of humics in high arctic subsurface DOM result in a very different subsurface composition than what is found in the NT. Hence, there is some applicability of the processes that govern DOM, yet compiling DOM compositions between the high-arctic and NT indicate modifications would need to be made to the conceptual diagram to encompass more arctic sites.

7.5 Conclusion

A conceptual diagram of the evolution in DOM composition is presented for different surface and subsurface DOM in the NT. Although data represents a select few sites in the NT, this conceptual diagram offers an initial characterization that can be easily adapted to incorporate DOM from other ecoregions in the NT. Further, the similarity in DOM composition observed from Yellowknife to Daring Lake suggests that DOM may not be all that different, especially across subsurface sites. However, some differences in high artic DOM are not encapsulated in the model that fits the low arctic and taiga shield. By acknowledging how DOM composition varies across the landscape, and different sources and processes may alter this composition, we can better estimate how DOM will respond changes in processes that drive DOM fate across the NT.

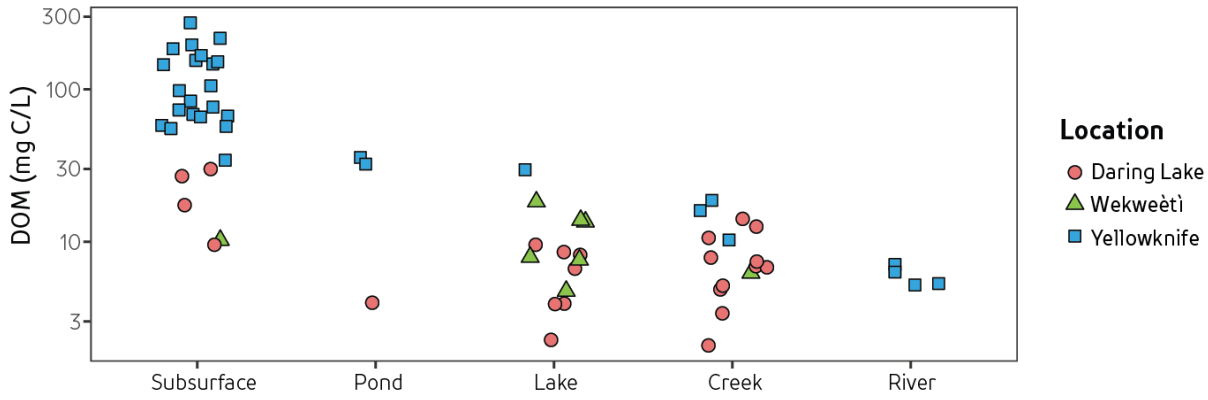

FIGURE 7.1: Dissolved organic matter concentration (DOM; logarithmic scale) for different subsurface ('Sub') and surface water sites at Daring Lake, Wekweètì, and Yellowknife. Numerous samples collected at the same site are represented by a single averaged point. Random scatter is incorporated into the x-axis to clearly show different data points.

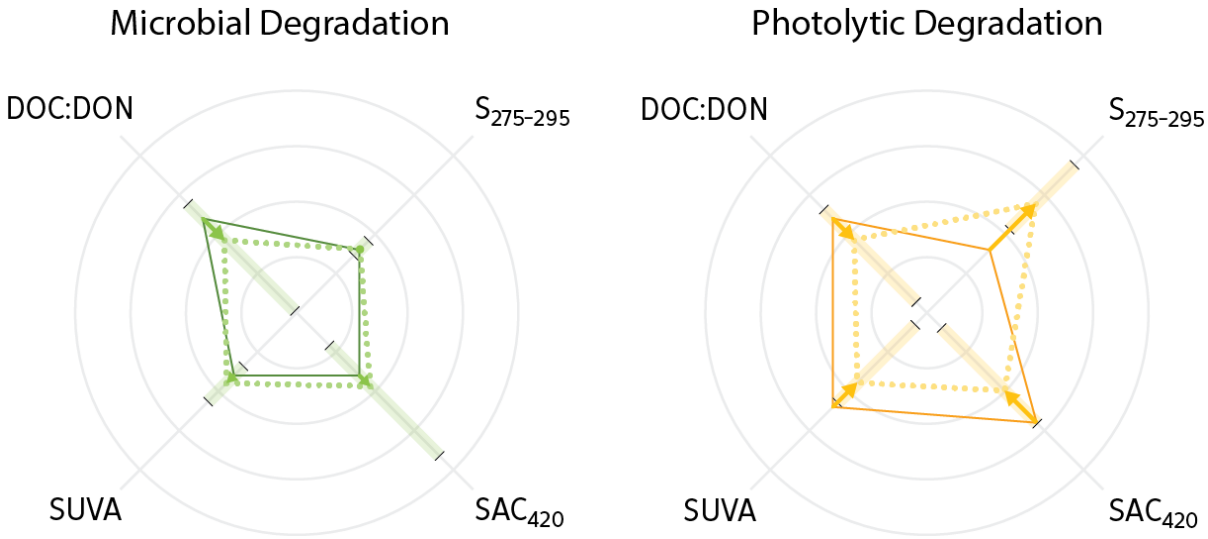

FIGURE 7.2: Summary of the relative effect of microbial (green; left) and photolytic (yellow; right) decomposition upon dissolved organic matter (DOM) composition measures using a hypothetical initial (dark line) and final (dotted line) DOM composition. The arrows represent the average change in each compositional metric using all samples, while the shaded box represents the greatest increase and decrease quantified from the experimental incubations (see Chapters 4 and 5). The shape of the initial composition is irrelevant as the percent change from each parameter is plotted. The Composition Wheel is defined by dissolved organic carbon to organic nitrogen ratio (DOC:DON), slope from 275 to 295nm (S_{275}), spectral absorption coefficient at 420 nm (SAC_{420}), and specific UV-absorbance at 255nm (SUVA). Microbial degradation represents the change determined over 30 days for all samples, whereas photolytic degradation represents the loss after 500 E/m^2 for all samples (corresponds to 13 and 18 days of continual sunlight in the low and high arctic, respectively).

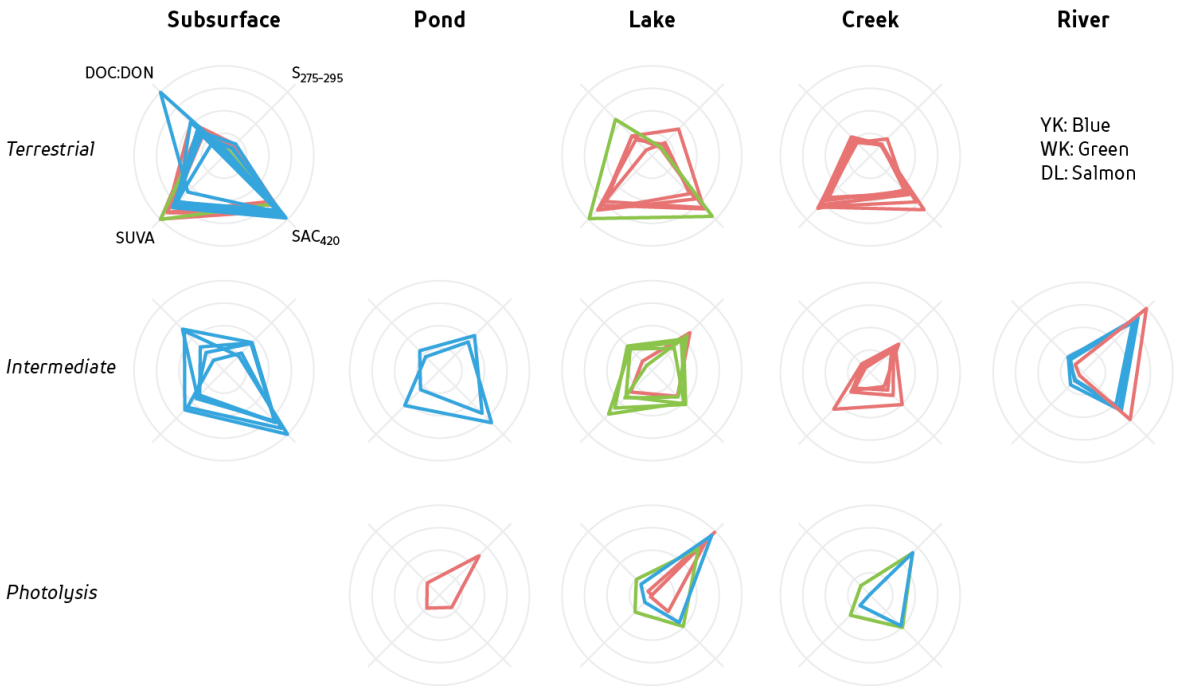

FIGURE 7.3: Dissolved organic matter (DOM) composition wheels for different hydrological sites from Yellowknife (YK), Wekweètì (WK), and Daring Lake (DL), Northwest Territories. DOM was categorized as either having terrestrial, photolytic, or intermediate characteristics based on sampling location and similarities to observed effects of degradation experiments on DOM metrics. Composition Wheels were represented by dissolved organic carbon to organic nitrogen ratio (DOC:DON), slope from 275 to 295nm (S275), proportion of the humic substances fraction (HSF), and specific UV-absorbance at 255nm (SUVA).

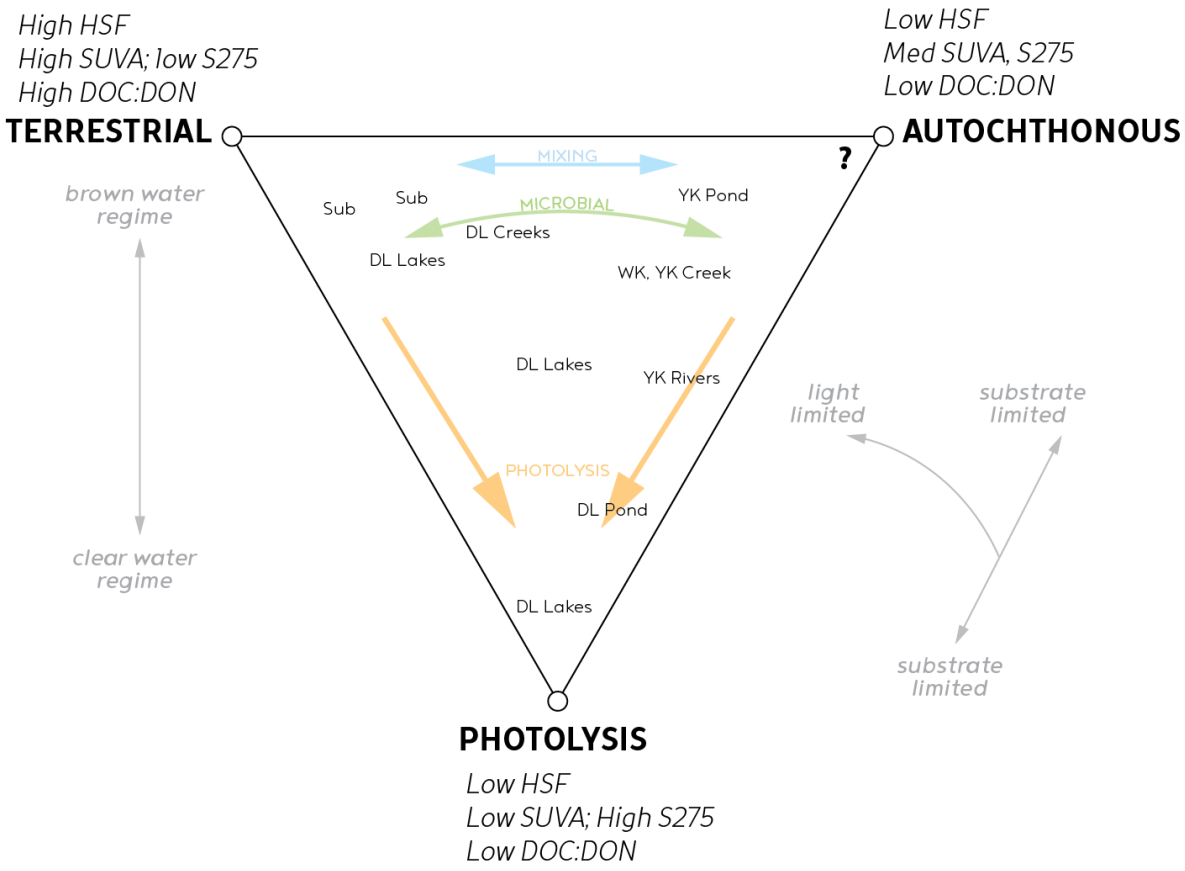

FIGURE 7.4: Conceptual diagram of dissolved organic matter (DOM) in the Northwest Territories based on microbial and photolytic degradation experiments and on the initial DOM present in the dataset. End-member (Terrestrial, Photolysis, Autochthonous) represent important source or processing characteristics, while arrows within the triangle represent how different processes 'move' DOM across the conceptual diagram. Greyed arrows on the side represent similar DOM evolution hypotheses[113,264]. The question mark indicates where data is lacking for a clear autochthonous-sourced DOM sample.

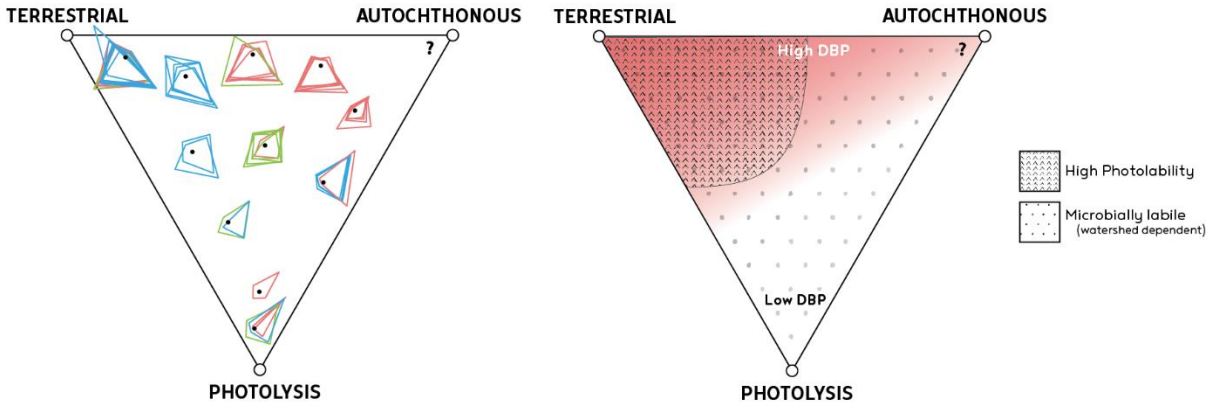

FIGURE 7.5: Example of using the dissolved organic matter (DOM) conceptual diagram to either trace DOM evolution in the environment (NT samples taken from Figure 7.3; left) or use to identify DOM compositions that are easily degraded (dots: microbially labile; triangles: photolytically labile) or easily form disinfection by-product (DBP; red-shading: darker means higher propensity to form DBP).

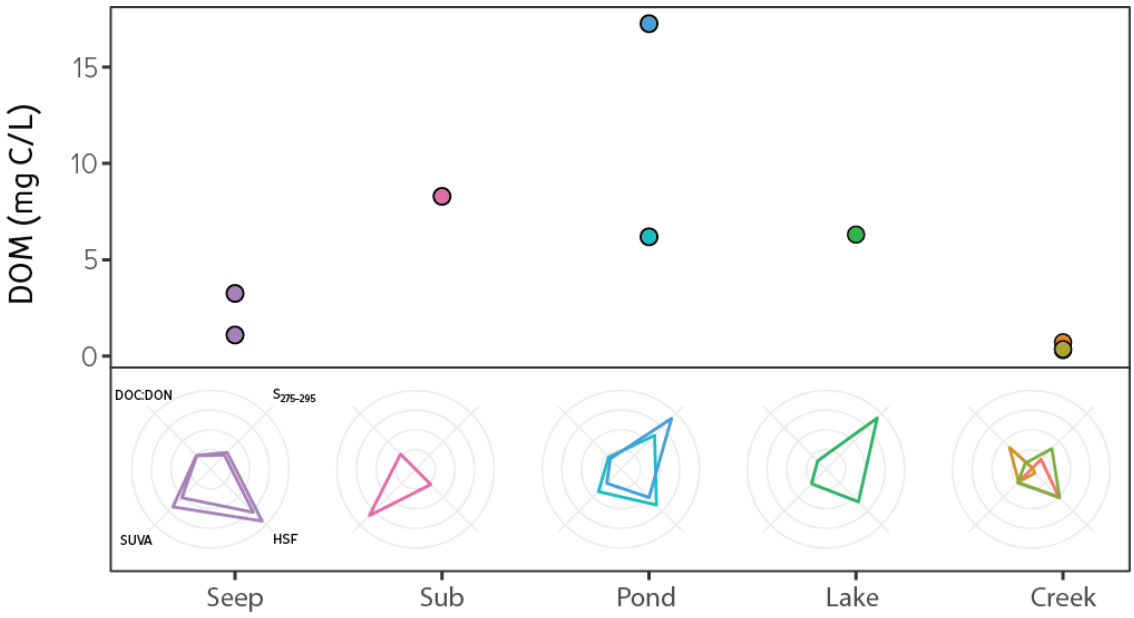

FIGURE 7.6: Dissolved organic matter concentration (DOM mg C/L; upper panel) and composition wheel (lower panel) for different hydrologic sites from the Lake Hazen Watershed, Nunavut. Composition wheels were based on dissolved organic carbon to organic nitrogen ratio (DOC:DON), slope from 275 to 295nm (S275), proportion of the humic substances fraction (HSF), and specific UV-absorbance at 255nm (SUVA).

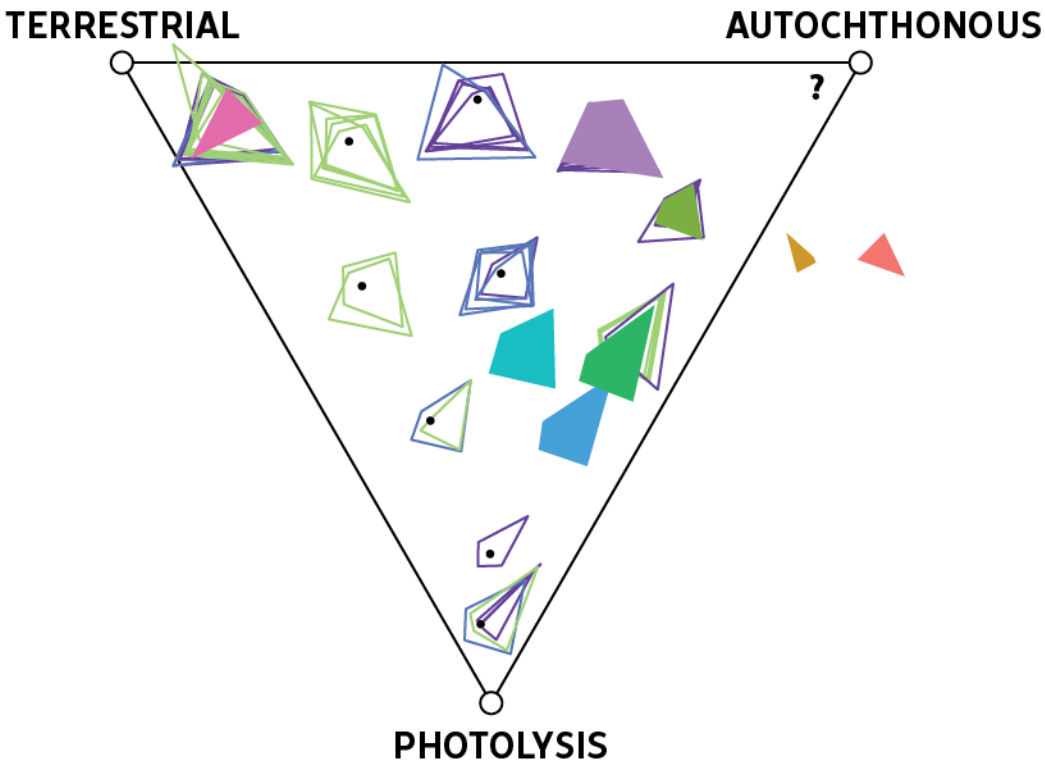

FIGURE 7.7: Application of the NT DOM conceptual diagram (hollow shapes) for high arctic DOM samples (solid shapes). Composition Wheels on the right side not in the triangle represent DOM from a glacial creek that were not similar to any of the defined end-members. Subsurface DOM, although different than all other subsurface samples, was plotted by 'terrestrial' as it was collected directly from the subsurface.

Chapter 8

Summary & Future Research

8.1 Original Scientific Contributions

The overall goal of this PhD thesis is to quantify differences in DOM concentration and composition across three northern ecoregions in Canada and to determine how DOM composition influences photolytic and microbial degradation rates. Summarized below are the major findings from each chapter.

The Northwest Territories (NT) represents an area of Canada rapidly undergoing change in response to a warming climate[10,11,147]. The objective of the first data chapter was to quantify the geochemical response to a warming climate from systems draining the taiga shield (Yellowknife and Cameron River) and taiga plains (Marian River) near Yellowknife, NT. Statistical analysis of long-term climatic parameters from the area and hydrologic variables from these rivers was used to investigate the magnitude of change in mean annual air temperature, total precipitation, monthly and annual discharge, and various geochemical parameter concentrations and fluxes (Chapter 2). Mean monthly air temperatures near Yellowknife significantly increased in winter (January to April), June, and July, with an annual increase in 3.2×10^{-2} °C/yr over the 80-year timeframe. No significant changes to the annual discharge of the Yellowknife or Cameron rivers occurred; however, increased average monthly discharge during the winter months was observed in the Yellowknife River over the 35-year dataset. Mean annual solute concentrations significantly increased within the Yellowknife and Cameron rivers over the 30-year time period, which in the absence of a change in discharge, indicated a shift towards deeper, potentially mineral-rich, subsurface flow pathways. Although concentrations of DOM did not change over time in any of the rivers, warming mean annual air temperatures in the area are nearing a threshold of -2°C, found to enhance DOM mobility in discontinuous permafrost areas[28]. Baseline conditions were easily defined for the Cameron River due to unchanging monthly and annual discharge, as well as for the Marian River, exhibiting strong seasonality in geochemistry but no trend with time. Conversely, changes to river discharge and water quality in the Yellowknife River suggest a dynamic and unidirectional trend, likely representative of increasing subsurface flow pathways. Hence, long-term records of climate, hydrology, and discharge indicate differences in the response from three

rivers near Yellowknife, and provide evidence on how these systems may continue to respond to a warming climate.

A variety of metrics can be used to characterize differences in DOM composition among surface and subsurface waters. The objective of the second data chapter was to determine which simple measures of DOM composition best explain the variability in DOM encountered across a variety of Canadian ecoregions (Chapter 3). Different DOM compositional measures included ultra-violet (UV) and visible absorbance, elemental ratios, and size-exclusion chromatography. Principal components analysis was applied to the DOM dataset and compositional measures with the highest contributions to the first and second principal component axes were determined to best represent variations in DOM composition. These measures included specific UV-absorbance at 255nm (SUVA), spectral slope between 275 and 295 nm ($S_{275\text{-}295}$), elemental ratios (DOC:DON), and the proportion of humic-substances fraction (HSF). Composition Wheels, a novel tool to visualize differences in DOM composition, were assembled using these four measures and used to quantify how different aspects of DOM change along the aquatic continuum. Overall, subsurface DOM, easily identified by high values of HSF and SUVA and low $S_{275\text{-}295}$, was similar across all sampling location compared to surface water DOM. More variability in composition was encountered among surface water DOM, likely reflecting differences in water residence time, exposure to photolysis, or *in situ* production of DOM. Hence, differences in DOM composition can be easily utilized to compare or trace the evolution of DOM composition across the aquatic continuum.

Processing of DOM can alter the amount, form, and reactivity of DOM exported from a watershed. Microbial processing is often the most important driver of DOM transformation and loss, yet few loss rates are found from sites in the Canadian subarctic and high arctic. The objective of the third data chapter was to quantify the range in the proportion of DOM lost during an incubation experiment, as well as quantify dark DOM loss rates from different hydrologic sites in three ecoregions: the taiga shield (Yellowknife, NT), southern arctic (Daring Lake, NT), and northern arctic (Lake Hazen, NU; Chapter 4). Results from a 30-day microbial incubation experiment commonly used to define biodegradable DOM (BDOM) show a total decrease between 1 to 27% from the original DOM concentration. Northern arctic DOM contained the lowest initial DOM concentrations and proportion of BDOM (1 to 11%), indicating that DOM is persistent within these systems. The highest BDOM proportions were observed in DOM in a southern arctic creek (27%) and taiga shield subsurface (17%). At similar incubation durations, proportions of BDOM

from this study are higher than other studies conducted in the NT, but overall lower when compared to other circumpolar areas such as Siberia or Alaska. Highest 1st-order degradation rate constants were observed from DOM in the taiga shield subsurface (7.3 $x10^{-3}$ d^{-1}) and a southern arctic pond (11.2 $x10^{-3}$ d^{-1}), while the remaining ten samples had a narrow range between 1.4 to 4.0 $x10^{-3}$ d^{-1}. Changes to DOM composition due to microbial degradation were generally unique to a specific sample. Further, traditional measures of DOM composition, such as spectral absorbance at 255 nm (SUVA) or spectral slope, were not good *a priori* predictors of BDOM proportion or degradation rate. However, the change in SUVA or SAC_{420} were better suited to quantify changes to DOM composition during microbial degradation as they showed the largest changes. Hence, location is more important for determining microbial lability than DOM composition and decreases to SUVA and SAC_{420} provide sensitive indicators of microbial degradation.

Photolytic degradation is an important driver of DOM fate in sub-arctic and arctic systems, particularly in shallow surface waters. The overall objective of the fourth data chapter was to determine the influence of DOM composition on photolytic DOM loss and quantify photodegradation rates (Chapter 5). The percentage loss in DOM was similar across locations (between 13 to 19% after 500 E/m^2, which corresponds to roughly 13 and 18 days of constant sunlight in the southern and northern arctic, respectively) even though initial DOM characteristics were different. However, photolytic yield (total amount of DOM lost divided by total irradiation) suggest DOM from these sites contain lower amounts of photolabile DOM than studies conducted in elsewhere. DOM composition is important for photolysis as DOM composition responded in a predictable manner across all sites: loss of humic, UV-visible light absorbing components, and the production of smaller, low-molecular weight DOM components. Photolysis of DOM followed a 1st-order rate equation with highest rates from southern arctic subsurface DOM (17 $x10^{-4}$ m^2/E) and lowest from northern arctic DOM (1.6 to 4.2 $x10^{-4}$ m^2/E) and taiga shield subsurface (4.1 $x10^{-4}$ m^2/E). Linear degradation rates, used to compare all photolysed samples and literature values, ranged between 0.4 to 30 x 10^{-3} m^2/E and were lower by one to two orders of magnitude than similar experiments conducted in Siberia, Russia, and Bylot Island, Canada. Further, unlike microbial degradation, photolytic degradation rates could be predicted using initial SUVA, SAC_{420}, and $S_{275-295}$ metrics. The importance of characterizing DOM composition to predict DOM lability is demonstrated by quantifying the contrasting influences of microbial and photolytic degradation on DOM compositional metrics. Thus, the sub-arctic and arctic locations sampled in this study are a

unique region onto itself with lower photolytic and microbial lability than other locations (i.e. eastern Boreal Canada, Alaska, or Siberia).

Dissolved organic matter adversely impacts drinking water quality via the formation of disinfection by-products (DBP) during the chlorination of drinking water supplies. The objective of the fifth data chapter was to quantify the relationship between DOM composition and DBP formation across various subsurface and surface water DOM encountered in the NT (Chapter 6). This objective was completed using two approaches: 1) assessing the occurrence of DOM and DBP within NT community drinking water supplies as reported, and 2) determining how differences in DOM composition relate to DBP formation. Public water quality records of 33 communities, obtained from the Government of Northwest Territories Municipal and Community Affairs website, showed that DOM and DBP were prevalent across the NT. Only 11% of all records (n= 520) contained values above the Canadian Council of Ministers of the Environment (CCME) maximum acceptable concentration. However, differences in storage times, point of sampling, different analytical laboratories, and time left to react, can all influence the amount of DBP formed making comparisons among sites difficult. Chlorination and DBP formation was measured in DOM samples collected from various surface and subsurface sites from the taiga shield (Yellowknife and Wekweètì, NT), southern arctic (Daring Lake, NT) ecoregions. Differences in the disinfection demand (DD; amount of chlorine added to obtain a chlorine residual) versus DOM concentration, as well as DBP:DOM, across samples indicated that DOM concentration alone was not a good predictor of DBP formation or DD. In both surface and subsurface environments, high DBP concentrations were formed from DOM with a terrestrial-like signature. Further, simple UV-absorbance measures provided useful information to predict DBP formation. Degradation experiments show that photolysis decreased the formation of DBP per carbon atom, yet microbial degradation increased the amount of DBP formed per DOM carbon atom. Hence, DOM concentration and composition were both important when considering drinking water treatability, especially in the NT where permafrost degradation, changing precipitation regimes, and warming temperatures may result in higher loadings of terrestrial DOM into surface waters used as drinking water resources.

A conceptual model to the evolution of DOM in the NT was created based on data and interpretations from the previous chapters. A three end-member model (Terrestrial, Photolytic, and Autochthonous) was determined based on similarities in DOM composition among sites, similarities

to DOM characteristics observed in literature, and results from the previous incubation experiments that identified specific indicators of microbial or photolytic processes on DOM composition. The conceptual model can be used to identify how different drivers influence DOM composition. Further, processing of DOM results in similar metrics regardless of initial composition. However, the conceptual model does not encapsulate some of the DOM compositions observed in the high arctic. This conceptual model provides a tool to link changes in DOM composition with effects upon DBP formation or ecosystem processes.

8.2 Future DOM Research in Sub-Arctic and Arctic Environments

The dataset presented in this thesis finds DOM composition can differ across relatively small spatial scales. Although this thesis was able to capture the heterogeneity in DOM composition, the data does not represent an instrumented flow path. Further, effective use of these degradation rates requires an accurate estimate of the time DOM may spend within a body of water or subsurface. Quantifying hydrologic flow paths, contributing areas, and both surface and subsurface water residence times would help constrain potential rates of degradation (i.e., exposure to sunlight, degradation in subsurface, time spent within a watershed) and improve estimates of DOM processing within these systems. Although the presence of permafrost can complicate hydrologic modelling and transport in the subsurface, there is a need to constrain and understand the quantity and timing of flows that transport DOM between terrestrial and aquatic systems.

Source characteristics of DOM need to be better quantified to trace DOM evolution within these systems. To enhance our understanding of DOM among different environments, more information is needed on the characterization of autochthonous DOM sources in NT surface waters and the impact of *in situ* DOM on local carbon cycling. Data from this thesis can strongly identify terrestrial sources of DOM or the influence of photolysis; however research is lacking in the connection between DOM composition and its impact on ecosystem functioning[141]. Autochthonous DOM comprised a biologically-available form of carbon within the Mackenzie Delta[130] but more data are needed to better constrain characteristics and rates of internal DOM production from different sub-arctic and arctic areas. Recent work in the Yukon River Basin, Alaska, highlighted the importance of internally derived carbon fixed from atmospheric carbon dioxide, rather than from terrestrial sources such as soils or degrading permafrost[316]. Determining the presence, composition, and fate of permafrost-derived carbon would be beneficial to help identify and predict the specific

response of permafrost-mobilized DOM on the carbon cycle under various climate change scenarios. Research from Siberia and Alaska have found ancient permafrost to be easily degraded and rapidly assimilated into biomass rather than mineralized into carbon dioxide[85,96,100]. The use of both stable and radioactive carbon isotopes offers a useful tool that would aid in constraining different terrestrial and aquatic DOM sources and processing, as well as identifying the presence of permafrost carbon. Quantifying the importance of *in situ* and permafrost-derived DOM using a suite of isotopic and geochemical measures would help delineate and constrain various sources that influence DOM reactivity.

Changes to the diversity and functioning of terrestrial and aquatic microbial communities can influence the fate of northern carbon. Incubation experiments rely on the microbial consortia during time of sampling, without any characterization or identification of key communities that may influence degradation rates. Recent work has shown how permafrost degradation results in rapid shifts to microbial community assemblages that directly impact the biogeochemical functioning of thaw ponds, as well as rates of carbon and nitrogen cycling within these systems[227,321–325]. The basic use of the term 'inoculum' greatly generalizes a breadth of microbial information that can be better utilized to constrain future predictions of carbon lability and cycling. Quantifying the influence of the microbial community upon DOM cycling is an important avenue to continue research as differences in community assemblages and functioning will alter DOM fate with a warming climate.

Further research is needed to enhance our understanding of how differences in DOM composition impact drinking water parameters, such as the association between DOM and trace metal mobility or toxicity. One avenue is explored in this thesis (production of DBP); however, there are a number of DOM-related water quality concerns that can be addressed. For instance, use of Proton Binding Index[60] could identify how differences in DOM composition affect the ability of DOM to interact with metals. Further, differences in the amount and source of freshwater organic matter have been found to influence mercury methylation rates and photodemethylation within the water column and lake or pond sediments[228,326–328]. The DOM database collected from this thesis could be used to further the understanding of the relationship between DOM lability, DOM composition, metal complexation, and mercury methylation rates, providing informative relationships in terms of aquatic health and drinking water quality.

Appendix A

Chapter 2 – Supplementary Figures

Summary of Concentration and Flux Chemistry

TABLE A: Annual (bold) and monthly (regular) cation and anion concentrations for the entire time period for the Yellowknife (YK; 1988 to 2012), Cameron (CAM; 1988 to 2012), and Marian (MAR; 2000 to 2012) rivers in the Northwest Territories, Canada. Average values are given with 1-standard devation (σ) and number of samples (*n*). Alkalinity is measured as the total concentration of $CaCO_3$.

	CATIONS												ANIONS								
RIVER	**K^+** (mg/L)			**Na^+** (mg/L)			**Ca^{2+}** (mg/L)			**Mg^{2+}** (mg/L)			**Cl^-** (mg/L)			**SO_4^{2-}** (mg/L)			**Alkalinity** (mg/L)		
	Avg	σ	*n*	*Avg*	σ	*n*	*Avg*	σ	*n*	*Avg*	σ	*n*	*Avg*	σ	*n*	*Avg*	σ	*n*	*Avg*	σ	*n*
YK	**0.96**	**0.14**	***255***	**1.74**	**0.43**	***253***	**5.31**	**1.31**	***257***	**1.92**	**0.43**	***255***	**1.76**	**0.25**	***255***	**3.45**	**0.99**	***249***	**18.6**	**2.9**	***243***
Jan	0.99	0.15	*21*	1.74	0.36	*21*	4.85	0.99	*22*	1.75	0.40	*22*	1.74	0.15	*20*	3.18	0.48	*21*	18.4	2.9	*21*
Feb	1.01	0.14	*18*	1.85	0.38	*18*	5.61	2.24	*19*	1.91	0.52	*19*	1.79	0.31	*19*	3.98	1.92	*19*	19.2	3.0	*17*
Mar	0.99	0.12	*22*	1.80	0.40	*23*	4.97	1.14	*23*	1.90	0.56	*23*	1.82	0.28	*23*	3.35	0.58	*22*	18.8	2.9	*19*
Apr	1.03	0.13	*20*	1.87	0.46	*19*	5.58	1.35	*20*	2.11	0.42	*19*	1.83	0.32	*17*	3.90	1.05	*20*	18.6	2.9	*20*
May	0.96	0.16	*25*	1.72	0.38	*25*	5.06	1.13	*25*	1.88	0.50	*25*	1.76	0.21	*26*	3.61	1.01	*25*	18.3	3.0	*23*
Jun	0.94	0.12	*26*	1.73	0.38	*26*	5.31	1.07	*26*	1.94	0.32	*26*	1.76	0.20	*27*	3.25	0.80	*24*	18.6	2.6	*23*
Jul	0.94	0.13	*22*	1.69	0.46	*22*	5.61	1.20	*22*	2.03	0.41	*22*	1.71	0.21	*23*	3.53	1.28	*22*	19.2	2.6	*21*
Aug	0.91	0.12	*23*	1.70	0.41	*22*	5.37	1.33	*23*	1.95	0.42	*22*	1.75	0.37	*22*	3.17	0.65	*21*	18.5	3.3	*24*
Sep	0.92	0.15	*24*	1.63	0.48	*23*	5.61	1.62	*24*	1.97	0.45	*24*	1.71	0.22	*24*	3.44	0.85	*23*	18.1	3.4	*22*
Oct	0.91	0.14	*20*	1.73	0.41	*20*	5.15	0.99	*20*	1.86	0.41	*20*	1.68	0.26	*20*	3.47	1.04	*19*	18.7	2.6	*20*
Nov	0.95	0.18	*16*	1.75	0.59	*16*	5.37	1.27	*15*	1.85	0.34	*15*	1.78	0.24	*16*	3.27	0.37	*15*	18.6	3.0	*15*
Dec	1.00	0.15	*18*	1.76	0.46	*18*	5.35	1.11	*18*	1.87	0.37	*18*	1.79	0.25	*18*	3.30	0.65	*18*	18.8	2.7	*18*
CAM	**1.14**	**0.16**	***229***	**2.20**	**0.36**	***230***	**8.50**	**1.74**	***232***	**2.48**	**0.47**	***231***	**2.33**	**0.48**	***224***	**4.24**	**1.21**	***227***	**28.0**	**4.2**	***231***
Jan	1.21	0.14	*20*	2.30	0.27	*20*	8.58	1.33	*21*	2.52	0.37	*21*	2.23	0.50	*19*	4.58	1.07	*21*	29.8	3.4	*21*
Feb	1.29	0.16	*14*	2.52	0.32	*14*	9.72	2.12	*15*	2.72	0.66	*15*	2.60	0.48	*15*	4.72	1.07	*13*	32.5	2.8	*15*
Mar	1.29	0.16	*15*	2.64	0.28	*15*	9.72	1.60	*15*	2.83	0.52	*15*	2.91	0.68	*15*	4.45	0.89	*15*	32.8	2.7	*15*
Apr	1.28	0.12	*23*	2.51	0.33	*23*	9.41	1.71	*23*	2.82	0.53	*23*	2.52	0.57	*21*	4.62	1.27	*23*	30.9	3.4	*23*
May	1.15	0.16	*19*	2.15	0.33	*20*	8.15	1.72	*20*	2.48	0.40	*19*	2.46	0.29	*18*	3.93	1.10	*20*	26.6	4.0	*20*
Jun	1.06	0.10	*21*	1.96	0.30	*21*	7.63	1.53	*21*	2.28	0.37	*21*	2.25	0.39	*21*	3.83	0.62	*20*	25.3	3.2	*20*
Jul	1.07	0.11	*22*	2.07	0.32	*22*	8.19	1.45	*22*	2.37	0.41	*22*	2.22	0.40	*21*	4.31	1.23	*22*	25.5	3.2	*22*
Aug	1.05	0.09	*26*	1.98	0.20	*26*	7.57	1.44	*26*	2.24	0.37	*26*	2.23	0.30	*25*	3.91	0.99	*25*	25.7	3.3	*26*
Sep	1.08	0.10	*20*	2.06	0.24	*20*	8.52	1.86	*20*	2.48	0.39	*20*	2.12	0.36	*20*	4.28	1.98	*20*	26.3	3.2	*20*
Oct	1.02	0.15	*22*	2.04	0.30	*22*	8.04	1.44	*22*	2.34	0.33	*22*	2.01	0.35	*22*	4.39	1.66	*21*	26.1	2.9	*22*

Nov	1.08	0.14	*14*	2.11	0.28	*14*	8.45	1.88	*14*	2.38	0.47	*14*	2.23	0.38	*14*	3.76	0.67	*14*	27.4	4.5	*14*
Dec	1.24	0.15	*13*	2.36	0.28	*13*	9.15	1.55	*13*	2.54	0.52	*13*	2.42	0.37	*13*	4.08	0.44	*13*	30.7	3.3	*13*
MAR	**1.13**	**0.22**	***166***	**2.09**	**0.37**	***166***	**18.4**	6.86	***166***	**7.91**	**3.00**	***168***	**1.48**	**0.28**	***159***	**15.7**	**8.04**	***163***	**59.1**	**23.8**	***165***
Jan	1.11	0.31	*13*	2.23	0.25	*12*	20.4	4.27	*13*	9.14	2.11	*13*	1.53	0.15	*11*	15.7	4.42	*13*	71.2	21.2	*13*
Feb	1.17	0.16	*11*	2.21	0.27	*11*	19.7	4.08	*12*	8.88	2.43	*12*	1.42	0.22	*12*	12.2	3.24	*12*	70.6	23.0	*12*
Mar	1.16	0.13	*15*	2.22	0.17	*15*	20.1	3.14	*15*	9.56	1.80	*15*	1.57	0.25	*15*	11.6	2.65	*15*	74.9	19.3	*15*
Apr	1.17	0.12	*14*	2.17	0.17	*14*	21.0	2.81	*14*	9.99	1.64	*14*	1.46	0.19	*12*	13.1	3.53	*14*	72.1	18.7	*14*
May	1.00	0.30	*16*	1.77	0.36	*16*	15.1	6.90	*16*	6.17	3.00	*16*	1.24	0.27	*14*	13.5	9.80	*16*	47.5	20.5	*16*
Jun	1.09	0.18	*15*	1.77	0.28	*15*	12.4	4.69	*15*	4.77	1.75	*15*	1.36	0.32	*15*	13.1	8.69	*15*	36.4	12.8	*15*
Jul	1.22	0.26	*15*	2.03	0.37	*15*	15.5	6.39	*15*	6.85	3.27	*15*	1.44	0.24	*15*	13.7	6.43	*15*	45.6	28.2	*15*
Aug	1.10	0.20	*17*	2.04	0.38	*17*	15.9	7.58	*17*	7.45	3.71	*17*	1.41	0.23	*17*	14.3	5.74	*16*	57.3	25.8	*16*
Sep	1.13	0.28	*13*	2.06	0.38	*14*	18.0	6.26	*14*	7.78	3.19	*14*	1.51	0.30	*14*	19.0	9.02	*14*	52.7	21.7	*14*
Oct	1.09	0.22	*15*	2.16	0.44	*15*	22.5	10.6	*15*	8.37	2.56	*15*	1.54	0.28	*15*	21.4	10.3	*12*	57.0	19.4	*14*
Nov	1.15	0.21	*11*	2.32	0.42	*11*	21.0	7.72	*10*	7.78	3.18	*11*	1.76	0.22	*9*	26.9	9.24	*10*	64.4	17.2	*10*
Dec	1.19	0.17	*11*	2.37	0.35	*11*	22.4	6.23	*10*	9.17	2.55	*11*	1.68	0.32	*10*	19.3	7.71	*11*	69.1	20.0	*11*

Table A2: Annual (bold) and monthly (regular) nutrient and field parameters for the entire time period for the Yellowknife (YK; 1988 to 2012), Cameron (CAM; 1988 to 2012), and Marian (MAR; 2000 to 2012) rivers in the Northwest Territories, Canada. Average values are given with 1-standard devation (σ) and number of samples (*n*).

RIVER	OTHER								Nutrients											
	Tot. Diss. Solids (mg/L)			**pH**		**Spec. Cond.** (uS/cm)			**NH_3** (mg N/L)			**NO_3^-+NO_2^-** (mg N/L)			**TP** (mg/L)			**DOC** (mg/L)		
	Avg	σ	*n*	*Avg*	*n*	*Avg*	σ	*n*	*Avg*	σ	*n*	*Avg*	σ	*n*	*Avg*	σ	*n*	*Avg*	σ	*n*
YK	**32.6**	**12.4**	***258***	**7.37**	***261***	**53.2**	**6.6**	***264***	**0.013**	**0.015**	***213***	**0.042**	**0.041**	***238***	**0.015**	**0.028**	***261***	**5.06**	**0.72**	***245***
Jan	34.8	16.5	*23*	7.22	*23*	51.5	5.5	*23*	0.014	0.010	*19*	0.055	0.025	*22*	0.010	0.006	*22*	4.92	0.56	*20*
Feb	28.5	9.2	*20*	7.24	*20*	53.3	7.5	*20*	0.010	0.014	*15*	0.054	0.020	*17*	0.023	0.057	*20*	4.99	0.72	*17*
Mar	28.4	12.6	*23*	7.17	*23*	52.7	5.5	*23*	0.019	0.026	*20*	0.060	0.027	*20*	0.013	0.019	*23*	4.96	0.43	*22*
Apr	34.6	7.8	*17*	7.32	*18*	55.2	6.8	*20*	0.012	0.015	*16*	0.058	0.039	*19*	0.010	0.005	*18*	4.87	0.80	*19*
May	33.3	12.8	*26*	7.39	*26*	52.1	5.6	*27*	0.009	0.006	*22*	0.038	0.037	*26*	0.011	0.008	*27*	5.21	0.74	*27*
Jun	36.5	14.0	*26*	7.43	*27*	53.0	4.5	*27*	0.011	0.011	*21*	0.030	0.050	*24*	0.011	0.009	*27*	5.00	0.59	*25*
Jul	33.7	12.9	*23*	7.51	*23*	54.3	6.1	*23*	0.013	0.014	*19*	0.041	0.067	*19*	0.012	0.007	*23*	5.31	0.53	*23*
Aug	34.6	9.3	*23*	7.53	*23*	52.8	6.7	*24*	0.010	0.008	*18*	0.027	0.053	*22*	0.010	0.004	*23*	5.16	0.61	*20*
Sep	33.0	16.4	*24*	7.46	*24*	51.6	7.9	*24*	0.009	0.004	*20*	0.029	0.045	*21*	0.027	0.056	*24*	5.43	1.27	*22*
Oct	29.2	8.5	*20*	7.41	*20*	54.8	8.9	*20*	0.012	0.018	*16*	0.030	0.032	*17*	0.019	0.036	*20*	5.01	0.73	*19*
Nov	28.4	11.0	*15*	7.40	*16*	54.0	8.6	*15*	0.017	0.020	*13*	0.039	0.025	*15*	0.012	0.017	*16*	4.65	0.37	*15*
Dec	33.7	9.3	*18*	7.30	*18*	54.5	6.2	*18*	0.016	0.022	*14*	0.053	0.017	*16*	0.023	0.036	*18*	5.00	0.68	*16*
CAM	**48.9**	**13.2**	***188***	**7.48**	***230***	**74.3**	**9.6**	***231***	**0.011**	**0.009**	***189***	**0.032**	**0.030**	***165***	**0.014**	**0.015**	***193***	**6.95**	**0.72**	***181***
Jan	50.9	7.7	*16*	7.46	*20*	78.4	7.5	*21*	0.029	0.010	*17*	0.033	0.023	*15*	0.011	0.006	*15*	6.85	0.54	*15*
Feb	52.6	9.0	*14*	7.37	*15*	83.2	7.6	*14*	0.013	0.007	*13*	0.060	0.031	*13*	0.013	0.011	*14*	6.99	0.41	*12*
Mar	50.6	16.1	*14*	7.44	*14*	87.5	6.0	*15*	0.009	0.004	*14*	0.067	0.040	*12*	0.015	0.017	*14*	6.77	0.52	*13*
Apr	57.6	12.4	*17*	7.32	*23*	83.5	6.5	*23*	0.007	0.003	*18*	0.056	0.028	*16*	0.010	0.004	*18*	6.82	0.62	*18*
May	50.9	9.2	*16*	7.38	*20*	71.1	9.7	*20*	0.008	0.006	*16*	0.027	0.021	*13*	0.014	0.015	*17*	7.08	0.88	*16*
Jun	48.8	6.5	*18*	7.55	*21*	67.8	5.8	*21*	0.008	0.005	*17*	0.016	0.018	*14*	0.009	0.003	*18*	7.18	0.79	*16*
Jul	47.5	14.6	*17*	7.60	*22*	68.4	6.3	*22*	0.008	0.006	*17*	0.018	0.015	*13*	0.011	0.006	*18*	7.27	0.80	*18*
Aug	47.7	12.7	*19*	7.59	*26*	68.8	7.0	*26*	0.008	0.004	*20*	0.014	0.011	*16*	0.013	0.006	*21*	7.28	0.90	*19*
Sep	43.0	14.1	*15*	7.59	*20*	70.5	6.7	*20*	0.009	0.006	*16*	0.016	0.020	*14*	0.019	0.021	*16*	6.91	0.67	*17*
Oct	43.6	15.4	*20*	7.48	*22*	69.4	6.6	*22*	0.009	0.008	*20*	0.025	0.032	*18*	0.013	0.014	*18*	6.69	0.64	*14*
Nov	38.8	17.0	*11*	7.51	*14*	72.0	9.0	*14*	0.009	0.003	*10*	0.027	0.022	*11*	0.025	0.039	*12*	6.59	0.61	*12*
Dec	54.5	14.1	*11*	7.44	*13*	80.0	6.5	*13*	0.019	0.005	*11*	0.026	0.020	*10*	0.020	0.020	*12*	6.72	0.77	*11*
MAR	**105.0**	**34.3**	***165***	**7.75**	***167***	**159**	**51.6**	***168***	**0.015**	**0.012**	***162***	**0.061**	**0.058**	***149***	**0.037**	**0.030**	***160***	**6.85**	**1.11**	***141***
Jan	114.9	29.4	*13*	7.60	*13*	182	31.8	*13*	0.014	0.005	*13*	0.084	0.043	*12*	0.015	0.005	*13*	6.98	0.58	*11*
Feb	95.8	18.2	*12*	7.59	*12*	170	28.0	*12*	0.012	0.013	*12*	0.101	0.039	*11*	0.014	0.012	*11*	6.78	0.55	*11*
Mar	106	16.3	*14*	7.64	*14*	181	21.8	*15*	0.012	0.007	*14*	0.092	0.052	*12*	0.016	0.014	*14*	6.86	0.86	*12*
Apr	109	17.9	*14*	7.70	*14*	178	15.9	*14*	0.010	0.008	*14*	0.085	0.055	*14*	0.030	0.046	*13*	6.18	0.56	*12*
May	78.6	41.2	*16*	7.82	*16*	132	51.3	*16*	0.012	0.009	*16*	0.038	0.050	*15*	0.021	0.009	*16*	6.68	1.36	*14*
Jun	86.0	26.0	*15*	7.70	*15*	106	35.5	*15*	0.015	0.011	*15*	0.050	0.075	*12*	0.048	0.019	*15*	6.50	1.17	*13*
Jul	101	47.7	*15*	7.82	*15*	135	55.5	*15*	0.021	0.020	*14*	0.060	0.091	*12*	0.045	0.022	*14*	6.79	0.92	*13*

Aug	113	42.1	*16*	7.84	*17*	149	58.8	*17*	0.019	0.012	*17*	0.040	0.061	*15*	0.048	0.019	*16*	6.84	1.11	*13*
Sep	116	32.7	*14*	7.92	*14*	157	43.4	*14*	0.018	0.016	*13*	0.037	0.035	*13*	0.070	0.047	*13*	6.93	1.57	*14*
Oct	122	41.2	*14*	7.88	*15*	184	71.7	*15*	0.015	0.013	*14*	0.050	0.050	*13*	0.059	0.024	*13*	7.08	1.09	*13*
Nov	105	22.6	*11*	7.73	*11*	168	63.0	*11*	0.018	0.009	*9*	0.043	0.038	*11*	0.037	0.019	*11*	7.29	0.77	*8*
Dec	118	30.2	*11*	7.64	*11*	187	43.6	*11*	0.020	0.007	*11*	0.065	0.044	*9*	0.033	0.029	*11*	7.81	1.98	*7*

Detection Limits

TABLE A3: Detection limits for all geochemical analyses on the Yellowknife, Cameron, and Marian rivers. Some parameters did not include samples that were below the detection limit (BDL). Multiple detection limits represent the range of limits encountered over the entire geochemical record.

Parameter	Detection Limit
K^+ (mg/L)	*No samples BDL*
Na^+ (mg/L)	*No samples BDL*
Ca^{2+} (mg/L)	*No samples BDL*
Mg^{2+} (mg/L)	*No samples BDL*
Cl^- (mg/L)	*No samples BDL*
SO_4^{2-} (mg/L)	<3
Alkalinity (total as $CaCO_3$ mg/L)	*No samples BDL*
NH_3 (mg N/L)	<0.005, <0.01
NO_2^-+NO_3^- (mg N/L)	<0.005, <0.010, <0.008
DOC (mg/L)	*No samples BDL*
TP (mg/L)	<0.006, <0.004, <0.01, <0.003

Climate Analysis

Z-scores were calculated for average annual temperatures and for total annual precipitation around Yellowknife, NT (Fig A1). Average values were calculated using values from 1951 to 1980, as done by Serreze et al. (2000). Increasing trends are observed for both average annual air temperature and total annual precipitation, indicating changes to climate over time.

FIGURE A1: Calculated z-score values for average annual temperature (A) and total annual precipitation (B) for the city of Yellowknife, NT. Included are linear regression lines.

Yellowknife & Cameron River Discharge

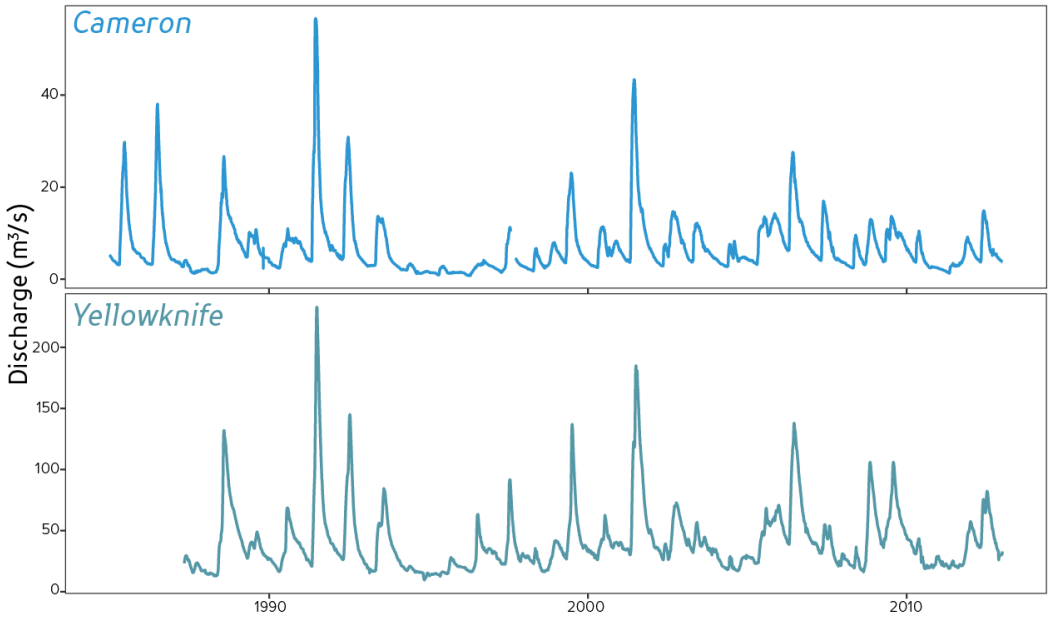

FIGURE A2: Daily measurements of discharge for the Cameron (top) and Yellowknife (bottom) rivers with time. Seasonality is easily seen by high flow during the spring and low flow during winter months.

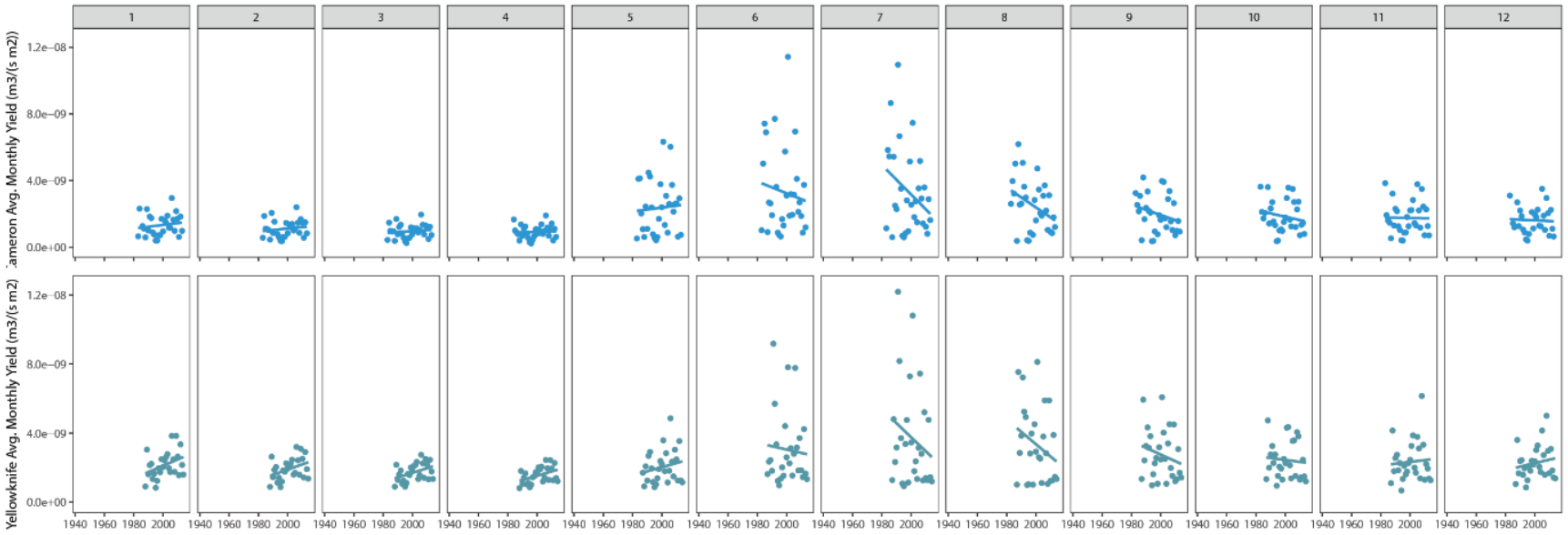

FIGURE A3: Average monthly discharge normalized to watershed area for the Yellowknife and Cameron Rivers.

Discharge-Concentration Relationships

Cations

A range of cation concentrations were found at various discharge measurements (Figure A4). No clear pattern or trend exists between concentration and discharge. A positive relationship between Na^+ concentration and discharge was observed in the Yellowknife river while a negative relationship with discharge was observed in the Cameron River. The Cameron River contains higher cation concentrations during lower discharge in the winter season than the Yellowknife River (Figure A4).

Anions

Chloride and sulphate concentrations were not well correlated with discharge in either the Yellowknife or Cameron rivers (Figure A5). However, a positive relationship between alkalinity and discharge is found in the Yellowknife River. An inverse relationship between alkalinity and discharge is found in the Cameron River. Lowest concentrations of alkalinity were observed during high flow in spring and summer months. Within the Yellowknife River, alkalinity appeared to be divided into a higher and lower group of values. Seasonality did not help predict anion concentrations and discharge in the Yellowknife River. Higher concentrations with lower flow during winter seasons are found in the Cameron River for both chloride and alkalinity, but not sulphate.

Nutrients

For both rivers, concentrations of inorganic nitrogen species (NH_3 and NO_3^-+NO_2^-) decreased with increased flow (Figure A6), while DOC concentrations increase with higher flows. There was no relationship between TP concentration and overall discharge for either river. For both rivers, lower flows in winter had the higher concentrations of nutrients, whereas highest flows in spring and summer had the lowest concentrations (Figure A6).

Other Parameters

No clear relationship between measurements of discharge with either TDS, pH, or specific conductivity were found in the Yellowknife River (Figure A7), while no relationship between discharge and either TDS or pH was found in the Cameron River. However, an inverse relationship between discharge and specific conductivity was observed in the Cameron River. Further, low flows

during the winter had high values of TDS, pH and specific conductivity, whereas high flows during the spring and summer contained lower values (Figure A7), suggesting a dilution response to spring snowmelt.

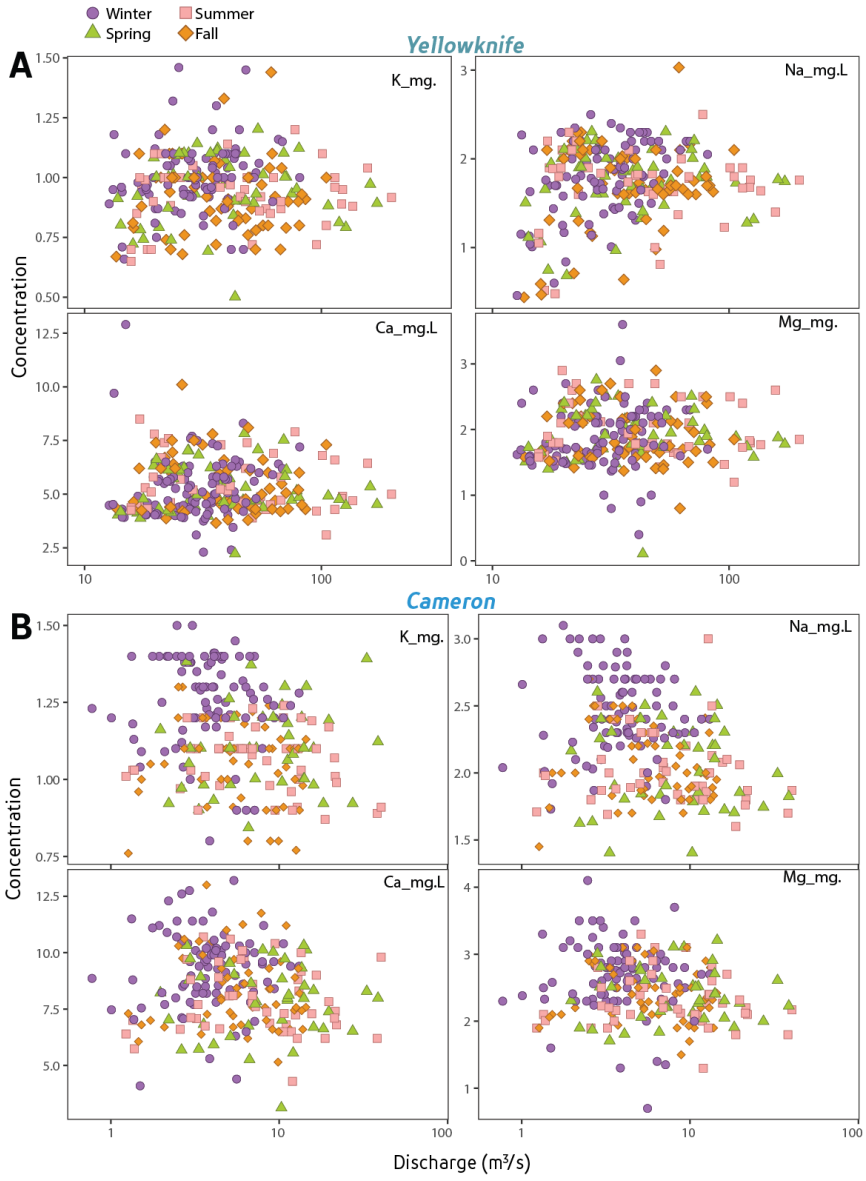

FIGURE A4: Concentration of cations versus discharge (logarithmic scale) for the Yellowknife (A) and Cameron (B) rivers for winter (purple circles), spring (green triangles), summer (pink squares), and fall (orange triangles).

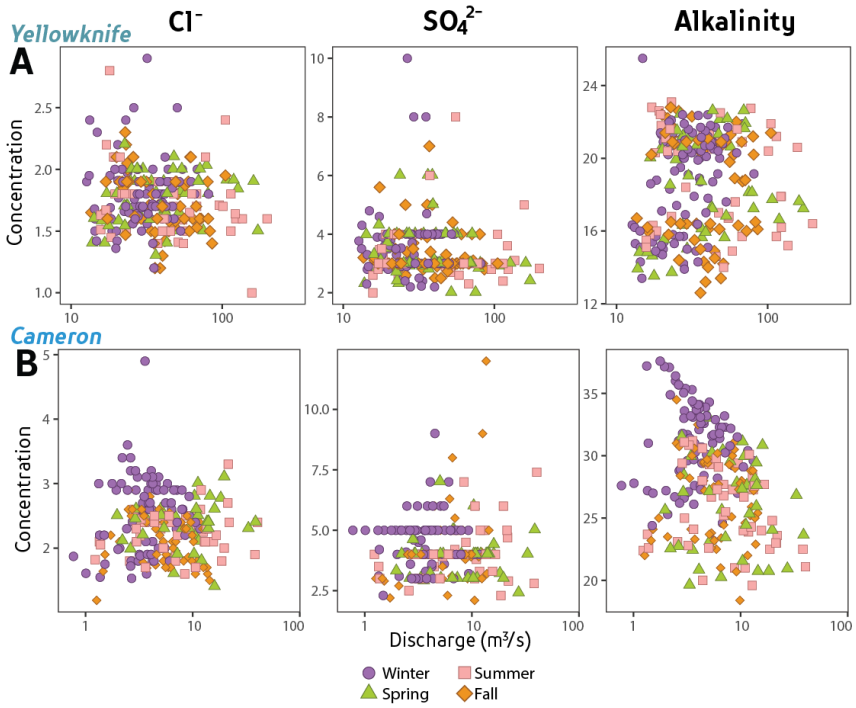

FIGURE A5: Concentration of anions versus discharge (logarithmic scale) for the Yellowknife (A) and Cameron (B) rivers for winter (purple circles), spring (green triangles), summer (pink squares), and fall (orange triangles).

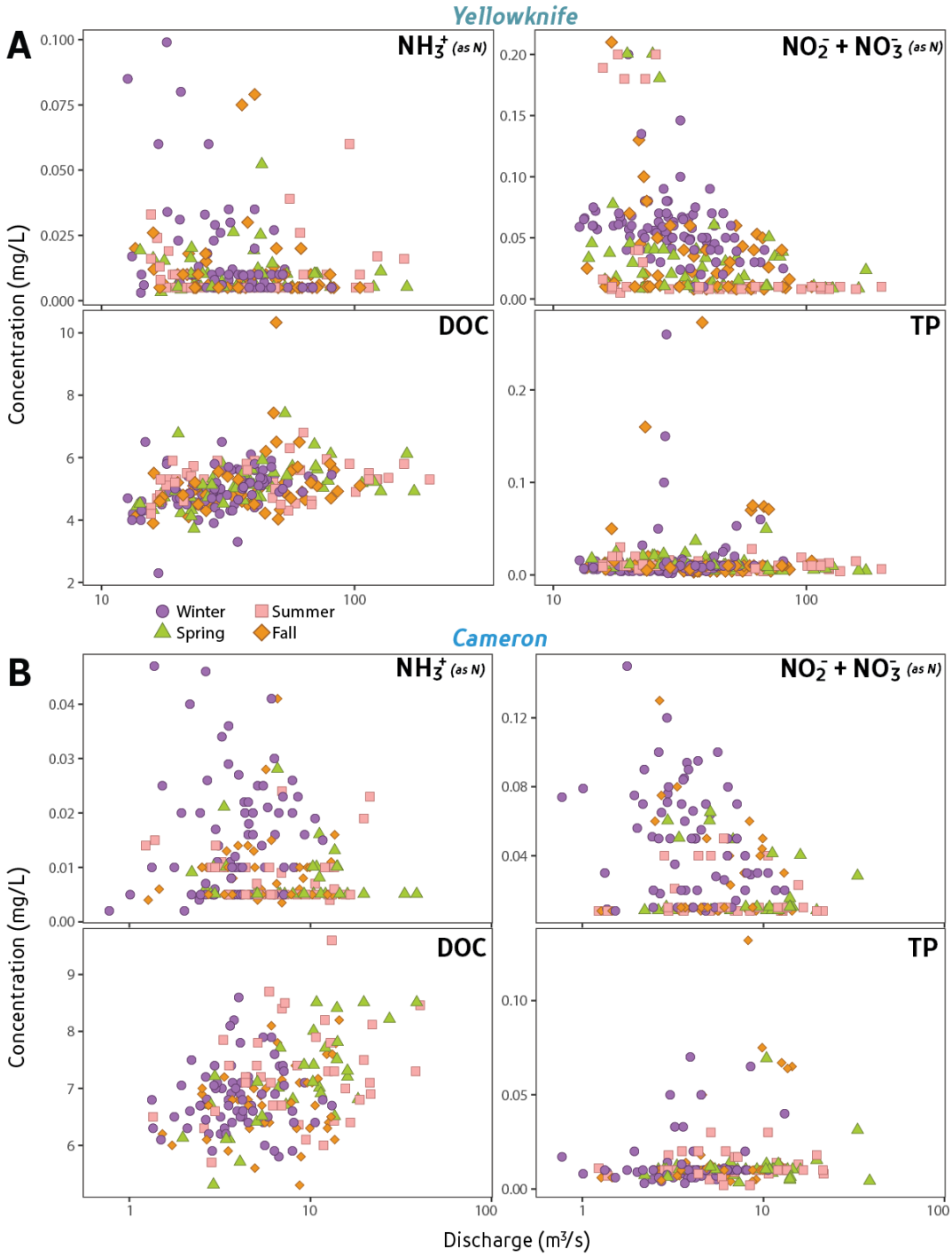

FIGURE A6: Concentration of nutrients versus discharge (logarithmic scale) for the Yellowknife (A) and Cameron (B) rivers for winter (purple circles), spring (green triangles), summer (pink squares), and fall (orange triangles).

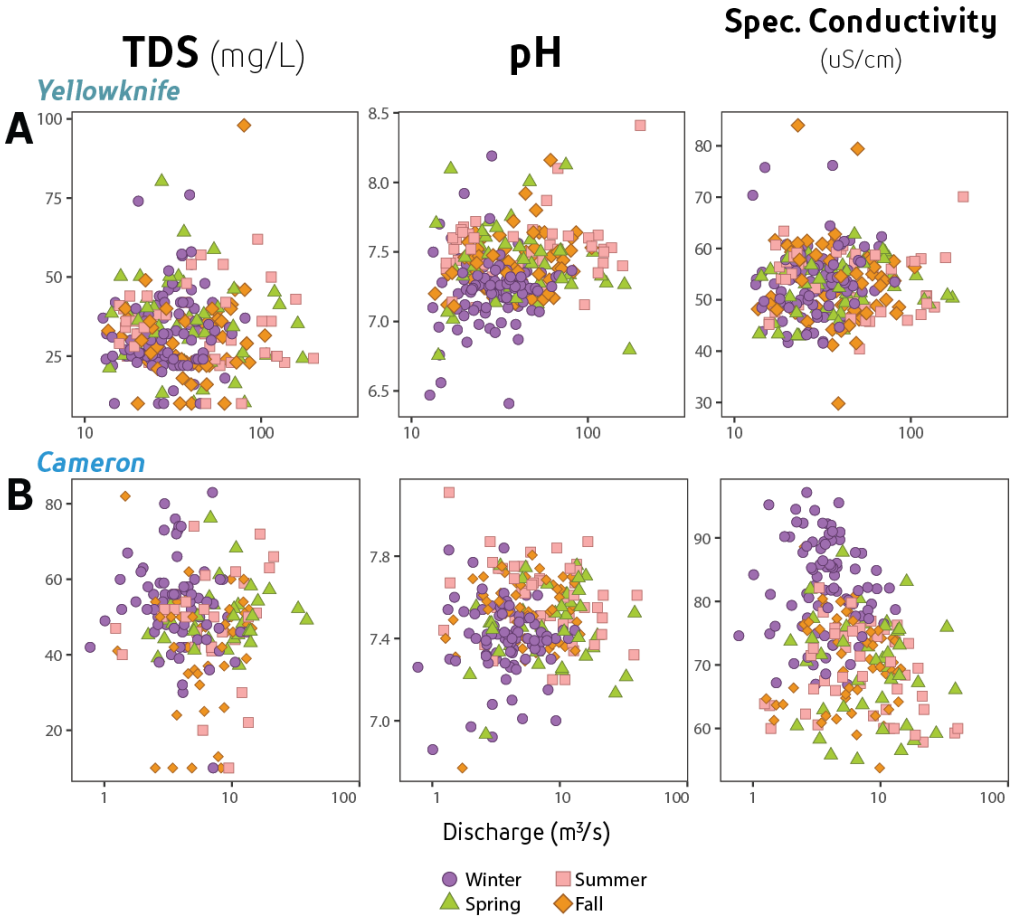

FIGURE A7: Total dissolved solids (TDS), pH, and specific conductivity versus discharge (logarithmic scale) for the Yellowknife (A) and Cameron (B) rivers for winter (purple circles), spring (green triangles), summer (pink squares), and fall (orange triangles).

Appendix B

Chapter 3 – Supplementary Figures

TABLE B1: Environmental description for all sampling sites, with the number of total samples taken for DOM concentration and at least one compositional measure (n_{DOC}), and number of samples used from that site in PCA analysis (n_{PCA}).

Name	Location	n_{DOC}	n_{PCA}	Description
SURFACE WATERS				
IISD-Experimental Lakes Area, ON (ELA)	49° 39' 40"N, 93° 43' 48"W Ontario, Canada	**74**	**45**	Boreal forest, underlain by Precambrian bedrock with discontinuous surficial layer of sandy-gravel till. Sampled from 2010 to 2016.
Lakes		*49*	*36*	
Creeks		*25*	*9*	
Grand River, ON (GR)	43° 30' 41"N, 80° 29' 43"W Ontario, Canada	**39**	-	Surrounding land predominately agricultural and flows past six wastewater treatment plants. Sampled from 6 consecutive locations along a 90km stretch every two months from 2011 to 2012.
Yellowknife, NT (YK)	62° 27' 14"N, 114° 22' 18"W Northwest Territories, Canada	**23**	**20**	Samples from the Taiga Shield underlain by discontinuous permafrost. Surface waters are surrounded by bedrock and peat pleataux around Yellowknife. Sampled in July or October between 2013 and 2017.
Lakes		*2*	*2*	
Ponds		*8*	*7*	
Rivers		*10*	*9*	
Creek		*3*	*2*	
Mackenzie River, NT (MK)	63° 14' 17"N, 123° 34' 0"W Northwest Territories, Canada	**13**	-	Samples taken by the Community Based Monitoring network along the Mackenzie River in July and August of 2015. Samples ranged from WHERE to Inuvik. River flows through Taiga Shield and Taiga Plains.
Rivers		*13*	-	
Wekweeti, NT (WK)	64° 11' 24"N, 114° 11' 10"W Northwest Territories, Canada	**11**	**11**	Situated in the Taiga Shield, below treeline, continuous permafrost. Samples taken in Octber of 2015 and 2016.
Lakes		*9*	*9*	
Creeks		*2*	*2*	
Daring Lake, NT (DL)	64° 31' 29"N, 111° 40' 24"W Northwest Territories, Canada	**19**	**19**	Found in the Southern Arctic above treeline, continuous permafrost.
Lakes		*7*	*7*	
Ponds		*1*	*1*	
Creeks		*11*	*11*	
Lake Hazen, NU (LH)	81° 49' 30"N, 71° 19' 26"W Nunavut, Canada	**160**	**12**	Tundra located in the high arctic; Lake Hazen Watershed is considered a local polar oasis.
Lakes		*38*	*2*	
Ponds		*18*	*4*	
Creeks		*41*	*1*	
Rivers		*32*	*0*	
Seeps		*31*	*5*	
GROUND WATERS				

Name	Location	n	nPCA	Description
Turkey Lakes Watershed, ON (TLW)	47° 2’ 54”N, 84° 24’ 25”W Ontario, Canada	**16**	-	Relatively un-impacted watershed in the Great Lakes-St. Lawrence forest region. Area consists of Precambrian bedrock and surficial glacial deposits of glaciofluvial outwash. Samples collected from depths ranging between 0.90 - 6.89m below surface.
IISD-Experimental Lakes Area, ON (ELA)	49° 39’ 40”N, 93° 43’ 48”W Ontario, Canada	**17**	-	Piezometers constructed in transect along a wetland, ranging from 0.70 - 3.85m below surface.
Nottawasaga Aquifer, ON (NW)	44° 7’ 26”N, 79° 49’ 12”W Ontario, Canada	**6**	-	Surficial deposits of glaciolacustrine deposits in an agriculturally-impacted aquifer. Samples collected from single multi-level piezometer within an unconfined surficial sand aquifer at depths of 4.35m, 5.13m, 6.68m, 9.90m, and 11.3m below surface.
Black Brook Watershed, NB (BBK)	47° 6’ 11”N, 67° 45’ 40”W New Brunswick, Canada	**15**	-	Site is an agriculturally-impacted aquifer. Surficial deposits of till and small deposits of glacial outwash. Samples taken from twelve domestic wells and three multi-level piezometers (6.1 - 30m below surface).
Long Point, ON (LP)	42° 34’ 46”N, 80° 22’ 57”W Ontario, Canada	**23**	-	Unconfined sand aquifer atop of a clay aquitard. Piezometers range from 1 to 4m below surface. Sampling of groundwater containing a septic plume.
Yellowknife, NT (YK)	62° 27’ 14”N, 114° 22’ 18”W Northwest Territories, Canada	**33**	**16**	Peat plateau sites underlain by sporadic discontinuous permafrost. Piezometers are above the permafrost boundary and depths range from 0.10 - 0.50m below surface.
Wekweeti, NT (WK)	64° 11’ 24”N, 114° 11’ 10”W Northwest Territories, Canada	**1**	**1**	Piezometers installed at deepest extent of active-layer (~0.5m below surface). Sampled 1-2 m away from lake shore in organic-rich peat.
Daring Lake, NT (DL)	64° 31’ 29”N, 111° 40’ 24”W Northwest Territories, Canada	**4**	**4**	??
Lake Hazen, NU (LH)	81° 49’ 30”N, 71° 19’ 26”W Nunavut, Canada	**17**	**2**	Samples taken from piezometer installed at deepest extent of active-layer (~0.25m). Location was in a subcatchment containing organic-rich soil. Flow direction was through wetland into nearby lake. Organic-rich layer underlain by silt or clay material.

Table B2: Summary data of all samples for DOM concentration (mg C/L), SUVA, slope between 275-295nm, DOC:DON, and proportion of humic substances.

	DOC (mg/L)					SUVA (L / (mg m))					S275-295 (nm-1)					DOC:DON					Prop. Humic Substances				
	Mean	σ (±)	Min	Max	n	Mean	σ (±)	Min	Max	n	Mean	σ (±)	Min	Max	n	Mean	σ (±)	Min	Max	n	Mean	σ (±)	Min	Max	n
Lake Hazen																									
Seep	1.4	1.1	0.3	3.9	31	6.2	2.9	1.1	12.0	26	0.0141	0.0015	0.0110	0.0174	26	21	17	4	74	19	0.76	0.06	0.65	0.80	5
Sub	6.7	3.7	2.4	15.7	17	8.8	4.0	2.1	18.6	15	0.0108	0.0035	0.0050	0.0163	15	19	16	5	76	17	0.44	0.34	0.21	0.68	2
Pond	12.1	7.8	3.7	24.0	18	4.5	1.3	2.7	7.6	18	0.0237	0.0051	0.0154	0.0321	18	21	8	11	45	18	0.60	0.05	0.56	0.68	4
Lake	2.7	3.0	0.1	6.9	38	4.0	0.8	1.9	4.7	18	0.0229	0.0029	0.0170	0.0257	18	15	4	9	21	10	0.57	0.05	0.50	0.61	5
Creek	1.2	2.0	0.1	8.0	41	4.1	2.1	1.5	10.0	25	0.0154	0.0035	0.0079	0.0217	25	16	10	2	34	9	0.49	0.15	0.21	0.63	6
River	0.5	0.4	0.1	1.4	32	4.2	1.9	1.5	7.7	22	0.0154	0.0046	0.0101	0.0264	23	-	-	-	-	-	0.43	0.15	0.22	0.68	10
Daring Lake																									
Sub	21.0	9.3	9.6	30.0	4	9.4	0.6	8.7	10.2	4	0.0128	0.0008	0.0116	0.0134	4	43	5	37	50	4	0.73	0.05	0.68	0.78	4
Pond	4.0	-	4.0	4.0	1	3.8	-	3.8	3.8	1	0.0199	-	0.0199	0.0199	1	28	-	28	28	1	0.40	NA	0.40	0.40	1
Lake	6.1	2.8	2.3	9.5	7	6.3	3.1	2.2	9.1	7	0.0179	0.0050	0.0127	0.0253	7	26	8	15	36	7	0.57	0.16	0.30	0.74	7
Creek	7.4	3.7	2.1	14.1	11	6.6	2.2	2.6	8.9	11	0.0157	0.0036	0.0133	0.0254	11	27	5	20	35	11	0.59	0.10	0.41	0.75	11
Wekweètì																									
Sub	10.2	-	10.2	10.2	1	10.3	-	10.3	10.3	1	0.0120	-	0.0120	0.0120	1	39	-	39	39	1	0.70	NA	0.70	0.70	1
Lake	10.8	5.35	4.5	18.3	9	6.7	2.2	4.3	10.2	9	0.0175	0.0032	0.0127	0.0222	9	36	13	20	62	9	0.61	0.11	0.50	0.81	9
Creek	6.2	0.4	6.0	6.5	2	4.8	0.0	4.8	4.8	2	0.0205	0.0001	0.0204	0.0206	2	25	10	18	32	2	0.57	0.08	0.51	0.62	2
Yellowknife																									
Sub	113	56.0	34.2	273	33	7.3	1.4	5.0	9.6	17	0.0136	0.0024	0.0100	0.0178	17	47	22	9	124	32	0.77	0.05	0.63	0.83	29
Pond	34.4	2.9	29.5	36.9	8	5.8	1.2	3.9	6.9	7	0.0180	0.0012	0.0164	0.0200	7	32	6	20	40	8	0.70	0.05	0.65	0.77	8
Lake	29.7	1.9	28.3	31.0	2	3.1	1.8	1.8	4.4	2	0.0246	0.0077	0.0192	0.0300	2	27	5	23	30	2	0.53	0.12	0.44	0.61	2
Creek	15.6	4.6	10.3	18.7	3	4.2	1.0	3.5	5.6	4	0.0195	0.0021	0.0170	0.0221	4	25	16	5	45	4	0.55	0.00	0.55	0.55	2
River	5.9	1.6	3.8	8.92	10	3.4	0.6	2.3	4.2	10	0.0226	0.0021	0.0200	0.0258	10	29	14	15	52	10	0.59	0.03	0.56	0.63	9
Mackenzie River																									
River	4.7	0.7	3.7	5.9	13	6.9	0.8	5.3	7.8	13	0.0172	0.0019	0.0149	0.0205	13	26	3	20	30	13	-	-	-	-	-
IISD-ELA																									
Sub	47.8	22.3	18.0	86.1	17	-	-	-	-	-	-	-	-	-	0	-	-	-	-	-	0.37	0.14	0.14	0.62	17
Lake	7.5	2.7	2.8	14. 6	49	6.4	4.6	1.4	21.2	32	0.0178	0.0042	0.0092	0.0308	32	30	14	19	105	41	0.50	0.09	0.32	0.75	56
Creek	23.4	11.9	10.3	63.6	25	8.4	1.9	5.3	11.1	22	0.0137	0.0013	0.0118	0.0160	22	48	11	34	82	22	0.81	0.02	0.74	0.85	17
Turkey Lakes Watershed																									
Sub	2.87	3.8	0.9	16.7	16	-	-	-	-	-	-	-	-	-	-	-	-	-	-	-	0.50	0.17	0.18	0.77	16
Nottawasaga																									
Sub	2.1	0.5	1.5	3.0	6	-	-	-	-	-	-	-	-	-	-	-	-	-	-	-	0.55	0.08	0.48	0.70	6
Grand River																									
River	6.1	1.0	4.0	8.0	39	-	-	-	-	-	-	-	-	-	-	10	7	3	34	39	0.66	0.05	0.51	0.75	39
Long Point																									
Sub	3.3	1.5	1.7	8.0	23	-	-	-	-	-	-	-	-	-	-	-	-	-	-	-	0.62	0.08	0.49	0.76	23
Black Brook Watershed																									
Sub	0.7	0.5	0.2	2.1	15	-	-	-	-	-	-	-	-	-	-	-	-	-	-	-	0.54	0.10	0.41	0.69	15

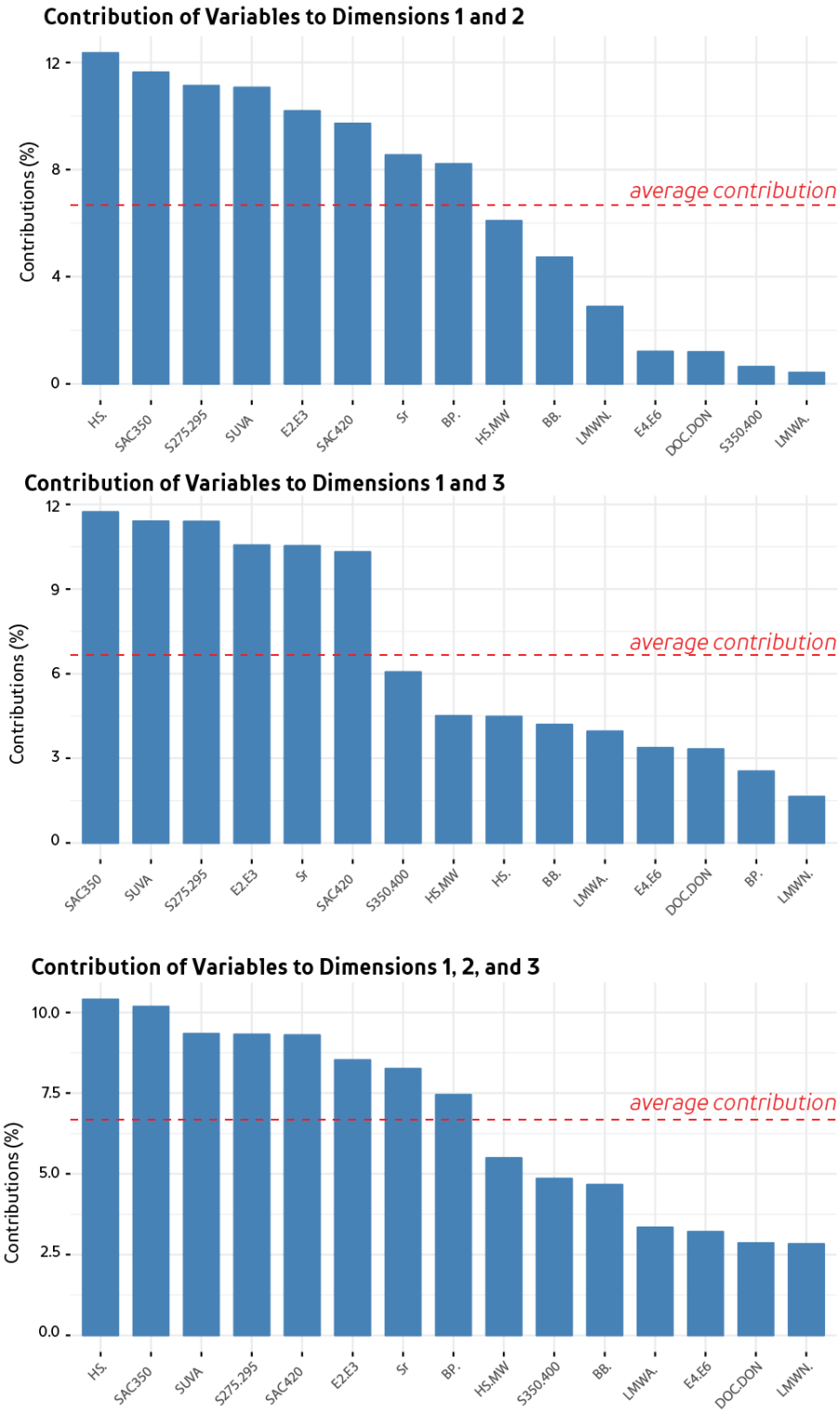

FIGURE B1: Contribution of each variable within the PCA to dimensions 1 and 2 (top graph), dimensions 1 and 3 (middle graph), and dimensions 1, 2 and 3 (bottom graph).

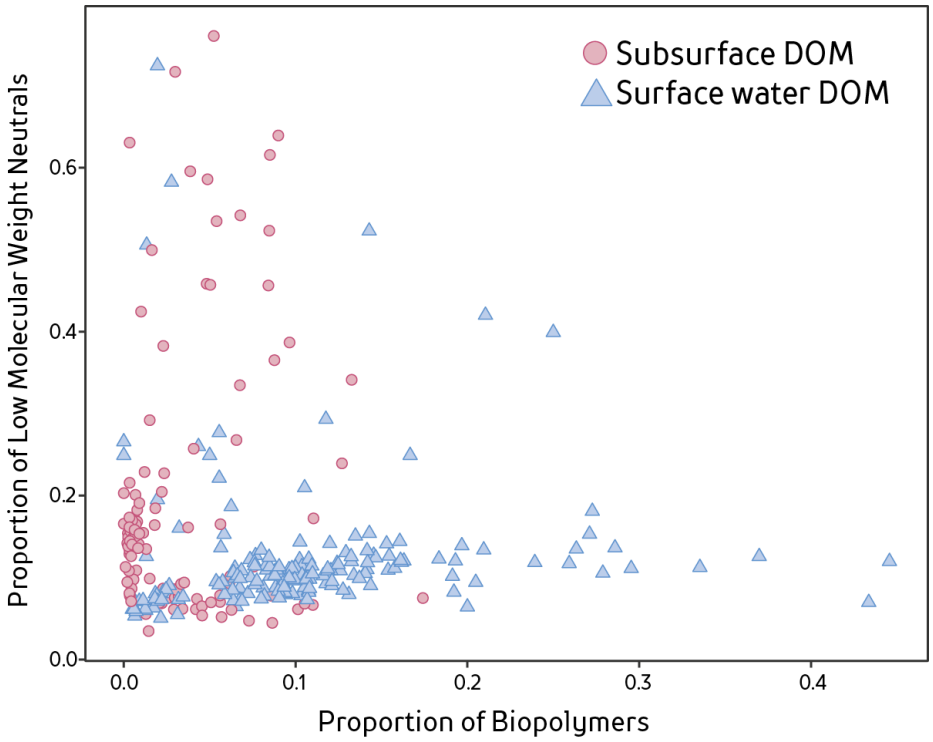

FIGURE B2: Proportion of low-molecular weight neutrals versus proportion of biopolymers for DOM from subsurface (pink circles) and surface water (lavender triangles) sites.

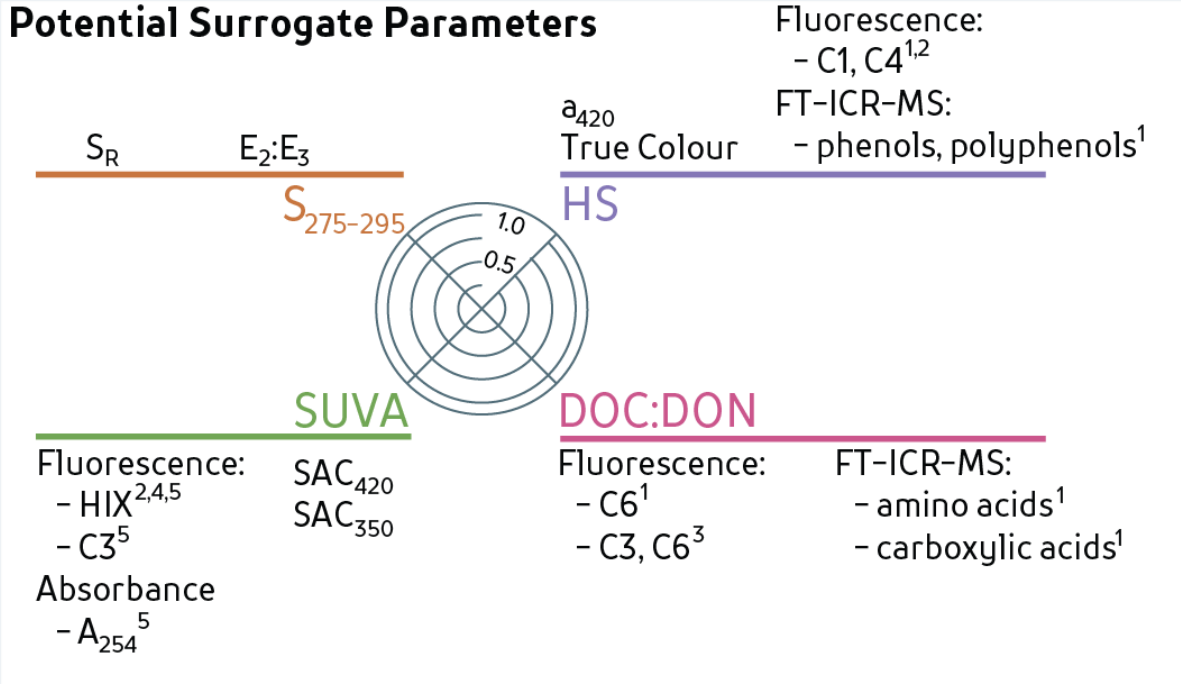

FIGURE B3: Surrogate parameters for each axis of the Composition Wheel.

Appendix C

Chapter 4 & 5 – Dissolved Inorganic Carbon

Microbial Degradation DIC

Concentrations of DIC were calculated from initial and final samples from Yellowknife and Daring Lake (Table C1). DIC was not calculated from Lake Hazen sites due to minimal change in overall dissolved organic matter (DOM; mg C/L) concentration and high background DIC.

Samples for DIC were collected in pre-weighed 12 mL Labco Exetainer vials and capped with no headspace using baked septa caps. Analysis involved withdrawing 6 mL of sample while simultaneously injecting 6 mL of helium and transferring the sample to another Exetainer filled with helium. Both exetainers were acidified using 0.05 mL of H_2SO_4 and another 6mL was added to the initial exetainer, resulting in both vials containing 12 mL of helium and 6 mL of sample. Vials were then placed on a shaker for 2 hours to allow for equilibration between liquid and gas phases. The concentration of headspace carbon dioxide (CO_2) was measured for each exetainer using a Varian CP-3800 Gas Chromatograph and dissolved concentrations of CO_2 were calculated according to Henry's Law.

Table C1: Subset of Yellowknife incubation samples to compare the loss of dissolved organic matter (DOM) with the pH, concentration of dissolved inorganic carbon (DIC), and total change in DIC.

	DOM Loss	**pH**		**DIC (mg C/L)**		**ΔDIC (mg C/L)**
	mg C/L	*Initial*	*Final*	*Initial*	*Final*	mg C/L
Subsurface	14.4	5.5	5.6	30.9	29.1	-1.8
Pond	3.3	5.3	5.5	8.8	8.2	-0.6
Creek	2.0	5.8	5.6	13.8	12.5	-1.3

Photolytic Degradation DIC

Table C2: Dissolved inorganic carbon and headspace carbon dioxide concentrations for 2014 photolysis samples for three treatments: original (t=0), 'Photo' (photolysed sample), and 'Dark'.

Sample	**DIC (mg/L)**			**CO_2 (ppm)**	
	Original	Photo	Dark	Original	Photo
Subsurface 1 (P2)	29	25	32	353	4480
Subsurface 2 (P5)	5.0	13	6.0	353	3765
River	5.6	6.1	6.0	353	1328

Appendix D

Chapter 6 – DBP Supplementary Information

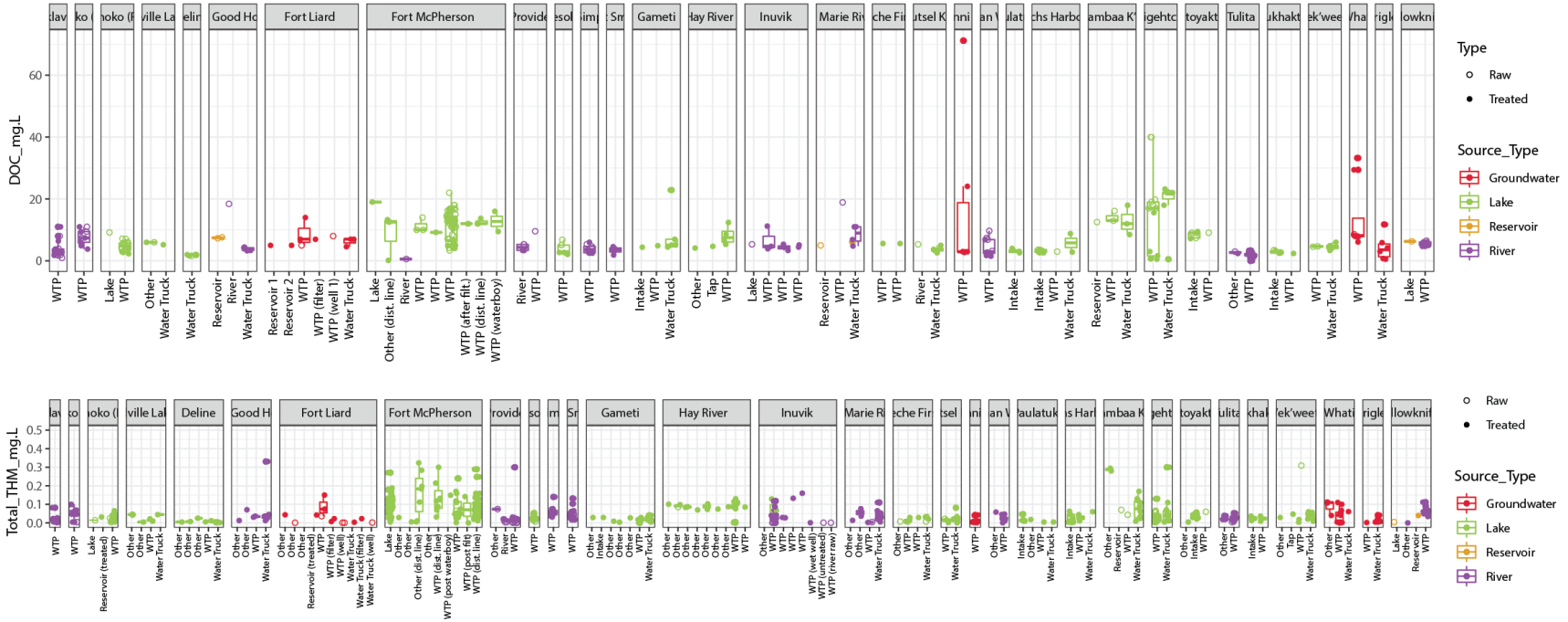

FIGURE D1: Water quality data of dissolved organic matter (DOM mg C/L; top) and total trihalomethane (THM mg/L; bottom) concentration for different sample locations in each community. Solid dots represent treated samples, whereas hollow dots are raw samples. Different colours represent the different water sources.

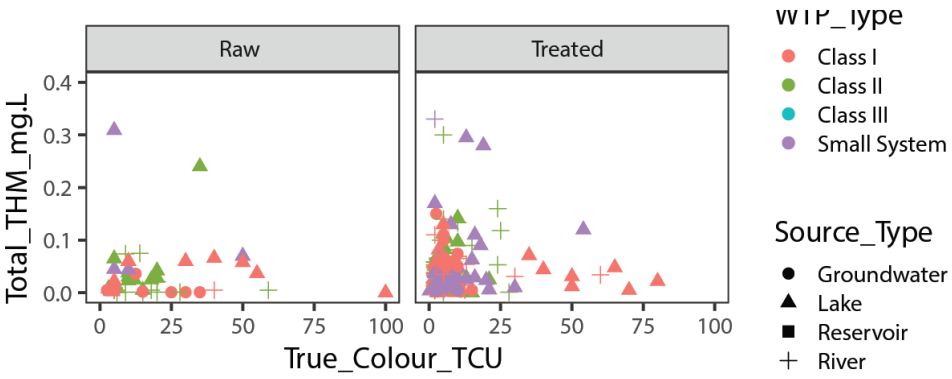

FIGURE D2: Water quality data of trihalomethane concentration (THM, mg/L) versus True Colour (TCU) for raw (left panel) and treated (right panel) samples compiled from the public database. Different colours represent different water treatment plant types, while different shapes represent the water source.

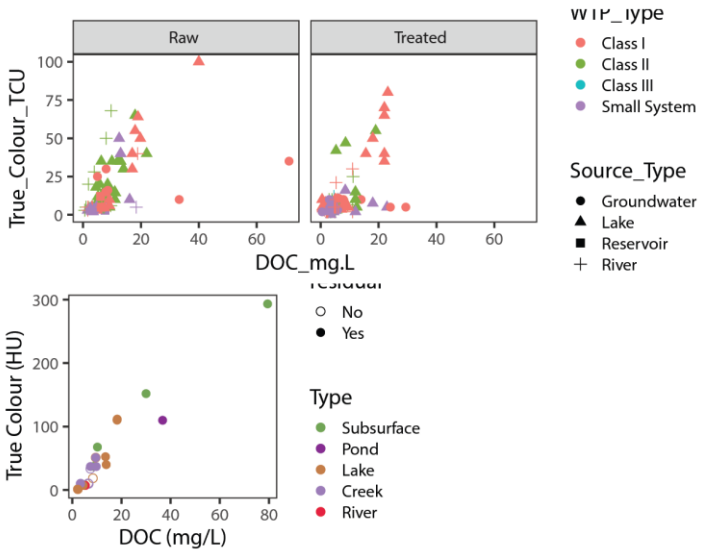

FIGURE D3: True colour versus dissolved organic matter (DOM, mg C/L) concentration for water quality database (top) and field data (bottom).

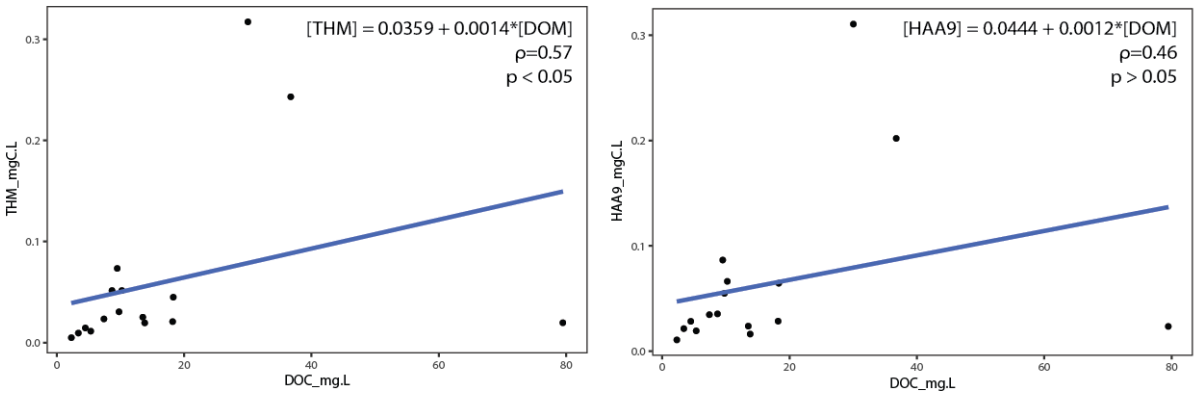

FIGURE D4: Overall trihalomethane (THM; left panel) and haloacetic acid (HAA9; right panel) concentration versus dissolved organic matter concentration (DOM) for all field samples.

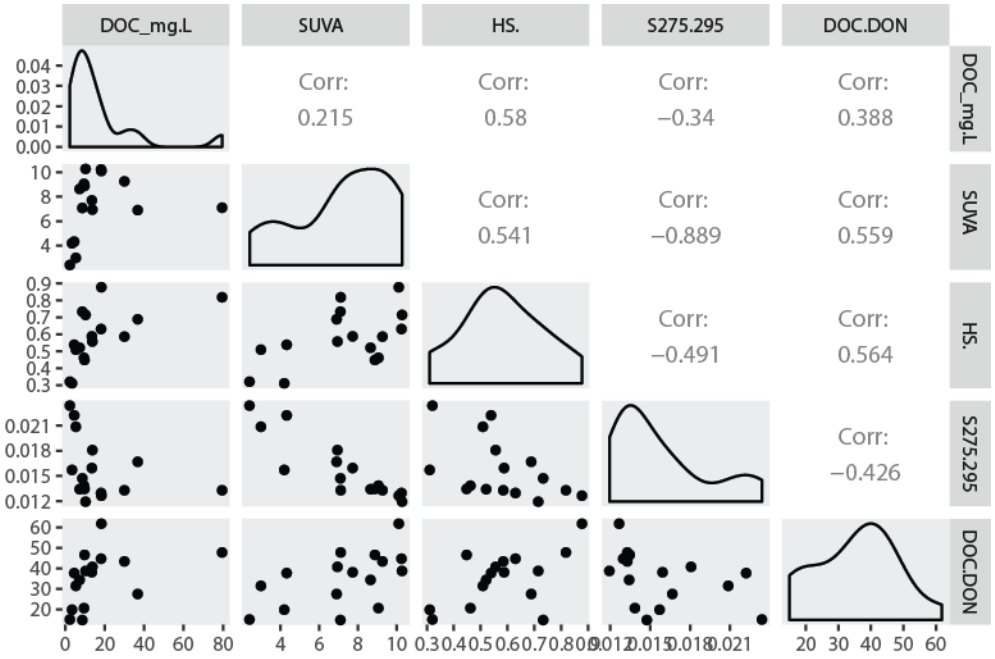

FIGURE D5: Correlation matrix for different dissolved organic matter (DOM) metrics: concentration (mg C/L); specific ultraviolet absorbance at 255 nm (SUVA, L/(mg·m)), proportion of humic substances fraction (HSF), slope ratio between 275 to 295 nm ($S_{275\text{-}295}$, nm^{-1}), and molar dissolved organic carbon to dissolved organic nitrogen ratio (DOC:DON).

Appendix E
Field Photos

Yellowknife, NT:

Photo of the 'Airport Site' that contains the pond with floating bog around it. Dead trees are called 'drunken trees' due to the degradation of underlying permafrost and subsequent flooding of roots.

Typical view of lakes near Yellowknife with sedges and black spruce.

Wekweètì, NT:

Landscape outside of Wekweètì (trees are more sparse than Yellowknife, continuous permafrost underneath).

Lake Hazen, NU:

Panorama of the Lake Hazen Watershed from atop a northern mountain slope looking southward towards Lake Hazen. The general lack of vegetation and moisture characteristic of the watershed is in stark contrast be a few small, productive areas as seen on the left hand side of the photo.

Looking at Lake Hazen (ice covered), the camp (directly at the crack in ice between the island and nearshore), and the smaller Skeleton Lake sub-catchment (productive green landscape with a series of lakes).

Looking out from Lake Hazen. Note the clarity of the lake (able to see rocks submerged beneath the surface).

References

(1) French, H. M.; Slaymaker, O. *Changing Cold Environments: A Canadian Perspective*; French, H. M., Slaymaker, O., Eds.; Wiley-Blackwell, 2011.

(2) Downing, J. A.; Prairie, Y. T.; Cole, J. J.; Duarte, C. M.; Tranvik, L. J.; Striegl, R. G.; McDowell, W. H.; Kortelainen, P.; Caraco, N. F.; Melack, J. M.; et al. The Global Abundance and Size Distribution of Lakes, Ponds, and Impoundments. *Limnol. Oceanogr.* **2006**, *51* (5), 2388–2397. https://doi.org/10.4319/lo.2006.51.5.2388.

(3) Tranvik, L. J.; Downing, J. A.; Cotner, J. B.; Loiselle, S. A.; Striegl, R. G.; Ballatore, T. J.; Dillon, P.; Finlay, K.; Fortino, K.; Knoll, L. B.; et al. Lakes and Reservoirs as Regulators of Carbon Cycling and Climate. *Limnol. Oceanogr.* **2009**, *54* (1), 17. https://doi.org/10.4319/lo.2009.54.6_part_2.2298.

(4) Rautio, M.; Dufresne, F.; Laurion, I.; Bonilla, S.; Vincent, W. F.; Christoffersen, K. S. Shallow Freshwater Ecosystems of the Circumpolar Arctic. *Écoscience* **2011**, *18* (3), 204–222. https://doi.org/10.2980/18-3-3463.

(5) Heginbottom, J. A.; Dubreuil, M. A.; Harker, P. A. Canada - Permafrost. In *National Atlas of Canada*; National Atlas Information Service, Natural Resources Canada: Ottawa, ON, Canada, 1995.

(6) Spence, C.; Woo, M. K. Hydrology of the Northwestern Subarctic Canadian Shield. In *Cold Region Atmospheric and Hydrologic Studies*; Woo, M., Ed.; Springer-Verlag: Berlin, Heidelberg, 2008; pp 235–256.

(7) Bednarski, J. M. *Surficial Geology, Lady Franklin Bay Area, Nunavut, NTS 120-C and Part of NTS 120-D*; 2015. https://doi.org/10.4095/296212.

(8) Smith, I. R. Late Quaternary Glacial History of Lake Hazen Basin and Eastern Hazen Plateau, Northern Ellesmere Island, Nunavut, Canada. *Can. J. Earth Sci.* **1999**, *36* (9), 1547–1565. https://doi.org/10.1139/e99-046.

(9) Serreze, M. C.; Barry, R. G. *The Arctic Climate System*; Cambridge University Press: Cambridge, 2014. https://doi.org/10.1017/CBO9781139583817.

(10) Schindler, D. W.; Smol, J. P. Cumulative Effects of Climate Warming and Other Human Activities on Freshwaters of Arctic and Subarctic North America. *Ambio* **2006**, *35* (4), 160–168.

(11) Serreze, M. C.; Barry, R. G. Processes and Impacts of Arctic Amplification: A Research Synthesis. *Glob. Planet. Change* **2011**, *77* (1–2), 85–96. https://doi.org/10.1016/j.gloplacha.2011.03.004.

(12) Burn, C. R.; Kokelj, S. V. The Environment and Permafrost of the Mackenzie Delta Area. *Permafr. Periglac. Process.* **2009**, *20* (2), 83–105. https://doi.org/10.1002/ppp.655.

(13) Serreze, M. C.; Walsh, J. E.; Osterkamp, T.; Dyurgerov, M.; Romanovsky, V.; Oechel, W. C.; Morison, J.; Zhang, T.; Barry, R. G. Observational Evidence of Recent Change in the Northern High-Latitude Environment. *Clim. Change* **2000**, *46*, 159–207.

(14) St. Jacques, J. M.; Sauchyn, D. J. Increasing Winter Baseflow and Mean Annual Streamflow from Possible Permafrost Thawing in the Northwest Territories, Canada. *Geophys. Res. Lett.* **2009**, *36* (1), 1–6. https://doi.org/10.1029/2008GL035822.

(15) Gustafsson, Ö.; Van Dongen, B. E.; Vonk, J. E.; Dudarev, O. V.; Semiletov, I. P. Widespread Release of Old Carbon across the Siberian Arctic Echoed by Its Large Rivers. *Biogeosciences* **2011**, *8*, 1737–1743. https://doi.org/10.5194/bg-8-1737-2011.

(16) Notz, D.; Stroeve, J. Observed Arctic Sea-Ice Loss Directly Follows Anthropogenic CO2 Emission. *Science (80-.).* **2016**, *354* (6313), 1–9. https://doi.org/10.1126/science.aag2345.

(17) Bintanja, R.; Andry, O. Towards a Rain-Dominated Arctic. *Nat. Clim. Chang.* **2017**, *7* (March), 263–268. https://doi.org/10.1038/nclimate3240.

(18) Tank, S. E.; Fellman, J. B.; Hood, E.; Kritzberg, E. S. Beyond Respiration: Controls on Lateral Carbon Fluxes across the Terrestrial-Aquatic Interface. *Limnol. Oceanogr. Lett.* **2018**. https://doi.org/10.1002/lol2.10065.

(19) Sharma, S.; Blagrave, K.; Magnuson, J. J.; O'Reilly, C. M.; Oliver, S.; Batt, R. D.; Magee, M. R.; Straile, D.; Weyhenmeyer, G. A.; Winslow, L.; et al. Widespread Loss of Lake Ice around the Northern Hemisphere in a Warming World. *Nat. Clim. Chang.* **2019**, *9* (3), 227–231. https://doi.org/10.1038/s41558-018-0393-5.

(20) Lehnherr, I.; St Louis, V. L.; Sharp, M.; Gardner, A. S.; Smol, J. P.; Schiff, S. L.; Muir, D. C. G.; Mortimer, C. A.; Michelutti, N.; Tarnocai, C.; et al. The World's Largest High Arctic Lake Responds Rapidly to Climate Warming. *Nat. Commun.* **2018**, *9* (1), 1–9. https://doi.org/10.1038/s41467-018-03685-z.

(21) Van Der Kolk, H. J.; Heijmans, M. M. P. D.; Van Huissteden, J.; Pullens, J. W. M.; Berendse, F. Potential Arctic Tundra Vegetation Shifts in Response to Changing Temperature, Precipitation and Permafrost Thaw. *Biogeosciences* **2016**, *13* (22), 6229–6245. https://doi.org/10.5194/bg-13-6229-2016.

(22) Warren, F. J.; Lemmen, D. S. *Canada in a Changing Climate: Sector Perspectives on Impacts and Adaptation*; Ottawa, ON, 2014.

(23) McGuire, D. A.; Anderson, L. G.; Christensen, T. R.; Dallimore, S.; Guo, L.; Hayes, D. J.; Heimann, M.; Lorenson, T. D.; MacDonald, R. W.; Roulet, N. Sensitivity of the Carbon Cycle in the Arctic to Climate Change. *Ecol. Monogr.* **2009**, *79* (4), 523–555.

(24) Abbott, B. W.; Jones, J. B.; Schuur, E. A. G.; Chapin III, F. S.; Bowden, W. B.; Bret-Harte, M. S.; Epstein, H. E.; Flannigan, M. D.; Harms, T. K.; Hollingsworth, T. N.; et al. Biomass Offsets Little or None of Permafrost Carbon Release from Soils, Streams, and Wildfire: An Expert Assessment. *Environ. Res. Lett.* **2016**, *11* (3), 034014. https://doi.org/10.1088/1748-9326/11/3/034014.

(25) Kuhry, P.; Grosse, G.; Harden, J. W.; Hugelius, G.; Koven, C. D.; Ping, C.-L.; Schirrmeister, L.; Tarnocai, C. Characterisation of the Permafrost Carbon Pool. *Permafr. Periglac. Process.* **2013**, *24* (2), 146–155. https://doi.org/10.1002/ppp.1782.

(26) Schuur, E. A. G.; Abbott, B. W.; Bowden, W. B.; Brovkin, V.; Camill, P.; Canadell, J. G.; Chanton, J. P.; Chapin, F. S.; Christensen, T. R.; Ciais, P.; et al. Expert Assessment of Vulnerability of Permafrost Carbon to Climate Change. *Clim. Change* **2013**, *119* (2), 359–374. https://doi.org/10.1007/s10584-013-0730-7.

(27) McClelland, J. W. W.; Holmes, R. M.; Peterson, B. J.; Raymond, P. A.; Striegl, R. G.; Zimov, S. A.; Zimov, N. S.; Tank, S. E.; Spencer, R. G. M.; Staples, R.; et al. Particulate Organic Carbon

and Nitrogen Export from Major Arctic Rivers. *Global Biogeochem. Cycles* **2016**, *30* (0428), 1–19. https://doi.org/10.1002/2015GB005351.

(28) Frey, K. E.; Smith, L. C. Amplified Carbon Release from Vast West Siberian Peatlands by 2100. *Geophys. Res. Lett.* **2005**, *32* (9), L09401. https://doi.org/10.1029/2004GL022025.

(29) Dutta, K.; Schuur, E. A. G.; Neff, J. C.; Zimov, S. A. Potential Carbon Release from Permafrost Soils of Northeastern Siberia. *Glob. Chang. Biol.* **2006**, *12*, 2336–2351. https://doi.org/10.1111/j.1365-2486.2006.01259.x.

(30) O'Donnell, J. A.; Aiken, G. R.; Walvoord, M. A.; Raymond, P. A.; Butler, K. D.; Dornblaser, M. M.; Heckman, K. Using Dissolved Organic Matter Age and Composition to Detect Permafrost Thaw in Boreal Watersheds of Interior Alaska. *J. Geophys. Res. Biogeosciences* **2014**, *119* (11), 2155–2170. https://doi.org/10.1002/2014JG002695.

(31) Hilton, R. G.; Galy, V.; Gaillardet, J.; Dellinger, M.; Bryant, C.; O'Regan, M.; Gröcke, D. R.; Coxall, H.; Bouchez, J.; Calmels, D. Erosion of Organic Carbon in the Arctic as a Geological Carbon Dioxide Sink. *Nature* **2015**, *524* (7563), 84–87. https://doi.org/10.1038/nature14653.

(32) Mann, P. J.; Eglinton, T. I.; McIntyre, C. P.; Zimov, N. S.; Davydova, A.; Vonk, J. E.; Holmes, R. M.; Spencer, R. G. M. Utilization of Ancient Permafrost Carbon in Headwaters of Arctic Fluvial Networks. *Nat. Commun.* **2015**, *6* (1), 7856. https://doi.org/10.1038/ncomms8856.

(33) Sulzberger, B.; Arey, J. S. Impacts of Polar Changes on the UV-Induced Mineralization of Terrigenous Dissolved Organic Matter. *Environ. Sci. Technol.* **2016**, *50* (13), 6621–6631. https://doi.org/10.1021/acs.est.5b05994.

(34) Wauthy, M.; Rautio, M.; Christoffersen, K. S.; Forsström, L.; Laurion, I.; Mariash, H. L.; Peura, S.; Vincent, W. F. Increasing Dominance of Terrigenous Organic Matter in Circumpolar Freshwaters Due to Permafrost Thaw. *Limnol. Oceanogr. Lett.* **2018**. https://doi.org/10.1002/lol2.10063.

(35) Fritz, M.; Opel, T.; Tanski, G.; Herzschuh, U.; Meyer, H.; Eulenburg, A.; Lantuit, H. Dissolved Organic Carbon (DOC) in Arctic Ground Ice. *Cryosphere* **2015**, *9* (2), 737–752. https://doi.org/10.5194/tc-9-737-2015.

(36) Schädel, C.; Schuur, E. A. G.; Bracho, R.; Elberling, B.; Knoblauch, C.; Lee, H.; Luo, Y.; Shaver, G. R.; Turetsky, M. R. Circumpolar Assessment of Permafrost C Quality and Its Vulnerability over Time Using Long-Term Incubation Data. *Glob. Chang. Biol.* **2014**, *20* (2), 641–652. https://doi.org/10.1111/gcb.12417.

(37) Laurion, I.; Vincent, W. F.; MacIntyre, S.; Retamal, L.; Dupont, C.; Francus, P.; Pienitz, R. Variability in Greenhouse Gas Emissions from Permafrost Thaw Ponds. *Limnol. Oceanogr.* **2010**, *55* (1), 115–133. https://doi.org/10.4319/lo.2010.55.1.0115.

(38) Evans, C. D.; Futter, M. N.; Moldan, F.; Valinia, S.; Frogbrook, Z.; Kothawala, D. N. Variability in Organic Carbon Reactivity across Lake Residence Time and Trophic Gradients. *Nat. Geosci.* **2017**, *10* (11), 832–835. https://doi.org/10.1038/NGEO3051.

(39) Myers-Pigg, A. N.; Louchouarn, P.; Amon, R. M. W.; Prokushkin, A.; Pierce, K.; Rubtsov, A. Labile Pyrogenic Dissolved Organic Carbon in Major Siberian Arctic Rivers: Implications for Wildfire-Stream Metabolic Linkages. **2015**, 1–9. https://doi.org/10.1002/2014GL062762.Received.

(40) Lupascu, M.; Wadham, J. L.; Hornibrook, E. R. C.; Pancost, R. D. Temperature Sensitivity of Methane Production in the Permafrost Active Layer at Stordalen, Sweden: A Comparison with Non-Permafrost Northern Wetlands. *Arctic, Antarct. Alp. Res.* **2012**, *44* (4), 469–482. https://doi.org/10.1657/1938-4246-44.4.469.

(41) Elberling, B.; Michelsen, A.; Schädel, C.; Schuur, E. A. G.; Christiansen, H. H.; Berg, L.; Tamstorf, M. P.; Sigsgaard, C. Long-Term CO2 Production Following Permafrost Thaw. *Nat. Clim. Chang.* **2013**, *3* (October), 890–894. https://doi.org/10.1038/nclimate1955.

(42) Schuur, E. a. G.; McGuire, a. D.; Schädel, C.; Grosse, G.; Harden, J. W.; Hayes, D. J.; Hugelius, G.; Koven, C. D.; Kuhry, P.; Lawrence, D. M.; et al. Climate Change and the Permafrost Carbon Feedback. *Nature* **2015**, *520* (7546), 171–179. https://doi.org/10.1038/nature14338.

(43) Wik, M.; Varner, R. K.; Anthony, K. W.; MacIntyre, S.; Bastviken, D. Climate-Sensitive Northern Lakes and Ponds Are Critical Components of Methane Release. *Nat. Geosci.* **2016**, No. January. https://doi.org/10.1038/ngeo2578.

(44) Mack, M. C.; Schuur, E. A. G.; Bret-Harte, M. S.; Shaver, G. R.; Chapin, F. S. Ecosystem Carbon Storage in Arctic Tundra Reduced by Long-Term Nutrient Fertilization. *Nature* **2004**, *431* (7007), 440–443. https://doi.org/10.1038/nature02887.

(45) Emmerton, C. A.; Louis, V. L. S.; Lehnherr, I.; Graydon, J. A.; Kirk, J. L.; Rondeau, K. J. The Importance of Freshwater Systems to the Net Atmospheric Exchange of Carbon Dioxide and Methane with a Rapidly Changing High Arctic Watershed. *Biogeosciences* **2016**, *13* (20), 5849–5863. https://doi.org/10.5194/bg-13-5849-2016.

(46) Wild, B.; Gentsch, N.; Čapek, P.; Diáková, K.; Alves, R. J. E.; Bárta, J.; Gittel, A.; Hugelius, G.; Knoltsch, A.; Kuhry, P.; et al. Plant-Derived Compounds Stimulate the Decomposition of Organic Matter in Arctic Permafrost Soils. *Sci. Rep.* **2016**, *6* (April), 25607. https://doi.org/10.1038/srep25607.

(47) Vonk, J. E.; Gustafsson, Ö. Permafrost-Carbon Complexities. *Nat. Geosci.* **2013**, *6* (9), 675–676. https://doi.org/10.1038/ngeo1937.

(48) Cooper, M. D. A.; Estop-Aragonés, C.; Fisher, J. P.; Thierry, A.; Garnett, M. H.; Charman, D. J.; Murton, J. B.; Phoenix, G. K.; Treharne, R.; Kokelj, S. V.; et al. Limited Contribution of Permafrost Carbon to Methane Release from Thawing Peatlands. *Nat. Clim. Chang.* **2017**, *7* (June), 507–511. https://doi.org/10.1038/NCLIMATE3328.

(49) Mueller, K. K.; Fortin, C.; Campbell, P. G. C. Spatial Variation in the Optical Properties of Dissolved Organic Matter (DOM) in Lakes on the Canadian Precambrian Shield and Links to Watershed Characteristics. *Aquat. Geochemistry* **2012**, *18* (1), 21–44. https://doi.org/10.1007/s10498-011-9147-y.

(50) Kellerman, A. M.; Dittmar, T.; Kothawala, D. N.; Tranvik, L. J. Chemodiversity of Dissolved Organic Matter in Lakes Driven by Climate and Hydrology. *Nat. Commun.* **2014**, *5* (MAY), 1–8. https://doi.org/10.1038/ncomms4804.

(51) Larson, J. H.; Frost, P. C.; Xenopoulos, M. A.; Williams, C. J.; Morales-Williams, A. M.; Vallazza, J. M.; Nelson, J. C.; Richardson, W. B. Relationships Between Land Cover and Dissolved Organic Matter Change Along the River to Lake Transition. *Ecosystems* **2014**, *17* (8), 1413–1425. https://doi.org/10.1007/s10021-014-9804-2.

(52) Dawson, J. J. C.; Billett, M. F.; Hope, D.; Palmer, S. M.; Claire, M.; Deacon, C. M. Sources and Sinks of Aquatic Carbon in a Peatland Stream Continuum. *Biogeochemistry* **2004**, *70*, 71–92.

(53) Schindler, D. W.; Curtis, P. J.; Parker, B. R.; Stainton, M. P. Consequences of Climate Warming and Lake Acidification for UV-B Penetration in North American Boreal Lakes. *Nature* **1996**, *379* (22), 705–708.

(54) Williamson, C. E.; Morris, D. P.; Pace, M. L.; Olson, O. G. Dissolved Organic Carbon and Nutrients as Regulators of Lake Ecosystems : Resurrection of a More Integrated Paradigm. *Limnol. Oceanogr.* **1999**, *44* (3), 795–803.

(55) Strock, K. E.; Theodore, N.; Gawley, W. G.; Ellsworth, A. C.; Saros, J. E. Increasing Dissolved Organic Carbon Concentrations in Northern Boreal Lakes: Implications for Lake Water Transparency and Thermal Structure. *J. Geophys. Res. Biogeosciences* **2017**, *122* (5), 1022–1035. https://doi.org/10.1002/2017JG003767.

(56) Pilla, R. M.; Williamson, C. E.; Zhang, J.; Smyth, R. L.; Lenters, J. D.; Brentrup, J. A.; Knoll, L. B.; Fisher, T. J. Browning-Related Decreases in Water Transparency Lead to Long-Term Increases in Surface Water Temperature and Thermal Stratification in Two Small Lakes. *J. Geophys. Res. Biogeosciences* **2018**. https://doi.org/10.1029/2017JG004321.

(57) Biddanda, B. A.; Cotner, J. B. Love Handles in Aquatic Ecosystems: The Role of Dissolved Organic Carbon Drawdown, Resuspended Sediments, and Terrigenous Inputs in the Carbon Balance of Lake Michigan. *Ecosystems* **2002**, *5* (5), 431–445. https://doi.org/10.1007/s10021-002-0163-z.

(58) Bauer, M.; Heitmann, T.; Macalady, D. L.; Blodau, C. Electron Transfer Capacities and Reaction Kinetics of Peat Dissolved Organic Matter. *Environ. Sci. Technol.* **2007**, *41* (1), 139–145. https://doi.org/10.1021/es061323j.

(59) Moore, D. R. J. *Water Quality Ambient Water Quality Criteria for Organic Carbon in British Columbia*; 1998.

(60) Al-Reasi, H. a; Wood, C. M.; Smith, D. S. Characterization of Freshwater Natural Dissolved Organic Matter (DOM): Mechanistic Explanations for Protective Effects against Metal Toxicity and Direct Effects on Organisms. *Environ. Int.* **2013**, *59*, 201–207. https://doi.org/10.1016/j.envint.2013.06.005.

(61) Baken, S.; Degryse, F.; Verheyen, L.; Merckx, R.; Smolders, E. Metal Complexation Properties of Freshwater Dissolved Organic Matter Are Explained by Its Aromaticity and by Anthropogenic Ligands. *Environ. Sci. Technol.* **2011**, *45* (7), 2584–2590. https://doi.org/10.1021/es103532a.

(62) French, T. D.; Houben, A. J.; Desforges, J.-P. W.; Kimpe, L. E.; Kokelj, S. V.; Poulain, A. J.; Smol, J. P.; Wang, X.; Blais, J. M. Dissolved Organic Carbon Thresholds Affect Mercury Bioaccumulation in Arctic Lakes. *Environ. Sci. Technol.* **2014**, *48* (6), 3162–3168. https://doi.org/10.1021/es403849d.

(63) Lescord, G. L.; Emilson, E. J. S.; Johnston, T. A.; Branfireun, B. A.; Gunn, J. M. Optical Properties of Dissolved Organic Matter and Their Relation to Mercury Concentrations in Water and Biota Across a Remote Freshwater Drainage Basin. *Environ. Sci. Technol.* **2018**, *52* (6), 3344–3353. https://doi.org/10.1021/acs.est.7b05348.

(64) Matilainen, A.; Vepsäläinen, M.; Sillanpää, M. Natural Organic Matter Removal by Coagulation during Drinking Water Treatment: A Review. *Adv. Colloid Interface Sci.* **2010**, *159* (2), 189–197. https://doi.org/10.1016/j.cis.2010.06.007.

(65) Matilainen, A.; Gjessing, E. T.; Lahtinen, T.; Hed, L.; Bhatnagar, A.; Sillanpää, M. An Overview of the Methods Used in the Characterisation of Natural Organic Matter (NOM) in Relation to Drinking Water Treatment. *Chemosphere* **2011**, *83* (11), 1431–1442. https://doi.org/10.1016/j.chemosphere.2011.01.018.

(66) Worrall, F.; Burt, T. P. Changes in DOC Treatability: Indications of Compositional Changes in DOC Trends. *J. Hydrol.* **2009**, *366* (1–4), 1–8. https://doi.org/10.1016/j.jhydrol.2008.11.044.

(67) Krasner, S. W.; Weinberg, H. S.; Richardson, S. D.; Pastor, S. J.; Chinn, R.; Sclimenti, M. J.; Onstad, G. D.; Thruston, A. D. Occurrence of a New Generation of Disinfection Byproducts. *Environ. Sci. Technol.* **2006**, *40* (23), 7175–7185. https://doi.org/10.1021/es060353j.

(68) Awad, J.; van Leeuwen, J.; Chow, C.; Drikas, M.; Smernik, R. J.; Chittleborough, D. J.; Bestland, E. Characterization of Dissolved Organic Matter for Prediction of Trihalomethane Formation Potential in Surface and Sub-Surface Waters. *J. Hazard. Mater.* **2016**, *308*, 430–439. https://doi.org/10.1016/j.jhazmat.2016.01.030.

(69) Dahlén, J.; Bertilsson, S.; Pettersson, C. Effects of UV-A Radiation on Dissolved Organic Matter in Humic Surface Waters. *Environ. Int.* **1996**, *22* (5), 501–506.

(70) Stedmon, C. a; Markager, S.; Bro, R. Tracing Dissolved Organic Matter in Aquatic Environments Using a New Approach to Fluorescence Spectroscopy. *Mar. Chem.* **2003**, *82* (3–4), 239–254. https://doi.org/10.1016/S0304-4203(03)00072-0.

(71) Weishaar, J. L.; Aiken, G. R.; Bergamaschi, B. A.; Fram, M. S.; Fujii, R.; Mopper, K. Evaluation of Specific Ultraviolet Absorbance as an Indicator of the Chemical Composition and Reactivity of Dissolved Organic Carbon. *Environ. Sci. Technol.* **2003**, *37* (20), 4702–4708. https://doi.org/10.1021/es030360x.

(72) Jaffé, R.; Yamashita, Y.; Maie, N.; Cooper, W. T.; Dittmar, T.; Dodds, W. K.; Jones, J. B.; Myoshi, T.; Ortiz-Zayas, J. R.; Podgorski, D. C.; et al. Dissolved Organic Matter in Headwater Streams: Compositional Variability across Climatic Regions of North America. *Geochim. Cosmochim. Acta* **2012**, *94*, 95–108. https://doi.org/10.1016/j.gca.2012.06.031.

(73) Spencer, R. G. M.; Butler, K. D.; Aiken, G. R. Dissolved Organic Carbon and Chromophoric Dissolved Organic Matter Properties of Rivers in the USA. *J. Geophys. Res. Biogeosciences* **2012**, *117* (3). https://doi.org/10.1029/2011JG001928.

(74) Poulin, B. a; Ryan, J. N.; Aiken, G. R. Effects of Iron on Optical Properties of Dissolved Organic Matter. *Environ. Sci. Technol.* **2014**, No. Iii, 1–20. https://doi.org/10.1021/es502670r.

(75) Huber, S. A.; Balz, A.; Abert, M.; Pronk, W. Characterisation of Aquatic Humic and Non-Humic Matter with Size-Exclusion Chromatography – Organic Carbon Detection – Organic Nitrogen Detection (LC-OCD-OND). *Water Res.* **2011**, *45* (2), 879–885. https://doi.org/10.1016/j.watres.2010.09.023.

(76) Perminova, I. V; Dubinenkov, I. V; Kononikhin, A. S.; Konstantinov, A. I.; Zherebker, A. Y.; Andzhushev, M. a; Lebedev, V. a; Bulygina, E.; Holmes, R. M.; Kostyukevich, Y. I.; et al. Molecular Mapping of Sorbent Selectivities with Respect to Isolation of Arctic Dissolved

Organic Matter as Measured by Fourier Transform Mass Spectrometry. *Environ. Sci. Technol.* **2014**, *48* (13), 7461–7468. https://doi.org/10.1021/es5015423.

(77) Hunt, A. P.; Parry, J. D.; Hamilton-Taylor, J. Further Evidence of Elemental Composition as an Indicator of the Bioavailability of Humic Substances to Bacteria. *Limnol. Oceanogr.* **2000**, *45* (1), 237–241.

(78) Fellman, J. B.; D'Amore, D. V.; Hood, E.; Boone, R. D. Fluorescence Characteristics and Biodegradability of Dissolved Organic Matter in Forest and Wetland Soils from Coastal Temperate Watersheds in Southeast Alaska. *Biogeochemistry* **2008**, *88* (2), 169–184. https://doi.org/10.1007/s10533-008-9203-x.

(79) Hutchins, R. H. S.; Aukes, P. J. K.; Schiff, S. L.; Dittmar, T.; Prairie, Y. T.; del Giorgio, P. A. The Optical, Chemical, and Molecular Dissolved Organic Matter Succession Along a Boreal Soil-Stream-River Continuum. *J. Geophys. Res. Biogeosciences* **2017**, *122* (11), 2892–2908. https://doi.org/10.1002/2017JG004094.

(80) Kellerman, A. M.; Guillemette, F.; Podgorski, D. C.; Aiken, G. R.; Butler, K. D.; Spencer, R. G. M. Unifying Concepts Linking Dissolved Organic Matter Composition to Persistence in Aquatic Ecosystems. *Environ. Sci. Technol.* **2018**, *52* (5), 2538–2548. https://doi.org/10.1021/acs.est.7b05513.

(81) Kellerman, A. M.; Kothawala, D. N.; Dittmar, T.; Tranvik, L. J. Persistence of Dissolved Organic Matter in Lakes Related to Its Molecular Characteristics. *Nat. Geosci.* **2015**, *8* (May). https://doi.org/10.1038/ngeo2440.

(82) Wickland, K. P.; Aiken, G. R.; Butler, K. D.; Dornblaser, M. M.; Spencer, R. G. M.; Striegl, R. G. Biodegradability of Dissolved Organic Carbon in the Yukon River and Its Tributaries: Seasonality and Importance of Inorganic Nitrogen. *Global Biogeochem. Cycles* **2012**, *26* (3), 1–14. https://doi.org/10.1029/2012GB004342.

(83) Hansen, A. M.; Kraus, T. E. C.; Pellerin, B. A.; Fleck, J. A.; Downing, B. D.; Bergamaschi, B. A. Optical Properties of Dissolved Organic Matter (DOM): Effects of Biological and Photolytic Degradation. *Limnol. Oceanogr.* **2016**, *61* (3), 1015–1032. https://doi.org/10.1002/lno.10270.

(84) Sulzberger, B.; Durisch-Kaiser, E. Chemical Characterization of Dissolved Organic Matter (DOM): A Prerequisite for Understanding UV-Induced Changes of DOM Absorption Properties and Bioavailability. *Aquat. Sci.* **2009**, *71* (2), 104–126. https://doi.org/10.1007/s00027-008-8082-5.

(85) Ward, C. P.; Nalven, S. G.; Crump, B. C.; Kling, G. W.; Cory, R. M. Photochemical Alteration of Organic Carbon Draining Permafrost Soils Shifts Microbial Metabolic Pathways and Stimulates Respiration. *Nat. Commun.* **2017**, 1–8. https://doi.org/10.1038/s41467-017-00759-2.

(86) Molot, L. A.; Dillon, P. J. Photolytic Regulation of Dissolved Organic Carbon in Northern Lakes. *Global Biogeochem. Cycles* **1997**, *11* (3), 357–365. https://doi.org/10.1029/97GB01198.

(87) Ward, C. P.; Cory, R. M. Complete and Partial Photo-Oxidation of Dissolved Organic Matter Draining Permafrost Soils. *Environ. Sci. Technol.* **2016**, *50* (7), 3545–3553. https://doi.org/10.1021/acs.est.5b05354.

(88) Amon, R. M. W.; Rinehart, A. J.; Duan, S.; Louchouarn, P.; Prokushkin, A.; Guggenberger, G.; Bauch, D.; Stedmon, C.; Raymond, P. a.; Holmes, R. M.; et al. Dissolved Organic Matter

Sources in Large Arctic Rivers. *Geochim. Cosmochim. Acta* **2012**, *94*, 217–237. https://doi.org/10.1016/j.gca.2012.07.015.

(89) Evans, C. D.; Monteith, D. T.; Cooper, D. M. Long-Term Increases in Surface Water Dissolved Organic Carbon: Observations, Possible Causes and Environmental Impacts. *Environ. Pollut.* **2005**, *137* (1), 55–71. https://doi.org/10.1016/j.envpol.2004.12.031.

(90) Roiha, T.; Peura, S.; Cusson, M.; Rautio, M. Allochthonous Carbon Is a Major Regulator to Bacterial Growth and Community Composition in Subarctic Freshwaters. *Sci. Rep.* **2016**, *6* (May), 34456. https://doi.org/10.1038/srep34456.

(91) Kritzberg, E. S.; Ekström, S. M. Increasing Iron Concentrations in Surface Waters - A Factor behind Brownification? *Biogeosciences* **2012**, *9*, 1465–1478. https://doi.org/10.5194/bg-9-1465-2012.

(92) Weyhenmeyer, G. A.; Prairie, Y. T.; Tranvik, L. J. Browning of Boreal Freshwaters Coupled to Carbon-Iron Interactions along the Aquatic Continuum. *PLoS One* **2014**, *9* (2), e88104. https://doi.org/10.1371/journal.pone.0088104.

(93) Drake, T. W.; Wickland, K. P.; Spencer, R. G. M.; McKnight, D. M.; Striegl, R. G. Ancient Low–Molecular-Weight Organic Acids in Permafrost Fuel Rapid Carbon Dioxide Production upon Thaw. *Proc. Natl. Acad. Sci.* **2015**, *112* (45), 13946–13951. https://doi.org/10.1073/pnas.1511705112.

(94) Drake, T. W.; Guillemette, F.; Hemingway, J. D.; Chanton, J. P.; Podgorski, D. C.; Zimov, N. S.; Spencer, R. G. M. The Ephemeral Signature of Permafrost Carbon in an Arctic Fluvial Network. *J. Geophys. Res. Biogeosciences* **2018**, No. 2015. https://doi.org/10.1029/2017JG004311.

(95) O'Donnell, J. a.; Aiken, G. R.; Walvoord, M. a.; Butler, K. D. Dissolved Organic Matter Composition of Winter Flow in the Yukon River Basin: Implications of Permafrost Thaw and Increased Groundwater Discharge. *Global Biogeochem. Cycles* **2012**, *26* (4), n/a-n/a. https://doi.org/10.1029/2012GB004341.

(96) Vonk, J. E.; Mann, P. J.; Davydov, S.; Davydova, A.; Spencer, R. G. M.; Schade, J.; Sobczak, W. V.; Zimov, N. S.; Zimov, S. A.; Bulygina, E.; et al. High Biolability of Ancient Permafrost Carbon upon Thaw. *Geophys. Res. Lett.* **2013**, *40* (11), 2689–2693. https://doi.org/10.1002/grl.50348.

(97) Wang, Y.; Xu, Y.; Spencer, R. G. M.; Zito, P.; Kellerman, A. M.; Podgorski, D.; Xiao, W.; Wei, D.; Rashid, H.; Yang, Y. Selective Leaching of Dissolved Organic Matter from Alpine Permafrost Soils on the Qinghai-Tibetan Plateau. *J. Geophys. Res. Biogeosciences* **2018**. https://doi.org/10.1002/2017JG004343.

(98) Panneer Selvam, B.; Lapierre, J.-F.; Guillemette, F.; Voigt, C.; Lamprecht, R. E.; Biasi, C.; Christensen, T. R.; Martikainen, P. J.; Berggren, M. Degradation Potentials of Dissolved Organic Carbon (DOC) from Thawed Permafrost Peat. *Sci. Rep.* **2017**, *7*, 45811. https://doi.org/10.1038/srep45811.

(99) Cory, R. M.; Ward, C. P.; Crump, B. C.; Kling, G. W. Sunlight Controls Water Column Processing of Carbon in Arctic Fresh Waters. *Science (80-.).* **2014**, *345* (6199), 925–928. https://doi.org/10.1126/science.1253119.

(100) Stubbins, A.; Mann, P. J.; Powers, L.; Bittar, T. B.; Dittmar, T.; McIntyre, C. P.; Eglinton, T. I.; Zimov, N. S.; Spencer, R. G. M. Low Photolability of Yedoma Permafrost Dissolved Organic Carbon. *J. Geophys. Res. Biogeosciences* **2017**, *122* (1), 200–211. https://doi.org/10.1002/2016JG003688.

(101) Laurion, I.; Mladenov, N. Dissolved Organic Matter Photolysis in Canadian Arctic Thaw Ponds. *Environ. Res. Lett.* **2013**, *8* (3), 035026. https://doi.org/10.1088/1748-9326/8/3/035026.

(102) Ritson, J. P.; Graham, N. J. D.; Templeton, M. R.; Clark, J. M.; Gough, R.; Freeman, C. The Impact of Climate Change on the Treatability of Dissolved Organic Matter (DOM) in Upland Water Supplies: A UK Perspective. *Sci. Total Environ.* **2014**, *473–474*, 714–730. https://doi.org/10.1016/j.scitotenv.2013.12.095.

(103) Semiletov, I.; Pipko, I.; Gustafsson, Ö.; Anderson, L. G.; Sergienko, V.; Pugach, S.; Dudarev, O.; Charkin, A.; Gukov, A.; Bröder, L.; et al. Acidification of East Siberian Arctic Shelf Waters through Addition of Freshwater and Terrestrial Carbon. *Nat. Geosci.* **2016**, No. April. https://doi.org/10.1038/NEGO2695.

(104) Metcalfe, D. B.; Hermans, T. D. G.; Ahlstrand, J.; Becker, M.; Berggren, M.; Björk, R. G.; Björkman, M. P.; Blok, D.; Chaudhary, N.; Chisholm, C.; et al. Patchy Field Sampling Biases Understanding of Climate Change Impacts across the Arctic. *Nat. Ecol. Evol.* **2018**, *2* (9), 1443–1448. https://doi.org/10.1038/s41559-018-0612-5.

(105) Mallory, M. L.; Gilchrist, H. G.; Janssen, M.; Major, H. L.; Merkel, F.; Provencher, J. F.; Strøm, H. Financial Costs of Conducting Science in the Arctic: Examples from Seabird Research. *Arct. Sci.* **2018**, *4* (4), 624–633. https://doi.org/10.1139/as-2017-0019.

(106) Amon, R. M. W.; Meon, B. The Biogeochemistry of Dissolved Organic Matter and Nutrients in Two Large Arctic Estuaries and Potential Implications for Our Understanding of the Arctic Ocean System. *Mar. Chem.* **2004**, *92* (1–4), 311–330. https://doi.org/10.1016/j.marchem.2004.06.034.

(107) Frey, K. E.; Siegel, D. I.; Smith, L. C. Geochemistry of West Siberian Streams and Their Potential Response to Permafrost Degradation. *Water Resour. Res.* **2007**, *43* (August 2006). https://doi.org/10.1029/2006WR004902.

(108) Mann, P. J.; Davydova, a.; Zimov, N. S.; Spencer, R. G. M.; Davydov, S.; Bulygina, E.; Zimov, S. A.; Holmes, R. M. Controls on the Composition and Lability of Dissolved Organic Matter in Siberia's Kolyma River Basin. *J. Geophys. Res.* **2012**, *117* (G1), G01028. https://doi.org/10.1029/2011JG001798.

(109) Wickland, K. P.; Neff, J. C.; Aiken, G. R. Dissolved Organic Carbon in Alaskan Boreal Forest: Sources, Chemical Characteristics, and Biodegradability. *Ecosystems* **2007**, *10* (8), 1323–1340. https://doi.org/10.1007/s10021-007-9101-4.

(110) Ward, C. P.; Cory, R. M. Chemical Composition of Dissolved Organic Matter Draining Permafrost Soils. *Geochim. Cosmochim. Acta* **2015**, *167*, 63–79. https://doi.org/10.1016/j.gca.2015.07.001.

(111) Abbott, B. W.; Larouche, J. R.; Jones, J. B.; Bowden, W. B.; Balser, a. W. Elevated Dissolved Organic Carbon Biodegradability from Thawing and Collapsing Permafrost. *J. Geophys. Res.* **2014**, *119*, 2049–2063. https://doi.org/10.1002/2014JG002678.Received.

(112) Balcarczyk, K. L.; Jones, J. B.; Jaffé, R.; Maie, N. Stream Dissolved Organic Matter Bioavailability and Composition in Watersheds Underlain with Discontinuous Permafrost. *Biogeochemistry* **2009**, *94* (3), 255–270. https://doi.org/10.1007/s10533-009-9324-x.

(113) Cory, R. M.; Harrold, K. H.; Neilson, B. T.; Kling, G. W. Controls on Dissolved Organic Matter (DOM) Degradation in a Headwater Stream: The Influence of Photochemical and Hydrological Conditions in Determining Light-Limitation or Substrate-Limitation of Photo-Degradation. *Biogeosciences Discuss.* **2015**, *12* (13), 9793–9838. https://doi.org/10.5194/bgd-12-9793-2015.

(114) Holmes, R. M.; McClelland, J. W.; Raymond, P. a.; Frazer, B. B.; Peterson, B. J.; Stieglitz, M. Lability of DOC Transported by Alaskan Rivers to the Arctic Ocean. *Geophys. Res. Lett.* **2008**, *35* (3), L03402. https://doi.org/10.1029/2007GL032837.

(115) Larouche, J. R.; Abbott, B. W.; Bowden, W. B.; Jones, J. B. The Role of Watershed Characteristics, Permafrost Thaw, and Wildfire on Dissolved Organic Carbon Biodegradability and Water Chemistry in Arctic Headwater Streams. *Biogeosciences* **2015**, *12* (14), 4221–4233. https://doi.org/10.5194/bg-12-4221-2015.

(116) Reyes, F. R.; Lougheed, V. L. Rapid Nutrient Release from Permafrost Thaw in Arctic Aquatic Ecosystems. *Arctic, Antarct. Alp. Res.* **2015**, *47* (1), 35–48. https://doi.org/10.1657/AAAR0013-099.

(117) Thompson, M. S.; Giesler, R.; Karlsson, J.; Klaminder, J. Size and Characteristics of the DOC Pool in Near-Surface Subarctic Mire Permafrost as a Potential Source for Nearby Freshwaters. *Arctic, Antarct. Alp. Res.* **2015**, *47* (1), 49–58.

(118) Roehm, C. L.; Giesler, R.; Karlsson, J. Bioavailability of Terrestrial Organic Carbon to Lake Bacteria: The Case of a Degrading Subarctic Permafrost Mire Complex. *J. Geophys. Res. Biogeosciences* **2009**, *114* (3), 1–10. https://doi.org/10.1029/2008JG000863.

(119) Kokfelt, U.; Rosén, P.; Schoning, K.; Christensen, T. R.; Förster, J.; Karlsson, J.; Reuss, N.; Rundgren, M.; Callaghan, T. V.; Jonasson, C.; et al. Ecosystem Responses to Increased Precipitation and Permafrost Decay in Subarctic Sweden Inferred from Peat and Lake Sediments. *Glob. Chang. Biol.* **2009**, *15* (7), 1652–1663. https://doi.org/10.1111/j.1365-2486.2009.01880.x.

(120) Jonasson, C.; Sonesson, M.; Christensen, T. R.; Callaghan, T. V. Environmental Monitoring and Research in the Abisko Area-an Overview. *Ambio* **2012**, *41 Suppl 3* (Supplement 3), 178–186. https://doi.org/10.1007/s13280-012-0301-6.

(121) Walvoord, M. A.; Striegl, R. G. Increased Groundwater to Stream Discharge from Permafrost Thawing in the Yukon River Basin: Potential Impacts on Lateral Export of Carbon and Nitrogen. *Geophys. Res. Lett.* **2007**, *34* (12). https://doi.org/10.1029/2007GL030216.

(122) Toohey, R. C.; Herman-Mercer, N. M.; Schuster, P. F.; Mutter, E. A.; Koch, J. C. Multidecadal Increases in the Yukon River Basin of Chemical Fluxes as Indicators of Changing Flowpaths, Groundwater, and Permafrost. *Geophys. Res. Lett.* **2016**, *43* (23), 12,120-12,130. https://doi.org/10.1002/2016GL070817.

(123) O'Donnell, J. A.; Aiken, G. R.; Kane, E. S.; Jones, J. B. Source Water Controls on the Character and Origin of Dissolved Organic Matter in Streams of the Yukon River Basin, Alaska. *J. Geophys. Res.* **2010**, *115* (G3), G03025. https://doi.org/10.1029/2009JG001153.

(124) Harms, T. K.; Edmonds, J. W.; Genet, H.; Creed, I. F.; Aldred, D.; Balser, A.; Jones, J. B. Catchment Influence on Nitrate and Dissolved Organic Matter in Alaskan Streams across a Latitudinal Gradient. *J. Geophys. Res. G Biogeosciences* **2016**, *121* (2), 350–369. https://doi.org/10.1002/2015JG003201.

(125) Aiken, G. R.; Spencer, R. G. M.; Striegl, R. G.; Schuster, P. F.; Raymond, P. A. Influences of Glacier Melt and Permafrost Thaw on the Age of Dissolved Organic Carbon in the Yukon River Basin. *Global Biogeochem. Cycles* **2014**, *28*, 525–537. https://doi.org/10.1002/2013GB004764.

(126) Lessels, J. S.; Tetzlaff, D.; Carey, S. K.; Smith, P.; Soulsby, C. A Coupled Hydrology-Biogeochemistry Model to Simulate Dissolved Organic Carbon Exports from a Permafrost Influenced Catchment. *Hydrol. Process.* **2015**, *44* (0), n/a-n/a. https://doi.org/10.1002/hyp.10566.

(127) Thompson, M. S.; Wrona, F. J.; Prowse, T. D. Shifts in Plankton, Nutrient and Light Relationships in Small Tundra Lakes Caused by Localized Permafrost Thaw. *Arctic* **2012**, *65* (4), 367–376.

(128) Littlefair, C. A.; Tank, S. E.; Kokelj, S. V. Retrogressive Thaw Slumps Temper Dissolved Organic Carbon Delivery to Streams of the Peel Plateau, NWT, Canada. *Biogeosciences* **2017**, *14* (23), 5487–5505. https://doi.org/10.5194/bg-14-5487-2017.

(129) Littlefair, C. A.; Tank, S. E. Biodegradability of Thermokarst Carbon in a Till-Associated, Glacial Margin Landscape: The Case of the Peel Plateau, NWT, Canada. *J. Geophys. Res. Biogeosciences* **2018**, *123* (10), 3293–3307. https://doi.org/10.1029/2018JG004461.

(130) Tank, S. E.; Lesack, L. F. W.; Gareis, J. a. L.; Osburn, C. L.; Hesslein, R. H. Multiple Tracers Demonstrate Distinct Sources of Dissolved Organic Matter to Lakes of the Mackenzie Delta, Western Canadian Arctic. *Limnol. Oceanogr.* **2011**, *56* (4), 1297–1309. https://doi.org/10.4319/lo.2011.56.4.1297.

(131) Gareis, J. a. L.; Lesack, L. F. W.; Bothwell, M. L. Attenuation of in Situ UV Radiation in Mackenzie Delta Lakes with Varying Dissolved Organic Matter Compositions. *Water Resour. Res.* **2010**, *46* (9), n/a-n/a. https://doi.org/10.1029/2009WR008747.

(132) Tank, S. E.; Striegl, R. G.; Mcclelland, J. W.; Kokelj, S. V. Multi-Decadal Increases in Dissolved Organic Carbon and Alkalinity Flux from the Mackenzie Drainage Basin to the Arctic Ocean. *Environ. Res. Lett.* **2016**, *11* (5), 54015. https://doi.org/10.1088/1748-9326/11/5/054015.

(133) Negandhi, K.; Laurion, I.; Whiticar, M. J.; Galand, P. E.; Xu, X.; Lovejoy, C. Small Thaw Ponds: An Unaccounted Source of Methane in the Canadian High Arctic. *PLoS One* **2013**, *8* (11). https://doi.org/10.1371/journal.pone.0078204.

(134) Wang, J.; Lafrenière, M. J.; Lamoureux, S. F.; Simpson, A. J.; Gélinas, Y.; Simpson, M. J. Differences in Riverine and Pond Water Dissolved Organic Matter Composition and Sources in Canadian High Arctic Watersheds Affected by Active Layer Detachments. *Environ. Sci. Technol.* **2018**, *52* (3), 1062–1071. https://doi.org/10.1021/acs.est.7b05506.

(135) Pautler, B. G.; Simpson, A. J.; McNally, D. J.; Lamoureux, S. F.; Simpson, M. J. Arctic Permafrost Active Layer Detachments Stimulate Microbial Activity and Degradation of Soil Organic Matter. *Environ. Sci. Technol.* **2010**, *44* (11), 4076–4082.

https://doi.org/10.1021/es903685j.

(136) Woods, G. C.; Simpson, M. J.; Pautler, B. G.; Lamoureux, S. F.; Lafrenière, M. J.; Simpson, A. J. Evidence for the Enhanced Lability of Dissolved Organic Matter Following Permafrost Slope Disturbance in the Canadian High Arctic. *Geochim. Cosmochim. Acta* **2011**, *75* (22), 7226–7241. https://doi.org/10.1016/j.gca.2011.08.013.

(137) Lamoureux, S. F.; Lafrenière, M. J. Seasonal Fluxes and Age of Particulate Organic Carbon Exported from Arctic Catchments Impacted by Localized Permafrost Slope Disturbances. *Environ. Res. Lett.* **2014**, *9* (4), 045002. https://doi.org/10.1088/1748-9326/9/4/045002.

(138) Fouché, J.; Lafrenière, M. J.; Rutherford, K.; Lamoureux, S. F. Seasonal Hydrology and Permafrost Disturbance Impacts on Dissolved Organic Matter Composition in High Arctic Headwater Catchments. *Arct. Sci.* **2017**, *0* (January), 1–28. https://doi.org/10.1139/AS-2016-0031.

(139) Olefeldt, D.; Roulet, N. T. *Permafrost Conditions in Peatlands Regulate Magnitude, Timing and Chemical Composition of Catchment Dissolved Organic Carbon Export.*; 2014. https://doi.org/10.1111/gcb.12607.

(140) Spence, C.; Kokelj, S. V.; Kokelj, S. A.; McCluskie, M.; Hedstrom, N. Evidence of a Change in Water Chemistry in Canada's Subarctic Associated with Enhanced Winter Streamflow. *J. Geophys. Res. Biogeosciences* **2015**, *120* (1), 113–127. https://doi.org/10.1002/2014JG002809.

(141) Creed, I. F.; Bergström, A. K.; Trick, C. G.; Grimm, N. B.; Hessen, D. O.; Karlsson, J.; Kidd, K. A.; Kritzberg, E.; McKnight, D. M.; Freeman, E. C.; et al. Global Change-Driven Effects on Dissolved Organic Matter Composition: Implications for Food Webs of Northern Lakes. *Glob. Chang. Biol.* **2018**, *24* (8), 3692–3714. https://doi.org/10.1111/gcb.14129.

(142) Hirsch, R. M.; Slack, J. R.; Smith, R. A. Techniques of Trend Analysis for Monthly Water Quality Data. *Water Resour. Res.* **1982**, *18* (1), 107–121.

(143) Hirsch, R. M.; Alexander, R. B.; Smith, R. A. Selection of Methods for the Detection and Estimation of Trends in Water Quality. *Water Resour. Res.* **1991**, *27* (5), 803–813.

(144) Billen, G.; Garnier, J.; Ficht, A.; Cun, C. Modeling the Response of Water Quality in the Seine River Estuary to Human Activity in Its Watershed over the Last 50 Years. *Estuaries* **2001**, *24* (6B), 977–993. https://doi.org/10.2307/1353011.

(145) Interlandi, S. J.; Crockett, C. S. Recent Water Quality Trends in the Schuylkill River, Pennsylvania, USA: A Preliminary Assessment of the Relative Influences of Climate, River Discharge and Suburban Development. *Water Res.* **2003**, *37* (8), 1737–1748. https://doi.org/10.1016/S0043-1354(02)00574-2.

(146) Worrall, F.; Burt, T. P.; Shedden, R. Long Term Trends of Riverine Dissolved Organic Matter. *Biogeochemistry* **2003**, *64* (2), 13. https://doi.org/10.1023/A:1024924216148.

(147) Coleman, K. A.; Palmer, M. J.; Korosi, J. B.; Kokelj, S. V.; Jackson, K.; Hargan, K. E.; Courtney Mustaphi, C. J.; Thienpont, J. R.; Kimpe, L. E.; Blais, J. M.; et al. Tracking the Impacts of Recent Warming and Thaw of Permafrost Peatlands on Aquatic Ecosystems: A Multi-Proxy Approach Using Remote Sensing and Lake Sediments. *Boreal Environ. Res.* **2015**, *20* (3), 363–377.

(148) Spence, C.; Kokelj, S. V.; Ehsanzadeh, E. Precipitation Trends Contribute to Streamflow

Regime Shifts in Northern Canada. In *Cold Region Hydrology in a Changing Climate*; 2011; pp 3–8.

(149) Lumb, A.; Halliwell, D.; Sharma, T. Application of CCME Water Quality Index to Monitor Water Quality: A Case Study of the Mackenzie River Basin, Canada. *Environ. Monit. Assess.* **2006**, *113* (1–3), 411–429. https://doi.org/10.1007/s10661-005-9092-6.

(150) McClelland, J. W.; Déry, S. J.; Peterson, B. J.; Holmes, R. M.; Wood, E. F. A Pan-Arctic Evaluation of Changes in River Discharge during the Latter Half of the 20th Century. *Geophys. Res. Lett.* **2006**, *33* (6), 2–5. https://doi.org/10.1029/2006GL025753.

(151) Déry, S. J.; Stadnyk, T. A.; MacDonald, M. K.; Gauli-Sharma, B. Recent Trends and Variability in River Discharge across Northern Canada. *Hydrol. Earth Syst. Sci.* **2016**, *20* (12), 4801–4818. https://doi.org/10.5194/hess-20-4801-2016.

(152) Rood, S. B.; Kaluthota, S.; Philipsen, L. J.; Rood, N. J.; Zanewich, K. P. Increasing Discharge from the Mackenzie River System to the Arctic Ocean. *Hydrol. Process.* **2016**, *160* (August 2016), 150–160. https://doi.org/10.1002/hyp.10986.

(153) Spence, C.; Kokelj, S. A.; Kokelj, S. V.; Hedstrom, N. The Process of Winter Streamflow Generation in a Subarctic Precambrian Shield Catchment. *Hydrol. Process.* **2014**, *28* (14), 4179–4190. https://doi.org/10.1002/hyp.10119.

(154) Kokelj, S. V.; Lacelle, D.; Lantz, T. C.; Tunnicliffe, J.; Malone, L.; Clark, I. D.; Chin, K. S. Thawing of Massive Ground Ice in Mega Slumps Drives Increases in Stream Sediment and Solute Flux across a Range of Watershed Scales. *J. Geophys. Res. Earth Surf.* **2013**, *118* (2), 681–692. https://doi.org/10.1002/jgrf.20063.

(155) Salmon, V. G.; Soucy, P.; Mauritz, M.; Celis, G.; Natali, S. M.; Mack, M. C.; Schuur, E. A. G. Nitrogen Availability Increases in a Tundra Ecosystem during Five Years of Experimental Permafrost Thaw. *Glob. Chang. Biol.* **2016**, *22* (5), 1927–1941. https://doi.org/10.1111/gcb.13204.

(156) Keuper, F.; Bodegom, P. M.; Dorrepaal, E.; Weedon, J. T.; Hal, J.; Logtestijn, R. S. P.; Aerts, R. A Frozen Feast: Thawing Permafrost Increases Plant-Available Nitrogen in Subarctic Peatlands. *Glob. Chang. Biol.* **2012**, *18* (6), 1998–2007. https://doi.org/10.1111/j.1365-2486.2012.02663.x.

(157) Wrona, F. J.; Johansson, M.; Culp, J. M.; Jenkins, A.; Mård, J.; Myers-Smith, I. H.; Prowse, T. D.; Vincent, W. F.; Wookey; A., P.; et al. Transitions in Arctic Ecosystems: Ecological Implications of a Changing Hydrological Regime. *J. Geophys. Res. Biogeosciences* **2016**, 650–674. https://doi.org/10.1002/2015JG003133.Received.

(158) MacLean, R.; Oswood, M.; Irons III, J.; McDowell, W. H. The Effect of Permafrost on Stream Biogeochemistry : A Case Study of Two Streams in the Alaskan (U.S.A.) Taiga. *Biogeochemistry* **1999**, *47*, 239–267.

(159) Keller, K.; Blum, J. D.; Kling, G. W. Geochemistry of Soils and Streams on Surfaces of Varying Ages in Arctic Alaska. *Arctic, Antarct. Alp. Res.* **2007**, *39* (1), 84–98. https://doi.org/10.1657/1523-0430(2007)39[84:GOSASO]2.0.CO;2.

(160) Petrone, K. C.; Jones, J. B.; Hinzman, L. D.; Boone, R. D. Seasonal Export of Carbon, Nitrogen, and Major Solutes from Alaskan Catchments with Discontinuous Permafrost. *J. Geophys.*

Res. **2006**, *111* (G2), G02020. https://doi.org/10.1029/2005JG000055.

(161) Frey, K. E.; McClelland, J. W. Impacts of Permafrost Degradation on Arctic River Biogeochemistry. *Hydrol. Process.* **2009**, *23*, 169–182. https://doi.org/10.1002/hyp.

(162) Ciais, P.; Sabine, C.; Bala, G.; Bopp, L.; Brovkin, V.; Canadell, J.; Chhabra, A.; DeFries, R.; Galloway, J.; Heimann, M.; et al. Carbon and Other Biogeochemical Cycles. In *Climate Change 2013: The Physical Science Basis. Contribution of Working Group I to the Fifth Assessment Report of the Intergovernmental Panel on Climate Change*; Stocker, T. F., Qin, D., Plattner, G.-K., Tignor, M., Allen, S. K., Boschung, J., Nauels, A., Xia, Y., Bex, V., Midgley, P. M., Eds.; Cambridge University Press: Cambridge, United Kingdom and New York, NY, 2013; pp 465–570. https://doi.org/10.1017/CBO9781107415324.015.

(163) Striegl, R. G.; Aiken, G. R.; Dornblaser, M. M.; Raymond, P. A.; Wickland, K. P. A Decrease in Discharge-Normalized DOC Export by the Yukon River during Summer through Autumn. *Geophys. Res. Lett.* **2005**, *32* (21), 3–6. https://doi.org/10.1029/2005GL024413.

(164) Kicklighter, D. W.; Hayes, D. J.; McClelland, J. W.; Peterson, B. J.; McGuire, A. D.; Melillo, J. M. Insights and Issues with Simulating Terrestrial DOC Loading of Arctic River Networks. *Ecol. Appl.* **2013**, *23* (8), 1817–1836. https://doi.org/10.1890/11-1050.1.

(165) Ecosystem Classification Group. *Ecological Regions of the Northwest Territories - Taiga Shield*; Yellowknife, NT, Canada, 2008.

(166) Ecosystem Classification Group. *Ecological Regions of the Northwest Territories - Taiga Plains*; Yellowknife, NT, Canada, 2009.

(167) Smith, S. L.; Romanovsky, V. E.; Lewkowicz, A. G.; Burn, C. R.; Allard, M.; Clow, G. D.; Yoshikawa, K.; Throop, J. Thermal State of Permafrost in North America: A Contribution to the International Polar Year. *Permafr. Periglac. Process.* **2010**, *21* (2), 117–135. https://doi.org/10.1002/ppp.690.

(168) Morse, P. D.; Wolfe, S. A.; Kokelj, S. V.; Gaanderse, A. J. R. The Occurrence and Thermal Disequilibrium State of Permafrost in Forest Ecotopes of the Great Slave Region, Northwest Territories, Canada. *Permafr. Periglac. Process.* **2015**, *27* (2), 145–162. https://doi.org/10.1002/ppp.1858.

(169) Kokelj, S. A. *Hydrologic Overview of the North and South Slave Regions*; Yellowknife, NT, Canada, 2003.

(170) Woo, M. K.; Mielko, C. Flow Connectivity of a Lake-Stream System in a Semi-Arid Precambrian Shield Environment. In *Cold Region Atmospheric and Hydrologic Studies. The Mackenzie GEWEX Experience*; Woo, M., Ed.; Springer-Verlag: Berlin, Heidelberg, 2008; Vol. 2, pp 221–233. https://doi.org/10.1007/978-3-540-75136-6_12.

(171) Runkel, R. L.; Crawford, C. G.; Cohn, T. A. *Load Estimator (LOADEST): A FORTRAN Program for Estimating Constituent Loads in Streams and Rivers: U.S. Geological Survey Techniques and Methods Book 4*; U.S. Geological Survey, 2004.

(172) Booth, G.; Raymond, P.; Oh, N.-H. LoadRunner <http://Environment.Yale.Edu/Raymond/Loadrunner/>. Yale University: New Haven, CT 2007.

(173) Yue, S.; Pilon, P.; Phinney, B.; Cavadias, G. The Influence of Autocorrelation on the Ability to

Detect Trend in Hydrological Series. *Hydrol. Process.* **2002**, *16* (9), 1807–1829. https://doi.org/10.1002/hyp.1095.

(174) Connon, R. F.; Quinton, W. L.; Craig, J. R.; Hayashi, M. Changing Hydrologic Connectivity Due to Permafrost Thaw in the Lower Liard River Valley, NWT, Canada. *Hydrol. Process.* **2014**, *28* (14), 4163–4178. https://doi.org/10.1002/hyp.10206.

(175) Åkerman, H. J.; Johansson, M. Thawing Permafrost and Thicker Active Layers in Sub-Arctic Sweden. *Permafr. Periglac. Process.* **2008**, *19*, 279–292. https://doi.org/10.1002/ppp.626.

(176) Lyon, S. W.; Destouni, G.; Giesler, R.; Humborg, C.; Mörth, M.; Seibert, J.; Karlsson, J.; Troch, P. A. Estimation of Permafrost Thawing Rates in a Sub-Arctic Catchment Using Recession Flow Analysis. *Hydrol. Earth Syst. Sci. Discuss.* **2009**, *13* (1), 595–604. https://doi.org/10.5194/hessd-6-63-2009.

(177) Yi, S.; Woo, M. K.; Arain, M. A. Impacts of Peat and Vegetation on Permafrost Degradation under Climate Warming. *Geophys. Res. Lett.* **2007**, *34* (16), 1–5. https://doi.org/10.1029/2007GL030550.

(178) Vihma, T.; Screen, J.; Tjernström, M.; Newton, B.; Zhang, X.; Popova, V.; Deser, C.; Holland, M.; Prowse, T. The Atmospheric Role in the Arctic Water Cycle: A Review on Processes, Past and Future Changes, and Their Impacts. *J. Geophys. Res. Biogeosciences* **2016**, *121* (3), 586–620. https://doi.org/10.1002/2015JG003132.

(179) Wolfe, S. A.; Kerr, D. E. Surficial Geology, Yellowknife Area, Northwest Territories, Parts of NTS85-J/7, NTS 85-J/8, NTS 85-J/9, and NTS 85-J/10. Geological Survey of Canada 2014, p Canadian Geoscience Map 183 (preliminary). https://doi.org/10.4095/293725.

(180) Lantz, T. C.; Kokelj, S. V. Increasing Rates of Retrogressive Thaw Slump Activity in the Mackenzie Delta Region, N.W.T., Canada. *Geophys. Res. Lett.* **2008**, *35* (6), 1–5. https://doi.org/10.1029/2007GL032433.

(181) Malone, L.; Lacelle, D.; Kokelj, S. V.; Clark, I. D. Impacts of Hillslope Thaw Slumps on the Geochemistry of Permafrost Catchments (Stony Creek Watershed, NWT, Canada). *Chem. Geol.* **2013**, *356*, 38–49. https://doi.org/10.1016/j.chemgeo.2013.07.010.

(182) Kendrick, M. R.; Huryn, A. D.; Bowden, W. B.; Deegan, L. A.; Findlay, R. H.; Hershey, A. E.; Peterson, B. J.; Beneš, J. P.; Schuett, E. B. Linking Permafrost Thaw to Shifting Biogeochemistry and Food Web Resources in an Arctic River. *Glob. Chang. Biol.* **2018**, *24* (12), 5738–5750. https://doi.org/10.1111/gcb.14448.

(183) Walvoord, M. A.; Voss, C. I.; Wellman, T. P. Influence of Permafrost Distribution on Groundwater Flow in the Context of Climate-Driven Permafrost Thaw: Example from Yukon Flats Basin, Alaska, United States. *Water Resour. Res.* **2012**, *48* (7), 1–17. https://doi.org/10.1029/2011WR011595.

(184) Neff, J. C.; Finlay, J. C.; Zimov, S. A.; Davydov, S. P.; Carrasco, J. J.; Schuur, E. A. G.; Davydova, A. I. Seasonal Changes in the Age and Structure of Dissolved Organic Carbon in Siberian Rivers and Streams. *Geophys. Res. Lett.* **2006**, *33* (23), L23401. https://doi.org/10.1029/2006GL028222.

(185) Kasischke, E. S.; Turetsky, M. R. Recent Changes in the Fire Regime across the North American Boreal Region - Spatial and Temporal Patterns of Burning across Canada and

Alaska. *Geophys. Res. Lett.* **2006**, *33* (9). https://doi.org/10.1029/2006GL025677.

(186) Veraverbeke, S.; Rogers, B. M.; Goulden, M. L.; Jandt, R. R.; Miller, C. E.; Wiggins, E. B.; Randerson, J. T. Lightning as a Major Driver of Recent Large Fire Years in North American Boreal Forests. *Nat. Clim. Chang.* **2017**, *7* (7), 529–534. https://doi.org/10.1038/nclimate3329.

(187) Bayley, S. E.; Schindler, D. W.; Beaty, K. G.; Parker, B. R.; Stainton, M. P. Effects of Multiple Fires on Nutrient Yields from Streams Draining Boreal Forest and Fen Watersheds: Nitrogen and Phosphorus. *Can. J. Fish. Aquat. Sci.* **1992**, *49* (3), 584–596. https://doi.org/10.1139/f92-068.

(188) Chorover, J.; Vitousek, P. M.; Everson, D. A.; Esperanza, A. M.; Turner, D. Solution Chemistry Profiles of Mixed-Conifer Forests before and after Fire. *Biogeochemistry* **1994**, *26* (2), 115–144. https://doi.org/10.1007/BF02182882.

(189) Government of the Northwest Territories; NWT Centre for Geomatics. Inventory of Landscape Change http://apps.geomatics.gov.nt.ca (accessed Jul 27, 2017).

(190) Benner, R.; Benitez-Nelson, B.; Kaiser, K.; Amon, R. M. W. Export of Young Terrigenous Dissolved Organic Carbon from Rivers to the Arctic Ocean. *Geophys. Res. Lett.* **2004**, *31* (5). https://doi.org/10.1029/2003GL019251.

(191) Giesler, R.; Lyon, S. W.; Mörth, C. M.; Karlsson, J.; Karlsson, E. M.; Jantze, E. J.; Destouni, G.; Humborg, C. Catchment-Scale Dissolved Carbon Concentrations and Export Estimates across Six Subarctic Streams in Northern Sweden. *Biogeosciences* **2014**, *11* (2), 525–537. https://doi.org/10.5194/bg-11-525-2014.

(192) Dillon, P. J.; Molot, L. A. Effect of Landscape Form on Export of Dissolved Organic Carbon, Iron, and Phosphorus from Forested Stream Catchments. *Water Resour. Res.* **1997**, *33* (11), 2591–2600. https://doi.org/10.1029/97WR01921.

(193) Andersson, J. O.; Nyberg, L. Spatial Variation of Wetlands and Flux of Dissolved Organic Carbon in Boreal Headwater Streams. *Hydrol. Process.* **2008**, *22* (12), 1965–1975. https://doi.org/10.1002/hyp.6779.

(194) Tarnocai, C.; Kettles, I. M.; Lacelle, B. Soil Organic Content of Canadian Peatlands. Geological Survey of Canada 2011, p Open File 6561.

(195) Tank, S. E.; Frey, K. E.; Striegl, R. G.; Raymond, P. A.; Holmes, R. M.; McClelland, J. W.; Peterson, B. J. Landscape-Level Controls on Dissolved Carbon Flux from Diverse Catchments of the Circumboreal. *Global Biogeochem. Cycles* **2012**, *26* (3), 1–15. https://doi.org/10.1029/2012GB004299.

(196) Collins, M.; Knutti, R.; Arblaster, J.; Dufresne, J.-L.; Fichefet, T.; Friedlingstein, P.; Gao, X.; Gutowski, W. J.; Johns, T.; Krinner, G.; et al. Long-Term Climate Change: Projections, Commitments and Irreversibility. In *Climate Change 2013: The Physical Science Basis. Contribution of Working Group I to the Fifth Assessment Report of the Intergovernmental Panel on Climate Change*; Stocker, T. F., Qin, D., Plattner, G.-K., Tignor, M., Allen, S. K., Boschung, J., Nauels, A., Xia, Y., Bex, V., Midgley, P. M., Eds.; Cambridge University Press: Cambridge, United Kingdom and New York, NY, 2013; pp 1029–1136.

(197) Bring, A.; Fedorova, I.; Dibike, Y.; Hinzman, L.; Mård, J.; Mernild, S. H.; Prowse, T.; Semenova, O.; Stuefer, S. L. L.; Woo, M. K. Arctic Terrestrial Hydrology: A Synthesis of

Processes, Regional Effects and Research Challenges. *J. Geophys. Res. Biogeosciences* **2016**, *121* (3), 621–649. https://doi.org/10.1002/2015JG003131.

(198) Instanes, A.; Kokorev, V.; Janowicz, R.; Bruland, O.; Sand, K.; Prowse, T. Changes to Freshwater Systems Affecting Arctic Infrastructure and Natural Resources. *J. Geophys. Res. G Biogeosciences* **2016**, *121* (3), 567–585. https://doi.org/10.1002/2015JG003125.

(199) Helms, J. R.; Stubbins, A.; Ritchie, J. D.; Minor, E. C.; Kieber, D. J.; Mopper, K. Absorption Spectral Slopes and Slope Ratios as Indicators of Molecular Weight, Source, and Photobleaching of Chromophoric Dissolved Organic Matter. *Limnol. Oceanogr.* **2008**, *53* (3), 955–969. https://doi.org/10.4319/lo.2008.53.3.0955.

(200) Larsen, L. G.; Aiken, G. R.; Harvey, J. W.; Noe, G. B.; Crimaldi, J. P. Using Fluorescence Spectroscopy to Trace Seasonal DOM Dynamics, Disturbance Effects, and Hydrologic Transport in the Florida Everglades. *J. Geophys. Res.* **2010**, *115*, 1–14. https://doi.org/10.1029/2009JG001140.

(201) Mead, J. The Control of Fe and PH on the Photodegradation and Characterization of Dissolved Organic Matter in Small, Oligotrophic Canadian Shield Freshwaters, University of Waterloo, 2017.

(202) Kothawala, D. N.; Stedmon, C. A.; Müller, R. A.; Weyhenmeyer, G. A.; Köhler, S. J.; Tranvik, L. J. Controls of Dissolved Organic Matter Quality: Evidence from a Large-Scale Boreal Lake Survey. *Glob. Chang. Biol.* **2014**, *20*, 1101–1114. https://doi.org/10.1111/gcb.12488.

(203) Massicotte, P.; Asmala, E.; Stedmon, C.; Markager, S. Global Distribution of Dissolved Organic Matter along the Aquatic Continuum: Across Rivers, Lakes and Oceans. *Sci. Total Environ.* **2017**, *609*, 180–191. https://doi.org/10.1016/j.scitotenv.2017.07.076.

(204) Hur, J.; Park, M.-H.; Schlautman, M. a. Microbial Transformation of Dissolved Leaf Litter Organic Matter and Its Effects on Selected Organic Matter Operational Descriptors. *Environ. Sci. Technol.* **2009**, *43* (7), 2315–2321. https://doi.org/10.1021/es802773b.

(205) Creed, I. F.; Mcknight, D. M.; Pellerin, B. A.; Green, M. B.; Bergamaschi, B. A.; Aiken, G. R.; Burns, D. A.; Findlay, S. E. G.; Shanley, J. B.; Striegl, R. G.; et al. The River as a Chemostat : Fresh Perspectives on Dissolved Organic Matter Flowing down the River Continuum. *Can. J. Fish. Aquat. Sci.* **2015**, *14* (April), 1–14.

(206) Lehmann, J.; Kleber, M. The Contentious Nature of Soil Organic Matter. *Nature* **2015**, *528*, 60–68. https://doi.org/10.1038/nature16069.

(207) Schmidt, M. W. I.; Torn, M. S.; Abiven, S.; Dittmar, T.; Guggenberger, G.; Janssens, I. a; Kleber, M.; Kögel-Knabner, I.; Lehmann, J.; Manning, D. a C.; et al. Persistence of Soil Organic Matter as an Ecosystem Property. *Nature* **2011**, *478* (7367), 49–56. https://doi.org/10.1038/nature10386.

(208) Marín-Spiotta, E.; Gruley, K. E.; Crawford, J.; Atkinson, E. E.; Miesel, J. R.; Greene, S.; Cardona-Correa, C.; Spencer, R. G. M. Paradigm Shifts in Soil Organic Matter Research Affect Interpretations of Aquatic Carbon Cycling: Transcending Disciplinary and Ecosystem Boundaries. *Biogeochemistry* **2014**, *117* (2–3), 279–297. https://doi.org/10.1007/s10533-013-9949-7.

(209) Koehler, B.; Von Wachenfeldt, E.; Kothawala, D. N.; Tranvik, L. J. Reactivity Continuum of

Dissolved Organic Carbon Decomposition in Lake Water. *J. Geophys. Res. Biogeosciences* **2012**, *117* (1), 1–14. https://doi.org/10.1029/2011JG001793.

(210) Koehler, B.; Tranvik, L. J. Reactivity Continuum Modeling of Leaf, Root, and Wood Decomposition across Biomes. *J. Geophys. Res. G Biogeosciences* **2015**, *120* (7), 1196–1214. https://doi.org/10.1002/2015JG002908.

(211) Catalán, N.; Casas-Ruiz, J. P.; von Schiller, D.; Proia, L.; Obrador, B.; Zwirnmann, E.; Marce, R. Biodegradation Kinetics of Dissolved Organic Matter Chromatographic Fractions in an Intermittent River. *J. Geophys. Res. Biogeosciences* **2017**, 131–144. https://doi.org/10.1002/2016JG003512.

(212) R Core Team. R: A Language and Environment for Statistical Computing. R Foundation for Statistical Computing: Vienna, Austria 2016.

(213) Chen, M.; Maie, N.; Parish, K.; Jaffé, R. Spatial and Temporal Variability of Dissolved Organic Matter Quantity and Composition in an Oligotrophic Subtropical Coastal Wetland. *Biogeochemistry* **2013**, *115* (1–3), 167–183. https://doi.org/10.1007/s10533-013-9826-4.

(214) Her, N.; Amy, G. L.; Foss, D.; Cho, J.; Yoon, Y.; Kosenka, P. Optimization of Method for Detecting and Characterizing NOM by HPLC-Size Exclusion Chromatography with UV and on-Line DOC Detection. *Environ. Sci. Technol.* **2002**, *36* (5), 1069–1076.

(215) Bodmer, P.; Heinz, M.; Pusch, M.; Singer, G. A.; Premke, K. Carbon Dynamics and Their Link to Dissolved Organic Matter Quality across Contrasting Stream Ecosystems. *Sci. Total Environ.* **2016**, *553*, 574–586. https://doi.org/10.1016/j.scitotenv.2016.02.095.

(216) Tercero Espinoza, L. A.; ter Haseborg, E.; Weber, M.; Frimmel, F. H. Investigation of the Photocatalytic Degradation of Brown Water Natural Organic Matter by Size Exclusion Chromatography. *Appl. Catal. B Environ.* **2009**, *87* (1–2), 56–62. https://doi.org/10.1016/j.apcatb.2008.08.013.

(217) Fichot, C. G.; Benner, R. The Spectral Slope Coefficient of Chromophoric Dissolved Organic Matter ($S_{275\text{-}295}$) as a Tracer of Terrigenous Dissolved Organic Carbon in River-Influenced Ocean Margins. *Limnol. Oceanogr.* **2012**, *57* (5), 1453–1466. https://doi.org/10.4319/lo.2012.57.5.1453.

(218) Jaffé, R.; McKnight, D.; Maie, N.; Cory, R. M.; McDowell, W. H.; Campbell, J. L. Spatial and Temporal Variations in DOM Composition in Ecosystems: The Importance of Long-Term Monitoring of Optical Properties. *J. Geophys. Res.* **2008**, *113* (G4), 1–15. https://doi.org/10.1029/2008JG000683.

(219) Jane, S. F.; Winslow, L. A.; Remucal, C. K.; Rose, K. C. Long-Term Trends and Synchrony in Dissolved Organic Matter Characteristics in Wisconsin, USA, Lakes: Quality, Not Quantity, Is Highly Sensitive to Climate. *J. Geophys. Res. Biogeosciences* **2017**, *122* (3), 546–561. https://doi.org/10.1002/2016JG003630.

(220) Cleveland, C. C.; Neff, J. C.; Townsend, A. R.; Hood, E. Composition, Dynamics, and Fate of Leached Dissolved Organic Matter in Terrestrial Ecosystems: Results from a Decomposition Experiment. *Ecosystems* **2004**, *7* (3), 275–285. https://doi.org/10.1007/s10021-003-0236-7.

(221) Bourbonniere, R. Distribution Patterns of Dissolved Organic Matter Fractions in Natural Waters from Eastern Canada. *Org. Geochem.* **1989**, *14* (1), 97–107.

https://doi.org/10.1016/0146-6380(89)90023-5.

(222) Kawasaki, N.; Matsushige, K.; Komatsu, K.; Kohzu, A.; Nara, F. W.; Ogishi, F.; Yahata, M.; Mikami, H.; Goto, T.; Imai, A. Fast and Precise Method for HPLC-Size Exclusion Chromatography with UV and TOC (NDIR) Detection: Importance of Multiple Detectors to Evaluate the Characteristics of Dissolved Organic Matter. *Water Res.* **2011**, *45* (18), 6240–6248. https://doi.org/10.1016/j.watres.2011.09.021.

(223) Romera-Castillo, C.; Chen, M.; Yamashita, Y.; Jaffé, R. Fluorescence Characteristics of Size-Fractionated Dissolved Organic Matter: Implications for a Molecular Assembly Based Structure? *Water Res.* **2014**, *55C*, 40–51. https://doi.org/10.1016/j.watres.2014.02.017.

(224) Chin, Y.-P.; Aiken, G. R.; O'Loughlin, E. Molecular Weight, Polydispersity, and Spectroscopic Properties of Aquatic Humic Substances. *Environ. Sci. Technol.* **1994**, *28* (11), 1853–1858. https://doi.org/10.1021/es00060a015.

(225) Curtis, P. J.; Schindler, D. W. Hydrologic Control of Dissolved Organic Matter in Low-Order Precambrian Shield Lakes. *Biogeochemistry* **1997**, *36* (1), 125–138. https://doi.org/10.1023/A:1005787913638.

(226) Spencer, R. G. M.; Mann, P. J.; Dittmar, T.; Eglinton, T. I.; Mcintyre, C.; Holmes, R. M.; Zimov, N. S.; Stubbins, A. Detecting the Signature of Permafrost Thaw in Arctic Rivers. *Geophys. Res. Lett.* **2015**, 1–6. https://doi.org/10.1002/2015GL063498.

(227) Deshpande, B. N.; Crevecoeur, S.; Matveev, A.; Vincent, W. F. Bacterial Production in Subarctic Peatland Lakes Enriched by Thawing Permafrost. *Biogeosciences* **2016**, *13* (15), 4411–4427. https://doi.org/10.5194/bg-13-4411-2016.

(228) MacMillan, G. A.; Girard, C.; Chételat, J.; Laurion, I.; Amyot, M. High Methylmercury in Arctic and Subarctic Ponds Is Related to Nutrient Levels in the Warming Eastern Canadian Arctic. *Environ. Sci. Technol.* **2015**, *49* (13), 7743–7753. https://doi.org/10.1021/acs.est.5b00763.

(229) Tank, S. E.; Lesack, L. F. W.; Hesslein, R. H. Northern Delta Lakes as Summertime CO2 Absorbers within the Arctic Landscape. *Ecosystems* **2009**, *12* (1), 144–157. https://doi.org/10.1007/s10021-008-9213-5.

(230) Guillemette, F.; del Giorgio, P. A. Reconstructing the Various Facets of Dissolved Organic Carbon Bioavailability in Freshwater Ecosystems. *Limnol. Oceanogr.* **2011**, *56* (2), 734–748. https://doi.org/10.4319/lo.2011.56.2.0734.

(231) Mostovaya, A.; Koehler, B.; Guillemette, F.; Brunberg, A. K.; Tranvik, L. J. Effects of Compositional Changes on Reactivity Continuum and Decomposition Kinetics of Lake Dissolved Organic Matter. *J. Geophys. Res. Biogeosciences* **2016**, *121* (7), 1733–1746. https://doi.org/10.1002/2016JG003359.

(232) Berggren, M.; Laudon, H.; Jansson, M. Aging of Allochthonous Organic Carbon Regulates Bacterial Production in Unproductive Boreal Lakes. *Limnol. Oceanogr.* **2009**, *54* (4), 1333–1342. https://doi.org/10.4319/lo.2009.54.4.1333.

(233) Guillemette, F.; McCallister, S. L.; Del Giorgio, P. A. Differentiating the Degradation Dynamics of Algal and Terrestrial Carbon within Complex Natural Dissolved Organic Carbon in Temperate Lakes. *J. Geophys. Res. Biogeosciences* **2013**, *118* (3), 963–973. https://doi.org/10.1002/jgrg.20077.

(234) Amon, R. M. W.; Benner, R. Bacterial Utilization of Different Size Classes of Dissolved Organic Matter. *Limnol. Oceanogr.* **1996**, *41* (1), 41–51.

(235) Lapierre, J. F.; del Giorgio, P. A. Partial Coupling and Differential Regulation of Biologically and Photochemically Labile Dissolved Organic Carbon across Boreal Aquatic Networks. *Biogeosciences* **2014**, *11* (20), 5969–5985. https://doi.org/10.5194/bg-11-5969-2014.

(236) Vachon, D.; Prairie, Y. T.; Guillemette, F.; del Giorgio, P. A. Modeling Allochthonous Dissolved Organic Carbon Mineralization Under Variable Hydrologic Regimes in Boreal Lakes. *Ecosystems* **2017**, *20* (4), 781–795. https://doi.org/10.1007/s10021-016-0057-0.

(237) Boudreau, B. P.; Ruddick, B. R. On a Reactive Continuum Representation of Organic Matter Diagenesis. *American Journal of Science*. 1991, pp 507–538. https://doi.org/10.2475/ajs.291.5.507.

(238) Vonk, J. E.; Tank, S. E.; Bowden, W. B.; Laurion, I.; Vincent, W. F.; Alekseychik, P.; Amyot, M.; Billett, M. F.; Canário, J.; Cory, R. M.; et al. Reviews and Syntheses: Effects of Permafrost Thaw on Arctic Aquatic Ecosystems. *Biogeosciences* **2015**, *12* (23), 7129–7167. https://doi.org/10.5194/bg-12-7129-2015.

(239) McDowell, W. H.; Zsolnay, A.; Aitkenhead-Peterson, J.; Gregorich, E. G.; Jones, D. L.; Jödemann, D.; Kalbitz, K.; Marschner, B.; Schwesig, D. A Comparison of Methods to Determine the Biodegradable Dissolved Organic Carbon from Different Terrestrial Sources. *Soil Biol. Biochem.* **2006**, *38* (7), 1933–1942. https://doi.org/10.1016/j.soilbio.2005.12.018.

(240) Sleighter, R. L.; Cory, R. M.; Kaplan, L. a.; Abdulla, H. A. N.; Hatcher, P. G. A Coupled Geochemical and Biogeochemical Approach to Characterize the Bioreactivity of Dissolved Organic Matter from a Headwater Stream. *J. Geophys. Res. Biogeosciences* **2014**, *119* (8), 1520–1537. https://doi.org/10.1002/2013JG002600.

(241) Wang, Y.; Hammes, F.; Boon, N.; Egli, T. Quantification of the Filterability of Freshwater Bacteria through 0.45, 0.22, and 0.1 Mm Pore Size Filters and Shape-Dependent Enrichment of Filterable Bacterial Communities. *Environ. Sci. Technol.* **2007**, *41* (20), 7080–7086. https://doi.org/10.1021/es0707198.

(242) Kerner, M.; Hohenberg, H.; Ertl, S.; Reckermann, M.; Spitzy, A. Self-Organization of Dissolved Organic Matter to Micelle-like Microparticles in River Water. *Nature* **2003**, *422* (6928), 150–154. https://doi.org/10.1038/nature01469.

(243) Kalbitz, K.; Schwesig, D.; Schmerwitz, J.; Kaiser, K.; Haumaier, L.; Glaser, B.; Ellerbrock, R.; Leinweber, P. Changes in Properties of Soil-Derived Dissolved Organic Matter Induced by Biodegradation. *Soil Biol. Biochem.* **2003**, *35* (8), 1129–1142. https://doi.org/10.1016/S0038-0717(03)00165-2.

(244) Hood, E.; Williams, M. W.; Mcknight, D. M. Sources of Dissolved Organic Matter (DOM) in a Rocky Mountain Stream Using Chemical Fractionation and Stable Isotopes. *Biogeochemistry* **2005**, *74*, 231–255. https://doi.org/10.1007/s10533-004-4322-5.

(245) Roiha, T.; Laurion, I.; Rautio, M. Carbon Dynamics in Highly Heterotrophic Subarctic Thaw Ponds. *Biogeosciences* **2015**, *12* (23), 7223–7237. https://doi.org/10.5194/bg-12-7223-2015.

(246) Attermeyer, K.; Catalán, N.; Einarsdottir, K.; Freixa, A.; Groeneveld, M.; Hawkes, J. A.; Bergquist, J.; Tranvik, L. J. Organic Carbon Processing During Transport Through Boreal

Inland Waters: Particles as Important Sites. *J. Geophys. Res. Biogeosciences* **2018**, *123* (8), 2412–2428. https://doi.org/10.1029/2018JG004500.

(247) Kothawala, D. N.; von Wachenfeldt, E.; Koehler, B.; Tranvik, L. J. Selective Loss and Preservation of Lake Water Dissolved Organic Matter Fluorescence during Long-Term Dark Incubations. *Sci. Total Environ.* **2012**, *433*, 238–246. https://doi.org/10.1016/j.scitotenv.2012.06.029.

(248) Wiegner, T. N.; Seitzinger, S. P. Seasonal Bioavailability of Dissolved Organic Carbon and Nitrogen from Pristine and Polluted Freshwater Wetlands. *Limnol. Oceanogr.* **2004**, *49* (5), 1703–1712. https://doi.org/10.4319/lo.2004.49.5.1703.

(249) del Giorgio, P. A.; Cole, J. J. Bacterial Growth Efficiency in Natural Aquatic Systems. *Annu. Rev. Ecol. Syst.* **1998**, *29* (1), 503–541. https://doi.org/10.1146/annurev.ecolsys.29.1.503.

(250) Burpee, B.; Saros, J. E.; Northington, R. M.; Simon, K. S. Microbial Nutrient Limitation in Arctic Lakes in a Permafrost Landscape of Southwest Greenland. *Biogeosciences Discuss.* **2015**, *12* (14), 11863–11890. https://doi.org/10.5194/bgd-12-11863-2015.

(251) Frey, K. E.; Sobczak, W. V.; Mann, P. J.; Holmes, R. M. Optical Properties and Bioavailability of Dissolved Organic Matter along a Flow-Path Continuum from Soil Pore Waters to the Kolyma River, Siberia. *Biogeosciences Discuss.* **2015**, *12* (15), 12321–12347. https://doi.org/10.5194/bgd-12-12321-2015.

(252) Michaelson, G. J.; Ping, C. L.; Kling, G. W.; Hobbie, J. E. The Character and Bioactivity of Dissolved Organic Matter at Thaw and in the Spring Runoff Waters of the Arctic Tundra North Slope, Alaska. *J. Geophys. Res.* **1998**, *103* (D22), 28939. https://doi.org/10.1029/98JD02650.

(253) Fellman, J. B.; Hood, E.; D'Amore, D. V.; Edwards, R. T.; White, D. Seasonal Changes in the Chemical Quality and Biodegradability of Dissolved Organic Matter Exported from Soils to Streams in Coastal Temperate Rainforest Watersheds. *Biogeochemistry* **2009**, *95* (2), 277–293. https://doi.org/10.1007/s10533-009-9336-6.

(254) Obernosterer, I.; Benner, R. Competition between Biological and Photochemical Processes in the Mineralization of Dissolved Organic Carbon. *Limnol. Oceanogr.* **2004**, *49* (1), 117–124. https://doi.org/10.4319/lo.2004.49.1.0117.

(255) Reche, I.; Pace, M. L.; Cole, J. J. Modeled Effects of Dissolved Organic Carbon and Solar Spectra on Photobleaching in Lake Ecosystems. *Ecosystems* **2000**, *3*, 419–432. https://doi.org/10.1007/s100210000038.

(256) Brisco, S.; Ziegler, S. Effects of Solar Radiation on the Utilization of Dissolved Organic Matter DOM) from Two Headwater Streams. *Aquat. Microb. Ecol.* **2004**, *37*, 197–208.

(257) Stubbins, A.; Spencer, R. G. M.; Chen, H.; Hatcher, P. G.; Mopper, K.; Hernes, P. J.; Mwamba, V. L.; Mangangu, A. M.; Wabakanghanzi, J. N.; Six, J. Illuminated Darkness: Molecular Signatures of Congo River Dissolved Organic Matter and Its Photochemical Alteration as Revealed by Ultrahigh Precision Mass Spectrometry. *Limnol. Oceanogr.* **2010**, *55* (4), 1467–1477. https://doi.org/10.4319/lo.2010.55.4.1467.

(258) Cory, R. M.; Crump, B. C.; Dobkowski, J. a; Kling, G. W. Surface Exposure to Sunlight Stimulates CO2 Release from Permafrost Soil Carbon in the Arctic. *Proc. Natl. Acad. Sci. U. S.*

A. **2013**, *110* (9), 3429–3434. https://doi.org/10.1073/pnas.1214104110.

(259) Porcal, P.; Dillon, P. J.; Molot, L. A. Seasonal Changes in Photochemical Properties of Dissolved Organic Matter in Small Boreal Streams. *Biogeosciences* **2013**, *10*, 553–5543. https://doi.org/10.5194/bg-10-5533-2013.

(260) Vähätalo, A. V.; Salkinoja-Salonen, M.; Taalas, P.; Salonen, K. Spectrum of the Quantum Yield for Photochemical Mineralization of Dissolved Organic Carbon in a Humic Lake. *Limnol. Oceanogr.* **2000**, *45* (3), 664–676. https://doi.org/10.4319/lo.2000.45.3.0664.

(261) Koehler, B.; Landelius, T.; Weyhenmeyer, G. A.; Machida, N.; Tranvik, L. J. Sunlight-Induced Carbon Dioxide Emissions from Inland Waters. *Global Biogeochem. Cycles* **2014**, *28* (7), 696–711. https://doi.org/10.1002/2014GB004850.

(262) Girard, C.; Leclerc, M.; Amyot, M. Photodemethylation of Methylmercury in Eastern Canadian Arctic Thaw Pond and Lake Ecosystems. *Environ. Sci. Technol.* **2016**, *50* (7), 3511–3520. https://doi.org/10.1021/acs.est.5b04921.

(263) Köhler, S.; Buffam, I.; Jonsson, A.; Bishop, K. H. Photochemical and Microbial Processing of Stream and Soil Water Dissolved Organic Matter in a Boreal Forested Catchment in Northern Sweden. *Aquat. Sci.* **2002**, *64*, 269–281.

(264) Berggren, M.; Klaus, M.; Panneer Selvam, B.; Ström, L.; Laudon, H.; Jansson, M.; Karlsson, J. Quality Transformation of Dissolved Organic Carbon during Water Transit through Lakes: Contrasting Controls by Photochemical and Biological Processes. *Biogeosciences Discuss.* **2017**, *15* (2), 1–22. https://doi.org/10.5194/bg-2017-279.

(265) Twardowski, M. S.; Donaghay, P. L. Photobleaching of Aquatic Dissolved Materials: Absorption Removal, Spectral Alteration, and Their Interrelationship. *J. Geophys. Res.* **2002**, *107* (C8), 3091. https://doi.org/10.1029/1999JC000281.

(266) Winter, A. R.; Fish, T. A. E.; Playle, R. C.; Smith, D. S.; Curtis, P. J. Photodegradation of Natural Organic Matter from Diverse Freshwater Sources. *Aquat. Toxicol.* **2007**, *84*, 215–222. https://doi.org/10.1016/j.aquatox.2007.04.014.

(267) Franke, D.; Hamilton, M. W.; Ziegler, S. E. Variation in the Photochemical Lability of Dissolved Organic Matter in a Large Boreal Watershed. *Aquat. Sci.* **2012**, *74*, 751–768. https://doi.org/10.1007/s00027-012-0258-3.

(268) Cory, R. M.; McKnight, D. M.; Chin, Y.-P.; Miller, P.; Jaros, C. L. Chemical Characteristics of Fulvic Acids from Arctic Surface Waters: Microbial Contributions and Photochemical Transformations. *J. Geophys. Res. Biogeosciences* **2007**, *112* (G4), n/a-n/a. https://doi.org/10.1029/2006JG000343.

(269) Ziegler, S.; Benner, R. Effects of Solar Radiation on Dissolved Organic Matter Cycling in a Subtropical Seagrass Meadow. *Limnol. Oceanogr.* **2000**, *45* (2), 257–266.

(270) Lafleur, P. M.; Humphreys, E. R. Spring Warming and Carbon Dioxide Exchange over Low Arctic Tundra in Central Canada. *Glob. Chang. Biol.* **2008**, *14* (4), 740–756. https://doi.org/10.1111/j.1365-2486.2007.01529.x.

(271) Laliberté, J.; Bélanger, S.; Frouin, R. Evaluation of Satellite-Based Algorithms to Estimate Photosynthetically Available Radiation (PAR) Reaching the Ocean Surface at High Northern Latitudes. *Remote Sens. Environ.* **2016**, *184*, 199–211. https://doi.org/10.1016/j.rse.2016.06.014.

(272) Opsahl, S.; Benner, R.; Amon, R. M. W.; Dec, N. Major Flux of Terrigenous Dissolved Organic Matter Through the Arctic Ocean Major Flux of Terrigenous Dissolved Organic Matter through the Arctic Ocean. *Limnology* **2007**, *44* (8), 2017–2023.

(273) Williamson, C. E.; Zepp, R. G.; Lucas, R. M.; Madronich, S.; Austin, A. T.; Ballaré, C. L.; Norval, M.; Sulzberger, B.; Bais, A. F.; McKenzie, R. L.; et al. Solar Ultraviolet Radiation in a Changing Climate. *Nat. Clim. Chang.* **2014**, *4* (6), 434–441. https://doi.org/10.1038/nclimate2225.

(274) Weyhenmeyer, G. A.; Fröberg, M.; Karltun, E.; Khalili, M.; Kothawala, D. N.; Temnerud, J.; Tranvik, L. J. Selective Decay of Terrestrial Organic Carbon during Transport from Land to Sea. *Glob. Chang. Biol.* **2012**, *18* (1), 349–355. https://doi.org/10.1111/j.1365-2486.2011.02544.x.

(275) Finstad, A. G.; Helland, I. P.; Ugedal, O.; Hesthagen, T.; Hessen, D. O. Unimodal Response of Fish Yield to Dissolved Organic Carbon. *Ecol. Lett.* **2014**, *17* (1), 36–43. https://doi.org/10.1111/ele.12201.

(276) Marshall, I. B.; Schut, P. H.; Ballard, M. *A National Ecological Framework for Canada: Attribute Data*; Ecosystem Stratification Working Group, Agriculture and Agri-Food Canada & Environment Canada: Ottawa, ON, Canada, 1999.

(277) Ministry of the Environment. *Technical Support Document for Ontario Drinking Water Standards, Objectives and Guidelines*; 2003.

(278) Rook, J. J. Chlorination Reactions of Fulvic Acids in Natural-Waters. *Environ. Sci. Technol.* **1977**, *11* (5), 478–482.

(279) Trussell, R. R.; Umphres, M. D. The Formation of Trihalomethanes. *J. Am. Water Work. Assoc.* **1978**, *70*, 604–612.

(280) Singer, P. C.; Obolensky, A.; Greiner, A. DBPs in Chlorinated North Carolina Drinking Waters. *J. Am. Water Work. Assoc.* **1995**, *87* (10), 83–92.

(281) Roberts, M. G.; Singer, P. C.; Obolensky, A. Comparing Total HAA and Total THM Concentrations Using ICR Data. *J. / Am. Water Work. Assoc.* **2002**, *94* (3), 103–114.

(282) White, D. M.; Garland, D. S.; Narr, J.; Woolard, C. R. Natural Organic Matter and DBP Formation Potential in Alaskan Water Supplies. *Water Res.* **2003**, *37* (4), 939–947. https://doi.org/10.1016/S0043-1354(02)00425-6.

(283) Richardson, S. D.; Plewa, M. J.; Wagner, E. D.; Schoeny, R.; DeMarini, D. M. Occurrence, Genotoxicity, and Carcinogenicity of Regulated and Emerging Disinfection by-Products in Drinking Water: A Review and Roadmap for Research. *Mutat. Res. - Rev. Mutat. Res.* **2007**, *636* (1–3), 178–242. https://doi.org/10.1016/j.mrrev.2007.09.001.

(284) Lavonen, E. E.; Gonsior, M.; Tranvik, L. J.; Schmitt-kopplin, P.; Kohler, S. J. Selective Chlorination of Natural Organic Matter: Identification of Previously Unknown Disinfection Byproducts. *Environ. Sci. Technol.* **2013**, *47*, 2264–2271.

(285) Singer, P. C. DBPs in Drinking Water: Additional Scientific and Policy Considrerations for Public Health Protection. *J. Am. Water Work. Assoc.* **2006**, *98* (10), 73–80.

(286) Roe, J.; Baker, A.; Bridgeman, J. Relating Organic Matter Character to Trihalomethanes Formation Potential: A Data Mining Approach. *Water Sci. Technol. Water Supply* **2008**, *8* (6), 717–723. https://doi.org/10.2166/ws.2008.150.

(287) Gallard, H.; von Gunten, U. Chlorination of Natural Organic Matter: Kinetics of Chlorination and of THM Formation. *Water Res.* **2002**, *36* (1), 65–74. https://doi.org/10.1016/S0043-1354(01)00187-7.

(288) Zeng, T.; Arnold, W. A. Clustering Chlorine Reactivity of Haloacetic Acid Precursors in Inland Lakes. *Environ. Sci. Technol.* **2014**, *48* (1), 139–148. https://doi.org/10.1021/es403766n.

(289) Hua, G.; Reckhow, D. A.; Abusallout, I. Correlation between SUVA and DBP Formation during Chlorination and Chloramination of NOM Fractions from Different Sources. *Chemosphere* **2015**, *130*, 82–89. https://doi.org/10.1016/j.chemosphere.2015.03.039.

(290) Golea, D. M.; Upton, A.; Jarvis, P.; Moore, G.; Sutherland, S.; Parsons, S. A.; Judd, S. J. THM and HAA Formation from NOM in Raw and Treated Surface Waters. *Water Res.* **2017**, *112*, 226–235. https://doi.org/10.1016/j.watres.2017.01.051.

(291) Li, C. W.; Korshin, G. V; Benjamin, M. M. Monitoring DBP Formation with Differential UV Spectroscopy. *J. Am. Water Work. Assoc.* **1998**, *90* (8), 88–100. https://doi.org/10.1002/j.1551-8833.1998.tb08488.x.

(292) Chang, E. E.; Chiang, P. C.; Ko, Y. W.; Lan, W. H. Characteristics of Organic Precursors and Their Relationship with Disinfection By-Products. *Chemosphere* **2001**, *44* (5), 1231–1236. https://doi.org/10.1016/S0045-6535(00)00499-9.

(293) Ates, N.; Kitis, M.; Yetis, U. Formation of Chlorination By-Products in Waters with Low SUVA-Correlations with SUVA and Differential UV Spectroscopy. *Water Res.* **2007**, *41* (18), 4139–4148. https://doi.org/10.1016/j.watres.2007.05.042.

(294) Department of Municipal and Community Affairs. *Report on Drinking Water 2016*; 2016.

(295) Pardhan-Ali, A.; Wilson, J.; Edge, V. L.; Furgal, C.; Reid-Smith, R.; Santos, M.; McEwen, S. A. A Descriptive Analysis of Notifiable Gastrointestinal Illness in the Northwest Territories, Canada, 1991-2008. *BMJ Open* **2012**, *2* (4), 1–10. https://doi.org/10.1136/bmjopen-2011-000732.

(296) Goldhar, C.; Bell, T.; Wolf, J. Vulnerability to Freshwater Changes in the Inuit Settlement Region of Nunatsiavut, Labrador: A Case Study from Rigolet. *Arctic* **2014**, *67* (1), 71–83. https://doi.org/10.14430/arctic4365.

(297) Monteith, D. T.; Stoddard, J. L.; Evans, C. D.; de Wit, H. A.; Forsius, M.; Høgåsen, T.; Wilander, A.; Skjelkvåle, B. L.; Jeffries, D. S.; Vuorenmaa, J.; et al. Dissolved Organic Carbon Trends Resulting from Changes in Atmospheric Deposition Chemistry. *Nature* **2007**, *450* (7169), 537–540. https://doi.org/10.1038/nature06316.

(298) Solomon, C. T.; Jones, S. E.; Weidel, B. C.; Buffam, I.; Fork, M. L.; Karlsson, J.; Larsen, S.; Lennon, J. T.; Read, J. S.; Sadro, S.; et al. Ecosystem Consequences of Changing Inputs of Terrestrial Dissolved Organic Matter to Lakes: Current Knowledge and Future Challenges. *Ecosystems* **2015**, No. January. https://doi.org/10.1007/s10021-015-9848-y.

(299) Martin, D.; Bélanger, D.; Gosselin, P.; Brazeau, J.; Furgal, C.; Déry, S. Drinking Water and Potential Threats to Human Health in Nunavik: Adaptation Strategies under Climate Change Conditions. *Arctic* **2007**, *60* (2), 195–202.

(300) Harper, S. L.; Edge, V. L.; Schuster-Wallace, C. J.; Berke, O.; McEwen, S. A. Weather, Water Quality and Infectious Gastrointestinal Illness in Two Inuit Communities in Nunatsiavut,

Canada: Potential Implications for Climate Change. *Ecohealth* **2011**, *8* (1), 93–108. https://doi.org/10.1007/s10393-011-0690-1.

(301) Wright, C. J.; Sargeant, J. M.; Edge, V. L.; Ford, J. D.; Farahbakhsh, K.; Shiwak, I.; Flowers, C.; Harper, S. L. Water Quality and Health in Northern Canada: Stored Drinking Water and Acute Gastrointestinal Illness in Labrador Inuit. *Environ. Sci. Pollut. Res.* **2017**, 1–13. https://doi.org/10.1007/s11356-017-9695-9.

(302) Chow, A. T.; Díaz, F. J.; Wong, K.-H.; O'Geen, A. T.; Dahlgren, R. a; Wong, P.-K. Photochemical and Bacterial Transformations of Disinfection By-Product Precursors in Water. *J. Environ. Qual.* **2013**, *42* (5), 1589–1595. https://doi.org/10.2134/jeq2013.01.0022.

(303) Deborde, M.; von Gunten, U. Reactions of Chlorine with Inorganic and Organic Compounds during Water Treatment-Kinetics and Mechanisms: A Critical Review. *Water Res.* **2008**, *42* (1–2), 13–51. https://doi.org/10.1016/j.watres.2007.07.025.

(304) Molot, L. A.; Dillon, P. J. Colour - Mass Balances and Colour - Dissolved Organic Carbon Relationships in Lakes and Streams in Central Ontario. *Can. J. Fish. Aquat. Sci.* **1997**, *54* (12), 2789–2795. https://doi.org/10.1139/cjfas-54-12-2789.

(305) Baker, A.; Spencer, R. G. M. Characterization of Dissolved Organic Matter from Source to Sea Using Fluorescence and Absorbance Spectroscopy. *Sci. Total Environ.* **2004**, *333* (1–3), 217–232. https://doi.org/10.1016/j.scitotenv.2004.04.013.

(306) Reckhow, D. A.; Rees, P. L. S.; Bryan, D. Watershed Sources of Disinfection Byproduct Precursors. *Water Sci. Technol. Water Supply* **2004**, *4* (4), 61–69.

(307) Pellerin, B. A.; Hernes, P. J.; Saraceno, J.; Spencer, R. G. M.; Bergamaschi, B. A. Microbial Degradation of Plant Leachate Alters Lignin Phenols and Trihalomethane Precursors. *J. Environ. Qual.* **2010**, *39* (3), 946. https://doi.org/10.2134/jeq2009.0487.

(308) Yang, X.; Guo, W.; Shen, Q. Formation of Disinfection Byproducts from Chlor(Am)Ination of Algal Organic Matter. *J. Hazard. Mater.* **2011**, *197*, 378–388. https://doi.org/10.1016/j.jhazmat.2011.09.098.

(309) Clark, G. F.; Stark, J. S.; Johnston, E. L.; Runcie, J. W.; Goldsworthy, P. M.; Raymond, B.; Riddle, M. J. Light-Driven Tipping Points in Polar Ecosystems. *Glob. Chang. Biol.* **2013**, *19* (12), 3749–3761. https://doi.org/10.1111/gcb.12337.

(310) Nevalainen, L.; Luoto, T. P.; Rantala, M. V.; Galkin, A.; Rautio, M. Role of Terrestrial Carbon in Aquatic UV Exposure and Photoprotective Pigmentation of Meiofauna in Subarctic Lakes. *Freshw. Biol.* **2015**, *60* (11), 2435–2444. https://doi.org/10.1111/fwb.12670.

(311) Dilling, W. L.; Tefertiller, N. B.; Kallos, G. J. Evaporation Rates and Reactivities of Methylene Chloride, Chloroform, 1,1,1 -Trichloroethane, Trichloroethylene, Tetrachloroethylene, and Other Chlorinated Compounds in Dilute Aqueous Solutions. *Environ. Sci. Technol.* **1975**, *9* (9), 833–838. https://doi.org/10.1021/es60107a008.

(312) Weaver, W. A.; Li, J.; Wen, Y.; Johnston, J.; Blatchley, M. R.; Blatchley, E. R. Volatile Disinfection By-Product Analysis from Chlorinated Indoor Swimming Pools. *Water Res.* **2009**, *43* (13), 3308–3318. https://doi.org/10.1016/j.watres.2009.04.035.

(313) Jagals, P.; Jagals, C.; Bokako, T. C. The Effect of Container-Biofilm on the Microbiological Quality of Water Used from Plastic Household Containers. *J. Water Health* **2003**, *1* (3), 101–

108.

(314) Xu, J.; Huang, C.; Shi, X.; Dong, S.; Yuan, B.; Nguyen, T. H. Role of Drinking Water Biofilms on Residual Chlorine Decay and Trihalomethane Formation: An Experimental and Modeling Study. *Sci. Total Environ.* **2018**, *642*, 516–525. https://doi.org/10.1016/j.scitotenv.2018.05.363.

(315) Bertilsson, S.; Jones, J. B. Supply of Dissolved Organic Matter to Aquatic Ecosystems: Autochthonous Sources. In *Aquatic Ecosystems: Interactivity of Dissolved Organic Matter*; Findlay, S. E. G., Sinsabaugh, R. L., Eds.; Academic Press, 2003; p 512.

(316) Bogard, M. J.; Kuhn, C. D.; Johnston, S. E.; Striegl, R. G.; Holtgrieve, G. W.; Dornblaser, M. M.; Spencer, R. G. M.; Wickland, K. P.; Butman, D. E. Negligible Cycling of Terrestrial Carbon in Many Lakes of the Arid Circumpolar Landscape. *Nat. Geosci.* **2019**. https://doi.org/10.1038/s41561-019-0299-5.

(317) McKnight, D. M.; Andrews, E. D.; Spaulding, S. A.; Aiken, G. R. Aquatic Fulvic Acids in Algal-rich Antarctic Ponds. *Limnol. Oceanogr.* **1994**, *39* (8), 1972–1979. https://doi.org/10.4319/lo.1994.39.8.1972.

(318) *Climate Change 2013 - The Physical Science Basis*; Intergovernmental Panel on Climate Change, Ed.; Cambridge University Press: Cambridge, 2014. https://doi.org/10.1017/CBO9781107415324.

(319) Szkokan-Emilson, E. J.; Kielstra, B. W.; Arnott, S. E.; Watmough, S. A.; Gunn, J. M.; Tanentzap, A. J. Dry Conditions Disrupt Terrestrial–Aquatic Linkages in Northern Catchments. *Glob. Chang. Biol.* **2017**, *23* (1), 117–126. https://doi.org/10.1111/gcb.13361.

(320) Emmerton, C. A.; St Louis, V. L.; Lehnherr, I.; Humphreys, E. R.; Rydz, E.; Kosolofski, H. R. The Net Exchange of Methane with High Arctic Landscapes during the Summer Growing Season. *Biogeosciences Discuss* **2014**, *11*, 1673–1706. https://doi.org/10.5194/bgd-11-1673-2014.

(321) Comte, J.; Lovejoy, C.; Crevecoeur, S.; Vincent, W. F. Co-Occurrence Patterns in Aquatic Bacterial Communities across Changing Permafrost Landscapes. *Biogeosciences* **2016**, *13* (12), 175–190. https://doi.org/10.5194/bg-13-175-2016.

(322) Comte, J.; Monier, A.; Crevecoeur, S.; Lovejoy, C.; Vincent, W. F. Microbial Biogeography of Permafrost Thaw Ponds across the Changing Northern Landscape. *Ecography (Cop.).* **2015**, No. July, n/a-n/a. https://doi.org/10.1111/ecog.01667.

(323) Kaiser, K.; Canedo-Oropeza, M.; McMahon, R.; Amon, R. M. W. Origins and Transformations of Dissolved Organic Matter in Large Arctic Rivers. *Sci. Rep.* **2017**, *7* (1), 1–11. https://doi.org/10.1038/s41598-017-12729-1.

(324) Mackelprang, R.; Waldrop, M. P.; DeAngelis, K. M.; David, M. M.; Chavarria, K. L.; Blazewicz, S. J.; Rubin, E. M.; Jansson, J. K. Metagenomic Analysis of a Permafrost Microbial Community Reveals a Rapid Response to Thaw. *Nature* **2011**, *480* (7377), 368–371. https://doi.org/10.1038/nature10576.

(325) Negandhi, K.; Laurion, I.; Lovejoy, C. Bacterial Communities and Greenhouse Gas Emissions of Shallow Ponds in the High Arctic. *Polar Biol.* **2014**, *37*, 1669–1683. https://doi.org/10.1007/s00300-014-1555-1.

(326) Herrero Ortega, S.; Catalán, N.; Björn, E.; Gröntoft, H.; Hilmarsson, T. G.; Bertilsson, S.; Wu, P.; Bishop, K. H.; Levanoni, O.; Bravo, A. G. High Methylmercury Formation in Ponds Fueled

by Fresh Humic and Algal Derived Organic Matter. *Limnol. Oceanogr.* **2017**. https://doi.org/10.1002/lno.10722.

(327) Bravo, A. G.; Bouchet, S.; Tolu, J.; Björn, E.; Mateos-Rivera, A.; Bertilsson, S. Molecular Composition of Organic Matter Controls Methylmercury Formation in Lakes. *Nat. Commun.* **2017**, 1–9. https://doi.org/10.1038/ncomms14255.

(328) Lehnherr, I.; St Louis, V. L. Importance of Ultraviolet Radiation in the Photodemethylation of Methylmercury in Freshwater Ecosystems. *Environ. Sci. Technol.* **2009**, *43* (15), 5692–5698. https://doi.org/10.1021/es9002923.